UNIVERSITY OF SÃO PAULO

INSTITUTE OF CHEMISTRY

Graduate Program in Biological Sciences (Biochemistry)

YUNYS PÉREZ BETANCOURT

Cationic and biocompatible polymeric nanoparticles: preparation, characterization, and immunoadjuvant activity

Original version of the defended Thesis

São Paulo

Date of deposit at the SPG:

03/01/2022

YUNYS PÉREZ BETANCOURT

Nanopartículas poliméricas catiônicas e biocompatíveis: preparação, caracterização e atividade imunoadjuvante

Thesis presented to the Institute of Chemistry of the University of São Paulo to obtain the title of Doctor in Science (Biochemistry)

Supervisor: Prof. Dr. Ana Maria Carmona-Ribeiro

São Paulo

2022

Autorizo a reprodução e divulgação total ou parcial deste trabalho, por qualquer meio convencional ou eletronico, para fins de estudo e pesquisa, desde que citada a fonte.

Ficha Catalográfica elaborada eletronicamente pelo autor, utilizando o programa desenvolvido pela Seção Técnica de Informática do ICMC/USP e adaptado para a Divisão de Biblioteca e Documentação do Conjunto das Químicas da USP

Bibliotecária responsável pela orientação de catalogação da publicação:
Marlene Aparecida Vieira - CRB - 8/5562

Pérez-Betancourt, Yunys
P438c Cationic and biocompatible polymeric nanoparticles: preparation, characterization, and immunoadjuvant activity / Yunys Pérez-Betancourt. - São Paulo, 2022.
195 p.

Tese (doutorado) - Instituto de Química da Universidade de São Paulo. Departamento de Bioquímica.
Orientador: Carmona-Ribeiro, Ana Maria

1. Vaccines. 2. Vaccine adjuvants. 3. Cationic polymers. 4. Cationic Lipids. 5. Nanoparticles. I. T. II. Carmona-Ribeiro, Ana Maria , orientador.

Acknowledgements

I would love to thank many people and institutions that were vital to my work developed in Brazil.

I would like to thank Conselho Nacional de Desenvolvimento Científico y Tecnológico for a Ph.D. fellowship (CNPq 140091/2019-0).

Special thanks to Prof. Ana Maria Carmona-Ribeiro for accepting me in her laboratory, guiding my work and the experience and knowledge sharing with me.

Thanks to the Biocoloids group for receiving and helping me.

I am very grateful to Prof. Eliana Faquim-Mauro and her team for the support and granted resources for developing this thesis work.

Thank you, Bianca, for always being there to help me solve my troubles and help me with the experiments.

To Ramón and Yusvelis, my roommates and friends, the light of my blackouts using software and computers.

To my friend Gonzalo, his emotional support was vital to triumph in this task, thank you a lot.

...

Abstract

Pérez-Betancourt, Y. **Cationic and biocompatible polymeric nanoparticles: preparation, characterization, and immunoadjuvant activity**. 2022. 198 p. PhD Thesis. Graduate Program in Biochemistry. Instituto de Química, Universidade de São Paulo, São Paulo.

Adjuvants activate innate immunity by diverse mechanisms simulating the activity of danger signals present in entire pathogens but absent in purified antigens used in vaccines. Cationic nanoparticles (NPs) are promising adjuvants as they may show high colloidal stability, they adsorb oppositely charged antigens, and they increase antigens uptake by antigen-presenting cells (APC). The high toxicity displayed by isolated cationic lipids or polymers has hampered their use in vaccines. In this work, the toxicity of cationic materials is overcome by combining them with biocompatible polymers. Herein is described the preparation, characterization, toxicity, and immunoadjuvant activity of three cationic NPs, poly(diallyldimethylammchloride)/ovalbumin (PDDA/OVA), poly(methyl methacrylate)/dimethyldioctadecylammonium bromide/PDDA (PMMA/DODAB/PDDA), and PMMA/DODAB. NPs of PDDA/OVA were prepared by mixing PDDA and OVA; NPs of PMMA/DODAB/PDDA and PMMA/DODAB NPs were synthesized by emulsion polymerization of methyl methacrylate (MMA) in the presence of cationic components. Dispersion of NPs had their physical characteristics (mean hydrodynamic diameter (Dz), polydispersity (P), mean zeta-potential (ζ), and conductance (G)) determined by dynamic light scattering (DSL), turbidimetry, and scanning electron microscopy (SEM). The content of

PMMA, PDDA, and DODAB in NPs also was characterized. PDDA, OVA, PDDA/OVA, PMMA/DODAB/PDDA, PMMA/DODAB, DODAB large vesicles (DODAB-LV), and DODAB bilayer fragment (DODAB-BF) toxicity was evaluated measuring cell viability against fibroblast and macrophages. Immunoadjuvant activity was assessed by determining antibody production (IgG1, IgG2a), delayed-type hypersensitivity reaction (DTH), and cytokines profile. PDDA/OVA (0.01/0.1 mg/mL) NPs displayed Dz=170±4 nm, ζ=+30±2 mV, and P=0.11±0.01. Free PDDA exhibited dose-dependent toxicity exerted by disrupting fibroblast membranes. PDDA/OVA NPs elicited a T helper 2 (Th2) immune response represented by high IgG1 production and DTH similar to $Al(OH)_3$/OVA. On the other hand, PMMA/DODAB/PDDA NPs exhibited Dz=217±1 nm, ζ=+73±1 mV, and P=0.12±0.01. After 24h incubation, PMMA/DODAB/PDDA NPs at 0.05 mg/mL (used in mice immunization) were no toxic against fibroblast or macrophages. PMMA/DODAB/PDDA NPs elicited a dual Th1/Th2 immune response, IgG1 titers were four times higher than the titers quantified using $Al(OH)_3$ as the adjuvant. DTH for PMMA/DODAB/PDDA NPs was significantly higher than the those registered for OVA or Al(OH)3/OVA. Th1/Th2 dual response for PMMA/DODAB/PDDA was confirmed by cytokines profile showing higher production of IFN-γ, IL-4, IL-2, and IL-10 than controls. NPs of PMMA/DODAB displayed Dz=80±1 nm, ζ=+52±3 mV, and P=0.07±0.01. PMMA/DODAB NPs were less toxic than DODAB-BF and DODAB-LV, both against fibroblast and macrophages, at the concentration used for immunizations. The immune response generated by PMMA/DODAB NPs was dual Th1/Th2, IgG1 titers were comparable to those elicited by Al(OH)3, IgG2a titers, as well as DTH, were significantly higher than the ones produced by OVA or $Al(OH)_3$/OVA. Th1/Th2 dual response confirmation was attained by determining cytokines production, PMMA/DODAB

NPs generated both Th1 (IL-2, IFN-γ) and Th2 (IL-4) cytokines. In conslusion, obtained NPs were biocompatible, nanosized, showed high ζ and narrow particle size distribution. Cationic materials' immobilization decreases their toxicity in vitro. NPs enhanced the immune response as compared with OVA and $Al(OH)_3$/OVA. Bearing-PDDA NPs had a bias toward a Th2 type response with high titers of IgG1, while PMMA/DODAB NPs exhibited a dual Th1/Th2 response.

Keywords: vaccines, vaccine adjuvants, cationic polymers, cationic lipids, nanoparticles, antigen carriers, nanoparticles/protein and polymer/protein interaction.

Resumo

Pérez-Betancourt, Y. **Nanopartículas poliméricas catiônicas e biocompatíveis: preparação, caracterização e atividade imunoadjuvante**. 2022. 198 p. Tese de Doutorado. Programa de Pós-Graduação em Bioquímica. Instituto de Química, Universidade de São Paulo, São Paulo.

Os adjuvantes ativam a imunidade inata por diversos mecanismos que simulam a atividade dos sinais de perigo presentes em patógenos inteiros, mas ausentes em antígenos purificados. Nanopartículas (NPs) catiônicas são adjuvantes promissores, pois podem apresentar alta estabilidade coloidal, adsorver antígenos de carga oposta e aumentar a captação de antígenos pelas células apresentadoras de antígeno (APC). A alta toxicidade apresentada por lipídios ou polímeros catiônicos isolados tem dificultado seu uso em vacinas. Neste trabalho, a toxicidade de materiais catiônicos é superada combinando-os com polímeros biocompatíveis. É descrita a preparação, caracterização, toxicidade e atividade imunoadjuvante de três NPs catiônicas, cloreto de poli (dialildimetilamônio)/ovalbumina (PDDA/OVA), poli (metacrilato de metila)/brometo de dimetildioctadecilamônio/PDDA (PMMA/DODAB/PDMA) e PMMA/DODAB. NPs de PDDA/OVA foram preparadas misturando PDDA e OVA; NPs de PMMA/DODAB/PDDA e PMMA/DODAB foram sintetizados por polimerização em emulsão de metacrilato de metila (MMA) na presença dos componentes catiônicos. As dispersões de NPs tiveram suas características físicas (diâmetro hidrodinâmico médio (Dz), polidispersidade (P), potencial-zeta (ζ) e condutância (G)) determinadas por espalhamento de luz dinâmico (DSL), turbidimetria e microscopia

eletrônica de varredura (MEV). O conteúdo de PMMA, PDDA e DODAB em NPs também foi caracterizado. A toxicidade de PDDA, OVA, PDDA/OVA, PMMA/DODAB/PDDA, PMMA/DODAB, vesículas grandes de DODAB (DODAB-LV) e fragmento de bicamada de DODAB (DODAB-BF) foi avaliada medindo a viabilidade contra fibroblastos e macrófagos. A atividade imunoadjuvante foi avaliada pela determinação da produção de anticorpos (IgG1, IgG2a), reação de hipersensibilidade do tipo retardado (DTH) e perfil de citocinas. NPs de PDDA/OVA (0,01/0,1mg/mL) mostraram Dz=170±4nm, ζ=+30±2mV e P=0,11±0,01. PDDA livre exibiu toxicidade dependente da dose exercida pela ruptura das membranas dos fibroblastos. NPs de PDDA/OVA desencadearam uma resposta imune T helper-2 (Th2) representada por alta produção de IgG1 e DTH semelhante a $Al(OH)_3$/OVA. NPs de PMMA/DODAB/PDDA exibiram Dz=217±1nm, ζ=+73±1mV e P=0,12±0,01. Após 24h de incubação, NPs de PMMA/DODAB/PDDA a 0,05mg/mL (usados na imunização) não foram tóxicas contra fibroblastos ou macrófagos. NPs de PMMA/DODAB/PDDA desencadearam uma resposta imune dual Th1/Th2, títulos de IgG1 foram quatro vezes maiores que os títulos quantificados usando $Al(OH)_3$ como adjuvante. DTH para as NPs de PMMA/DODAB/PDDA foi significativamente maior que aqueles registrados para OVA ou $Al(OH)_3$/OVA. A resposta dual Th1/Th2 para PMMA/DODAB/PDDA foi confirmada pelo perfil de citocinas mostrando maior produção de IFN-γ, IL-4, IL-2 e IL-10 que os controles. NPs de PMMA/DODAB exibiram Dz=80±1nm, ζ=+52±3mV e P=0,07±0,01 e foram menos tóxicas do que DODAB-BF e DODAB-LV, tanto contra fibroblastos quanto macrófagos. A resposta imune gerada por NPs de PMMA/DODAB foi dual Th1/Th2, títulos de IgG1 foram comparáveis aos eliciados por $Al(OH)_3$, títulos de IgG2a, bem como DTH, foram significativamente maiores do que os produzidos por OVA ou $Al(OH)_3$/OVA. A confirmação

da resposta Th1/Th2 foi obtida através da determinação da produção de citocinas, NPs de PMMA/DODAB geraram citocinas Th1 (IL-2, IFN-γ) e Th2 (IL-4). Em conclusão, as NPs obtidas foram biocompatíveis, nanométricas, apresentaram ζ altos e distribuição de tamanho de partícula estreita. A imobilização de materiais catiônicos diminui sua toxicidade in vitro. NPs aumentaram a resposta imune comparado OVA e Al(OH) $_3$/OVA. NPs contendo PDDA induziram uma resposta Th2 com altos títulos de IgG1, enquanto NPs de PMMA/DODAB exibiram uma resposta dual Th1/Th2.

Palavras chaves: vacinas, adjuvantes para vacinas, polímeros catiônicos, lipídios catiônicos, nanopartículas, carreadores de antígenos, interação nanopartícula/proteína e polímero/proteína.

List of Figures

1.1 General mechanism of action of adjuvants. B lymphocytes (blue), antigen presenting cells (brown) and T lymphocytes (pink). Reproduced from (SHAKYA; NANDAKUMAR, 2013). 23

1.2 Chemical structure of poly(diallyldimethylammonium chloride) (PDDA). 29

1.3 Schematic representation of DODAB large vesicles (DODAB LV), DODAB bilayer fragments (DODAB BF), and chemical structure of DODAB. 34

1.4 Schematic illustration of the synthesis of PMMA/DODAB and PMMA/CTAB nanoparticles by emulsion polymerization using azobisisobutyronitrile (AIBN) as initiator. DODAB was used as bilayer fragment (DODAB BF), reproduced from (MATHIAZZI; CARMONA-RIBEIRO, 2020). 36

1.5 Chemical structures of methyl methacrylate (MMA) and poly(methyl methacrylate) (PMMA). 37

1.6 Scanning electron microscopy and schematic representation of PMMA/PDDA nanoparticles. Reproduced from (SANCHES et al., 2015). 38

Table of Contents

ACKNOWLEDGEMENTS 5

ABSTRACT 8

RESUMO 11

FIGURES LIST 12

1 INTRODUCTION 15

1.1 General aspects of vaccines and the immune system 15

1.1.1 Overview of immune responses 15

1.1.2 Vaccines, general aspects 18

1.2 Adjuvants 21

1.2.1 General mechanisms of action of adjuvants 21

1.2.2 Nanostructures as vaccine adjuvants 24

1.2.3 Cationic adjuvants 27

1.2.3.1 Interaction of cationic polymers with proteins 27

1.2.3.2 Cationic polymers as adjuvants 29

1.2.3.3 Cationic lipids and surfactants as adjuvants 32

1.2.3.4 Hybrid lipid/polymer cationic nanoparticles as adjuvants 34

1.2.3.5 Cationic nanostructure for vaccines design 38

2 OBJECTIVES 86

2.1 General objective 86

2.2 Specific objectives 86

3 MICROBICIDAL DISPERSIONS AND COATINGS FROM HYBRID NANOPARTICLES OF POLY (METHYL METHACRYLATE), POLY (DIALLYL DIMETHYL AMMONIUM) CHLORIDE, LIPIDS, AND SURFACTANTS 88

4 SIMPLE NANOPARTICLES FROM THE ASSEMBLY OF CATIONIC POLYMER AND ANTIGEN AS IMMUNOADJUVANTS 110

5 BIOCOMPATIBLE LIPID POLYMER CATIONIC NANOPARTICLES FOR ANTIGEN PRESENTATION 127

6 CATIONIC BIOCOMPATIBLE POLYMER/LIPID NANOPARTICLES AS IMMUNOADJUVANTS 145

7 CATIONIC NANOSTRUCTURES AS ADJUVANTS FOR VACCINES 163

8 CONCLUSIONS 181

9 PERSPECTIVES 183

BIBLIOGRAPHY 184

1 Introduction

1.1 General aspects of vaccines and the immune system

1.1.1 Overview of immune responses

Immune responses are categorized into innate and adaptive immunity; adaptive immunity is classified into humoral and cellular immunity. The function of humoral immunity is to eradicate extracellular pathogens present in blood or other biological fluids; antibodies produced by B lymphocytes are the main effector molecules in this type of response. On the other hand, cellular immunity is responsible for the elimination of intracellular pathogens and cancer cells; this type of immunity is mediated by CD8+ T lymphocytes. T and B lymphocytes express T cell receptors (TCR) and B cell receptors (BCR), respectively, and recognize a large variety of antigens (ABBAS; LICHTMAN; PILLAI, 2018).

When a pathogen invades the organism, T and B lymphocytes are activated through their corresponding receptors. At the same time, memory T and B lymphocytes are generated, allowing the host to respond more speedily and specifically, when the same pathogen invades the organism for a second time; this phenomenon constitutes the basis of vaccination. Vaccination resembles an actual microbial infection in a highly attenuated condition, and its role is to produce memory cells against specific pathogens (ABBAS; LICHTMAN; PILLAI, 2018; PULENDRAN; AHMED, 2011).

Innate immunity is carried out by a variety of cells, namely, leukocytes, macrophages, and dendritic cells (DCs) collectively termed phagocytes as they intake and kill pathogens (LIM; GRINSTEIN; ROTH, 2017). Innate immunity does not afford long-term immunity;

furthermore, it has more specificity than previously believed and is highly developed to distinguish foreign pathogens (ABBAS; LICHTMAN; PILLAI, 2018; AKIRA, 2011). This discrimination depends on a family of evolutionarily conserved receptors termed Toll Like Receptors (TLRs) (JANSSENS; BEYAERT, 2003; HALLMAN; RäMET; EZEKOWITZ, 2001). It is relevant to highlight that the activation of innate immunity is a requirement for inducing adaptive immunity (ABBAS; LICHTMAN; PILLAI, 2018; MEDZHITOV; JANEWAY, 2000).

According to the original theory of the immune response, DCs intake pathogens, digest their protein into small peptides, and express the antigenic peptides on their cell surface; DCs then migrate from the infected tissue to regional lymph nodes, where they present the antigenic peptides to naïve T cells (ABBAS; LICHTMAN; PILLAI, 2018). In the most recent theory, in addition to phagocytosis and digestion of pathogens, DCs must be activated to activate T cells. In normal tissues, cells die continuously, and dead cells are removed by DCs. Although the resulting autoantigens are displayed to T cells by DCs, T cells do not become activated because DCs are not activated, resulting in anergy. For an efficient activation of T cells, DCs must be activated; in the activated state, DCs over express co-stimulatory molecules (CD40, CD80, CD86) and produce specific cytokines (ABBAS; LICHTMAN; PILLAI, 2018; PAULIS et al., 2013).

The activities of B and T lymphocytes populations define the type of immune response against infections. After recognition of a specific antigen, B cells differentiate into plasma cells and release antigen-specific antibodies. However, the development of immunological memory on re-exposure to the same antigen occurs only when B cells have received “help” from T cells; this type of response is called T-cell dependent response. CD4+ T helper (Th) cells cannot recognize protein antigen unless presented after processing by

antigen-presenting cells (APCs) activated during the innate immune response. Activated Th cells release inflammatory mediators specific for a subpopulation of Th cells (Th1, Th2, and Th17), which has downstream implications for how effectively the pathogen is removed or contained. In general, Th1 cells eradicate intracellular pathogens. Th2 cells eliminate extracellular parasites, and Th17 cells eliminate extracellular bacteria and fungi. Activated CD8+ cytotoxic T lymphocytes kill cells directly or releasing of cytotoxins (ABBAS; LICHTMAN; PILLAI, 2018; CHAPLIN, 2010).

Activation of T lymphocytes depends on DCs, capable of processing and presenting antigenic peptides to T lymphocytes through a protein complex known as Major Histocompatibility Complex (MHC). The differentiation of Th lymphocytes into one specific phenotype (for exampe Th1, Th2, or Th17) is mediated by cytokines that regulate the immune response. For example, the interleukins IL-12 and IFN-γ are related to the induction of a Th1 pattern, while IL-4 and IL-5 are related to the induction of the Th2 pattern (ABBAS; LICHTMAN; PILLAI, 2018).

APCs, like DCs, play a paramount intermediary role between innate and adaptive responses and are critical in determining the direction of the adaptive immune response (ABBAS; LICHTMAN; PILLAI, 2018; STEINMAN; HEMMI, 2006). Therefore, the ideal vaccine would initiate an innate immune response capable of directing the adaptive immune response towards the efficient inactivation and removal of specific pathogens, followed by the development of immune memory. The inadequate ability of highly purified vaccines to induce protective immunity is connected to their failure to produce APCs maturation (PASQUALE et al., 2015; COFFMAN; SHER; SEDER, 2010).

1.1.2 Vaccines, general aspects

Vaccines were introduced by Edward Jenner in 1796 (RIEDEL, 2005). Vaccination is the process of mimicking the infection in the body, leading to the activation of the immune system to generate a potent immune response (PULENDRAN; AHMED, 2011; CHUMAKOV et al., 2021). The basis of vaccination is the immunological memory; it is the ability of the immune system to quickly and specifically recognize an antigen to which it was previously exposed (POLLARD; BIJKER, 2021; SALLUSTO et al., 2010).

Since their discovery, vaccines have been one of the most foremost advances in medicine. Through vaccines, it has been possible to reduce or eradicate the incidence of various infectious diseases; they are biological preparations that provide active adaptive immunity to a specific infectious disease (RODRIGUES; PLOTKIN, 2020). A vaccine usually contains an agent like the microorganism that causes the disease and is obtained, usually, from weakened or dead forms of the pathogen, its toxins, or one of its antigenic proteins (POLLARD; BIJKER, 2021). The vaccine stimulates the immune system to recognize the infectious agent as a threat and destroy it; also, recognize and destroy any class of microorganisms associated with this agent that it may encounter in the future (POLLARD; BIJKER, 2021; PULENDRAN; AHMED, 2011). Vaccines can be prophylactic, preventing the effects of a future natural infection with a specific pathogen; also, vaccines can be therapeutic, exerting their effect on an ongoing illness such as cancer (CHEN; YAN; HUANG, 2008; BRINKMAN et al., 2004; ESFAHANI et al., 2020).

Live attenuated vaccines contain debilitated variants of the pathogen, virus, or bacteria. These attenuated pathogens can replicate in the host, resulting in persisting immunity, these vaccines are highly effective; however, there are concerns regarding their capacity of

reverting to its virulent form (PULENDRAN; AHMED, 2011; MINOR, 2015). For example, the Venezuelan equine encephalitis vaccine needs to undergo only two-point mutations to return to virulent form, limiting its usefulness to vaccinating individuals exposed to high risk of infection (PASQUALE et al., 2015; STROMBERG et al., 2020).

Inactivated vaccines are prepared from a disease-causing microorganism; pathogens are chemical or physically treated to kill them (SANDERS; KOLDIJK; SCHUITEMAKER, 2015; CHUA; SEKIYA; JACKSON, 2018). These treatments make pathogens unable to replicate and eliminate their infectious potency (CHUA; SEKIYA; JACKSON, 2018). The disadvantage is that must be given additional injections to get a strong immune response and long-term immunity (PASQUALE et al., 2015). Inactivated vaccines do not replicate; however, safety is still a concern (SANDERS; KOLDIJK; SCHUITEMAKER, 2015; CHUA; SEKIYA; JACKSON, 2018). In the 1960s, a formalin-inactivated vaccine against the respiratory syncytial virus (RSV) killed an infant in a clinical trial; this tragedy has damaged the field of RSV vaccine, and no vaccine candidates had entered late-stage clinical trials so far (BLANCO et al., 2010).

Another class of commercially available vaccine is the inactivated toxoid; these vaccines are based on the toxin produced by certain types of bacteria, such as *Clostridium tetani* and *Corynebacterium diphtheriae* (WEINBERGER, 2017). These traditional vaccines are still in use because they are highly potent. However, this approach cannot be used in numerous vaccines because of safety issues, and some pathogens cannot be cultured in industrial conditions (FINDLOW; KNUF, 2019).

The limitations above described led to the introduction of subunit and recombinant protein vaccines (PASQUALE et al., 2015). Vaccines obtained from purified antigens such as

recombinant proteins or proteins isolated from pathogens improved the vaccine's development, as they demonstrated to be safe, without the ability to revert to virulent forms; besides, this type of vaccines are easier to manufacture and characterize (PASQUALE et al., 2015; KARCH; BURKHARD, 2016). However, purified antigens are poor immunogens due to the lack of danger signals that are molecules present in entire pathogens. Danger signals activate innate immunity through their receptors; examples of these molecules are lipopolysaccharide (LPS) and double-stranded RNA (GALLUCCI; MATZINGER, 2001; HENGGE et al., 2001; GARG; AGOSTINIS, 2017). In general, danger signals are also known as pathogen-associated molecular patterns (PAMPs). Then, adjuvants were introduced into vaccines formuation to increase the immunogenicity of these weaker antigens and help to improve the overall potency of low-immunogenic subunit vaccines; the general function of adjuvants is to activate cells of innate immunity (PASQUALE et al., 2015; COFFMAN; SHER; SEDER, 2010).

In DNA vaccines, the idea is that genes codifying for microbial antigens are introduced into cells to produce antigens (GHAFFARIFAR, 2018). The adaptive immune response generated against a DNA vaccine depends on the type of cell that is transfected by the DNA; it is thought that the antigen-presenting cells initiate a CD8+ T cell response (DUPUIS et al., 2000; DENIS-MIZE et al., 2003). In addition, activated CD8+ T lymphocytes can kill cells that present the antigen on MHC class I molecules, decreasing the expression of the DNA vaccine (CUI, 2005; HASSON; AL-BUSAIDI; SALLAM, 2015). In this type of vaccine, plasmids must be delivered into the cell nucleus to produce mRNA. The fact constitutes a significant limitation, demanding special adjuvants able to meet this condition (SINGH et al., 2000; KHAN, 2013).

RNA vaccines are a type of vaccine that uses a copy of mRNA to produce an immune response (PARDI et al., 2018). The vaccine transfects a synthetic mRNA molecule into immune cells, such as dendritic cells; once in cells, mRNA serves as a template for the synthesis of antigenic proteins; these proteins stimulate an adaptive immune response (ZHANG et al., 2019a; SCHLAKE et al., 2012). Normally, mRNA is inoculated using cationic nanoparticles obtained from cationic lipids that protect the RNA strands from degradation and drive to an increased internalization in the antigen-presenting cells (CARMONA-RIBEIRO; PéREZ-BETANCOURT, 2020; SAHIN; KARIKó; TüRECI, 2014; FAN et al., 2018). The advantages of RNA vaccines over subunit vaccines are their easy design and superior production speed, lower production cost, and the induction of cellular (Th1) and humoral (Th2) immunity (ZHANG et al., 2019a). A disadvantage of mRNA vaccines is that they require storage temperatures of -80 ℃ (NANOMEDICINE. . . , 2020).

1.2 Adjuvants

1.2.1 General mechanisms of action of adjuvants

Adjuvants are immunomodulatory molecules used with antigens in vaccine formulations to elicit a strong immune responses. The classical adjuvant used in human vaccines is based on aluminum salts, such as aluminum hydroxide, aluminum phosphate, and potassium aluminum sulfate (AWATE; BABIUK; MUTWIRI, 2013; MARRACK; MCKEE; MUNKS, 2009). Adjuvants have several potential benefits, such as reducing the frequency of vaccination, diminishing the dose of antigen per vaccine, raising the quality of the immune response, promoting immunity, and improving the stability of the final vaccine formulation (PASQUALE et al., 2015; AWATE; BABIUK; MUTWIRI, 2013; WANG; XU, 2020). The conventional

role of adjuvants is to enhance the immune response, represented as increasing antibody titer and blocking infections. However, a more current challenge is to generate adjuvants that can guide the response towards a more effective adaptive immune response, capable of eliminating specific pathogens (PASHINE; VALIANTE; ULMER, 2005; PASQUALE et al., 2015; POLLARD; BIJKER, 2021). In addition to increasing the immune response, adjuvants are extremely relevant as they intensify seroconversion in population groups with impaired immune systems (COFFMAN; SHER; SEDER, 2010; REED; ORR; FOX, 2013).

A general classification of adjuvants used clinical and experimentally is as immunomodulatory agents or as depots or passive vehicles (COFFMAN; SHER; SEDER, 2010; APOSTÓLICO et al., 2016). Immunomodulatory adjuvants are agonists of pattern recognition receptors (PRRs) associated with pathogens or damaged self-cells (SCHIJNS et al., 2020). For many adjuvants, the exact mechanism by which they potentiate the immune response is unknown. It is conjectured that adjuvants do not act directly on the adaptive immunity but exert their action on the innate immunity (COFFMAN; SHER; SEDER, 2010). It has been possible to reveal some fundamental mechanisms by which adjuvants act. Six well-studied mechanisms stand out, namely:

(1) sustained release of antigen at the injection site (depot effect) (AWATE; BABIUK; MUTWIRI, 2013),

(2) increasing the production of cytokines and chemokines (AWATE; BABIUK; MUTWIRI, 2013; REED; ORR; FOX, 2013),

(3) cell recruitment at the injection site (AWATE; BABIUK; MUTWIRI, 2013; AALST et al., 2017),

(4) increasing antigen uptake and presentation to antigen-presenting cells (CARMONA-RIBEIRO; PéREZ-BETANCOURT, 2020),

(5) activation and maturation of antigen-presenting cells (increased expression of MHC class II and expression of co-stimulatory molecules) and migration to draining lymph nodes (AWATE; BABIUK; MUTWIRI, 2013),

(6) activation of inflammasomes (IVANOV et al., 2020).

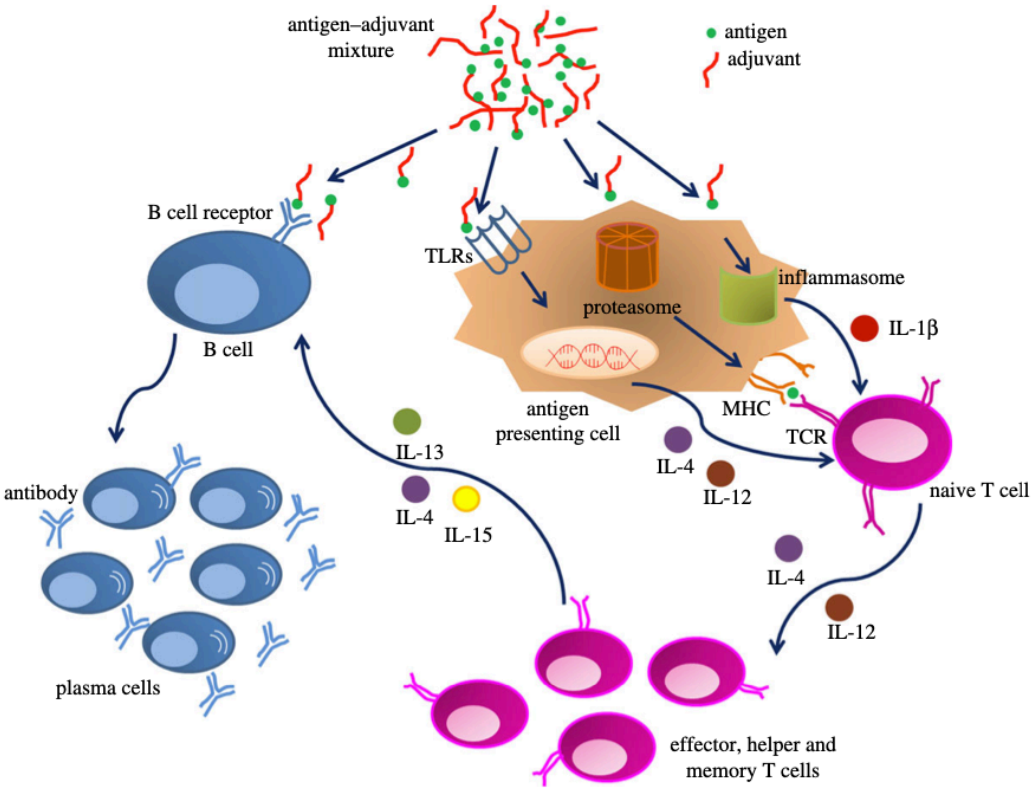


Figure 1.1: General mechanism of action of adjuvants. B lymphocytes (blue), antigen presenting cells (brown) and T lymphocytes (pink). Reproduced from (SHAKYA; NANDAKUMAR, 2013).

Figure 1.1 shows the general mechanism through which adjuvants act; it illustrates the stimulation of the humoral response (antibody production) and the cellular response (production of effector T cells, T helper cells, and memory T lymphocytes). The adjuvant forms a complex with the antigen, promoting the entry of the antigen to the antigen-presenting

cell. The antigen/adjuvant complexes interact with TLRs and stimulate T lymphocytes and cellular immunity. The complex activates B lymphocytes through the BCR, eliciting antibody production (SHAKYA; NANDAKUMAR, 2013). As mentioned before, inflammasomes (green structure in **Figure 1.1**) are receptors of damage associated molecular patterns (DAMPs) and are they activated by adjuvants; for instance, aluminum salts activate NLPR3 inflammasome (IVANOV et al., 2020). Proteasomes (orange structure in **Figure 1.1**) are protein complexes that process cytosolic antigenic protein before being presented in MHC class I (AWATE; BABIUK; MUTWIRI, 2013).

Particulate adjuvants, namely, aluminum salts, emulsions, liposomes, and particles (micro and nano), are considered the first generation of vaccine adjuvants (KURODA; COBAN; ISHII, 2013; SAROJA; LAKSHMI; BHASKARAN, 2011). This first generation can also be considered antigen-release systems that promote antigen uptake (PASQUALE et al., 2015; AWATE; BABIUK; MUTWIRI, 2013). The second generation of vaccine adjuvants can be described as combinational adjuvants, as they are composed of immune enhancers combined with the first generation of vaccine adjuvants (MUTWIRI et al., 2011). Aluminum salts, liposomal adjuvants, emulsions, or nanoparticles increase antigen presentation at the injection site, leading to locally high concentrations of antigen. Therefore, uptake by antigen-presenting cells such as dendritic cells, macrophages, and B cells is improved (WANG; XU, 2020; TIZARD, 2021).

1.2.2 Nanostructures as vaccine adjuvants

The application of nanotechnology in the field of medicine is broad as nanotechnology offers the possibility to design nanoparticles (diameter less than 1000 nm) varying in composition,

size, shape, and surface properties (KHAN; SAEED; KHAN, 2019). The nanoparticles size allows entry into the cells through the endocytosis mechanism, particularly pinocytosis (BEHZADI et al., 2017; ZHAO et al., 2014). Nanoparticles are implemented as either delivery systems to enhance the antigen processing and/or immunostimulants adjuvant to activate or enhance the immune response (ZHAO et al., 2014).

As delivery systems, nanoparticles can deliver antigen to the cells of the immune system; antigens and nanoparticles complexes are taken up by the immune cell, or act as a transient delivery system protecting the antigen and then releasing it at the target location. For nanoparticles to act as a delivery system, association of antigen and nanoparticle is typically necessary. For immune potentiator approaches, nanoparticles activate certain immune pathways, which might then enhance antigen processing and improve immunogenicity (GARG; DEWANGAN, 2020). The size of nanoparticles allows them to cross biological barriers easily; this fact makes nanoparticles suitable to deliver any class of drug and antigens (JIA et al., 2020; BLANCO; SHEN; FERRARI, 2015).

Using nanoparticles in vaccines offers two main advantages. Nanoparticles act as adjuvants and enhance the antigenicity of conjugated or adsorbed antigens and can act as an antigen themselves; in this way, they can mimic features of pathogens such as viruses (PATI; SHEVTSOV; SONAWANE, 2018; ZHU; WANG; NIE, 2014). Engineering nanoparticle surfaces to secure antigens attachment is a common practice; attachment of antigens has been reached through simple physical adsorption or more complex methods, such as chemical conjugation or encapsulation (ZHAO et al., 2014; PATRA et al., 2018). Antigens adsorption onto a nanoparticle relies on ionic or hydrophobic interaction mostly; therefore, the interaction between nanoparticle and antigen is relatively weak, which may lead to rapid

disassociation of antigen and nanoparticle in vivo (ZHAO et al., 2014; FOX et al., 2013).

Nanoparticles' size defines the cellular uptake mechanism such as endocytosis, phagocytosis, and micropinocytosis. These mechanisms are responsible for the uptake of a myriad of particle sizes and critical parameters that affect immunogenicity by promoting and inducing appropriate responses (BEHZADI et al., 2017; MANOLOVA et al., 2008; CARMONA-RIBEIRO, 2014). Nanoparticles traffic to the draining lymph nodes in a size-dependent manner; large particles (500–2000 nm) are associated with DCs at the injection site, the small ones (20–200 nm) and virus-like particles (VLP) (around 30 nm) are found in lymph-nodes-resident DCs and macrophages, suggesting free drainage of these particles to the lymph nodes; in vivo small but not large particles circulate freely to the lymph nodes, and it has been demonstrated that DCs are strictly required for transport of large particles from the injection site to the LN (MANOLOVA et al., 2008). Besides size, the charge of the surface of nanoparticles influences the uptake by antigen-presenting cells. Cationic nanoparticles are taken up by cells much more readily than those with negative surface charge, due to the anionic nature of cell membranes (CARMONA-RIBEIRO; PéREZ-BETANCOURT, 2020; HARUSH-FRENKEL et al., 2008). The higher internalization of cationic nanoparticles leads to important cell toxicity (HARUSH-FRENKEL et al., 2008; FRöHLICH, 2012). It has been reported that cationic nanoparticles can cross the cytoplasmatic membrane freely, a process known as direct translocation (LIN; ALEXANDER-KATZ, 2013; LI; MALMSTADT, 2013).

Nanoparticles-based vaccines (nanovaccines) are very promising because of the great benefits offered by being accurately captured by the antigen-presenting cells. They induce both rapid and durable humoral and cellular immunity, up-regulating genes and enhancing

antigenic processing. Nanoparticles can be delivered through multiple routes, maintain long-lived antigen stability and functionality, and enable antigen and adjuvant specific transport to antigen-presenting cells (mainly dendritic cells able to control immune tolerance and immunity). Particulate vaccines in vivo activate the NLRP3 (NOD-like receptor family) causing an influx of eosinophils and an up-regulation of MHC class II molecules expression and antigen-presentation cell activity (AWATE; BABIUK; MUTWIRI, 2013; PULENDRAN; ARUNACHALAM; O'HAGAN, 2021). After activation, the cytoplasmic NLRP3 protein promotes the production of pro-inflammatory cytokines such as IL-1β and IL-18 (BARON et al., 2015; YAZDI et al., 2010).

1.2.3 Cationic adjuvants

1.2.3.1 Interaction of cationic polymers with proteins

Cationic polymers are natural or synthetic compounds bearing positive charges or incorporating cationic entities into their structure. Cationic polymers by their property of permeabilizing cytoplasmic membranes are often used as delivery systems for therapeutic DNAs and RNAs; in addition, cationic polymers are also applied as protein delivery systems (SPROUSE; REINEKE; DAVIS, 2016; CARMONA-RIBEIRO; CARRASCO, 2013). The interaction between proteins and polyelectrolytes (PE) leads to the formation of complexes and coacervates/precipitates under specific conditions; the process is driven by non-specific and non-covalent interactions, mainly electrostatic interactions (KIZILAY; KAYITMAZER; DUBIN, 2011; WANG et al., 2019). The structure of the protein-PE complexes could be adjusted by modulating protein-PE interactions to meet the needs of different applications, such as biosensor development, protein separation, drug, and vaccine delivery, and tissue

engineering (WANG et al., 2019).

Two major theories have been proposed to explain protein-PE interactions, they are: the charge regulation theory and the charge anisotropy theory (WANG et al., 2019; KAYITMAZER et al., 2013). The charge regulation theory states that interaction between PEs and proteins is confined to a specific space (WANG et al., 2019; VALETTI; BRASSESCO; PICó, 2016). The presence of PEs could attract their corresponding protein counterion by Coulombic forces such that the microenvironment, including the local pH and ion distribution of the protein, is modified by the electrical field of the PE (WANG et al., 2019). Therefore, the protonation states of acidic or basic residues of proteins could be altered, leading to a different charge profile and electrostatic properties as compared to their normal pattern (WANG et al., 2019; GAO; HOLKAR; SRIVASTAVA, 2019).

Charge anisotropy theory centers on the electrostatic heterogeneity of proteins and not on the external influence exerted by PEs on their structures. When the protein and PE complexation occurs; the charge patches with equal and opposite charges interact with the PEs generating short-range attraction and long-range repulsion effects. Using a proper quantity of salts could screen the long-range repulsive forces, preserving the short-range attraction forces, leading to maximum binding affinity at a given ionic strength (WANG et al., 2019).

PDDA is a cationic polymer with a high density of positive charges due to the presence of one quaternary nitrogen per monomer (**Figure 1.2**), this makes PDDA a highly hydrophilic polymer (WANDREY; HERNáNDEZ-BARAJAS; HUNKELER, 1999). PDDA has numerous applications such as: purifying drinking water, developing methods for protein purification, tissue engineering, coating particles for numerous purposes, including drug delivery and

DNA vaccines, as a DNA transfection agent, and encapsulating mammalian cells (WANG et al., 2019; DAUTZENBERG; HOLZAPFEL; LUKANOFF, 1993; XU et al., 2012; BALL; CARRIèRE; BARBEAU, 2011); the chemical structure of PDDA is displayed on **Figure 1.2**.

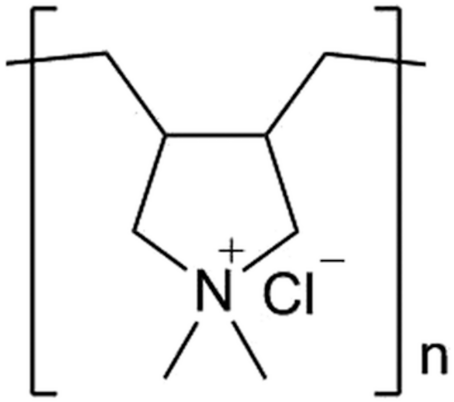


Figure 1.2: Chemical structure of poly(diallyldimethylammonium chloride) (PDDA).

1.2.3.2 Cationic polymers as adjuvants

Adjuvants' properties of polyelectrolytes have been investigated since some years ago (GALL; KNIGHT; HAMPSON, 1972). Cationic polymers, despite their cytotoxicity, constitute an important class of cationic adjuvants (FISCHER et al., 2003; MARTINEZ; KELLER; SCHLENOFF, 2011; MONNERY et al., 2017). Cationic polymers can form different supramolecular arrangements, ranging from simply complexing the polymer with the antigen (DNA, RNA, and proteins), driven by electrostatic interactions, to using polymers as a coating or particle core (SANCHES et al., 2015; ORTEGA-MUNOZ et al., 2016; WEGMANN et al., 2012). Polyelectrolytes combine simply with oppositely charged proteins and nucleic acids by electrostatic interactions (KAYITMAZER et al., 2013; WEGMANN et al., 2012; MEKA et al., 2017).

Polyethyleneimine (PEI) and chitosan are the most studied cationic polymers regarding

their adjuvant properties (WEGMANN et al., 2012; KHADEMI et al., 2018b). PEI is an organic, hydrophilic, and cationic polymer that exhibits a large density of positive charges and combines well with negatively charged molecules such as DNA, negatively charged antigens, or plasma membranes (SHEN et al., 2017). A relevant property of PEI is its ability to escape from endosomes after cell internalization, preventing the endosomal acidification. The high number of nitrogen atoms in the PEI molecule makes the polymer an excellent buffer at low pH (BENJAMINSEN et al., 2013; MENG et al., 2020). The proton sponge effect results in the influx of Cl^- ions and water, with osmotic swelling of the lysosome. After lysosomes swelling and rupture, antigens remain free in the cytoplasm, leading to the promotion of Th1 immune response (BENJAMINSEN et al., 2013).

PEI as an adjuvant protects antigens from enzymatic degradation (DéMOULINS et al., 2016), activates inflammasomes, up-regulates the transcription factor called interferon-3 regulatory factor (Irf-3) (WEGMANN et al., 2012), and other genes related to the immune response (REGNSTROM et al., 2003). The PEI-induced Th1 response is due to the polymer promoting the escape of the PEI/antigen complex from endosomes, allowing antigens to be processed through the proteasome and the resulting peptides presented through the MHC class I (CHEN et al., 2011). PEI promotes the release of double-stranded DNA by host cells, triggering Irf-3 dependent signaling (WEGMANN et al., 2012). Irf-3 is a transcription factor related to the activation of the innate response through the synthesis of type I interferon (DHANWANI; TAKAHASHI; SHARMA, 2018). In addition to Irf-3, PEI activates NLRP3 inflammasomes, a critical component of the innate immune system, which directs the immune response to a Th2 type (WEGMANN et al., 2012; SHEPPARD et al., 2014).

Several examples reported in the literature depict the ability of PEI to enhance the immune response. Biodegradable polymeric particles obtained from poly (lactic-co-glycolic acid) (PLGA) were functionalized with cationic surfactants, cetrimonium bromide (CTAB), lipids (DODAB), or cationic polymers, PEI or poly-L-lysine (PLL)) to improve antigen adsorption, colloidal stability, and immune response. The functionalization of particles with cationic polymers increased the adsorption of antigens, the proliferation of CD8+ and CD4+ T lymphocytes and the production of cytokines such as: TNF-α IFN-γ, IL-4 and IL-6 (SINGH et al., 2004; GU et al., 2019).

Gold nanorods functionalized with CTAB, PEI, or poly PDDA, three cationic materials, were characterized according to their physical characteristics, colloidal stability in biological fluids, ability to adsorb DNA plasmid, capacity to transfect cells, and type of immune response induced against an HIV DNA vaccine. The nanostructures functionalized with PDDA were the most stable; moreover, PDDA-functionalized nanorods showed the highest capacity to adsorb DNA and facilitated the expression of green fluorescent protein (GFP) after cells transfection with the corresponding plasmid. Functionalization with PDDA ensured the most powerful antibody titer with a predominance of IgG1 production; in addition, PDDA-functionalized nanostructures induced proliferation of T CD8+ and T CD4+ lymphocytes (XU et al., 2012).

Poly amino acids are another important class of cationic polymers used to carry antigens in vaccine formulations (LUHRS et al., 2002). Like other cationic polymers, they combine with negatively charged molecules spontaneously (WEGMANN et al., 2012; BOHIDAR et al., 2005). Poly-L-arginine (PLAr) on the surface of microcapsules obtained by layer-by-layer or spray-drying techniques increased particle uptake by antigen-presenting cells (LUHRS

et al., 2002; DEVRIENDT et al., 2013). A promising research reported the use of PLAr to carry peptides derived from tumor antigens to obtain a synthetic antitumor vaccine. The work reported that the subcutaneous injection of a mixture of PLAr and peptides induced numerous antigen-specific T cells in the systemic circulation for more than four months. Also, the authors reported the presence of numerous antigen-loaded antigen-presenting cells in the draining lymph nodes of vaccinated animals, suggesting that PLAr is a suitable adjuvant to deliver antigens to the lymph nodes. An additional relevant result is the absence of antibodies PLAr, allowing this compound to be used for numerous booster injections (MATTNER et al., 2002).

1.2.3.3 Cationic lipids and surfactants as adjuvants

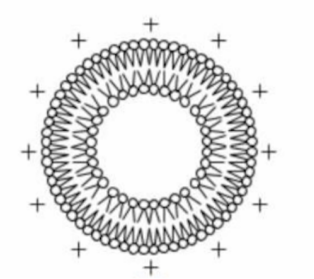
Cationic adjuvants obtained from lipids or cationic surfactants have been widely studied. Electrostatic attraction between the antigen and oppositely charged portions of the adjuvant leads to the loading of vaccines in cationic assemblies (CARMONA-RIBEIRO; PéREZ-BETANCOURT, 2020). For instance, from cationic DODAB bilayer is possible to obtain water dispersion of closed microstructures such as vesicles or open, nanosized bilayer fragments (BF); the formers are prepared by disrupting closed vesicles using a sonicator (TSURUTA et al., 1997; LINCOPAN et al., 2009; ROZENFELD et al., 2011; ROZENFELD et al., 2012). DODAB BF mixed with microorganism-derived vesicles was efficient in inducing a strong immune response against *Neisseria meningitidis* (ALMEIDA; GASPARI, 2018; SANTOS; LINCOPAN; GASPARI, 2018).

Probably, DODAB is the most investigated lipid among the synthetic cationic lipids; this molecule and its supramolecular assemblies have been studied from numerous points of

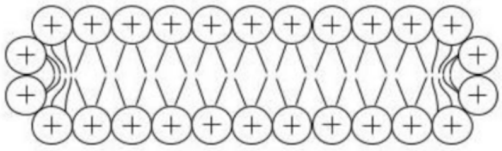
view. After the complexes adjuvant/antigen undergo endocytosis by antigen-presenting cells, the resulting peptides are displayed on MHC class I or MHC class II proteins (ROCHE; FURUTA, 2015). DODAB nanosized, cationic bilayer fragments (BF) combine with oppositely charged antigens, prompting a Th1-biased immune response (CARMONA-RIBEIRO; PéREZ-BETANCOURT, 2020; ROZENFELD et al., 2012; CARMONA-RIBEIRO, 2017a).

Also, DODAB assembles as closed vesicles or liposomes with a high capacity to activate the immune system (TSURUTA et al., 1997; ANDERLUZZI et al., 2021; KORSHOLM et al., 2007; KAUR et al., 2012; HENRIKSEN-LACEY et al., 2010). DODAB cationic liposomes do not promote de DCs maturation; alternatively, DODAB liposomes increase the antigen internalization by antigen-presenting cells (KORSHOLM et al., 2007; CARMONA-RIBEIRO, 2017b). Other investigations have revealed that the adjuvant mechanism of DODAB liposomes relies on depot effects (HENRIKSEN-LACEY et al., 2010; KAUR et al., 2012).

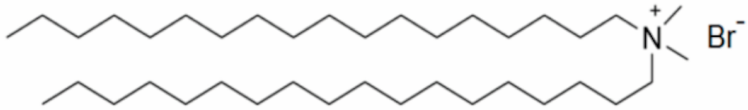
The comparison of different cationic platforms was performed to evaluate their suitability to deliver mRNA-based vaccines. All formulations contained either the non-ionizable cationic lipid 1,2-dioleoyl-3-trimethylammonium-propane (DOTAP) or DODAB were assessed according to physicochemical characteristics, in vitro transfection efficiency and efficacy as vaccine deliver. Results displayed that hybrid polymer/DOTAP nanoparticles, DOTAP liposomes and DODAB liposomes induced the highest antigen expression in vitro; polymer/DOTAP nanoparticles were the most potent in inducing humoral and cellular immunity in vivo (ANDERLUZZI et al., 2020). The structure of DODAB and schematic representations of DODAB large versicles, and bilayer fragments are shown in **Figure 1.3**.



DODAB LV



DODAB BF



DODAB

Figure 1.3: Schematic representation of DODAB large vesicles (DODAB LV), DODAB bilayer fragments (DODAB BF), and chemical structure of DODAB.

1.2.3.4 Hybrid lipid/polymer cationic nanoparticles as adjuvants

The idea of using hybrid lipid/polymers materials aims to combine lipids and polymers properties such as lipids' amphiphilic nature, the opportunity of high organizational level in the lipid-based structures, and the mechanical and resistance advantages obtainable by polymers (CARMONA-RIBEIRO; PéREZ-BETANCOURT, 2020). Coupling these materials enables overcoming significant limitations like degradation of bioactive incorporated principles, short circulation time of drugs and vaccines, and absence of controlled release (MUKHERJEE et al., 2019; DAVE et al., 2019). They have been reported various types of arrangement between lipids and polymers; the hybrid assemblies could be classified as lipid–polymer or polymer–lipid, depending on the position of each material in the structure; either the polymer or the lipid is in the inner part of the nanostructure (CARMONA-RIBEIRO;

PéREZ-BETANCOURT, 2020; NAVES et al., 2013; MATHIAZZI; CARMONA-RIBEIRO, 2020).

Lipids and polymers can assemble as hybrid materials guided by attractive, non-covalent, and weak but numerous interactions. For example, the principal forces driving bilayer deposition onto hydrophobic or hydrophilic nanoparticles or surfaces from bilayer vesicles or bilayer fragments (BF) are the electrostatic attraction, van der Waals attraction, and/or the hydrophobic effect (RIBEIRO; BRAGA; CARMONA-RIBEIRO, 2017; XAVIER; CARMONA-RIBEIRO, 2017). Lipid/polymer, or polymer/lipid nanoparticles have applications in biomolecular recognition (MOURA; CARMONA-RIBEIRO, 2006; CARMONA-RIBEIRO, 2010), drug delivery (MUKHERJEE et al., 2019; DAVE et al., 2019; CARMONA-RIBEIRO, 2020), vaccine design, and obtaining microbicidal materials (MATHIAZZI; CARMONA-RIBEIRO, 2020).

Hybrid and cationic lipid/polymer nanoparticles have been effective as an inducer of a robust immune response (KHADEMI et al., 2018a; ROSE et al., 2015; ZHANG et al., 2019b; ANDERLUZZI et al., 2020). For instance, poly lactic-co-glycolic acid (PLGA) and DODAB were combined to yield cationic nanoparticles for delivering a Mycobacterium tuberculosis nasal vaccine; PLGA/DODAB nanoparticles showed uniform size, spherical shape, and smooth surface. PLGA/DODAB nanoparticles loaded with HspX/EsxS antigen (a recombinant fused protein of M. tuberculosis) and with monophosphoryl lipid A (MPLA) increased the secretion of IFN-γ and IL-17 and enhanced IgA, IgG1, and IgG2a titers (ZHANG et al., 2019b).

In our laboratory, the good miscibility between PMMA and antimicrobial quaternary DODAB was first described (PEREIRA et al., 2008; MELO et al., 2011). Hybrid and cationic

PMMA/CTAB and PMMA/DODAB nanoparticles synthesized by emulsion polymerization of methyl methacrylate (MMA) in the presence of DODAB and CTAB, as emulsifiers, had their physical and antimicrobial properties determined. Nanoparticles were spherical and monodisperse, but the antimicrobial activity of the nanoparticles was lower than the one of free emulsifiers (DODAB or CTAB) (MATHIAZZI; CARMONA-RIBEIRO, 2020). A diagram of the process of synthesis of poly(methyl methacrylate) (PMMA)/emulsifier is depicted in **Figure 1.4**. PMMA/DODAB nanoparticles obtained by emulsion polymerization were investigated in the present work regarding their immunoadjuvant properties.

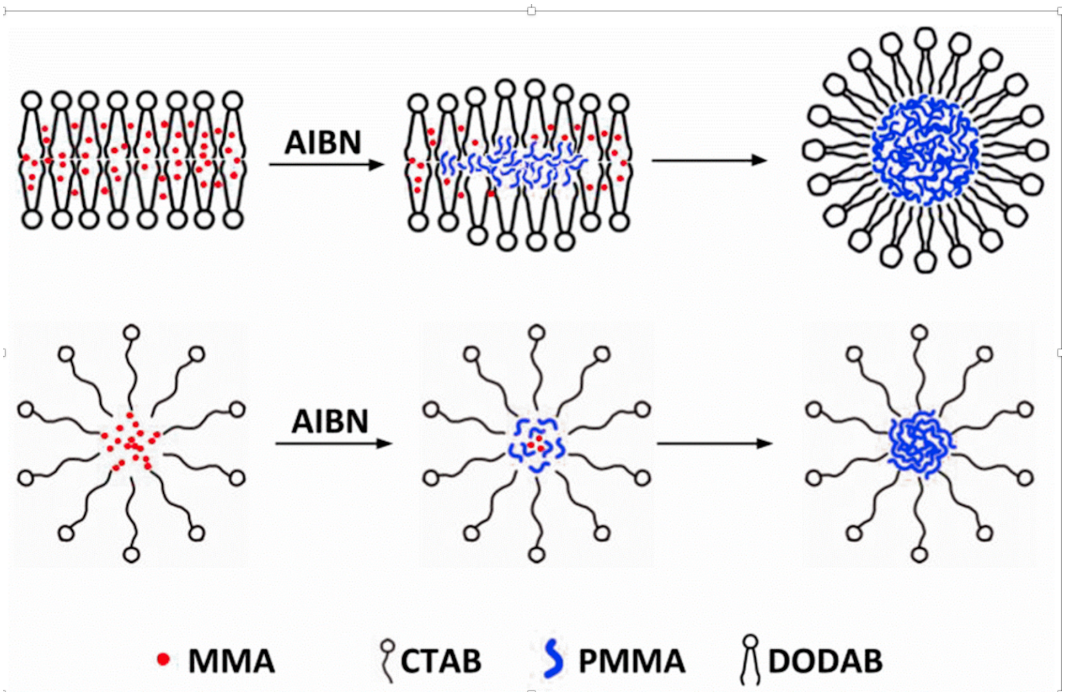


Figure 1.4: Schematic illustration of the synthesis of PMMA/DODAB and PMMA/CTAB nanoparticles by emulsion polymerization using azobisisobutyronitrile (AIBN) as initiator. DODAB was used as bilayer fragment (DODAB BF), reproduced from (MATHIAZZI; CARMONA-RIBEIRO, 2020).

PMMA is a synthetic and biocompatible polymer that displays great mechanical properties and low toxicity; moreover, PMMA shows slow degradation: Aliphatic CH_2-C- backbone of PMMA is connected to CH_3–(methyl) and CH_3–O–CO– (ester) side groups. The aliphatic

character of PMMA plays a very significant role in how this polymer behaves (RAHMAN et al., 2020; IDREES et al., 2020; HELLER et al., 2011). PMMA is acrylic polymer and belongs to the family of polymers that are formed by the polymerization of an alkyl acrylate ester; PMMA is generally synthesized from its liquid monomer, methyl methacrylate (MMA), using a radical polymerization initiator, such as benzoyl peroxide or AIBN (RAHMAN et al., 2020; GALVãO et al., 2018; SCHORK; RAY, 1987). The reaction is exothermic, and the temperature needs to be controlled for the polymerization to proceed properly. The duration of polymerization controls the molecular weight of the product formed and thus the length of PMMA chains obtained (RAHMAN et al., 2020; SCHORK; RAY, 1987). Chemical structures of MMA and PMMA are shown in **Figure 1.5**.

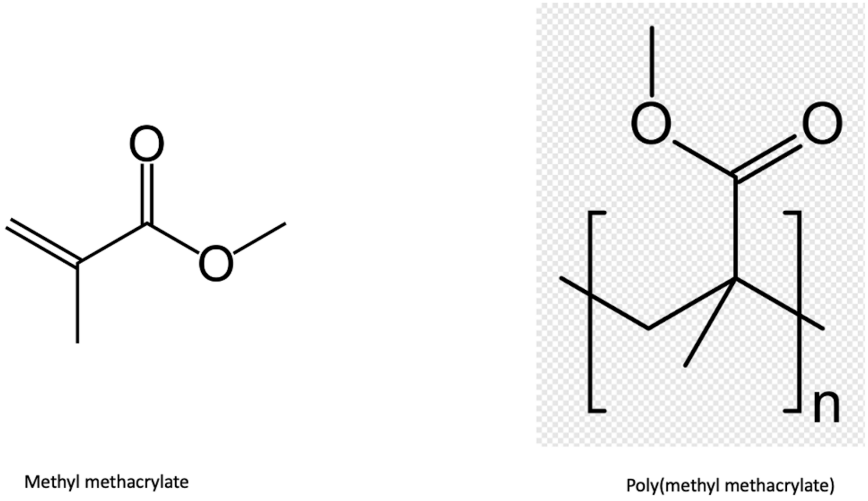


Figure 1.5: Chemical structures of methyl methacrylate (MMA) and poly(methyl methacrylate) (PMMA).

Another instance of hybrid lipid/polymer nanoparticles is represented by PMMA/DODAB/PDDA nanoparticles; these nanoparticles were obtained by emulsion polymerization of MMA in the presence of DODAB and PDDA as emulsifiers (GALVãO et al., 2018; RIBEIRO et al., 2019). The basis to obtain PMMA/DODAB/PDDA nanoparticles was reported by our group

in 2015; in this opportunity, only PDDA was used as an emulsifier and low conversion of MMA in PMMA was achieved (SANCHES et al., 2015). The scheme of the resulting nanoparticles (PMMA/PDDA) is displayed in **Figure 1.6**. The idea of including DODAB in the reaction aimed at increasing the yield of the PMMA synthesis (GALVãO et al., 2018; RIBEIRO et al., 2019). In this work, we also assessed the immunoadjuvant properties of PMMA/DODAB/PDDA nanoparticles.

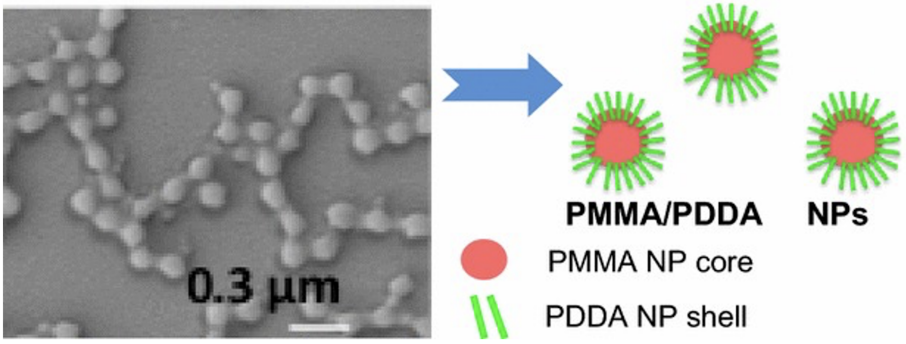


Figure 1.6: Scanning electron microscopy and schematic representation of PMMA/PDDA nanoparticles. Reproduced from (SANCHES et al., 2015).

1.2.3.5 Cationic nanostructure for vaccines design

biomimetics

MDPI

Review

Cationic Nanostructures for Vaccines Design

Ana Maria Carmona-Ribeiro * and Yunys Pérez-Betancourt

Biocolloids Laboratory, Instituto de Química, Universidade de São Paulo, São Paulo 05508-000, SP, Brazil; y.betancourt@usp.br

* Correspondence: amcr@usp.br

Received: 5 June 2020; Accepted: 3 July 2020; Published: 7 July 2020



Abstract: Subunit vaccines rely on adjuvants carrying one or a few molecular antigens from the pathogen in order to guarantee an improved immune response. However, to be effective, the vaccine formulation usually consists of several components: an antigen carrier, the antigen, a stimulator of cellular immunity such as a Toll-like Receptors (TLRs) ligand, and a stimulator of humoral response such as an inflammasome activator. Most antigens are negatively charged and combine well with oppositely charged adjuvants. This explains the paramount importance of studying a variety of cationic supramolecular assemblies aiming at the optimal activity in vivo associated with adjuvant simplicity, positive charge, nanometric size, and colloidal stability. In this review, we discuss the use of several antigen/adjuvant cationic combinations. The discussion involves antigen assembled to (1) cationic lipids, (2) cationic polymers, (3) cationic lipid/polymer nanostructures, and (4) cationic polymer/biocompatible polymer nanostructures. Some of these cationic assemblies revealed good yet poorly explored perspectives as general adjuvants for vaccine design.

Keywords: cationic nanoparticles; dioctadecyldimethylammonium bromide; poly (acrylates); biomimetic lipid/polymer nanoparticles; cationic polymer /biocompatible polymer assemblies; cationic adjuvants; cationic lipids; polycation

1. Introduction

Purified antigens in subunit vaccines usually lack the danger signals of full pathogens, resulting in poor immunogenicity [1]. Adjuvants then become essential components of modern vaccines, enhancing and guiding the immune response against each specific pathogen [2–5]. The only adjuvants licensed for human use worldwide are the aluminum-based salts like $Al(OH)_3$. Their water dispersions consist of polydisperse and large aggregated particles poorly dispersed in water that are positively charged at the pH of water and can combine with negatively charged antigens such as peptides, proteins, nucleic acids, and RNA [6–8]. Other cationic adjuvants based on nanoparticles [9–12], liposomes [13–15], cationic bilayer fragments [9,16,17], supported cationic bilayers on polymeric nanoparticles (NPs) [10], silica [18], or cationic polymers on superparamagnetic iron oxide NPs have also been proposed as effective micro- or nanomaterials able to effectively interact with antigens and antigen-presenting cells (APC) [19].

The uptake of antigen/cationic assemblies depends on size [20,21]. Virus-like NPs (20–200 nm mean diameter) are taken up by endocytosis via clathrin-coated vesicles, caveolae, or their independent receptors and are preferentially ingested by dendritic cells (DC) [22]. Bacteria-like microparticles (500–5000 nm diameter) undergo phagocytosis and primary ingestion by macrophages. Vaccines administered as particles in dispersion are internalized efficiently by APC either by endocytosis or phagocytosis or a combination of both mechanisms [23,24]. Particles with diameters below 500 nm, in particular NPs (40–100 nm diameter), are more efficient to promote CD8 and CD4 type 1 T-helper cell responses than the microparticles (diameters above 500 nm). Similarly,

to $Al(OH)_3$, large particles usually induce good antibody responses from T-helper cells type 2 [23]. Cationic micro- and nanoparticles are effectively taken up both by macrophages and dendritic cells. After electrostatics promotes the binding of cationic particles and assemblies to APCs, subsequent internalization takes place [12,14,21,25]. Antigens of *Mycobacterium tuberculosis* [15,26], *Chlamydia trachomatis* [12], *Neisseria meningitides* [17,27], *Taenia crassiceps* [9,10], and *Mycobacterium leprae* [13] carried by cationic particles, liposomes, or bilayer fragments containing dioctadecyldimethylammonium bromide (DODAB) cationic lipid enhanced the cellular and humoral antigen-specific immune response [15,16,28]. Excellent reviews are available on the use of a variety of cationic lipids such as dimethylaminoethane–carbamoyl–cholesterol (DC-Chol) and derivatives [29], 1,2-dioleoyl-3-trimethylammonium-propane (DOTAP) [30], DODAB [9,16,31], and others to present antigens [32].

In response to pathogens, the innate immune system recognizes the pathogen-associated molecular patterns (PAMPs) by means of the pattern recognition receptors (PRRs) on the surface and in endosomes of APCs [1,33]. As a second line of defense, the adaptive immune system developed by vertebrates consists in memory T and B cells that employ new synthesized antigen-specific receptors able to recognize pathogen-specific antigens when presented by major histocompatibility complexes (MHC) on the surface of an APC. The balance between activity of T or B cells relies on signals provided by the APC (such as co-stimulatory molecules and precise cytokines) in response to the priming by PAMPs [1]. In summary, the co-delivery of antigen and adjuvant to APCs in subunit vaccines results in up-regulation of co-stimulatory molecules essential for adequate T and B cells stimulation [1]. In order to formulate vaccines, a fundamental comprehension of innate and adaptive immune responses is required: the first PAMPS recognition is made via several receptors (innate immunity) leading to the responses able to activate and differentiate T helper cells with possible B cell (antibody-mediated) and CD8 T cell-mediated adaptive immune responses [33].

2. Assemblies from Cationic Lipids and Surfactants

Mimicking nature is a powerful approach for developing novel lipid-based devices for drug and vaccine delivery. Cationic biomimetic particles offered a suitable interfacial environment for adsorption, presentation, and targeting of antigens in vivo. Thereby, antigens can effectively be presented by tailored biomimetic particles for development of vaccines over a range of defined and controllable particle sizes [34]. Lipid supramolecular association with particles has been systematically studied on latex, silica, or drug particles over a range of experimental conditions in order to achieve optimal bilayer deposition onto each particle. The difficult step of vesicle disruption, especially for bilayers in the rigid gel state, was circumvented by using previously disrupted charged vesicles, namely charged bilayer fragments or disks (BF). BF, under appropriate conditions of the intervening medium, coalesced around particles for presentation of antigens to the immunological system [35].

Antigen loading in the vaccine can be driven in cationic assemblies by electrostatic attraction between the antigen and oppositely charged moieties of the adjuvant. For example, cationic DODAB bilayers in water dispersions are available as closed microstructures such as vesicles or open, nano-sized bilayer fragments (BF) obtained by ultrasonic disruption from closed vesicles [28,36–39]. These micro- or nano-structures efficiently combine with serum proteins [40], recombinant heat-shock proteins from micobacteria [13], purified extracts from parasites such as *Taenia crassiceps* [9,10], ovalbumin (OVA) model antigen [16], genetic material such as DNA [41–43], mono- or oligonucleotides such as CpG [44–46], and other oppositely charged biomolecules, drugs, nanoparticles, surfaces, or biological cells [28,41]. Several good reviews appeared on the use of a variety of cationic lipids and surfactants to formulate vaccines [21,32,47–49].

Examples of monocationic lipids are *N*-(1-(2,3-dioleyloxy)propyl)-*N*,*N*,*N*-trimethylammonium trimethyl chloride (DOTMA), dioleoyl-3-trimethylammonium-propane (chloride salt) (DOTAP), dimethyldioctadecylammonium bromide (DDAB or DODAB), dimethylaminoethane carbamoyl cholesterol (DC-Chol), 1,2-distearoyl-3-trimethylammonium-propane (chloride salt) (DSTAP), and

dimyristoyl-3-trimethylammonium-propane (chloride salt) (DMTAP). One example of a polycationic sphingolipid is *N*-palmitoyl d-erythro-sphingosyl-1-0-carbamoyl-spermine triacetate salt (CCS). Figure 1 shows the chemical structures of DOTMA, DOTAP, DODAB, CCS and DC-Chol.

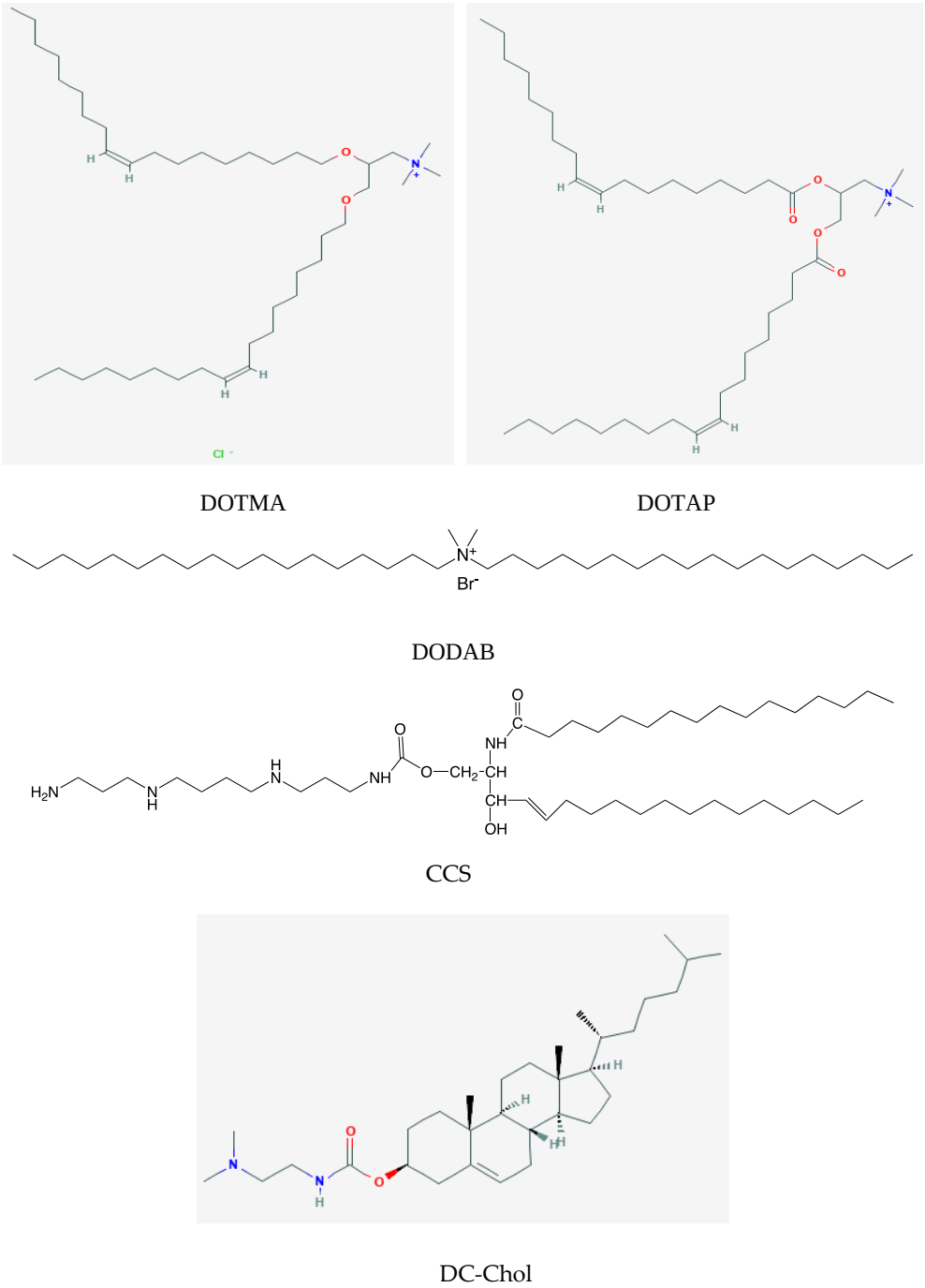


Figure 1. Chemical structure of cationic lipids or surfactants used to formulate vaccines. They bear the cationic charges of primary or secondary amino groups or quaternary ammonium nitrogens in their structures which combine with oppositely charged antigens. CCS is N-palmitoyl d-erythro-sphingosyl-1-0-carbamoyl-spermine triacetate salt. The CCS chemical structure was reprinted from [50] with permission from Elsevier, Copyright 2006.

In particular, CCS is a polycationic surfactant with one primary and two secondary amine groups self-assembling as micelles in aqueous phase; CCS required "helper" lipids such as cholesterol to form liposomes before being combined with the hemoaglutinin/neuraminidase antigens of influenza virus to elicit both Th1 and Th2 responses in mice immunized via the nasal route [50,51].

Among the synthetic lipids, DODAB is possibly the less expensive and the most studied synthetic lipid from several points of view such as its self-assembly as closed or open bilayers in aqueous solutions, its physico-chemical properties in aqueous solutions, its ability to interact with several oppositely charged molecules, nanostructures, nanoparticles, surfaces, and cells with a controllable cytotoxicity against mammalian cells lines; its combinations with a large variety of antigens were able to induce a Th1 response but did not improve the Th2 humoral response [9,13,16,28,37,52]. Among the other cationic lipids, only those with more fluid bilayers due to their double bonds in the hydrocarbon chains or to short hydrocarbon chains such as DOTAP or DMTAP, respectively, were able to elicit both Th1 and Th2 responses combined with antigens [50]. The sphingolipid CCS has a large polycationic polar head and inverted-cone molecular shape self-assembling as micelles. Bilayers were formed combining CCS with other neutral lipids such as dioleoyl phosphatidylethanolamine (DOPE) or cholesterol (Chol), at a CCS/helper lipid mole ratio of 1/1 to 4/1; these cationic assemblies were explored by Barenholz and coworkers to deliver influenza virus antigens by the intranasal route [50,51].

The intranasal (i.n.) is an advantageous mucosal route that allows rapid administration for large populations in the case of pandemics. A good example is the i.n. influenza vaccine, based on CCS combining carrier and adjuvant activities, which elicits, in mice, strong systemic (serum) and local (lung and nasal) humoral and cellular immunity. Unsized liposomes of DC-Chol, DODAB, and DSTAP resulted in low serum and local responses, while two others (DMTAP- and DOTAP-based vaccines) induced both systemic and local vigorous Th1 and Th2 immune responses [50]. However, only the vaccine formulated with CCS was equivalent or superior to the commercial vaccine co-administered with cholera toxin as an adjuvant [50]. Innovative mucosal vaccines against influenza [53] or other diseases were recently comprehensively reviewed [54].

Figure 2 illustrates the possible events for mucosal immunization driven by an antigen/adjuvant nano-assembly as reprinted with permission from Bernocchi et al. 2017, reference [54]. The possible routes for an antigen/adjuvant nano-assembly are depicted from Figure 2A–E where there is direct capture by dendritic cell in Figure 2A, antigen diffusion through the cell junctions in Figure 2B, M cells performing the sampling of the antigen/carrier assemblies and directing them to appropriate cells in their M cell pocket in Figure 2C, epithelial cells performing endocytosis of the NP/antigen for further deliverance to local dendritic cells (DC) and T cells which are able to boost the immune response in Figure 2D. At last in Figure 2E, once in endosomes, NP could release antigens and be exocytosed as free, unloaded, NP (E1) and/or induce the endosomal escape of the antigens (E2) that would be processed as an endogenous antigen and presented by MHC-I (E3). In the other way, also on Figure 2E, NP could be degraded in endo/lysosomes (E4), and the released antigen be processed as exogenous and presented by MHC-II (E5). This could lead to DC and CD8+ T cell activation and/or priming. The activated DC from these pathways then migrate to germinal centers or directly to lymph nodes to activate CD4+ T cells that in turn activate B cells. They undergo an IgA+ phenotype switch, migrate by the blood flow to the effector sites and produce secreted IgA (sIgA) as IgA+ plasma cells.

Once NP/Ag undergo endocytosis by APC, the epitopes of processed antigens can be presented as complexes with either major histocompatibility complex I (MHC-I) or major histocompatibility complex II (MHC-II) [55,56]. In the case of cationic lipids, the versatile DODAB can be dispersed as nanosized, cationic bilayer fragments (BF) able to combine with oppositely charged antigens in general, driving the immune response to a cell-mediated one (Th1) [9,16]. In a certain sense, the DODAB BF are discoidal and open nanostructures instead of closed, vesicular bilayers or liposomes, and antigen is expected to become adsorbed from the electrostatic attraction all around the disk-like bilayer so that desorption and endosomal escape might allow MHC-I presentation after trafficking from the cytosol to the endoplasmic reticulum. This would agree with findings by Korsholm and coworkers [57]; they

studied the mechanism of adjuvanticity for DODAB/OVA liposomes and found that these liposomes did not affect the maturation of murine bone-marrow-derived dendritic cells (BM-DCs) related to the surface expression of MHC-II, CD40, CD80, and CD86 but enhanced the uptake of OVA by BM-DCs via endocytosis; intraperitoneal injection of DODAB/OVA liposomes also enhanced the uptake of the antigen by peritoneal exudate cells and targeted the antigen preferentially to antigen-presenting cells, leading to enhanced uptake and presentation of antigen [57].

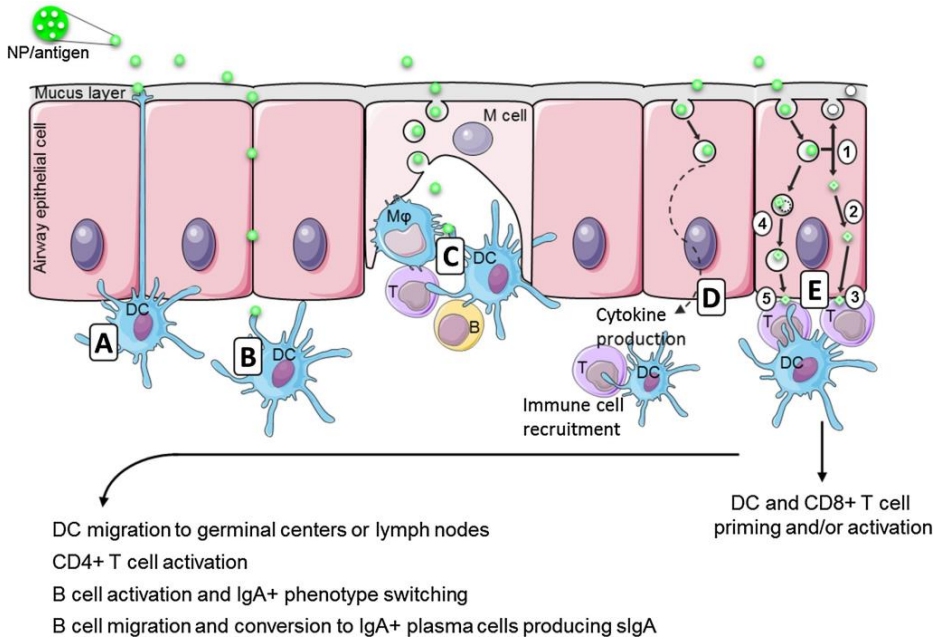


Figure 2. Mucosal immune induction in nasal and airways epithelia by antigen-loaded nanocarriers (NP/antigen). (**A**) Dendritic cells (DC) protruding arms, the transepithelial dendrites, directly capture the NP/antigen. (**B**) NP/antigen can also diffuse through epithelial junctions and reach the underlying DC. (**C**) The M cells create a pocket enriched in immune cells (DC, macrophages-Mφ and lymphocytes T) and perform the sampling of the luminal antigens so that the immune cells contact the NP/antigen. (**D**) The NP/antigen can also enter cells by endocytosis and deliver the antigens of the nanovaccine into the cells. The endocytosis of NP/antigen by the epithelial cells triggers the production of cytokines, defensines, and chemokines involved in local immune cells recruitment (DC and T cells) able to boost the immune response. (**E**) The endocytosis of NP/antigen can also be the first step of antigen presentation by epithelial cells. In endosomes, NP could release antigens and be exocytosed as free, unloaded, NP (E1) and/or induce the endosomal escape of the antigens (E2) that will be processed as an endogenous antigen and presented by major histocompatibility complex I (MHC-I) (E3). In the other way, NP could be degraded in endo/lysosomes (E4), and the released antigen will be processed as exogenous and presented by major histocompatibility complex II (MHC-II) (E5). This could lead to DC and CD8+ T cell activation and/or priming. The activated DC from these pathways then migrate to germinal centers or directly to lymph nodes to activate CD4+ T cells that in turn activate B cells. They undergo an IgA+ phenotype switch, migrate by the blood flow to the effector sites and produce secreted IgA (sIgA) as IgA+ plasma cells. Reprinted from [54] with permission from Elsevier, Copyright 2017.

Nano-sized formulations enter the cells by endocytosis following the *endo*-lysosomal pathway before the protein is delivered and degraded in the endosomes; the resulting peptides are complexed with MHC-II and presented on cell surface for activation of CD4+ T helper cells, stimulating cytokine secretion and humoral antibody responses (Th2). When the nanostructure promotes the protein escape from the endosomes to the cytosol, the protein may be degraded in the proteasome with the peptidic products of the degradation carried by transporters of antigen processing to the endoplasmic

reticulum where they combine with MHC-I. Cellular expression of peptide-associated MHC-I activates CD8+ T cells and cell-mediated immunity [58–61]. For effective control of tumors and pathogens by the immune system, neoplastic and infected cells must be targeted and destroyed by cytotoxic T lymphocytes (CTLs). While MHC-I conventionally present endogenous cytosolic antigens, the alternative pathway, termed cross-presentation, also allows the presentation of peptides derived from exogenous antigens by MHC-I [62]. As tumor antigens and pathogen-derived proteins are often not endogenously produced by antigen-presenting cells (APCs), this exogenous pathway is crucial for the generation of CD8+ CTL responses against these cell-associated antigens [63]. Enhancement of the targeting of exogenous antigens to the cross-presentation pathway may help develop effective vaccines against tumors, parasites, intracellular bacteria, and viruses. In summary, there are distinct intracellular routes for antigen uptake and presentation to attain CD4 and CD8 T cell activation and ideal antigen adjuvant systems should activate both of these pathways, thereby also inducing cross-presentation [58]. Since subunit vaccines are not effective in cytotoxic T cells activation, the association with adjuvants becomes crucial [64]. Interestingly, the antigen encapsulation in nanostructures (nanoparticles and bilayer nanodisks included) may direct the antigen presentation towards a different or combined immune response. This orientation can be affected by multiple factors, such as the mechanism of uptake, and is dependent upon the nanostructure physical properties such as the size, the outer surface charge, and also the inner particle charge. In our group, we observed that cationic nanodisks of DODAB BF complexed with the model antigen ovalbumin induced in vivo a large Th1 response and very low or absent humoral response [9,13,16], whereas NPs of PDDA/OVA, where the antigen was entangled with the cationic polymer PDDA, elicited potent Th2 humoral response in absence of the cell-mediated one [65]. Therefore, the ideal adjuvant should combine the ability of offering the antigen to be degraded inside the endosome with the ability to allow the antigen endosomal escape. Should we mix DODAB BF/antigen with PDDA/antigen to achieve the right balance between Th1 and Th2 responses?

The progress in gene or siRNA delivery to cells contributed substantially to the development of novel cationic lipids [66–68]. A particularly interesting class of cationic lipids is the lipopolyamines synthesized by Byk and coworkers in the 1990s aiming at DNA transfer to cells [69]. They were recently explored by Pizzuto and coworkers as single-component adjuvants able to elicit both Th1 and Th2 responses in absence of toxicity in vivo [70]. Figure 3 illustrates the ability of these polyamines to activate Toll-like receptor 2 (TLR2) and 4 (TLR4) besides inducing, in combination with OVA antigen, both IgG1 and IgG2a; OVA alone or Alum induced exclusively IgG1, and lipopolyamines induced both IgG1 and IgG2a antibodies production [70]. Figure 3A shows the chemical structure of the lipopolyamines. Figure 3B illustrates the uptake of lipopolyamines alone or complexed with ovalbumin by cultured human cell lines transfected with Toll-like Receptors (TLRs), leading to (1) secretion of inflammatory and type-I interferon cytokines able to trigger a Th1 response (cell-mediated immunity); (2) secretion of the interleukin-1beta (IL-1β) able to induce a Th2 response (humoral immune response). Figure 3C shows that the uptake of lipopolyamines/antigen complexes in vivo by intraperitoneal macrophages induced secretion of interleukin-5 (IL-5) and humoral immunity plus tumor necrosis factor-alpha (TNF-α) and gamma-interferon inducible protein (IP-10) [71], typical inducers of Th1 response (cell-mediated immune response) by the cultured macrophages.

On Figure 3 reproduced from Pizzuto and coworkers are shown two lipopolyamines with 12 or 18 carbon atoms in their alkyl chains; however, only the lipopolyamines with 12 or 14 carbon atoms in their alkyl chains activated TLR2- and TLR4-transfected cells, whereas the C18-lipopolyamine with very similar or identical polar head group activated only TLR2-transfected cells. The hypothesis cast to understand this was related to the fusogenic behavior of the lipopolyamines, since those with shorter lengths of the carbon chains (as those with C12 or C14) would be more fusogenic than those with long chains (as those with C18); thereby, the former would be taken up more easily by the cells. The possible toxicity in vivo of the lipopolyamine–OVA complexes was evaluated from determinations of liver enzymes alanine transaminase (ALT), aspartate transaminase (AST), and the inflammatory

cytokine tumor necrosis factor-alpha (TNF-α) in the serum plus histological examination of liver slices of the injected mice post-injection; no toxicity was detected, neither in serum nor on liver slices. The TLR stimulation and secretion of pro-inflammatory and interleukin-1beta (IL-1β) cytokines suggested that the C12 or C14-polyamines would be promising one-component vaccine adjuvants eliciting both humoral and cell-mediated responses [70].

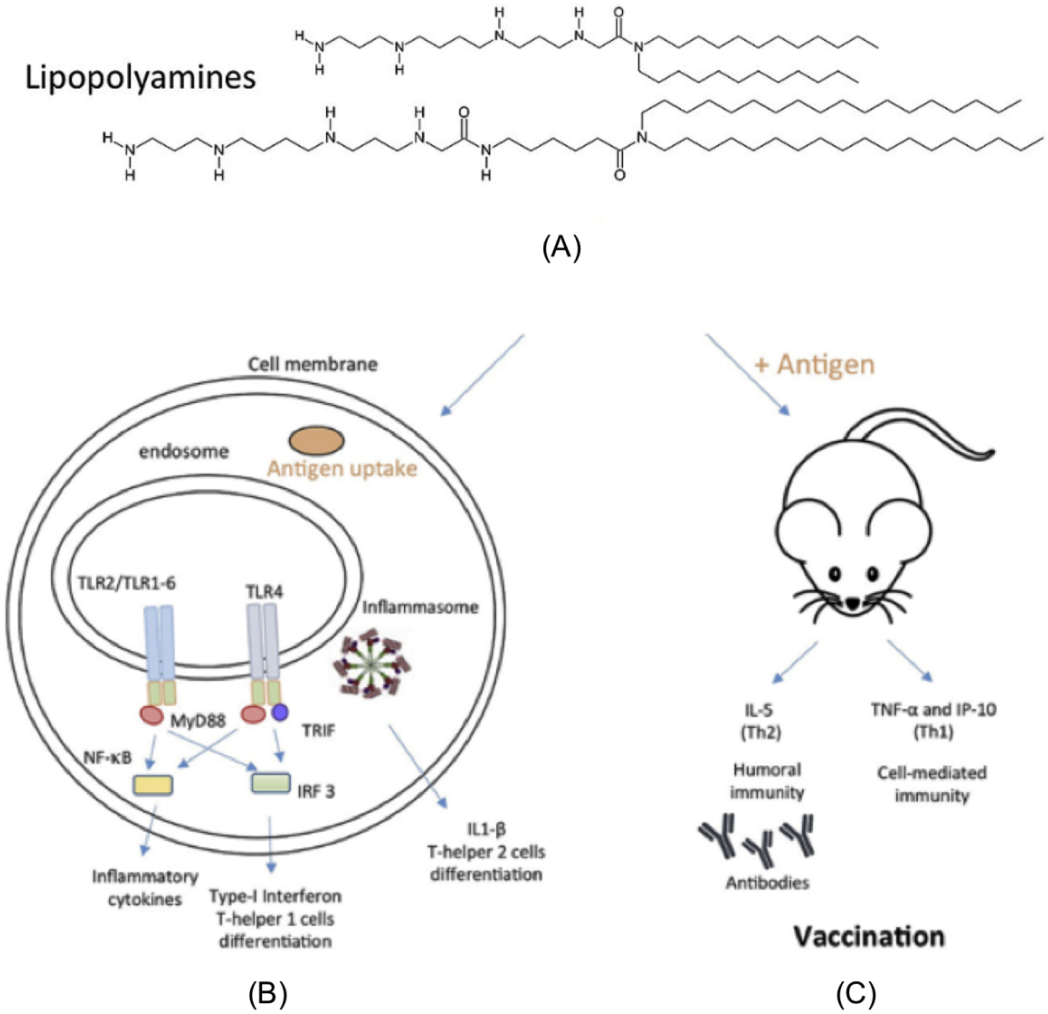


Figure 3. (**A**) Chemical structure of lipopolyamines (12 or 18 C). (**B**) Uptake of lipopolyamines alone or complexed with ovalbumin by cultured human cell lines transfected with Toll-like Receptors (TLRs), leading to 1) secretion of inflammatory and type-I interferon cytokines able to trigger a Th1 response (cell-mediated immunity); 2) secretion of the interleukin-1beta (IL-1β) able to induce a Th2 response (humoral immune response). (**c**) Uptake of lipopolyamines/antigen complexes in vivo by intraperitoneal macrophages induced secretion of interleukin-5 (IL-5) and humoral immunity plus tumor necrosis factor-alpha (TNF-α) and gamma-interferon inducible protein (IP-10) [71], typical inducers of Th1 response (cell-mediated immune response) by the cultured macrophages. Reprinted from [70] with permission from Elsevier, Copyright 2018.

Aluminum adjuvants typically activate the inflammasome pathway and Th 2 response [72] so that alum combinations with TLR agonists are needed to induce the cell-mediated Th 1 response against pathogens [5]. Pizzuto et al. also demonstrated that lipopolyamines induced IP-10, IL-6, and IL-1β secretion in murine macrophages and TNF-α in murine and human macrophages. TNF-α and

IL-6 are pro-inflammatory cytokines typical of the NF-κB induction. IP-10 is instead the signature of Type I IFN antiviral and T cell-stimulating response and is typical of the IRF induction. Finally, IL-1β secretion demonstrates the concomitant activation of the NF-κB pathway, which expresses pro-IL-1β, and of the inflammasome pathway that cleaves pro-IL-1 β. The activation of both TLR and inflammasome pathways combined with the carrier properties makes cationic lipid lipopolyamines excellent candidates as one-component vaccine adjuvants [70].

The mycobacterial cord factor trehalose-6,6′-dimycolate (TDM) present in the cell wall of mycobacteria and its synthetic adjuvant analog trehalose-6,6′-dibehenate (TDB) are glycolipids that trigger innate immunity. Bone-marrow-derived dendritic cells (BMDCs) stimulated with TDB induced Nlrp3 inflammasome-dependent IL-1β secretion; in vivo, in Nlrp3-deficient mice, recruitment of neutrophils by TDB was reduced, showing the essential role of the Nlrp3 inflammasome for the induction of an innate humoral immune response triggered by TDB [73].

In murine models of *Mycobacterium tuberculosis* (Mtb) infection, TDM administration drove the early pro-inflammatory M1-like macrophage response related to the granulomas of primary pathology; proinflammatory cytokines such as TNF-α, IL-1β, IL-6, and IL-12p40 were produced in lung tissue [74]. Furthermore, CD11b+CD45+ macrophages with a high surface expression of the pro-inflammatory CD38 and CD86 markers were found in lung lesions of mice at 7 days post-TDM introduction, but low phenotypic marker expression of anti-inflammatory M2-like markers CD206 and EGR-2 were present on macrophages. TDM played a role in establishment of the M1-like shift in the microenvironment during primary tuberculosis. Thus, the MTB cell wall cording factor TDM is a physiologically relevant and useful molecule for modeling early macrophage-mediated events during establishment of the tuberculosis-induced granuloma pathogenesis [74].

In order to improve fusion of cell membranes with DODAB bilayers, which are in the rigid gel state at room temperature [75], DODAB bilayer fluidity had to be increased by using DODAB combinations with other lipids and surfactants such as the glycolipid TDB [15,76], the surfactant monoolein (1-monooleoyl-rac-glycerol) [77], the C24:1 β-glucosylceramide [78] or the glycolipid de-O-acylated lipooligosaccharide (dLOS) as a booster vaccine against tuberculosis [79]. In particular, intranasal immunization with DODAB/TDB combined with influenza antigen A (H3N2) induced superior humoral and cell-mediated responses; there was an effective facilitation of uptake by DC, DC maturation in vitro, increased mucosal IgA production, increased IgG, IgG1, and IgG2b antibody titers in comparison with other formulations using cationic lipids after intranasal administration in vivo [80]. Immunization of mice with a mycobacterial fusion protein in DODAB-TDB liposomes induced a strong, specific Th1-type immune response characterized by substantial production of interferon-gamma mediated by CD4 T cells and high levels of IgG2b isotype antibodies [15]. The combinations of DODAB and monoolein improved the fusion of the liposomes with cell membranes, thereby allowing their use for mammalian cell transfection [81] and in vitro gene silencing [82]. These combinations also induced strong humoral and cell-mediated immune responses, producing antibodies (IgGs) against specific cell wall proteins of *Candida albicans* (CWSP) useful for fighting fungus infections [77,83]. Figure 4 illustrates the use and activity of DODAB/monoolein vesicles as adjuvants as reproduced from reference [77]. One should notice the inverted hexagonal phase of monoolein inside the liposome.

Another important line of research for vaccines against pathogens has been the use of cationic liposomes or DODAB bilayer fragments (BF) as adjuvants for intranasal immunization. The cationic DOTAP/DC-Chol liposomes combined with ovalbumin (OVA) were intranasally administered eliciting enhanced production of IgG antibodies in the serum (Th2 response) in immunized mice as well as mucosal IgA [84]. Immune responses for DODAB BF and alum complexes with outer membrane vesicles (OMV) of *Neisseria meningitidis* B administered by intranasal and subcutaneous routes in mice were compared; intranasal immunization produced a mixed Th1 and Th2 response, while subcutaneous immunization exhibited a Th1 profile only [27]. Non-replicating, nanometric membrane vesicles (MV) released both by Gram-positive and Gram-negative bacteria contain proteins, lipids, and nucleic acids that are effectively able to stimulate the innate and adaptive immune system [85,86]. In this regard,

the cationic lipids can add extra adjuvanticity. Furthermore, multiple antigens can decorate these MV; for example, outer MVs from attenuated *S. typhimurium* was successfully decorated with one, two, or three antigens from *M. tuberculosis* (ESAT6, Ag85B, and Rv2660c) and major outer membrane protein epitopes from *Chlamydia trachomatis;* in vitro data showed that the antigen Ag85B delivered by outer MVs is able to be recognized and processed by dendritic cells and subsequently activate *M. tuberculosis*-specific T cells [87].

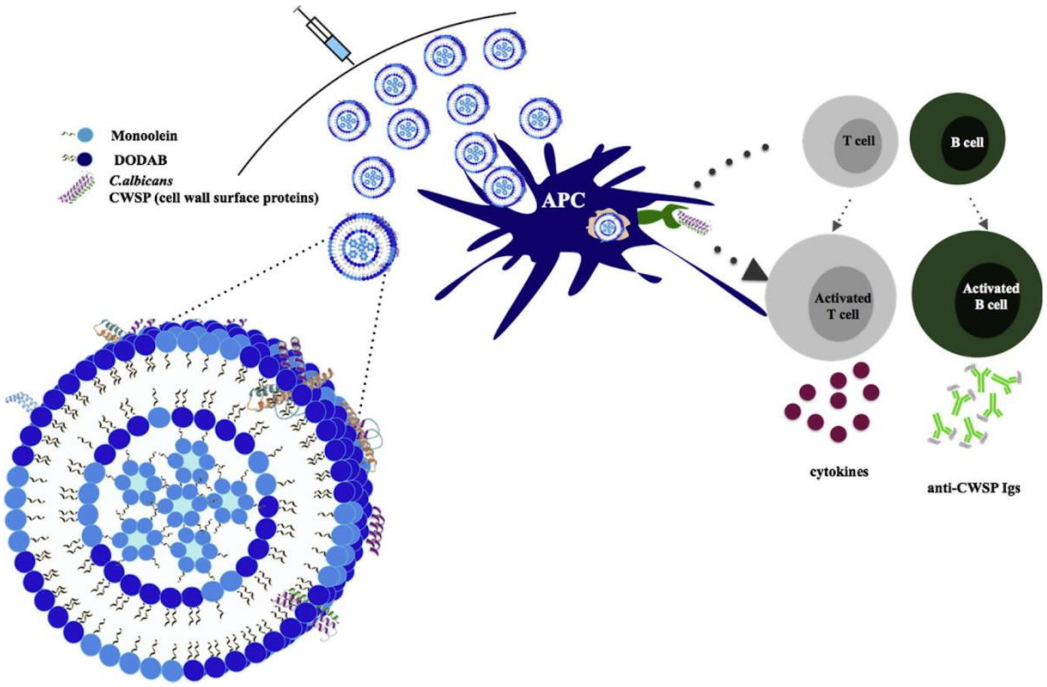


Figure 4. Activation of cell-mediated immunity and humoral response by DODAB/monoolein liposomes incorporating cell wall surface proteins of *Candida albicans* (CWSP). Reprinted from [77] with permission from Elsevier, Copyright 2015.

The development of effective intranasal vaccines is of great interest due to their potential to induce both mucosal and systemic immunity. Some oil-in-water nanoemulsion (NE) formulations containing various cationic and nonionic surfactants were used as adjuvants for the intranasal delivery of vaccine antigens. Association of NE droplets with the mucus protein mucin in vitro was important as were the cationic NE formulations that facilitated cellular uptake of the model antigen, ovalbumin (OVA), in a nasal epithelial cell line. NE-facilitated mucosal layer penetration and cellular uptake led to enhancement of the immune response [88].

In an interesting comparative study, several cationic lipids were evaluated regarding their effectiveness as humoral adjuvants while carrying the influenza antigen hemoagglutinin (HA) [89]. DDA or DODAB and other cationic lipids combined with a neutral lipid (DPPC) in a molar proportion of 1:1 were again evaluated as poor inducers of humoral response with exception of DC-Chol. The cationic liposomes contained a cationic compound (DDA or DODAB, 1,2-dipalmitoyl-3-trimethylammonium-propane DPTAP, DC-Chol, or 1,2-diacyl-sn-glycero-3-ethylphosphocholine (eDPPC) and a neutral phospholipid 1,2-dipalmitoyl-sn-glycero-3-phosphocholine (DPPC) and carried the influenza antigen HA; they were well characterized regarding hydrodynamic diameter, zeta potential, membrane fluidity, HA loading, and humoral immune response in subcutaneously immunized mice from the production of HA-specific antibodies by ELISA and HA-neutralizing antibodies by hemagglutination inhibition (HI) assay. Figure 5, reproduced from reference [89], shows that liposomes at 1:1 DC-Chol/DPPC combined with HA gave the inhibition of hemoagglutination

titers that could be related to the highest IgG1 and IgG2a titers compared to the other liposomal HA formulations and HA alone. Moreover, increasing the proportion of cationic lipid increased the incorporation of HA and the immune response [89]. One should notice that the physical state of the cationic bilayers was the rigid gel state in all cases and the physical state of the DC-Chol/DPPC bilayers was not determined in reference [89].

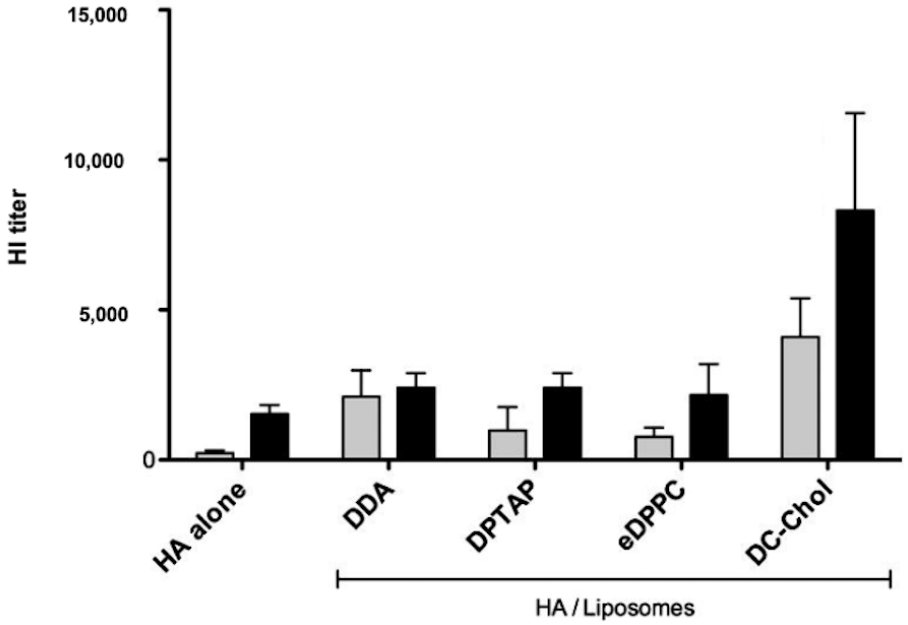


Figure 5. Hemagglutination inhibition (HI) assay for neutralizing antibodies against hemagglutinin (HA) elicited by combinations of HA with DDA/DPPC, DPTAP/DPPC, or DC-Chol/DPPC where DDA is dioctadecyldimethylammonium bromide, DPTAP is 1,2-dipalmitoyl-3-trimethylammonium-propane, DPPC is 1,2-dipalmitoyl-sn-glycero-3-phosphocholine, eDPPC is 1,2-diacyl-sn-glycero- 3-ethylphos phocholine and DC-Chol is 3β-[*N*-(*N*′,*N*′-Dimethylaminoethane)-carbamoyl] cholesterol. Reprinted from [89] with permission from Elsevier, Copyright 2012.

The mRNA technology for vaccines [90] has been recognized as representing a transformative technology to control infectious diseases [91] and to fight cancer [92]. For example, while constructing an mRNA vaccine against influenza, the mRNA encoding the HA antigen of influenza A H1N1 virus was delivered by cationic lipid nanoparticles (LPN) and induced protective immune responses in mice. The lipid nanoparticles comprised several lipids such as DOTAP, 1,2-dioleoyl-sn-glycero-3-phosphoethanolamine (DOPE), and 1, 2-distearoyl-sn-glycero-3-phosphoethanolamine-N-(methoxy(polyethylene glycol)-2000) (DSPE-mPEG2000) (50:50:1 mol/mol) [93]. The system allowed also the covalent binding of mannose (Man) to the PEG moiety so that targeting of the mannose -cationic NPs (LNP-man) to the mannose receptors on antigen-presenting cells such as macrophages and dendritic cells improved the delivery efficiency of the assembly. These cationic lipid/mRNA NPs could protect their mRNA cargo from degradation by nucleases and deliver the m-RNA into cells by electrostatic adsorption and fusion with the cell membrane. LNP-Man contained DOTAP, DOPE, and DSPE-PEG-Mannose (50:50:1 mol/mol). This vaccine was properly tested from administration by the intra-nasal route and induced excellent protection against influenza. The important issue of lipid-based anticancer vaccines was recently reviewed [94].

In order to ascertain whether antigen depot or lymphatic targeting would benefit long-term immunological memory, OVA antigen was encapsulated with DOTAP cationic liposomes (LP) or DOTAP-PEG-mannose liposomes (LP-Man) to generate depot or lymphatic-targeted liposome vaccines,

respectively [95]; in vivo imaging showed that LP accumulated near the injection site, whereas LP-Man accumulated in draining lymph nodes (LNs) and spleen enhancing the uptake by resident antigen-presenting cells. LP vaccines with depot effect induced higher anti-OVA IgG production than LP-Man vaccines on day 40 after priming but failed to mount an effective B-cell memory response upon OVA re-challenge after three months. In contrast, lymphatic-targeted LP-Man vaccines elicited sustained antibody production and robust recall responses three months after priming, suggesting that lymphatic targeting rather than antigen depot promoted the establishment of long-term memory responses [95].

Small interfering RNAs (siRNAs) are able to recognize a homologous mRNA sequence in the cell and induce its degradation; each siRNA molecule can inactivate several target RNAs in a sequence-specific manner [96]. The main problems in the development of siRNA-based drugs and vaccines for therapeutic use are the low efficiency of siRNA delivery to target cells and the degradation of siRNAs by nucleases in biological fluids [67]. Among the approaches used to deliver RNA are those based on non-saturated double-chained cationic lipids [97]. These lipids were shown to facilitate fusion with cell membranes [98]. Figure 6 shows the encapsulation of self-amplifying RNA based on alphavirus genome, which contains the genes encoding the alphavirus RNA replication machinery but lacks the genes encoding the viral structural proteins required for infection; the cationic liposome composition is also shown on the right as reproduced with permission from Geall and coworkers, 2012 [99]. The cationic lipid employed was 1,2-dilinoleyloxy-*N*,*N*-dimethyl-3-aminopropane (DLinDMA) with two double bonds per chain [98]. After immunization, replication and amplification of the RNA molecule occur exclusively in the cytoplasm of the transfected cells, thereby eliminating risks of genomic integration, cell transformation, and safety issues that occur for recombinant DNA, viral vectors, and pDNA vaccines. Furthermore, there is no need for crossing the nuclear membrane, a rate-limiting step for nonviral pDNA delivery.

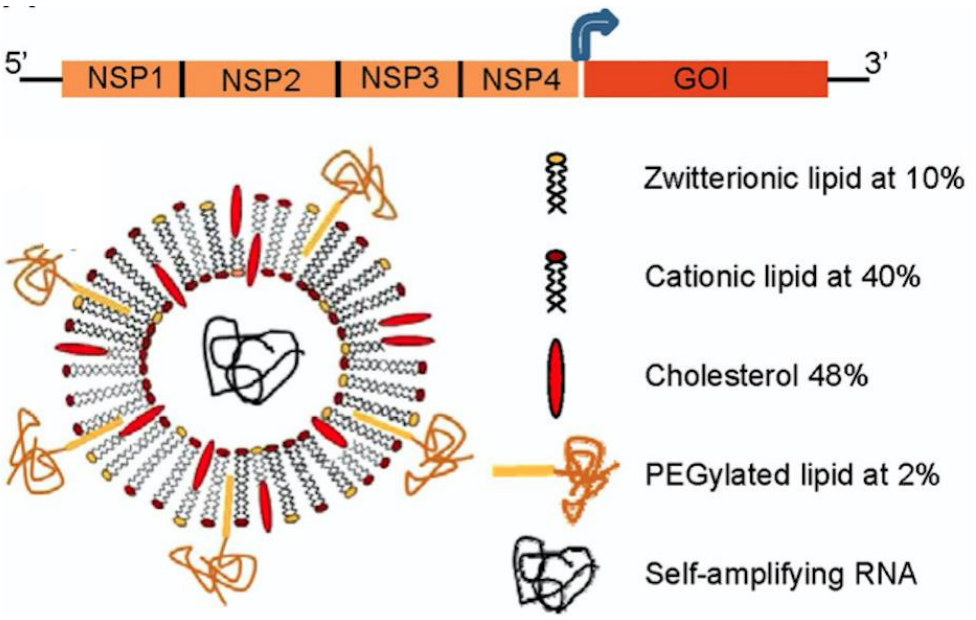


Figure 6. Self-amplifying RNA vaccines where this RNA derived from and alphavirus contains a 5′ cap, nonstructural genes (NSP1-4), 26S subgenomic promoter (dark blue arrow), the gene of interest, and a polyadenylated tail. The self-amplifying RNA was protected inside the cationic liposome with the composition shown in the legend on the right. Reprinted from [99].

Dendritic cells (DC) process and present antigens to T lymphocytes, inducing potent immune responses when encountered in association with activating signals, such as pathogen-associated

molecular patterns. Monophosphoryl lipid A (MPL) is a ligand of the Toll-like receptor-4 and has been used in several studies on vaccines [100]. Using combined therapy against murine model tumors, both MPL and IL-12 were included in cationic DOTAP liposomes for intratumoral injection [101]. In 4T1 murine model of breast cancer, the injection decreased cellular proliferation and increased serum levels of IL-1β and TNF-α. The addition of recombinant IL-12 further suppressed tumor growth and increased expression of IL-1β, TNF-α, and interferon-γ. IL-12 also increased the percentage of cytolytic T cells, DC, and F4/80(+) macrophages in the tumor. The combination of MPL and IL-12 elevated the levels of nitric oxide synthase 7-fold above basal levels in the tumor and caused cell cycle arrest and apoptosis, also inhibiting the growth of untreated tumor in the same animal and revealing the systemic activity of the formulation [101].

In another very interesting approach, sterically stabilized nanodisks based on high-density lipoproteins (HDL) carried MPL, CpG (ligand of Toll-like receptor-9), and antigen for personalized cancer immunotherapy; synthetic high-density lipoprotein (sHDL) nanodisks were composed of phospholipids and apolipoprotein A1 (ApoA1)-mimetic peptides (the peptides were named 22A because they were synthesized as 22-mer peptides, derived from the repeat α-helix domain of ApoA1) [102]. Thereby the endogenous role of HDL as a nanocarrier for cholesterol was explored in synthetic HDL that carried cholesteryl-CpG, neo-antigens, and tumor Ag peptides (neo-antigens identified via tumor DNA sequencing) to produce homogeneous, stable, and ultrasmall nanodisks in less than two hours at room temperature; nanodisks promoted co-delivery of Ag/CpG to draining lymph nodes; prolonged Ag presentation on antigen-presenting cells (APCs); elicited striking levels of broad-spectrum antitumor T-cell responses; and significantly inhibited tumor growth, also eradicating established tumors [102]. Cationic nanodisks of DODAB, also called DODAB bilayer fragments (BF), have also been used as adjuvants for carrying several antigens, CpG agonist, and oligonucleotides [16] directing excellent Th1 response and also Th2, depending on the administration route [see references [21,25,28]. Figure 7 schematically represents cross-sections of DODAB nanodisks carrying CpG and ovalbumin (OVA). DODAB BF have two major strategic advantages when compared to more sophisticated formulations: (1) DODAB is possibly the less expensive synthetic cationic lipid available nowadays, (2) DODAB dispersion as open bilayers in water solution can be rapidly performed by sonication with a macrotip, and (3) the nanometric size of the DODAB bilayer disks allows direct stimulation of APC in the draining lymph nodes [103].

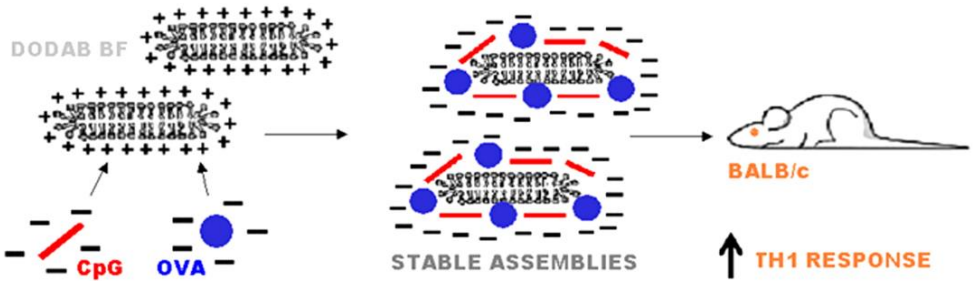


Figure 7. Schematic representation of cross sections for DODAB bilayer fragments (DODAB BF) used for carrying ovalbumin (OVA) and CpG agonist of Toll-like receptor 9. The final assemblies were anionic and directed excellent Th1 response in mice immunized subcutaneously. Curiously, addition of CpG to the assembly did not improve the immune response; DODAB was effective by itself. In addition, the nanosize of the assemblies was more important than the charge. Reprinted from [16] with permission from Elsevier, Copyright 2012.

Whereas DODAB BF harboring CpG did not improve the adjuvanticity of DODAB BF in vivo [16], DOTAP/DC-chol liposomes harboring CpG ODN as a mucosal adjuvant induced both antigen-specific mucosal IgA responses and balanced Th1/Th2 responses so that the combination resolved adverse effects of CpG ODN as mucosal adjuvant by means of dose minimization [104].

Human papillomavirus (HPV) is the most common sexually transmitted biological agent and causes precancer lesions and cancer; three prophylactic HPV vaccines targeting high-risk HPV types are available in many countries worldwide: 2-, 4- and 9-valent vaccines; all three of the vaccines use recombinant DNA technology and are prepared from the purified L1 protein that self-assembles to form HPV type-specific empty shells [105]. There are a few instances of using cationic lipids to formulate vaccines against HPV. DOTAP/oncoprotein E7 of papillomavirus was evaluated for its anti-cancer activity; E7 peptide formulated with DOTAP induced migration of activated dendritic cells (DC) to the draining lymph node (DLN) and efficiently generated functional antigen-specific CD8+ T lymphocyte infiltration and apoptosis at tumor sites; the effect did not change by adding CpG to the same formulation [106]. Efficient eradication of tumors in mice was also achieved using combinations of DOTAP/DOPE cationic liposomes with synthetic long peptides (SLP) derived from OVA alone or combined with different Toll-like receptors ligands including CpG; a single intradermal tailbase vaccination of tumor-bearing mice with a low dose of E7/poly(I:C)-liposomes led to complete clearance of the tumors in 100% of the mice; therapeutic vaccination with SLP could be clinically effective against HPV-induced premalignant lesions; induced antigen-specific CD8+ and CD4+ T cells and in vivo cytotoxicity against target cells after intradermal vaccination; at a low dose (1 nmol) of SLP, our liposomal formulations significantly controlled tumor outgrowth in two independent models (melanoma and HPV-induced tumors) and even cured 75%–100% of mice of their large established tumors; cured mice were fully protected from a second challenge with an otherwise lethal dose of tumor cells, indicating the potential of liposomal SLP in the formulation of powerful vaccines for cancer immunotherapy [107].

SLP-loaded (1,2-dioleoyl-3-(trimethyammonium) propane)-based cationic formulation as a therapeutic cancer vaccine was tested against two independent tumor models. The OVA-derived SLPs containing CTL and Th epitopes were loaded into DOTAP- based cationic liposomes combined with different TLR ligands [poly(I:C), Pam3CysK4, CpG], and the most potent formulations were applied in a foreign antigen (OVA)-expressing melanoma model. In an independent setting, HPV16 E7 SLP was formulated in the same liposomal system and analyzed as a therapeutic vaccine in the TC-1 HPV+ tumor model; both formulations were highly effective in the induction of cellular immunity and tumor control [107].

The humoral and cellular immune responses induced in mice against hepatitis B virus surface antigen (HBsAg) were examined when the antigen was either adsorbed to aluminum hydroxide or administered with DC-Chol. DC-Chol induced cellular immune responses to HbsAg and a balanced Th1/Th2 response, which enabled mice to overcome the inherited unresponsiveness to HBsAg encountered with aluminum-adjuvanted vaccine. Thus, the DC-Chol provided a signal to switch on both Th1 and Th2 responses for vaccination against hepatitis B virus [108].

An early model study on trafficking of cationic-liposome-DNA complexes in the cells attempted to reveal by electron microscopy the intracellular fate of gold-labeled structures. Cells treated with DOTMA liposome-DNA complexes demonstrated endocytosis of the liposome–DNA complexes in coated pits, which were seen in early endosomes, late endosomes, and lysosomes. In isolated alveolar type II cells, the gold-labeled DOTMA lipid apparently mixed with the contents of lamellar bodies. In most cells, gold particles were dispersed throughout the cytoplasmic matrix. In a small proportion of cells, a membrane system resembling the endoplasmic reticulum developed within the nucleus; this novel structure was also present in isolated nuclei from cells and then mixed with DOTMA-containing liposomes [109].

DNA vaccination technologies have been important in several areas despite the difficulties involving DNA transfection efficiency, prevention of DNA degradation, APC targeting, and enhancing DNA escape from endo/lysosomal compartments and attachment of virus-derived nuclear localization sequences facilitating nuclear entry of the DNA [110]. For example, DNA vaccines provide an attractive technology platform against anthrax bioterrorism agents; monovalent and bivalent anthrax plasmid DNA (pDNA) vaccines encoding genetically detoxified protective antigen (PA) and lethal factor (LF)

proteins were formulated in cationic lipids, and immune responses after two or three injections of cationic lipid-formulated PA, PA plus LF, or LF pDNAs were at least equivalent to two doses of anthrax vaccine adsorbed (AVA). High titers of anti-PA, anti-LF, and neutralizing antibody to lethal toxin (Letx) were achieved in all rabbits. All animals receiving PA or PA plus LF pDNA vaccines were protected. In addition, 5 of 9 animals receiving LF pDNA survived, and the time to death was significantly delayed in the others. Groups receiving three immunizations with PA or PA plus LF pDNA showed no increase in anti-PA, anti-LF, or Letx neutralizing antibody titers postchallenge, suggesting little or no spore germination. In contrast, titer increases were seen in AVA animals and in surviving animals vaccinated with LF pDNA alone. Preclinical evaluation of this cationic lipid-formulated bivalent PA and LF vaccine is complete, and the vaccine has received U.S. Food and Drug Administration Investigational New Drug allowance [111].

Early work involving cationic liposomes to carry plasmid encoding antigens revealed that the liposomes indeed protected the liposome-entrapped DNA from degradation in vivo, thereby resulting in greater antibody responses against the encoded antigen when compared with naked DNA, both given via the subcutaneous route; T-cell responses from analysis of interferon-γ and interleukin-4 levels in the spleens of mice treated with liposomes/DNA were also significantly higher than those measured in mice treated similarly with naked DNA [112–114]. More recently, Perrie and coworkers gave an excellent summary of the possible fate of cationic liposomes/DNA (L/DNA) assemblies injected by the subcutaneous route [115]. L/DNA assemblies injected locally are taken up by APC penetrating the site of injection or in the lymph nodes draining the injected site; the clearance of L/DNA from the site of injection depends on L/DNA size; the smaller the size, the more rapid the clearance through the anatomical barriers [116]. The L/DNA become dispersed throughout the lymph node either permeating along the sinuses or being taken up by cells such as macrophages; once within cells, L/DNA are digested by the lysosomes, leaving their contents within the lysosomes or escaping this degradation via fusion with the endosomal membrane (which happens due to the fusogenic lipid DOPE present in the liposomal bilayer) [117–119]. Thereby DNA is displaced from the complex and released into the cytosol for eventual episomal transfection so that cationic lipid and DOPE favor liposome-mediated -DNA immunization [115,117,118]. The possible fates of nanosized adjuvant/antigen assemblies were thoroughly discussed by Smith and coworkers, 2013 [120].

Lecithins are components of cell membranes consisting of combinations of phosphatidylcholine (PC), phosphatidylethanolamine (PE), phosphatidylserine (PS), and phosphatidylinositol (PI), plus other substances such as triglycerides and fatty acids; in particular, soy lecithin contains 21% PC, 22% PE, and 19% PI, along with other components. Lecithins are widely used for dispersing, emulsifying, and stabilizing a variety of pharmaceuticals often included in intramuscular and intravenous injectables, parenteral nutrition formulations, and topical products [121]. Hexadecyltrimethyl ammonium bromide (CTAB) surfactant added to lecithin nanoparticles yielded cationic particles with diameters in the range of 100–200 nm where soy lecithin was the matrix material and CTAB, the outer surfactant. The zeta potential of the particles was positive, reached a value of about 40 mV at a CTAB concentration of 2.5 mM, and was used to adsorb plasmid DNA and transfect cells efficiently, representing a potential carrier for DNA vaccines [122].

Cationic liposomes are commonly used as a transfection reagent for DNA, RNA, or proteins and as a co-adjuvant of antigens for vaccination trials. A high density of positive charges close to cell surface is likely to be recognized as a signal of danger by cells or contribute to trigger cascades that are classically activated by endogenous cationic compounds, though carrier/protein or carrier/nucleic acid might have anionic charges and still trigger significant immune responses. There are several cellular pathways, like pro-apoptotic and pro-inflammatory cascades, that can be induced by cationic liposomes, depending on their nature, size, and structural properties (nature of the lipid hydrophilic moieties, hydrocarbon tail, mode of organization) [123]. Their use and design for specific applications such as gene transport or as adjuvants certainly require more knowledge on their structure–function relationship. Excellent reviews are available on this nano-era regarding

applications of nanotechnology in immunology [120,124], progress in prophylactic and therapeutic nanovaccines [124], cancer nano-immunotherapy [125], nanomaterial interactions with the immune system [126], and liposomes formulations for vaccines [127,128].

3. Assemblies Based on Cationic Polymers

Similarly to cationic lipids, cationic polymers constitute another important class of cationic adjuvants despite their often-reported dose-dependent cytotoxicity that requires dose minimization [9,10,65,129–133]. They easily combine with oppositely charged proteins [40,134]. Biodegradable polymeric particles of poly (lactic-co-glycolic acid) (PLGA) have been combined with cationic surfactants or lipids or polymers (CTAB, DODAB, polyethyleneimine (PEI) or ε-poly-L-lysine (PLL)) for improving antigen adsorption, colloidal stability, and the immune response [135,136]. Nanocomplexes of PEI and antigens (influenza hemagglutinin or herpes simplex virus type-2 glycoprotein D) delivered by the mucosal route activated APC in vivo, promoting dendritic cell trafficking to draining lymph nodes besides eliciting a potent immune response against the viral subunit glycoproteins; a single intranasal administration elicited robust antibody-mediated protection [137]. Systemic administration of the same antigens with PEI induced both Th1/Th2 immune responses and higher titers of both antigen-binding and -neutralizing antibodies than alum [138].

The cationic antimicrobial polymer poly (diallyldimethylammonium chloride) (PDDA) is a poly-cation [139–141] able to combine with bovine serum albumin (BSA), yielding NPs with diameters around 50 nm [142,143]. In combination with HIV-1 DNA, nanorods of gold yielded particles of gold/PDDA/DNA, which elicited a Th2 response that was higher than the one obtained using PEI or cetyltrimethylammonium bromide (CTAB). Stimulated cellular and humoral immunity, as well as T cell proliferation, was obtained in comparison with naked HIV-1 Env plasmid DNA treatment in vivo [144]. Recently, NPs of PDDA/ovalbumin were prepared, characterized by their physical properties, and evaluated as stimulators of the OVA-specific immune response [65]. Dynamic light scattering (DLS) showed that these cationic PDDA/OVA NPs at reduced doses of cationic polymer had low size, positive zeta-potential, low polydispersity, good colloid stability, and low cytotoxicity against mammalian cells in culture eliciting potent Th2 OVA-specific immune response (high OVA-specific IgG1 and low OVA-specific IgG2a production); the OVA-specific antibody production was even higher than the one elicited by $Al(OH)_3$/OVA [65].

Polycations combine spontaneously with molecules of opposite charge like proteins and nucleic acids [65,137,142]; thus, the main use of polycations in the biomedical field is the delivery of bioactive molecules including DNA, RNA, and protein [145]. Polycations as adjuvants can be used in a variety of assemblies, ranging from the simple complexation of polymer with antigen driven by electrostatic interactions [65,138,146] to the use of the polymers as particle coatings or particle cores [147]. The spontaneous complexation of polycations with negatively charged antigens is the simplest way to use these systems as antigen carriers. Figure 8 shows the chemical structures of some cationic polymers that have been used as antigen carriers.

Polyethyleneimine (PEI) is an organic, hydrophilic, and cationic polymer that displays a strong positive charge density promoting the combination with negatively charged molecules such as DNA, negatively charged antigens, or plasma membranes [146]. An interesting quality of PEI is its ability to leak from endosomes after cell internalization due to its capacity for avoiding the endosomal acidification; the high number of nitrogen atoms in the PEI molecule makes the polymer an excellent buffer also at low pH [148]. This proton sponge effect is due to deprotonated PEI amino groups binding protons as they are pumped into the lysosome, resulting in the influx of Cl^- ions and water with lysosome osmotic swelling and stretching of the PEI molecule itself due to repulsion between protonated amino groups; thereby, there is rupture of the lysosomal membrane with release of lysosomal contents into the cytoplasm, the so-called endosomal escape leading to a cellular, Th1 response [149,150]. PEI as an adjuvant protects antigens from enzymatic degradation [151], activates the inflammasomes, up-regulates the transcription factor called interferon regulatory factor 3 (Irf-3) [137] and also other

immunostimulatory genes [152], induces Th1 immune response associated with endosomal escape and cross-presentation [153]; administered by the mucosal route, it improves the uptake of antigen and the activation of APCs [137,154]. PEI promotes dsDNA release by host cells triggering the Irf-3-dependent signaling [137]; Irf-3 is a transcription factor related with the activation of innate response by means of the synthesis of type I interferon [155]. Besides Irf-3, PEI activates Nlrp3 inflammasomes, a critical component of the innate immune system, which directs the immune response toward a Th2-biased type [137,138]. PEI as an adjuvant can induce Th1-, Th2-, or Th1/Th2- biased immune response; although PEI has the proton sponge effect to carry out the lysosomal escape, sometimes the escape does not occur, and antigens are presented via MHC class II, resulting in a Th1/Th2 or Th2 response [137,138,146]. PEI/antigen administered by intranasal route induced Th2 response [137], while PEI/antigen administered by a subcutaneous route yielded a Th1/Th2 mixed response [138].

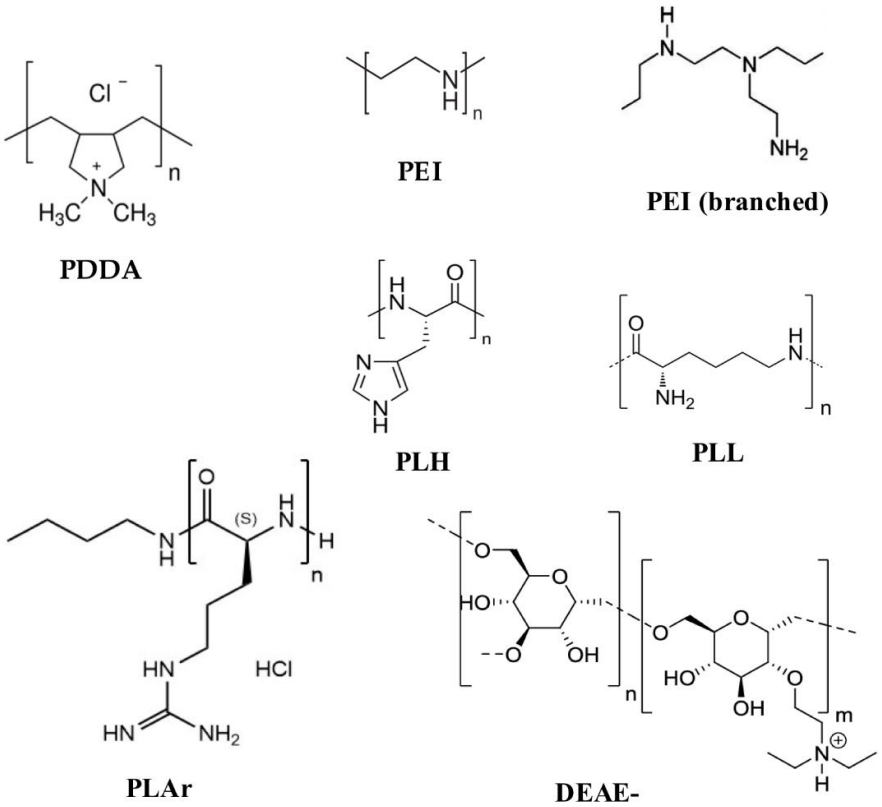


Figure 8. Chemical structures of some cationic polymers: poly (diallyldimethylammonium chloride) (PDDA), linear polyethyleneimine (PEI), branched polyethyleneimine (PEI), poly-L-arginine (PLAr), poly-L-lysine (PLL), poly-L-histidine (PLH), diethylaminoethyl-dextran (DEAE-).

Aiming at improving the mucosal response against major viral pathogens, glycoproteins derived from influenza A virus, herpes simplex virus type-2, or HIV-1 combined with PEI as particles in dispersion, administered as a single intranasal dose induced a robust protection from further lethal viral infection, which was superior to the one elicited by cholera toxin as an experimental mucosal adjuvant; these PEI/antigen nanoparticles were efficiently taken up by APCs in vitro, while in vivo they enhanced the DCs trafficking to draining lymph nodes. The nasal immunization with the recombinant envelope glycoprotein gp140 from HIV-1 carried by PEI induced high titer of antigen-specific IgA in vaginal lavages, demonstrating that nasal immunization can induce a systemic immune response. In Nlrp3-knockout mice, PEI/gp140 complexes elicited a Th1-biased immune response, suggesting

that in normal mice the NPs activated the inflammasome Nlrp3 towards a Th2-type response [137]. In continuation, four different PEI polymers such as linear PEI (40 and 160 kDa) and branched PEI (25 and 750 kDa) were combined with the gp 140 from HIV-1; after immunization, all elicited similar responses characterized by a moderate Th1-biased response. The comparison of PEI with alum showed significantly improved performance of PEI compared to alum. PEI-induced immune response was characterized by an intermediate IgG1/IgG2a endpoint titer ratio, indicating a mixed Th1/Th2 immune response as corroborated from analysis of cytokines profile using antigen-re-stimulated splenocytes from mice immunized with gp140 glycoprotein and PEI. Significant amounts of Th1 cytokines IL-2, TNF-α, and GM-CSF and the Th2-associated cytokine IL-5 were determined [138].

Eliciting a cell-mediated immune response is necessary for achieving effective vaccines against cancer and other major diseases like malaria; thus adjuvants able to enhance the antigen presentation via MHC I are needed. Chen and coworkers reported that PEI/OVA NPs, obtained from mixtures of PEI and OVA, promoted cross-presentation through the major MHC class I pathway. The mouse bone-marrow-derived dendritic cells stimulated in vitro with PEI/OVA NPs resulted in improved and more frequent OVA(257-264)/MHC I complex presentation on dendritic cell surfaces. Besides, DCs pulsed with PEI/OVA NPs but not those pulsed with OVA alone showed significant capacity to stimulate T cells [153]. Using DNA as antigens is an encouraging alternative for designing anticancer therapeutic vaccines. Complexes formed by OVA plasmid and PEI (PEI/DNA) were administered to animals, and the corresponding immune response and antitumor activity were assessed. Animals injected with the PEI/DNA complexes displayed antigen-specific cell lysis, and there was increased antigen presentation via MHC class I and significant lymphocyte infiltration at the intra-tumor inoculation sites; importantly, the vaccine injected either before or after the tumor cell inoculation repressed the tumor growth and increased the survival rate of animals [156].

Poly (diallyldimethylammonium chloride) (PDDA) is a synthetic and linear polycation that combines well with DNA [157,158] or protein [142,143]. Figure 9A,B show scanning electron micrographs of PDDA/OVA nanoparticles (NPs) under low and high magnification, respectively; these NPs elicited OVA-specific Th2 response in immunized mice, which was superior to the one elicited by alum [65].

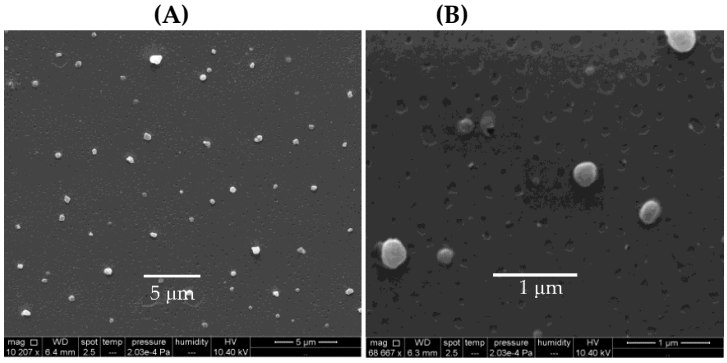


Figure 9. Scanning electron micrographs of PDDA/OVA NPs assembled at 0.1 mg·mL^{-1} OVA and 0.01 mg·mL^{-1} PDDA obtained under low (**A**) and high magnification (**B**). At the low PDDA dose employed, PDDA cytotoxicity was not significant against cells in culture. Reprinted from [65].

Biomedical uses for PDDA have mostly focused on the design of biosensors [159], transfection [158], or antimicrobial chemotherapy [139–141,160–163] probably due to its high toxicity [65,129]. PDDA, when combined with OVA, in water, formed cationic, nano-sized, and stable NPs that displayed a dose-dependent cytotoxicity, which could be easily controlled from the use of low doses. Interestingly, PDDA/OVA NPs induced a potent Th-2-type immunity (high ratio IgG1:IgG2a) and elicited an OVA-specific IgG1 antibody production higher than the one induced by OVA or $Al(OH)_3$/OVA; PDDA/OVA NPs displayed low cellular immune response as determined from footpad swelling tests

for detecting the delayed-type hypersensitivity reaction (DTH) and the low elicited production of IgG2a quantified in serum, both in immunized mice [65].

An important biomolecule that can be carried by cationic polymers is DNA, essential for DNA vaccines despite its relative delivery inefficiency when compared to viral vectors [164]. Cell internalization of the polyplexes (cationic polymer/DNA) and subsequent release of their cargo requires translocation across endosomal and/or nuclear membranes, a determinant factor for therapeutic efficiency, and hence, potential clinical impact. Polyplexes or lipoplexes (cationic lipid/DNA) essentially follow a similar intracellular route once captured by endocytosis [165,166]. Figure 10 shows the intracellular trafficking of a fluorescently labeled oligo-deoxynucleotide (ODN) carried in PEI/fluorescein isothiocyanate-labelled ODN (FITC-ODN) polyplexes; fluorescence is firstly inside the endosome, then in the cytosol after escaping from the endosome due to the endosomal burst, and finally in the cell nucleus as reproduced from ur Rehaman et al. 2013 [166]. The limited efficiency of ODN delivery to the nucleus relates to the fact that most endosomes did not burst.

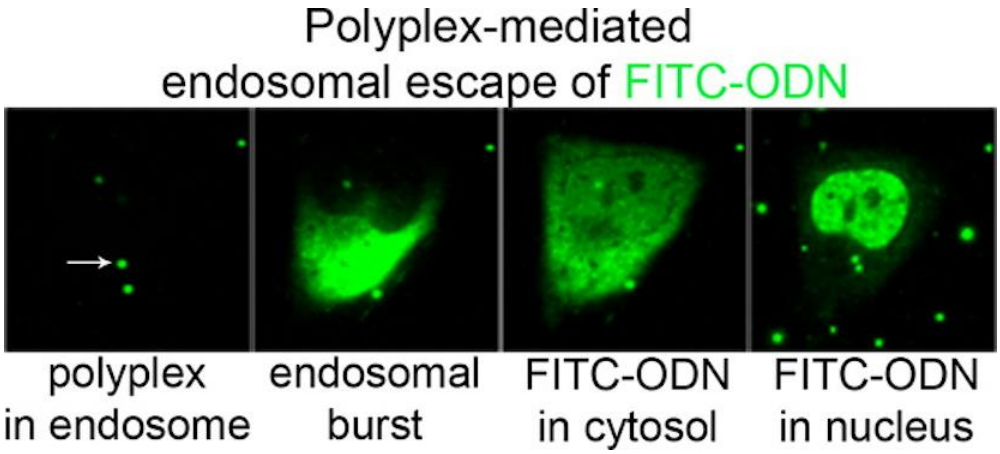


Figure 10. PEI-mediated cytosolic delivery of oligonucleotides occurs by endosomal bursting. HeLa cells were incubated with polyplexes carrying fluorescein isothiocyanate labeled oligo-deoxy nucleotides (FITC-ODNs) in green and monitored by time-lapse microscopy. Following internalization of the poly (ethylene imine) (PEI) polyplexes in endosomes, endosomal bursting occurs causing the release of ODNs into the cytosol. After an initial appearance throughout the cytosol, the ODNs rapidly accumulate in the nucleus. Reprinted from [165] with permission from 2013 American Chemical Society.

Diethylaminoethyl-dextran (DEAE-) polymer is a quaternary ammonium compound that contains three basic groups with different pKa values [167]. The polymer facilitates the adsorption and penetration of viral particles or bacteria into cells, suggesting that it is adequate for delivering antigens into the APCs [168]. DEAE- has delivered Venezuelan equine encephalomyelitis virus [169] and whole-cells *Vibrio cholerae* Inaba and Ogawa serotypes vaccines [170], although its adjuvant properties have been explored mainly for use in vaccines for veterinarian treatment [171]. DEAE-Dextran mixed with formalin-inactivated Venezuelan equine encephalomyelitis virus exhibited a significant adjuvant effect on the primary immune response in rhesus monkeys [169]. In a whole-cell vaccine, DEAE- combined with *Vibrio cholerae* produced a higher and longer-lasting antibody titer than the one elicited by vaccines without adjuvant; furthermore, there was a greater protection against cholera re-infection [170]. In a breast cancer model, DEAE- induced the production of IFN-beta inhibiting the gene expression of the vascular endothelial growth factor (VEGF) gene and the NOTCH1 gene both related to angiogenesis and tumorigenesis [172].

Poly (2-aminoethyl methacrylate) (PAEM) homopolymers with defined chain length and narrow molecular weight distribution were synthesized using atom transfer radical polymerization (ATRP) so that PAEM of different chain lengths (45, 75, and 150 repeating units) showed varying strength

in condensing plasmid DNA into narrowly dispersed nanoparticles. Longer polymer chain length resulted in higher levels of overall cellular uptake and nuclear uptake of plasmid DNA, but shorter polymer chains favored intracellular and intranuclear release of free plasmid from the polyplexes. Using a model antigen-encoding ovalbumin plasmid, transfected DCs activated naïve CD8(+) T cells to produce high levels of interferon-γ. Efficiency of transfection, DC maturation, and CD8(+) T cell activation showed varying degrees of polymer chain-length dependence, showing the importance of using structurally defined cationic polymers as carriers for DNA vaccines [173]. This model study emphasized the importance of well-defined chain length for cationic polymers in DNA vaccines; this type of cationic polymer poly (2-aminoethyl methacrylate) was also recently reviewed for exploring structure–function relationship while delivering DNA [174]. Excellent reviews are available on micro- and nanoparticles for DNA vaccine delivery [175] and on molecular delivery of plasmids for genetic vaccination [176].

Polyaminoacids are another important class of polycations used for carrying antigens in vaccine formulations [177]. Like other polycations, one major advantage of using them is their ability to combine spontaneously with molecules of negative charge, a phenomenon driven for electrostatic interactions. Within the group of polyaminoacids, poly-L-lysine and poly-L-arginine are among the most studied as adjuvants. For instance, poly-L-arginine on the surface of microcapsules obtained by layer-by-layer or spray-drying techniques supports the particles' uptake by the APCs [178,179]. Promising research reported the use of poly-L-arginine for carrying tumor antigen-derived peptides for synthesizing a synthetic antitumor vaccine; the work described that the subcutaneous injection of a mixture of poly-L-arginine and peptides induced a large number of antigen-specific T cells detectable in the systemic circulation for more than four months. Another important finding reported by the authors was the presence of numerous APCs loaded with antigen in the draining lymph nodes of vaccinated animals, suggesting that poly-L-arginine is a suitable carrier for targeting antigens into the lymph nodes. An additional relevant result is the absence of antibodies against poly-L-arginine, allowing this compound to be used for numerous booster injections [180].

Employing TLR agonists as adjuvants is an attractive alternative for stimulating a specific type of immunity like a Th1-biased response. Negatively charged TLR agonists could also be easily attached to polycations by electrostatic interactions [138]. The adjuvant activity of combinations between CpG ODN (ligand for Toll-like receptor 9) and different polycations such as poly-L-arginine, poly-L-lysine, poly-L-histidine, or chitosan in an OVA vaccination model, as well as poly-L-arginine and poly-L-histidine, but not poly-L-lysine or chitosan, improved efficiently both the IgG antibody production and the number of splenocytes secreting IFN-gamma after T CD8+ ex vivo stimulation. CpG-ODN/poly-L-arginine is better than complete Freund's adjuvant and aluminum salt as adjuvants and did not induce local toxicity [181]. The assembly of poly-L-arginine, CpG-ODN, and synthetic peptides induced an improved peptide-specific immune response as compared to the application of peptides with either of the immunomodulators alone. Poly-L-arginine synergized with oligodeoxynucleotides containing CpG-motifs (CpG-ODN) for enhanced and prolonged immune responses and prevented the CpG-ODN-induced systemic release of pro-inflammatory cytokines; CpG-ODN are known to be potent inducers of predominantly type 1-like immune responses, while polycationic amino acids, facilitate the uptake of antigens into antigen-presenting cells (APCs). The potentially harmful systemic release of pro-inflammatory cytokines induced upon injection of CpG-ODN was inhibited and long-lasting, and high numbers of antigen-specific T cells could be observed from fluorescence-labeled OVA even after only one injection of the vaccine [182].

Cationic polymers are also used for coating or functionalizing different types of NPs, namely, magnetic NPs, metallic NPs, ceramic NPs, hydrophobic NPs, or biocompatible polymer-based NPs. For instance, PEI has been used for coating SPIONs [19,183,184], silica NPs [185], or gold NPs [144,186]. Cationic and nanosized PEI-coated SPIONs in vitro activate macrophages and polarize them to an M1-like phenotype [184]. PEI-coated SPIONs obtained from the sonication of iron oxide suspension and PEI solution was used for carrying the plasmid-malaria DNA vaccine encoding VR1020-PyMSP119;

the intraperitoneal administration of the complex displayed high titers of antigen-specific IgG1 and IgG2a and improved the immunological memory after vaccination [19]. Another example of metallic nanoparticles functionalized with polycations was reported for Xu and coworkers; they coated gold nanorods with the polycations PEI or PDDA or with the surfactant CTAB and attached therapeutic HIV-1 DNA-vaccine. Gold nanorods coated with both polycations show the best capacity for packing DNA, and they were uptaken by DCs in a higher level than the ones coated with CTAB; polycation-coated gold nanorods induced a significant increase of the cellular and humoral immunity as determined by antibody titers (IgG1/IgG2 ratio) and T cell proliferation. It was also described that PDDA enhances a Th2 whereas PEI induces a Th1/Th2 immune response [144].

In situ silicifications and capping treatment produced PEI–silica–PEI coatings on Japanese encephalitis virus vaccine maintaining its immunogenicity better than the vaccines without adjuvant; this fact could be relevant in cases where keeping the vaccine under refrigerated condition is difficult [187]. PEI coating mesoporous silica micro-rods (MSR-PEI) significantly enhanced the antigenicity of a peptide antitumor vaccine. The antigen was coupled to the microstructure by simple adsorption enhancing host DCs activation and T cell response compared to controls; MSR-PEI/E7-peptide eradicated large established TC-1 lung tumors in ~80% of mice and generated immunological memory; MSR-PEI vaccine, using a pool of neoantigens, eliminated established lung metastases and controlled tumor growth [188].

Carboxylated polystyrene particles conjugated covalently with poly-L-lysine carried a DNA vaccine improving the immune Th-1 response; C57BL/6 mice were immunized with the NPs carrying an OVA plasmid yielding a high level of activated CD8 T cells and OVA-specific antibodies. The animals immunized with the poly-L-lysine-coated polystyrene NPs generated a significant antitumor response evidenced by the inhibition of tumor growth after challenging with the OVA expressing EG7 tumor cell line; NPs with diameters of 50 nm yielded the best activity [189].

In summary, polycations can be excellent adjuvants for vaccines, but a quantitative determination of toxicity should always be performed for determining the minimal doses where toxicity is absent and the adjuvant effect still occur; this includes also the equally toxic cationic polyaminoacids. One should notice also that cationic polymers in general are potent antimicrobials as often reviewed [139].

4. Hybrid Cationic Assemblies of Biocompatible Polymer/Cationic Polymer

Hybrid cationic polymer/biocompatible polymer assemblies are useful for improving the characteristics of delivery systems. For example, the use of biocompatible polymers decreases the toxicity of the systems, whereas the cationic polymers improve the colloidal stability, antigen loading capacity, and APCs internalization. Some researchers have used this approach for achieving improved delivery systems [136,190,191].

Biocompatible synthetic or natural polymers can improve body functions without interfering with its normal functioning or triggering side effects [192–194]. Some examples of biocompatible polymers are poly (lactic-co-glycolic acid) [195], poly (ε-caprolactone) (PCL) [196], poly (lactic acid) [197], poly (3- hydroxybutyrate-co-3-hydroxyvalerate) (PHBV) [198], chitosan [199,200], cellulose [201] and poly (acrylates) including poly (methyl methacrylate) (PMMA) [202,203]. Neutral or anionic biocompatible synthetic or natural polymers as polylactide-co-glycolide microparticles have been cationized with cationic lipid DODAB or cationic surfactant CTAB to assure combination with the oppositely charged DNA antigens to design DNA vaccines [135,204]. In another instance, DODAB cationic bilayer surrounded polystyrene sulfate particles available over a range of diameters [205–207] or silica particles [208,209]; recently optimal coverage with single cationic bilayers on the anionic polymeric or inorganic particles was achieved [207,209]. Synthetic biocompatible polymers such as PMMA were also hybridized with cationic polymers or cationic lipids or surfactants [160–163,210–213]. In summary, a variety of model hybrid and cationic delivery systems are already available to combine with a myriad of oppositely charged antigens for vaccine design [25,163,214,215].

In a brief overview, biocompatible polymers interact with biological systems without exerting significant damage or toxicity, displaying characteristics like biodegradability and/or biosorption. Their broad utility has been reported in different areas of medicine including orthopedics, tissue engineering, and drug and vaccine delivery; eventually, these materials also display intrinsic biological activity [192–194,216]. Medical devices or drug delivery systems based on biocompatible polymers have been approved by the Food and Drug Administration (FDA) [192–194,216]. Biocompatible polymers can be natural (e.g., chitosan, alginate, cellulose) or synthetic (e.g., polylactic acid, poly (lactic-co-glycolic acid)); some excellent reviews on biocompatible polymers are available [217,218]. One of the most promising delivery strategies for activating the immune system is the controlled release of antigens from a biodegradable polymeric matrix, the sustained liberation of antigens may induce strong immune responses [216,217]. Many biocompatible polymers have often been used as vaccine adjuvants such as the biocompatible and biodegradable poly (lactic acid) (PLA), poly (lactic-co-glycolic acid) (PLGA), and chitosan [216,219,220]. Figure 11 shows the chemical structures of some biocompatible polymers used for vaccine delivery.

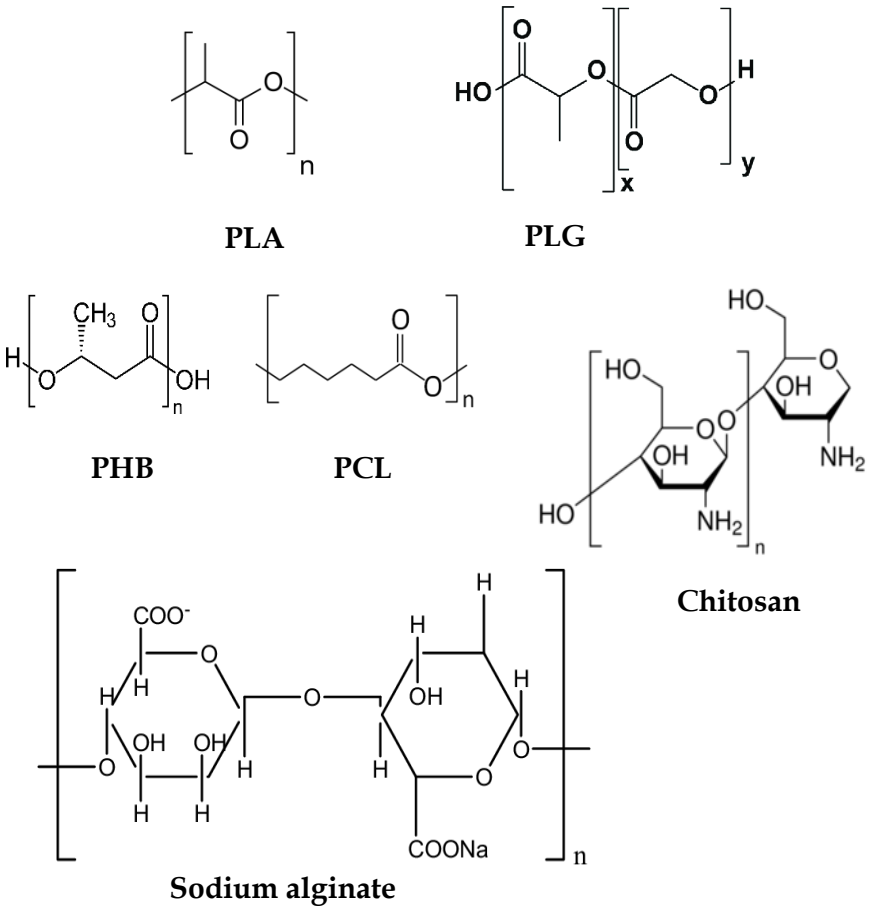


Figure 11. Chemical structure of some biocompatible polymers such as polylactic acid (PLA), poly (lactic-co-glycolic acid) (PLGA), polyhydroxybutyrate (PHB), polycaprolactone (PCL), chitosan, and sodium alginate.

As a first example of combination of cationic polymer and biocompatible polymer, assemblies of PEI and PLGA have often been used in vaccine delivery systems to carry antigens; they enhanced the antigen-specific antibody titer, lymphocyte proliferation, antigen internalization by phagocytic cells, and Th-1 typical cytokines production [136,221,222]. Biocompatible PLGA NPs were coated with

three different cationic polymers, PEI, chitosan, or ε-Poly-L-lysine (PLL), aiming at improving the antigen loading capacity of PLGA NPs and evaluating the immune response against OVA as model antigen. PLGA-PEI/OVA NPs displayed the highest OVA loading capacity and colloidal stability, improved lymphocyte proliferation, CD4/CD8 ratio, increased the production of OVA-specific IgG1 and IgG2a antibodies and the secretion of TNF-α, IFN-gamma, IL-4, and IL-6 [136]. Similarly, the cationic PEI-coated PLGA NPs encapsulating the immunopotentiator *Angelica sinensis* polysaccharide (ASP) significantly activated macrophages, induced the expression of MHC II and CD86 molecules and the production of IL-1β and IL-12p70 cytokines. The adsorption of the porcine circovirus type 2 (PCV2) antigen onto NPs improved the macrophages antigen internalization. Immunized mice significantly improved the production of PCV2-specific IgG and responded with a mixed Th-1/Th-2 biased immune response [221].

Microparticles of PLGA coated with branched or linear PEI were suitable for delivering DNA vaccines demonstrating low cytotoxicity and improvement of APCs internalization [223,224]. In an interesting approach, PEI/DNA complexes were entrapped into PLGA microspheres warranting protection against DNA degradation and efficient uptake by APCs in comparison to the one of naked DNA. The humoral response elicited by PLGA/PEI/DNA against an DNA-HIV-1 antigen was from two to three times higher than one elicited by naked DNA; the cytolytic T lymphocyte at low doses of the antigen was also improved by the complex [224].

Other pairs of polymers used for assembling polymer–polymer hybrid NPs were PLGA/chitosan or PLGA/chitosan-derivatives, these hybrid NPs also improved the uptake rates of antigen by APCs and enhanced the elicited immune response in vivo [191,225,226]. By a modified double emulsion solvent evaporation process, three different NPs based on PLGA were synthesized, chitosan-coated PLGA, glycol-chitosan-coated PLGA, and PLGA NPs, all of them with a diameter smaller than 200 nm and positive zeta potentials; the NPs were used as adjuvants for assessing their capability to induce an enhance immune response. After immunization, glycol-chitosan/PLGA NPs elicited the higher mucosal and systemic response when administered with hepatitis B surface antigen, associated due to in vitro mucoadhesion. Both coated NPs experimented on had less mucosal clearance than PLGA uncoated NPs, resulting in improvement of the immune response [226]; permanence of the vaccine at the mucosa improved the obtained response [226–228]. Slow antigen-releasing N-trimethyl-chitosan-coated-PLGA/OVA NPs with permanent cationic charges yielded high IgA production [229].

Assemblies of PLA with cationic polymer physical properties and immunoadjuvant activity were described [230,231]. Polycation-coated PLA NPs increased the expression of MHC and co-stimulatory molecules, enhanced cytokine production, activated and induced maturation of APC, and improved antibody titer [147,227]. PLA microspheres coated with PEI or chitosan or chitosan chloride significantly increased the loading antigen capacity according to the increment of surface charge; coating PLA microspheres with polycations also augmented the macrophages uptake rates of the adsorbed hepatitis B surface antigen, the expression of CD86, MHC I, MHC II, and the secretion of IL-1β, IL-6, TNF-α, and IL-12. Intraperitoneal administration of cationic microspheres carrying the antigen improved the production of antibodies as compared with aluminum-based adjuvant and free antigen; besides, the cationic microspheres elicited a Th-1 biased showing the assemblies adequacy for performing antiviral, antimalaria, and antitumor vaccines [227].

Chen and coworkers tested chitosan-decorated PLA microspheres carrying hepatitis surface antigen administered via commonly used parenteral administration routes and obtained robust immune responses such as maturation of DCs with overexpression of CD40, CD80, and IL-12 in contrast with the absence of these responses when aluminum-based adjuvant was used; in vivo tests showed increased IgG production induced by both the MPs and the alum-based adjuvants; only the MPs administered by intramuscular route could induce high IgG2a titer, Th-1 cytokines (IL-2, IL-12, and IFN-γ) and Th-2 cytokine IL-4 secretions, demonstrating that PLA-coated NPs improve the cellular and humoral

response [147]. Figure 12 shows a scanning electron micrograph of PLA microparticles coated by chitosan chloride and gives details on mean diameter, zeta-potential, and antigen loading [147].

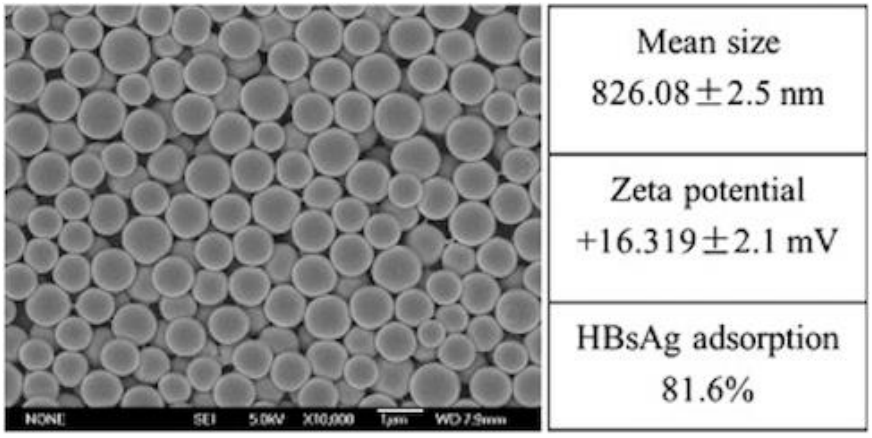


Figure 12. Scanning electron micrographs and dynamic light scattering Zetasizer analysis were used to characterize PLA microparticles (MP) modified by cationic chitosan chloride surface coating. Antigen adsorption was calculated by comparing the amount of antigen in supernatants after centrifugation with total input antigen (protein concentration was analytically determined). The load of HBsAg/particles was 3.2 (μg/mg). Reprinted from [147] with permission from Elsevier, Copyright 2014.

Alginate and chitosan are two versatile biopolymers widely used in drug delivery systems, as they are oppositely charged and it is relatively simple to obtain hybrid systems from them. Taking advantage of the physical–chemical properties of those polymers, one can obtain interesting systems for carrying a myriad of antigens like protein, DNA, or RNA antigen; for instance, it is possible to encapsulate the cargo into the hybrid assembly or to obtain surfaces positively or negatively charged for adsorbing antigens. Regarding the adjuvant properties, one of the main limitations of oral vaccines is that antigens suffer degradation into the gastric cavity losing their native structures and antigenicity; using alginate and chitosan, it is possible to avoid this phenomenon [232–234]. In an interesting work where hybrid NPs from chitosan and alginate were synthesized for vaccine delivery, it was shown that alginate coating antigen/chitosan complex is a good strategy for avoiding antigen degradation from gastric environment. The system showed a pattern of controlled release and low in vitro toxicity; furthermore, alginate/chitosan hybrid NPs elicited systemic and mucosal immune response exhibiting the highest titer of antibody as compared with the controls [234]. However, alginate/chitosan hybrid anionic NPs failed in inducing a Th1 response when the NPs and a hepatitis B virus antigen were administered by the subcutaneous route in a mouse model [235].

Alginate and PLL were assembled as NPs by ionotropic complexation method. The NPs displayed a diameter between 130 and 850 nm, a negative zeta-potential, and a sustained-release behavior regarding the encapsulated BSA. Additionally, the system showed low cytotoxicity and significant increment of BSA internalization in vitro [236].

Hybrid NPs from combinations of biocompatible and cationic polymers have been less studied as antigen carriers. For example, hybrid systems between PEI and alginate are little explored in the context of vaccine delivery, although there is evidence that the two polymers form complexes by electrostatic interactions [237]; combinations of PEI with alginate reduce significantly the toxicity of the polycation favoring the degradation of PEI [238]. Alginate/PEI hybrid systems formed nanogels able to incorporate and deliver antigens enhancing both cellular and humoral response. Nanogels facilitated antigen uptake by mouse bone-marrow DCs; promoted intracellular antigen degradation and cytosolic release, and increased antigen presentation via MHC I and II, vaccine-induced antibody

production, and CD8+ T cell-mediated tumor cell lysis, suggesting that the nanogels are potent immunoadjuvants [239].

PEI-coated PMMA NPs synthesized by emulsion polymerization combined well with DNA and are a suitable alternative for gene delivery, showing low cytotoxicity and high transfection capacity [240,241]; however, these works did not report evidence of the immunoadjuvant activity of those assemblies.

Using emulsion polymerization of the two co-monomers, interesting functionalities were reunited in the same polymeric particle: the cationic moiety represented by the quaternary ammonium nitrogen of comonomer 1 and the hydrophilic poly (ethyleneglycol) chains of comonomer 2; thereby poly (methylmethacrylate) (PMMA) was covalently modified to yield core–shell cationic nanoparticles that enhanced cellular responses induced by HIV-1 Tat DNA vaccination. These biocompatible core–shell cationic nanoparticles, composed of an inner hard core of poly (methylmethacrylate) (PMMA) and a hydrophilic tentacular shell bearing positively charged groups and poly (ethyleneglycol) chains covalently bound to the core electrostatically and reversibly adsorbed DNA, efficiently delivered it intracellularly and were not toxic in vitro or in mice [242]. Furthermore, two intramuscular (i.m.) immunizations (4 weeks apart) with a very low dose (1 microgram) of the plasmid PCV-tat delivered by these nanoparticles followed by one or two protein boosts induced significant antigen-specific humoral and cellular responses and greatly increased Th1-type T cell responses and CTLs against HIV-1 Tat [242]. Along similar lines, PEG was covalently bound to the cationic polymer poly (2-aminoethyl methacrylate hydrochloride) in order to improve the stability of nanstructures in vivo [243]. Figure 13 shows the core–shell microparticles obtained by Castaldello and coworkers, 2006, incorporating both functionalities, cationic charge and the stability, in aqueous medium imparted by PEG [242].

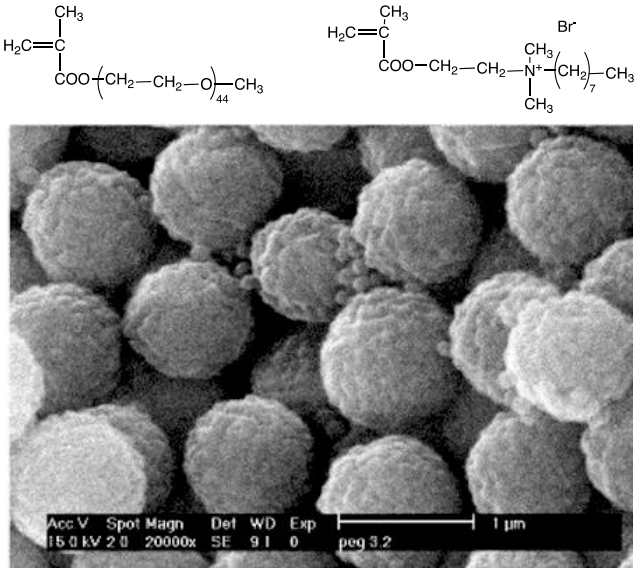


Figure 13. Scanning electron micrograph of PMMA core–PEG shell microparticles where the hydrophilic non-ionic co-monomer poly (ethylene glycol) methyl ether methacrylate and the cationic co-monomer 2-(dimethyloctyl) ammonium ethyl methacrylate bromine were used in the emulsion polymerization reaction. Reprinted from [242] with permission from Elsevier, Copyright 2011.

Non-covalent nanoparticle (NP) assemblies of PMMA, a synthetic, non-charged, and biocompatible polymer, and PDDA polycation have been described earlier by our group since the first report on the good compatibility and miscibility of PDDA with PMMA evaluated from microbicidal PMMA/PDDA NPs [160–163,210–214]. The synthesis of PMMA NPs by emulsion polymerization of MMA in the presence of PDDA yielded cationic, homodisperse, and stable NPs [160,212], which are presently being

evaluated in our group for possible applications as immunoadjuvants. In summary, it is possible to take advantage of the biocompatibility of PMMA and the cationic character of PDDA to investigate novel applications for these assemblies obtained in absence of any covalent linkage between the polymers. In addition, our group recently synthesized and characterized hybrid NPs from PMMA, PDDA, and surfactants that could be excellent alternatives for carrying antigen due to the combination of the biocompatibility of PMMA with the adjuvant properties of the cationic polymer PDDA and/or the cationic lipid DODAB [65,161,162]. Figure 14 shows the core–shell PMMA/PDDA NPs and a schematic picture of their nanostructure with PMMA in the core and PDDA non-covalently bound to PMMA, forming a surrounding shell [214]. One should notice that the hydrophobic PMMA is in the core and the cationic and hydrophilic PDDA is in the shell; upon increasing the ionic strength, the shell can collapse due to the screening of the PDDA charges [19–71].

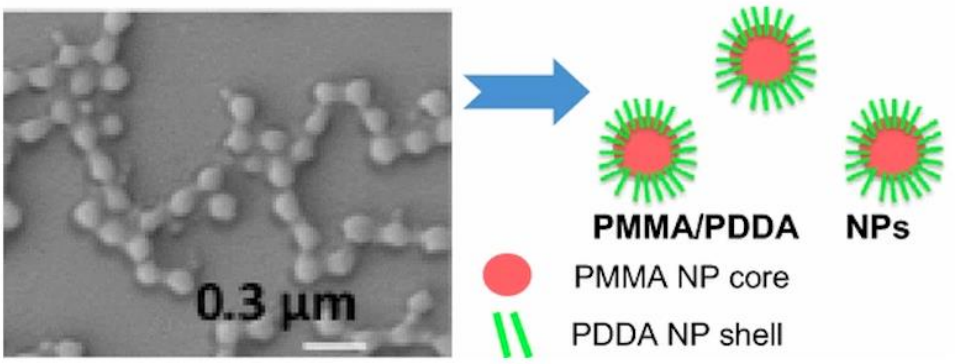


Figure 14. Scanning electron micrograph of PMMA/PDDA NPs and schematic representation of the PMMA/PDDA NPs structure with their core–shell nanostructure that occurs at low ionic strength. Reproduced from reference [160].

Antigen endosomal escape has been observed for protein loaded in cationic and porous maltodextrin NPs [244]. Figure 15 illustrates the endosomal escape or permanence of two types of cationic maltodextrin NPs, those modified with anionic lipids in their cores (named $DGNP^+$) and those with cationic cores (named NP^+). The OVA/NPs intracellular traffic was determined from fluorescence-labeled OVA. Both types of NPs efficiently delivered OVA to cells; however, whereas those with the anionic inner core delivered OVA to the cytosol and endoplasmic reticulum, those with the cationic core were less able to release OVA in the cytosol and delivered it to the endosomes. One should notice the punctuated distribution pattern of OVA delivered by NP+ into cells, typical of endosomal localization and the diffused OVA localization throughout the cytoplasm when OVA was delivered with DGNP+ NPs. Both NPs increased intracellular proteolysis of OVA; however, DGNP(+) facilitated OVA escape from endosomes [244].

Cancer vaccines targeting patient-specific tumor neo-antigens have recently emerged as a promising component of the immunotherapeutic treatment against the disease [245,246]. However, neo-antigenic peptides typically elicit weak $CD8^+$ T cell responses, so there is a need for universally applicable vaccine delivery strategies to enhance the immunogenicity of these peptides. Ideally, such vaccines could also be rapidly fabricated using chemically synthesized peptide antigens customized to an individual patient. An interesting approach for implementing the combination between biocompatible polymer and cationic polymer was achieved with the biocompatible propyl-acrylic acid and cationized antigen from covalently binding decalysine peptide to the antigen and then assembling this with the biocompatible polymer via electrostatic assembly; these NPs promoted cytosolic delivery of the antigen and MHC I presentation [245,247]. In addition, poly (acrylic acid) derivatives as mucoadhesive polymers might increase the epithelial permeability for carried antigens or drugs after easily crossing the mucus layer of the mucosae. The attachment to the mucus layer

could be achieved by exclusively non-covalent bonds such as ionic interactions, hydrogen bonds, and van der Waal's forces, leading also to a certain extent to opening of the tight junctions [248]. Figure 16 shows a schematic representation of the electrostatically stabilized NPs assembled by mixing decalysine-modified antigenic peptides and poly (propyl acrylic acid) (pPAA) poly-anion. NPs increased and prolonged antigen uptake and presentation on MHC-I (major histocompatibility complex class I) molecules expressed by dendritic cells with activation of $CD8^+$ T cells. The suitable intranasal immunization route inhibited formation of lung metastases in a murine melanoma model; further addition of the adjuvant α-galactosylceramide (α-GalCer) stimulated robust $CD8^+$ T cell responses, significantly increasing survival time in mice with established melanoma tumors [245]. On Figure 16a, poly (propylacrylic acid)-cationic peptide nanosized assemblies aiming at enhancing antigen endosomal escape and MHC-I antigen presentation are prepared. On Figure 16b, one should notice the simple simple and rapid mixing of decalysine-modified antigenic peptides with poly (propylacrylic acid) (pPAA) forming antigen-loaded nanoplexes, which are electrostatically stabilized nanoparticles. On Figure 16c the scheme shows the nanoplexes promoting cytosolic antigen delivery via endosomal escape, resulting in enhanced levels of antigen presentation on class I major histocompatibility complex (MHC-I).

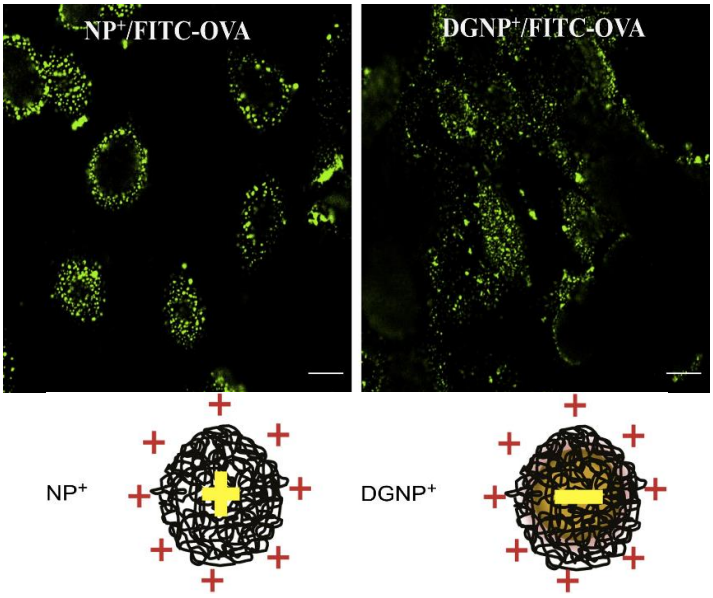


Figure 15. Comparison of ovalbumin (OVA) intracellular delivery by maltodextrin porous nanoparticles with outer and inner cationic charges (NP+) or outer cationic/inner anionic charges (DGNP+) using confocal microscopy to visualize OVA labeled with fluorescent markers (FITC-OVA). NP+ and DGNP+ were loaded with FITC–OVA and incubated for different periods with 16HBE cells. After 30 min incubation, cells were washed with PBS and fixed with 4% PAF. Intracellular FITC–OVA was visualized by confocal microscopy. Scale bar = 10 μm. Adapted from [244] with permission from Elsevier, Copyright 2012.

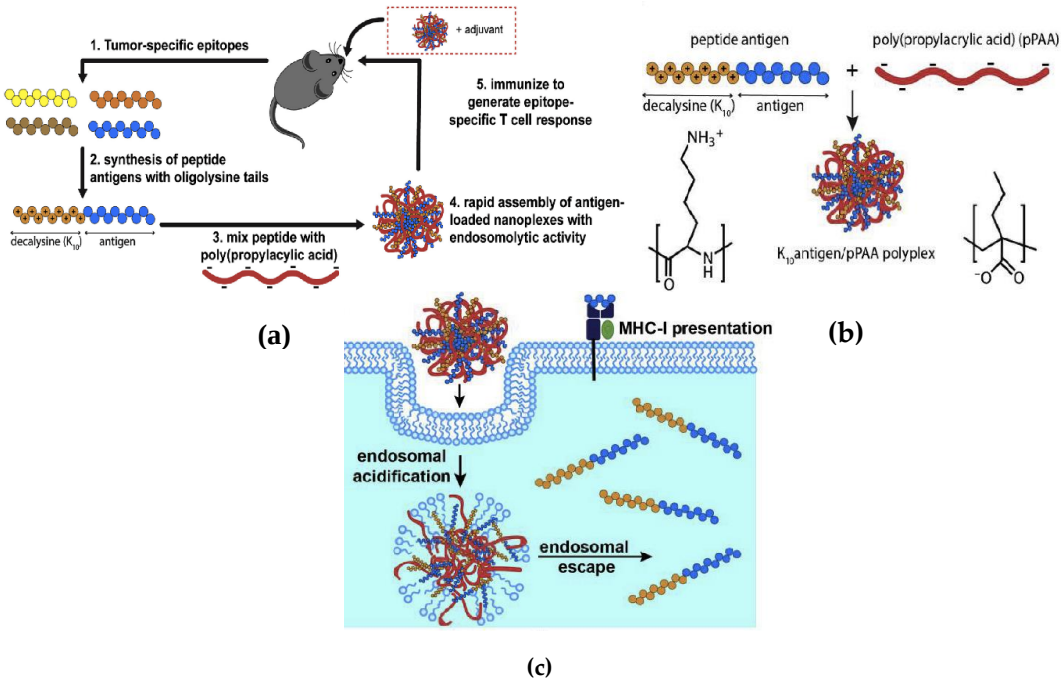


Figure 16. (**a**) Poly (propylacrylic acid)-cationic peptide nanosized assemblies for enhancing antigen endosomal escape and MHC-I antigen presentation. (**b**) Assembly of antigen-loaded nanoplexes via simple and rapid mixing of decalysine-modified antigenic peptides and pPAA, which generates electrostatically stabilized nanoparticles. (**c**) Schematic representation of nanoplexes promoting cytosolic antigen delivery via endosomal escape, resulting in enhanced levels of antigen presentation on class I major histocompatibility complex (MHC-I). Reprinted from [245] with permission from Elsevier, Copyright 2018.

Inside the endosome, PLGA erosion with release of the glycolic or lactic acids further reduced the pH, improving the antigen degradation and presentation through MHC-II [249,250]. Oral administration of antigens may lead to their uptake by microfold cells (M cells) in Peyer's patches of intestine to initiate protective immunity against infections, but limitations such as the lack of specificity of proteins toward M cells and degradation of proteins in the harsh environment of gastrointestinal (GI) tract had to be overcome. Mucoadhesive vehicle of thiolated eudragit (TE) microparticles transported an M cell-targeting peptide-fused model protein antigen [251]. Thereby, oral delivery of TE microparticulate antigens exhibited high transcytosis of antigens through M cells resulting in strong protective sIgA as well as systemic IgG antibody responses. The delivery system not only induced CD4+ T cell immune responses but also generated strong CD8+ T cell responses with enhanced production of IFN-γ in spleen [251]. Along similar lines, the mucoadhesive, cationic, and biocompatible chitosan in combination with poly-ε-caprolactone yielded NPs effective in immunization against influenza [252].

In conclusion, hybrid assemblies of polycation and biocompatible polymer have the advantages of reducing the toxicity of the cationic polymer and adding the interesting properties of muco-adhesiveness so important for mucosal vaccines.

5. Cationic Assemblies of Lipid–Polymer and Polymer–Lipid

Assemblies obtained from combining lipids and polymers gather the benefits of lipids' amphiphilic nature, possibility of high organizational level in the lipid-based structures, and the mechanical and resistance advantages offered by polymers; blending these materials, it is possible to overcome major limitations like degradation of bioactive incorporated principles, short circulation time of drugs and vaccines, and lack of controlled release [253,254]. Diverse types of arrangement between lipids and

polymers have been described; in general, these hybrid assemblies could be classified as lipid–polymer or polymer–lipid, depending on the position of each material in the hybrid structure; either the polymer or the lipid is in the inner part the nanostructure. In addition, polymer and lipid may mix, driven by intermolecular interactions, so that the lipid may become embedded in the polymer matrix displaying good compatibility with the polymer [210,212,213,253,254].

Lipids and polymers can assemble as hybrid materials driven by attractive, non-covalent, and weak but frequent multipoint interactions. For example, lipid deposition from charged bilayers onto oppositely charged spherical solid cores such as polymeric nanoparticles [37,205,255], silica [208,256–258], or hydrophobic drug aggregates [38,259] led to interesting and bioactive hybrid nanoparticles. The so-called biomimetic, lipid–polymer, or polymer–lipid NPs have been finding applications in biomolecular recognition [260], drug delivery [259,261–263], vaccine design [9,10,16,18,21,25,28,46,163], and antimicrobial chemotherapy [131,139–141,160,163,207,211,212,263–271].

The principal forces driving bilayer deposition onto hydrophobic or hydrophilic nanoparticles or surfaces from bilayer vesicles or bilayer fragments (BF) are the electrostatic attraction, van der Waals attraction, and/or the hydrophobic effect [37,205,255,256,258]. Medium composition, pH, and the ratio between the surface areas of the particles (Aparticles) and bilayers (Abilayers) also play a crucial role in achieving the optimal bilayer deposition on the particles: this ratio should be around 1 for complete coverage of all particles with bilayers [38,208,259–263]. The amount of added lipid must be sufficient to surround all particles in the dispersion with one bilayer; otherwise, poor colloidal stability may result with formation of aggregates. Figure 17 illustrates some possible interactions between one bilayer vesicle and two particles, vesicle, and particles with similar sizes [206].

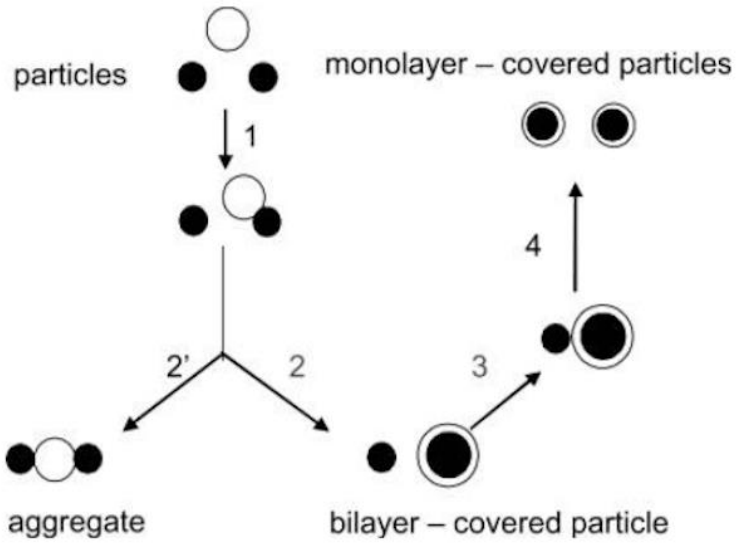


Figure 17. The interaction between one bilayer vesicle and two particles. In the first step (step **1**), electrostatic and/or van der Waals and/or hydrophobic attraction leads to aggregation of a vesicle and a particle. These same interaction forces may disrupt the vesicle bilayer and promote bilayer adsorption onto the microsphere (step **2**) and/or further aggregation with the other microsphere (step 2'). The adsorbed bilayer may attract the second microsphere (step **3**). The hydrophobic interaction between an eventually hydrophobic surface and the hydrocarbon chains in the bilayer may completely destroy the bilayer structure, flip-flopping the hydrocarbon chains onto the particle surface and generating a monolayer coverage on each microsphere (step **4**). Adapted from [206] with permission from Elsevier, Copyright 1999.

When lipid bilayers are the starting nanostructure, their physical state is an important factor determining lipid–particle interactions; bilayer vesicles in the rigid gel state do not disrupt upon

adhesion onto solid particles, so bilayer coverage does not take place [272]. For avoiding this difficulty, either the lipid has to be changed to a lipid able to form bilayers in the liquid-crystalline, more fluid state at room temperature, or flat and open bilayer fragments of the charged lipid (BF) has to be used. BFs not only can adsorb onto solid particles but also can independently function as scaffolds for deposition of a variety of bioactive molecules such as peptides [207,265,267,268], drugs [131,207,259,263, 264,269], antimicrobial polymers [139,141,163,266,273], proteins [21,25,28,40,46,140,141,163,260,264], oligonucleotides [16,46], or nucleic acids [41,42]. Adhesion of a DODAB vesicle layer onto the rough and highly hydrated surface of cells was electrostatically driven; cationic closed vesicles of DODAB at low ionic strength surrounded bacterial cells as a vesicle layer [274]; the absence of DODAB vesicle disruption upon interaction with the bacteria was depicted from absence of (14C)-sucrose leakage from the large vesicles in experiments where this marker was used to label the inner water compartment of the vesicles [275]. Given the quaternary ammonium moiety of the DODAB molecule, its antimicrobial effect was systematically evaluated and its differential cytotoxicity was reviewed [38].

Charged BFs are easily obtained from vesicles by ultrasonic disruption and have been used for the production of a variety of lipid-based biomimetic particles [37–39,41]. Deconstruction of the bilayer by solubilizing cationic lipid and drug or biocompatible polymer in a common solvent has also been a useful approach; this successfully allowed the obtaining of hybrid nanoparticles of hydrophobic drug/cationic lipid/ethanol in water dispersion surrounded or not by the biocompatible carboxy methyl cellulose biopolymer [276]. Another successful strategy was the optimization of single bilayer deposition onto silica nanoparticles from lipid films [209]. In order to ascertain whether bilayer coverage indeed took place, size distribution, polydispersity, and zeta-potential are often determined from dynamic light scattering (DLS) techniques [277] complemented by morphology evaluation from advanced electron microscopy techniques [131,160,212] and quantitative methods for obtaining adsorption isotherms [209]. Figure 18 shows some adsorption isotherms of the cationic lipid DODAB from DODAB films or from pre-formed bilayers onto silica particles where maximal adsorption values yielded an adsorbed amount consistent with bilayer deposition on silica for depositions from DODAB films [209].

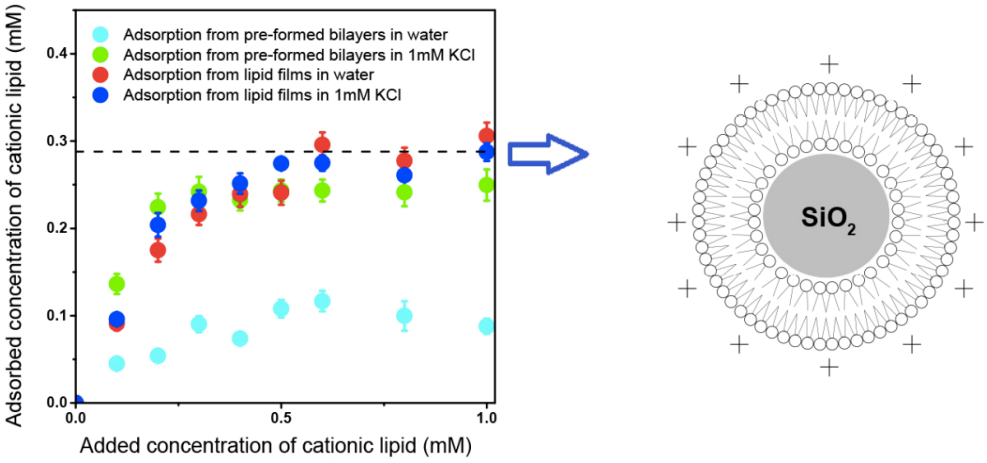


Figure 18. Adsorption isotherms for DODAB from films or pre-formed bilayer fragments (BF) onto silica (2 mg/mL). The dashed line at 0.288 mM DODAB represents the theoretical concentration corresponding to bilayer adsorption. Reproduced from [209].

If the lipid bilayers and the particles are oppositely charged, poor colloidal stability occurs at a critical lipid concentration where the size is maximum and the zeta-potential is zero [10,18,205,208,259, 263]. Above this critical lipid concentration, the particles exhibit zeta-potentials that are similar to that of the charged bilayer and recover colloidal stability [10,18,205,259]. Aggregates of hydrophobic drugs

dispersed in water have also been treated as particles and coated with lipids at high drug-to-lipid molar ratios [140,259,263]. More recently, protocols have evolved to employ bilayer disassembly and biopolymers for stabilization of very hydrophobic drugs such as indomethacin [163,276].

BFs combine well with several antigens and are available as cationic (made of DODAB) or anionic nanostructures (made of the anionic and synthetic lipid sodium dihexadecylphosphate or DHP), allowing combinations with both positively and negatively charged antigens. Transmission electron micrographs of DODAB BF [278] and DHP BF [279] are on Figure 19A,B, respectively.

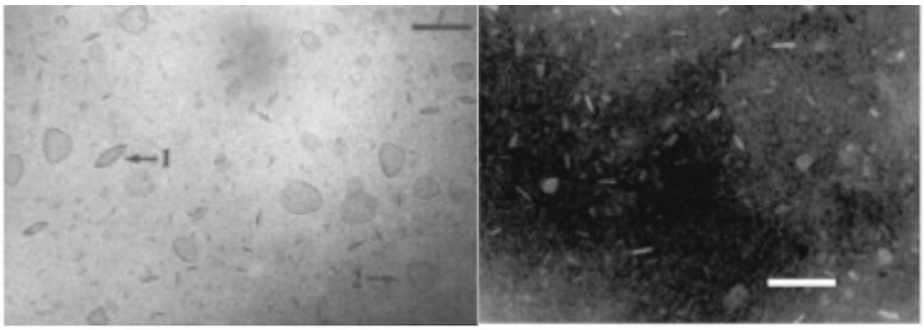


Figure 19. Lipid bilayer fragments of cationic and anionic synthetic lipids. (**A**) Bilayer fragments of dioctadecyldimethylammonium bromide (DODAB) visualized by cryo-transmission electron micrograph. Adapted from [278] with permission from 1995 American Chemical Society. (**B**) Bilayer fragments of sodium dihexadecylphosphate (DHP) visualized by transmission electron micrograph after negatively staining the sample. Disks were observed edge-on or face-on. Bars denote 100 nm Adapted from [279] with permission from 1991 American Chemical Society [278,279].

DODAB BFs loaded or unloaded with antibiotics were covered consecutively by a carboxymethylcellulose (CMC) and a poly (diallyl dimethyl ammonium chloride) (PDDA) layer [131,141] being efficiently captured by macrophages to deliver their antibiotic cargo against difficult intracellular pathogens, as are the mycobacteria [270]. The activity of DODAB BF/CMC or DODAB BF/CMC/PDDA in combination with antigens still requires further research.

The differential cytotoxicity of DODAB, its dose-dependent toxicity, and its ability to induce delayed-type hypersensitivity (DTH) in vivo, a marker for cell-mediated immune responses, pointed out the feasibility of using DODAB as an efficient immunoadjuvant mainly for veterinary uses but also in humans in a few instances [9,13,52,57,280–282]. Supramolecular assemblies of DODAB BF by themselves or after interaction with supporting particles were also combined with three different model antigens in separate and tested as immunoadjuvants [9]. DODAB-based immunoadjuvants carrying antigens at reduced DODAB dose (0.01–0.1 mM) induced superior DTH responses in mice in comparison to alum. Thus, the cationic immunoadjuvant was either reduced to a single-component, nanosized system—DODAB BF—or was a dispersion of cationic nanoparticles with controllable nature and size as obtained after covering silica or polystyrene sulfate latex (PSS) with a cationic DODAB bilayer. DODAB BF interacted with proteins via both the hydrophobic effect and the electrostatic attraction at low ionic strength. DODAB-based adjuvants exhibited good colloid stability while complexed with the antigens, complete absence of toxicity in mice (i.e., local or general reactions), and a remarkable induction of Th1 immune response at reduced doses of cationic and toxic DODAB lipid. DODAB vesicle disruption by probe sonication at low ionic strength (0.1–5.0 mM monovalent salt) produced DODAB BF which remained electrostatically stabilized in dispersion by the electrostatic repulsion in between fragments. DODAB BF also interacted with oppositely charged particles such as silica or polystyrene sulfate (PSS) latex to produce the cationic particulates. Figure 20 shows some

hybrid and cationic immunoadjuvants based on reduced DODAB doses and their compared DTH response [9,10,18].

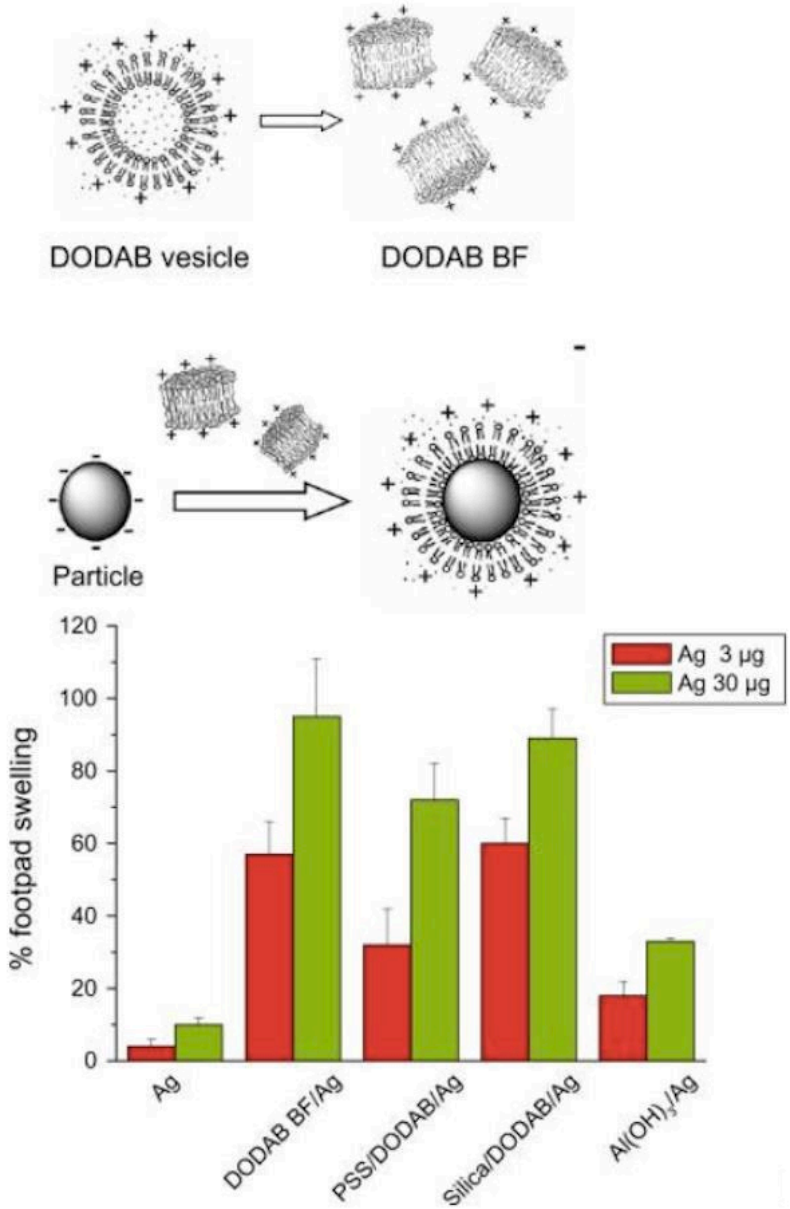


Figure 20. Schematic representation of nanometric dioctadecyldimethylammonium bromide (DODAB)-based adjuvants inducing delayed-type hypersensitivity (DTH) in mice as compared to alum. The same antigen (Ag) carried by each adjuvant was used for immunization. Ag was carried by DODAB BF at 0.1 mM DODAB (DODAB BF/Ag) or by polystyrene sulfate nanoparticles (PSS)/DODAB or by silica/DODAB particles at 0.01 or 0.05 mM DODAB (PSS/DODAB/Ag or silica/DODAB/Ag), respectively, or by alum ($Al(OH)_3$/Ag). After immunization, elicitation of the swelling response was done by injecting Ag alone in the mice footpad so that % footpad swelling was measured in comparison to alum [9,10,18]. At the DODAB doses employed, DODAB cytotoxicity was absent against mammalian cells in culture. Adapted from [9,10] with permission from Elsevier, Copyright 2007 and Copyright 2009 and reference [18].

An interesting approach was described in order to apply immunotherapy associated with chemotherapy against *Leishmania* infection: solid lipid NPs using soya phosphatidyl choline and stearic acid were prepared by solvent emulsification-evaporation method followed by ultrasonication. These solid NPs were loaded with amphotericin B before coating with chitosan and displayed diameters lower than 220 nm and positive zeta-potentials showing low hemolytic activity and antileishmanial activity higher than the one for commercial AmBisome or Fungizone. The NPs were taken up by J774A.1 macrophages, which activated the production of TNF-α and IL-12; importantly, cytotoxicity experiments in vitro and acute toxicity experiments in mice evidenced the safety of the formulation in comparison to marketed formulations [283].

Cationic and porous NPs from maltodextrin and the anionic lipid 1,2-dipalmitoyl-sn-glycero-3-phosphatidylglycerol (DPPG) were synthesized to evaluate their interaction with the nose mucosa; these NPs, combined with OVA displayed low toxicity, were efficiently taken up by airway epithelial cells and significantly improved the OVA delivery to the cells, increasing the permanence time of OVA at the nose mucosa to at least 6 h, in contrast to unformulated OVA, which remained 1.5 h only at the mucosa [284].

DODAB coating the biocompatible PLGA yielded cationic nanoparticles that elicited Th1 and Th17 responses [284,285]. Cationic NPs of PLGA, DODAB, and TDB in a nasal vaccine displayed nanometric sizes and high and positive zeta-potentials while carrying the outer-membrane protein (MOMP) antigen of *Chlamydia trachomatis,* inducing high titers of IgG2a, IFN-γ, and IL-17a [286].

Similarly, PLGA and DODAB were combined to yield cationic NPs for delivering a *Mycobacterium tuberculosis* nasal vaccine; PLGA/DODAB NPs showed uniform size, spherical shape, and smooth surface. PLGA/DODAB NPs loaded with HspX/EsxS antigen (a recombinant fused protein of *M. tuberculosis*) and with monophosphoryl lipid A (MPLA) increased the secretion of IFN-γ and IL-17 and enhanced the antibody titers of IgA, IgG1, and IgG2a [285]. In a different approach, cationic liposomes obtained from DOTAP, hyaluronic acid (HA), and PEG achieved a good immune response after intranasal vaccination with a recombinant antigen from *M. tuberculosis*; there was improved colloidal stability and prolonged antigen release. Besides, the typical cytotoxicity exerted by DOTAP was reduced 20-fold. DOTAP/HA/PEG NPs carrying OVA and MPLA promoted DCs maturation and up-regulation of co-stimulatory markers such as CD40, CD86, and MHC-II. Mice vaccinated with DOTAP/HA/PEG NPs carrying OVA and MPLA via intranasal route generated robust OVA-specific CD8(+) T cell and humoral responses; in addition, the intranasal inoculation of DOTAP/HA/PEG NPs co-loaded with MPLA and F1-V, a fused antigen from *Yersinia pestis*, induced a potent and long-lasting antibody production, evidencing that these hybrid liposome/polymer NPs are appropriate as a mucosal adjuvant [287].

PLGA/DC-Chol core/shell hybrid NPs synthesized by a double emulsion solvent evaporation method were tested as an adjuvant with the peculiarity that the antigen, OVA, was attached to the NPs in three different ways: inside the NPs (OVA in), adsorbed on the NPs (OVA ad), or both ways (OVA in/ad). After the internalization by DCs, FITC-OVA traffic from fluorescence microscopy showed that OVA ad and free OVA remained in the lysosomes, whereas OVA in or in/ad escaped from the endo-lysosome favoring cross-presentation. In vivo experiments showed that OVA in/ad provided not only adequate initial antigen exposure but also long-term antigen persistence at the injection inside. OVA in and OVA in/ad elicited significantly higher antigen-specific immune response than OVA ad [288].

Summarizing this topic, cationic lipids are very versatile and can either carry antigens by themselves via BF or impart positive charges to a variety of polymeric NPs under good control of their usual toxicity. They have the advantage of eliciting a potent cellular immune response in many instances. The adjuvant properties of the hybrid NPs have been often reviewed [21,25,34].

6. Conclusions

Cationic nanostructures such as the lipid-covered particles, the bilayer fragments, the cationic polymers, and the hybrid nanostructures of biocompatible and cationic polymers or lipids are interesting carriers with sizes below 100 nm. Their size directs them to the lymphatic vessels and antigen-presenting cells in the lymph nodes, and their positive charge allows efficient combination with important biomolecules such as peptides, proteins, nucleic acids, epitopes, and enhancers of the immune response.

The composition with lipids allows the inclusion of targeting in the microstructures that cannot directly reach the lymph nodes or that require special targeting to avoid degradation in the endosomes or to reach the cell nucleus.

The cationic nanostructures can protect the carried antigen for vaccine administration by the oral route and can increase the permanence time of the antigen/carrier assembly at the mucosae still enhancing the systemic immunity. The cationic nanostructures are particularly efficient in delivering antigens to APCs, allowing both antigen processing and presentation via MHC-II or processing and cross-presentation via MHC-I. The intracellular traffic depends on administration route and location of the antigen in the complex. The direct connection of the complex antigen/adjuvant to APCs in the lymph nodes avoids permanence at injection sites and local inflammatory reactions since they easily overcome the anatomical barriers due to their nanometric size. Their toxicity is easily controllable by using low concentrations of the cationic lipid or cationic polymer in the nanostructures.

There is a huge variety of cationic nanostructured materials available from nanomaterials science. However, most of them remain untested regarding their properties as immunoadjuvants or their intrinsic toxicity both in vitro and in vivo. This means that a huge area for biomedical research remains still unexplored and it is our hope that this review will be the trigger for further valuable research on vaccine design with novel cationic nanostructures.

Author Contributions: Conceptualization, A.M.C.-R. and Y.P.-B.; investigation, A.M.C.-R., and Y.P.-B.; resources, A.M.C.-R.; data curation, A.M.C.-R.; writing—original draft preparation, A.M.C.-R. and Y.P.-B.; writing—review and editing, A.M.C.-R. and Y.P.-B.; visualization, A.M.C.-R. and Y.P.-B.; supervision, A.M.C.-R.; project administration, A.M.C.-R.; funding acquisition, A.M.C.-R. All authors have read and agreed to the published version of the manuscript.

Funding: This research was funded by Conselho Nacional de Desenvolvimento Científico e Tecnológico (CNPq), grant numbers 302758/2019-4 and 302352/2014-7 and Fundação de Amparo à Pesquisa do Estado de São Paulo (FAPESP), grant number 2019/17685-2. Y.P-B was the recipient of a CNPq PhD fellowship grant number 140091/2019-0.

Conflicts of Interest: The authors declare no conflict of interest. The funders had no role in the design of the study; in the collection, analyses, or interpretation of data; in the writing of the manuscript, or in the decision to publish the results.

References

1. Abbas, A.K.; Lichtman, A.H.; Pillai, S. *Cellular and Molecular Immunology*, 9th ed.; Elsevier Ltd.: Philadelphia, PA, USA, 2018; ISBN 9780323479783.
2. Coffman, R.L.; Sher, A.; Seder, R.A. Vaccine adjuvants: Putting innate immunity to work. *Immunity* **2010**, *33*, 492–503. [CrossRef]
3. Bergmann-Leitner, E.S.; Leitner, W.W. Adjuvants in the driver's seat: How magnitude, type, fine specificity and longevity of immune responses are driven by distinct classes of immune potentiators. *Vaccines* **2014**, *2*, 252–296. [CrossRef]
4. Pasquale, A.; Preiss, S.; Silva, F.; Garçon, N. Vaccine adjuvants: From 1920 to 2015 and beyond. *Vaccines* **2015**, *3*, 320–343. [CrossRef]
5. Awate, S.; Babiuk, L.A.; Mutwiri, G. Mechanisms of action of adjuvants. *Front. Immunol.* **2013**, *4*, 114. [CrossRef]
6. HogenEsch, H.; O'Hagan, D.T.; Fox, C.B. Optimizing the utilization of aluminum adjuvants in vaccines: You might just get what you want. *NPJ Vaccines* **2018**, *3*, 51. [CrossRef]

7. Martiñón, S.; Cisneros, A.; Villicaña, S.; Hernández-Miramontes, R.; Mixcoha, E.; Calderón-Vargas, P. Chemical and immunological characteristics of aluminum-based, oil-water emulsion, and bacterial-origin adjuvants. *J. Immunol. Res.* **2019**, *2019*, 3974127. [CrossRef] [PubMed]
8. Apostólico, J.D.; Lunardelli, V.A.S.; Coirada, F.C.; Boscardin, S.B.; Rosa, D.S. Adjuvants: Classification, modus operandi, and licensing. *J. Immunol. Res.* **2016**, *2016*, 1459394. [CrossRef]
9. Lincopan, N.; Espindola, N.M.; Vaz, A.J.; da Costa, M.H.B.; Faquim-Mauro, E.; Carmona-Ribeiro, A.M. Novel immunoadjuvants based on cationic lipid: Preparation, characterization and activity in vivo. *Vaccine* **2009**, *27*, 5760–5771. [CrossRef] [PubMed]
10. Lincopan, N.; Espindola, N.M.; Vaz, A.J.; Carmona-Ribeiro, A.M. Cationic supported lipid bilayers for antigen presentation. *Int. J. Pharm.* **2007**, *340*, 216–222. [CrossRef] [PubMed]
11. Nawwab Al-Deen, F.M.; Selomulya, C.; Kong, Y.Y.; Xiang, S.D.; Ma, C.; Coppel, R.L.; Plebanski, M. Design of magnetic polyplexes taken up efficiently by dendritic cell for enhanced DNA vaccine delivery. *Gene Ther.* **2014**, *21*, 212–218. [CrossRef]
12. Rose, F.; Wern, J.E.; Gavins, F.; Andersen, P.; Follmann, F.; Foged, C. A strong adjuvant based on glycol-chitosan-coated lipid-polymer hybrid nanoparticles potentiates mucosal immune responses against the recombinant Chlamydia trachomatis fusion antigen CTH522. *J. Control. Release* **2018**, *271*, 88–97. [CrossRef] [PubMed]
13. Tsuruta, L.R.; Quintilio, W.; Costa, M.H.; Carmona-Ribeiro, A.M. Interactions between cationic liposomes and an antigenic protein: The physical chemistry of the immunoadjuvant action. *J. Lipid Res.* **1997**, *38*, 2003–2011. [PubMed]
14. Riehl, M.; Harms, M.; Hanefeld, A.; Baleeiro, R.B.; Walden, P.; Mader, K. Combining R-DOTAP and a particulate antigen delivery platform to trigger dendritic cell activation: Formulation development and in-vitro interaction studies. *Int. J. Pharm.* **2017**, *532*, 37–46. [CrossRef]
15. Davidsen, J.; Rosenkrands, I.; Christensen, D.; Vangala, A.; Kirby, D.; Perrie, Y.; Agger, E.M.; Andersen, P. Characterization of cationic liposomes based on dimethyldioctadecylammonium and synthetic cord factor from M. tuberculosis (trehalose 6,6′-dibehenate)-a novel adjuvant inducing both strong CMI and antibody responses. *Biochim. Biophys. Acta* **2005**, *1718*, 22–31. [CrossRef] [PubMed]
16. Rozenfeld, J.H.K.; Silva, S.R.; Raneia, P.A.; Faquim-Mauro, E.; Carmona-Ribeiro, A.M. Stable assemblies of cationic bilayer fragments and CpG oligonucleotide with enhanced immunoadjuvant activity in vivo. *J. Control. Release* **2012**, *160*, 367–373. [CrossRef] [PubMed]
17. de Almeida, A.F.; De Gaspari, E. Dioctadecyldimethylammonium bromide (DODAB-BF) as a new adjuvant for maternal-fetal immunization in mice against Neisseria meningitidis: Evaluation of humoral response. *Pathog. Dis.* **2018**, *76*. [CrossRef]
18. Lincopan, N.; Santana, M.R.; Faquim-Mauro, E.; da Costa, M.H.B.; Carmona-Ribeiro, A.M. Silica-based cationic bilayers as immunoadjuvants. *BMC Biotechnol.* **2009**, *9*, 5. [CrossRef]
19. Nawwab Al-Deen, F.; Ma, C.; Xiang, S.D.; Selomulya, C.; Plebanski, M.; Coppel, R.L. On the efficacy of malaria DNA vaccination with magnetic gene vectors. *J. Control. Release* **2013**, *168*, 10–17. [CrossRef]
20. Xiang, S.D.; Scholzen, A.; Minigo, G.; David, C.; Apostolopoulos, V.; Mottram, P.L.; Plebanski, M. Pathogen recognition and development of particulate vaccines: Does size matter? *Methods* **2006**, *40*, 1–9. [CrossRef]
21. Carmona-Ribeiro, A.M. Cationic Nanostructures for Vaccines. In *Immune Response Activation*; Duc, G.H.T., Ed.; IntechOpen: Rijeka, Croatia, 2014; pp. 1–45. ISBN 978-953-51-1374-4.
22. Pelkmans, L. Secrets of caveolae- and lipid raft-mediated endocytosis revealed by mammalian viruses. *Biochim. Biophys. Acta* **2005**, *1746*, 295–304. [CrossRef]
23. Fifis, T.; Gamvrellis, A.; Crimeen-Irwin, B.; Pietersz, G.A.; Li, J.; Mottram, P.L.; McKenzie, I.F.C.; Plebanski, M. Size-dependent immunogenicity: Therapeutic and protective properties of nano-vaccines against tumors. *J. Immunol.* **2004**, *173*, 3148–3154. [CrossRef] [PubMed]
24. O'Hagan, D.T.; MacKichan, M.L.; Singh, M. Recent developments in adjuvants for vaccines against infectious diseases. *Biomol. Eng.* **2001**, *18*, 69–85. [CrossRef]
25. Carmona-Ribeiro, A.M. Nanomaterials based on lipids for vaccine development. In *Micro and Nano Technologies*; Skwarczynski, M., Toth, I.B.T.M., Eds.; Elsevier: Oxford, UK, 2017; pp. 241–257. ISBN 978-0-323-39981-4.

26. Holten-Andersen, L.; Doherty, T.M.; Korsholm, K.S.; Andersen, P. Combination of the cationic surfactant dimethyl dioctadecyl ammonium bromide and synthetic mycobacterial cord factor as an efficient adjuvant for tuberculosis subunit vaccines. *Infect. Immun.* **2004**, *72*, 1608–1617. [CrossRef] [PubMed]
27. de Oliveira Santos, F.A.; Lincopan, N.; De Gaspari, E. Evaluation of intranasal and subcutaneous route of immunization in neonatal mice using DODAB-BF as adjuvant with outer membrane vesicles of Neisseria meningitis B. *Immunobiology* **2018**, *223*, 750–760. [CrossRef] [PubMed]
28. Carmona-Ribeiro, A.M. The versatile dioctadecyldimethylammonium bromide. In *Application and Characterization of Surfactants*; Najjar, R., Ed.; IntechOpen: Rijeka, Croatia, 2017; pp. 157–182. ISBN 9789535133261.
29. Ju, J.; Huan, M.L.; Wan, N.; Qiu, H.; Zhou, S.Y.; Zhang, B.L. Novel cholesterol-based cationic lipids as transfecting agents of DNA for efficient gene delivery. *Int. J. Mol. Sci.* **2015**, *16*, 5666–5681. [CrossRef] [PubMed]
30. Tada, R.; Suzuki, H.; Takahashi, S.; Negishi, Y.; Kiyono, H.; Kunisawa, J.; Aramaki, Y. Nasal vaccination with pneumococcal surface protein A in combination with cationic liposomes consisting of DOTAP and DC-chol confers antigen-mediated protective immunity against Streptococcus pneumoniae infections in mice. *Int. Immunopharmacol.* **2018**, *61*, 385–393. [CrossRef]
31. Milicic, A.; Kaur, R.; Reyes-Sandoval, A.; Tang, C.K.; Honeycutt, J.; Perrie, Y.; Hill, A.V.S. Small cationic DDA:TDB liposomes as protein vaccine adjuvants obviate the need for TLR agonists in inducing cellular and humoral responses. *PLoS ONE* **2012**, *7*, e34255. [CrossRef]
32. De Serrano, L.O.; Burkhart, D.J. Liposomal vaccine formulations as prophylactic agents: Design considerations for modern vaccines. *J. Nanobiotechnol.* **2017**, *15*, 83. [CrossRef]
33. Geijtenbeek, T.B.H.; Gringhuis, S.I. C-type lectin receptors in the control of T helper cell differentiation. *Nat. Rev. Immunol.* **2016**, *16*, 433–448. [CrossRef]
34. Carmona-Ribeiro, A.M. Biomimetic nanoparticles: Preparation, characterization and biomedical applications. *Int. J. Nanomed.* **2010**, *5*, 249–259. [CrossRef]
35. Carmona-Ribeiro, A.M. Biomimetic particles in drug and vaccine delivery. *J. Liposome Res.* **2007**, *17*, 165–172. [CrossRef] [PubMed]
36. Ribeiro, A.M.; Chaimovich, H. Preparation and characterization of large dioctadecyldimethylammonium chloride liposomes and comparison with small sonicated vesicles. *Biochim. Biophys. Acta* **1983**, *733*, 172–179. [CrossRef]
37. Carmona-Ribeiro, A.M. Synthetic amphiphile vesicles. *Chem. Soc. Rev.* **1992**, *21*, 209–214. [CrossRef]
38. Carmona-Ribeiro, A.M. Bilayer-forming synthetic lipids: Drugs or carriers? *Curr. Med. Chem.* **2003**, *10*, 2425–2446. [CrossRef] [PubMed]
39. Carmona-Ribeiro, A.M. Lipid bilayer fragments and disks in drug delivery. *Curr. Med. Chem.* **2006**, *13*, 1359–1370. [CrossRef]
40. Carvalho, L.A.; Carmona-Ribeiro, A.M. Interactions between cationic vesicles and serum proteins. *Langmuir* **1998**, *14*, 6077–6081. [CrossRef]
41. Carmona-Ribeiro, A.M. Interactions between cationic liposomes and drugs or biomolecules. *An. Acad. Bras. Cienc.* **2000**, *72*, 39–43. [CrossRef] [PubMed]
42. Rosa, H.; Petri, D.F.S.; Carmona-Ribeiro, A.M. Interactions between bacteriophage DNA and cationic biomimetic particles. *J. Phys. Chem. B* **2008**, *112*, 16422–16430. [CrossRef] [PubMed]
43. Kikuchi, I.S.; Carmona-Ribeiro, A.M. Interactions between DNA and Synthetic Cationic Liposomes. *J. Phys. Chem. B* **2000**, *104*, 2829–2835. [CrossRef]
44. Kikuchi, I.S.; Viviani, W.; Carmona-Ribeiro, A.M. Nucleotide Insertion in Cationic Bilayers. *J. Phys. Chem. A* **1999**, *103*, 8050–8055. [CrossRef]
45. Nantes, I.L.; Correia, F.M.; Faljoni-Alario, A.; Kawanami, A.E.; Ishiki, H.M.; Amaral, A.T.; Carmona-Ribeiro, A.M. Nucleotide conformational change induced by cationic bilayers. *Arch. Biochem. Biophys.* **2003**, *416*, 25–30. [CrossRef]
46. Rozenfeld, J.H.K.; Oliveira, T.R.; Lamy, M.T.; Carmona-Ribeiro, A.M. Interaction of cationic bilayer fragments with a model oligonucleotide. *Biochim. Biophys. Acta* **2011**, *1808*, 649–655. [CrossRef] [PubMed]
47. Azmi, F.; Ahmad Fuaad, A.A.H.; Skwarczynski, M.; Toth, I. Recent progress in adjuvant discovery for peptide-based subunit vaccines. *Hum. Vaccines Immunother.* **2014**, *10*, 778–796. [CrossRef] [PubMed]

48. Amorij, J.P.; Kersten, G.F.A.; Saluja, V.; Tonnis, W.F.; Hinrichs, W.L.J.; Slutter, B.; Bal, S.M.; Bouwstra, J.A.; Huckriede, A.; Jiskoot, W. Towards tailored vaccine delivery: Needs, challenges and perspectives. *J. Control. Release* **2012**, *161*, 363–376. [CrossRef]
49. Christensen, D.; Korsholm, K.S.; Andersen, P.; Agger, E.M. Cationic liposomes as vaccine adjuvants. *Expert Rev. Vaccines* **2011**, *10*, 513–521. [CrossRef]
50. Joseph, A.; Itskovitz-Cooper, N.; Samira, S.; Flasterstein, O.; Eliyahu, H.; Simberg, D.; Goldwaser, I.; Barenholz, Y.; Kedar, E. A new intranasal influenza vaccine based on a novel polycationic lipid—Ceramide carbamoyl-spermine (CCS): I. Immunogenicity and efficacy studies in mice. *Vaccine* **2006**, *24*, 3990–4006. [CrossRef]
51. Even-Or, O.; Samira, S.; Rochlin, E.; Balasingam, S.; Mann, A.J.; Lambkin-Williams, R.; Spira, J.; Goldwaser, I.; Ellis, R.; Barenholz, Y. Immunogenicity, protective efficacy and mechanism of novel CCS adjuvanted influenza vaccine. *Vaccine* **2010**, *28*, 6527–6541. [CrossRef]
52. Hilgers, L.A.; Snippe, H. DDA as an immunological adjuvant. *Res. Immunol.* **1992**, *143*, 494–496. [CrossRef]
53. Calzas, C.; Chevalier, C. Innovative mucosal vaccine formulations against influenza A virus infections. *Front. Immunol.* **2019**, *10*, 1605. [CrossRef]
54. Bernocchi, B.; Carpentier, R.; Betbeder, D. Nasal nanovaccines. *Int. J. Pharm.* **2017**, *530*, 128–138. [CrossRef]
55. Shen, H.; Ackerman, A.L.; Cody, V.; Giodini, A.; Hinson, E.R.; Cresswell, P.; Edelson, R.L.; Saltzman, W.M.; Hanlon, D.J. Enhanced and prolonged cross-presentation following endosomal escape of exogenous antigens encapsulated in biodegradable nanoparticles. *Immunology* **2006**, *117*, 78–88. [CrossRef] [PubMed]
56. Wang, C.; Li, P.; Liu, L.; Pan, H.; Li, H.; Cai, L.; Ma, Y. Self-adjuvanted nanovaccine for cancer immunotherapy: Role of lysosomal rupture-induced ROS in MHC class I antigen presentation. *Biomaterials* **2016**, *79*, 88–100. [CrossRef] [PubMed]
57. Korsholm, K.S.; Agger, E.M.; Foged, C.; Christensen, D.; Dietrich, J.; Andersen, C.S.; Geisler, C.; Andersen, P. The adjuvant mechanism of cationic dimethyldioctadecylammonium liposomes. *Immunology* **2007**, *121*, 216–226. [CrossRef] [PubMed]
58. Boraschi, D.; Italiani, P. From antigen delivery system to adjuvanticy: The board application of nanoparticles in vaccinology. *Vaccines* **2015**, *3*, 930–939. [CrossRef] [PubMed]
59. Brandtzaeg, P. Nature and function of gastrointestinal antigen-presenting cells. *Allergy* **2001**, *56*, 16–20. [CrossRef]
60. Bungener, L.; Huckriede, A.; Wilschut, J.; Daemen, T. Delivery of protein antigens to the immune system by fusion-active virosomes: A comparison with liposomes and ISCOMs. *Biosci. Rep.* **2002**, *22*, 323–338. [CrossRef]
61. Diebold, S.S.; Cotten, M.; Koch, N.; Zenke, M. MHC class II presentation of endogenously expressed antigens by transfected dendritic cells. *Gene Ther.* **2001**, *8*, 487–493. [CrossRef]
62. Heath, W.R.; Belz, G.T.; Behrens, G.M.N.; Smith, C.M.; Forehan, S.P.; Parish, I.A.; Davey, G.M.; Wilson, N.S.; Carbone, F.R.; Villadangos, J.A. Cross-presentation, dendritic cell subsets, and the generation of immunity to cellular antigens. *Immunol. Rev.* **2004**, *199*, 9–26. [CrossRef] [PubMed]
63. Sigal, L.J.; Crotty, S.; Andino, R.; Rock, K.L. Cytotoxic T-cell immunity to virus-infected non-haematopoietic cells requires presentation of exogenous antigen. *Nature* **1999**, *402*, 25–29. [CrossRef]
64. Sun, H.X.; Xie, Y.; Ye, Y.P. ISCOMs and ISCOMATRIX. *Vaccine* **2009**, *27*, 4388–4401. [CrossRef] [PubMed]
65. Perez-Betancourt, Y.; Tavora, B.C.; Colombini, M.; Faquim-Mauro, E.L.; Carmona-Ribeiro, A.M. Simple nanoparticles from the assembly of cationic polymer and antigen as immunoadjuvants. *Vaccines* **2020**, *8*, 105. [CrossRef] [PubMed]
66. Zhi, D.; Bai, Y.; Yang, J.; Cui, S.; Zhao, Y.; Chen, H.; Zhang, S. A review on cationic lipids with different linkers for gene delivery. *Adv. Colloid Interface Sci.* **2018**, *253*, 117–140. [CrossRef] [PubMed]
67. Chernikov, I.V.; Vlassov, V.V.; Chernolovskaya, E.L. Current development of siRNA bioconjugates: From research to the clinic. *Front. Pharmacol.* **2019**, *10*, 444. [CrossRef]
68. Scherman, D.; Rousseau, A.; Bigey, P.; Escriou, V. Genetic pharmacology: Progresses in siRNA delivery and therapeutic applications. *Gene Ther.* **2017**, *24*, 151–156. [CrossRef]
69. Byk, G.; Dubertret, C.; Escriou, V.; Frederic, M.; Jaslin, G.; Rangara, R.; Pitard, B.; Crouzet, J.; Wils, P.; Schwartz, B.; et al. Synthesis, activity, and structure–activity relationship studies of novel cationic lipids for DNA transfer. *J. Med. Chem.* **1998**, *41*, 229–235. [CrossRef]

70. Pizzuto, M.; Bigey, P.; Lachages, A.M.; Hoffmann, C.; Ruysschaert, J.M.; Escriou, V.; Lonez, C. Cationic lipids as one-component vaccine adjuvants: A promising alternative to alum. *J. Control. Release* **2018**, *287*, 67–77. [CrossRef] [PubMed]
71. Puapatanakul, P.; Chansritrakul, S.; Susantitaphong, P.; Ueaphongsukkit, T.; Eiam-Ong, S.; Praditpornsilpa, K.; Kittanamongkolchai, W.; Avihingsanon, Y. Interferon-inducible protein 10 and disease activity in systemic lupus erythematosus and lupus nephritis: A systematic review and meta-analysis. *Int. J. Mol. Sci.* **2019**, *20*, 4954. [CrossRef]
72. Eisenbarth, S.C.; Colegio, O.R.; O'Connor, W.; Sutterwala, F.S.; Flavell, R.A. Crucial role for the Nalp3 inflammasome in the immunostimulatory properties of aluminium adjuvants. *Nature* **2008**, *453*, 1122–1126. [CrossRef]
73. Schweneker, K.; Gorka, O.; Schweneker, M.; Poeck, H.; Tschopp, J.; Peschel, C.; Ruland, J.; Gross, O. The mycobacterial cord factor adjuvant analogue trehalose-6,6′-dibehenate (TDB) activates the Nlrp3 inflammasome. *Immunobiology* **2013**, *218*, 664–673. [CrossRef]
74. Nguyen, T.K.T.; D'Aigle, J.; Chinea, L.; Niaz, Z.; Hunter, R.L.; Hwang, S.A.; Actor, J.K. Mycobacterial trehalose 6,6′dimycolate-induced M1-type inflammation. *Am. J. Pathol.* **2020**, *190*, 286–294. [CrossRef]
75. Nascimento, D.B.; Rapuano, R.; Lessa, M.M.; Carmona-Ribeiro, A.M. Counterion effects on properties of cationic vesicles. *Langmuir* **1998**, *14*, 7387–7391. [CrossRef]
76. Henriksen-Lacey, M.; Bramwell, V.W.; Christensen, D.; Agger, E.M.; Andersen, P.; Perrie, Y. Liposomes based on dimethyldioctadecylammonium promote a depot effect and enhance immunogenicity of soluble antigen. *J. Control. Release* **2010**, *142*, 180–186. [CrossRef] [PubMed]
77. Carneiro, C.; Correia, A.; Collins, T.; Vilanova, M.; Pais, C.; Gomes, A.C.; Real Oliveira, M.E.C.D.; Sampaio, P. DODAB:monoolein liposomes containing Candida albicans cell wall surface proteins: A novel adjuvant and delivery system. *Eur. J. Pharm. Biopharm.* **2015**, *89*, 190–200. [CrossRef]
78. Martins, L.S.; Nomura, D.A.; Duarte, E.L.; Riske, K.A.; Lamy, M.T.; Rozenfeld, J.H.K. Structural characterization of cationic DODAB bilayers containing C24:1 beta-glucosylceramide. *Biochim. Biophys. Acta Biomembr.* **2019**, *1861*, 643–650. [CrossRef] [PubMed]
79. Ko, A.; Wui, S.R.; Ryu, J.I.; Lee, Y.J.; Hien, D.T.T.; Rhee, I.; Shin, S.J.; Park, S.A.; Kim, K.S.; Cho, Y.J.; et al. Potentiation of Th1-Type Immune Responses to Mycobacterium tuberculosis Antigens in Mice by Cationic Liposomes Combined with De-O-Acylated Lipooligosaccharide. *J. Microbiol. Biotechnol.* **2018**, *28*, 136–144. [CrossRef]
80. Qu, W.; Li, N.; Yu, R.; Zuo, W.; Fu, T.; Fei, W.; Hou, Y.; Liu, Y.; Yang, J. Cationic DDA/TDB liposome as a mucosal vaccine adjuvant for uptake by dendritic cells in vitro induces potent humoural immunity. *Artif. Cells Nanomed. Botechnol.* **2018**, *46*, 852–860. [CrossRef]
81. Silva, J.P.N.; Oliveira, A.C.N.; Casal, M.P.P.A.; Gomes, A.C.; Coutinho, P.J.G.; Coutinho, O.P.; Oliveira, M.E. DODAB:monoolein-based lipoplexes as non-viral vectors for transfection of mammalian cells. *Biochim. Biophys. Acta Biomembr.* **2011**, *1808*, 2440–2449. [CrossRef]
82. Oliveira, A.C.N.; Martens, T.F.; Raemdonck, K.; Adati, R.D.; Feitosa, E.; Botelho, C.; Gomes, A.C.; Braeckmans, K.; Real Oliveira, M.E. Dioctadecyldimethylammonium:monoolein nanocarriers for efficient in vitro gene silencing. *ACS Appl. Mater. Interfaces* **2014**, *6*, 6977–6989. [CrossRef]
83. Carneiro, C.; Correia, A.; Lima, T.; Vilanova, M.; Pais, C.; Gomes, A.C.; Real Oliveira, M.E.; Sampaio, P. Protective effect of antigen delivery using monoolein-based liposomes in experimental hematogenously disseminated candidiasis. *Acta Biomater.* **2016**, *39*, 133–145. [CrossRef]
84. Tada, R.; Hidaka, A.; Iwase, N.; Takahashi, S.; Yamakita, Y.; Iwata, T.; Muto, S.; Sato, E.; Takayama, N.; Honjo, E.; et al. Intranasal immunization with DOTAP cationic liposomes combined with DC-cholesterol induces potent antigen-specific mucosal and systemic immune responses in mice. *PLoS ONE* **2015**, *10*, e0139785. [CrossRef]
85. Jiang, L.; Schinkel, M.; van Essen, M.; Schiffelers, R.M. Bacterial membrane vesicles as promising vaccine candidates. *Eur. J. Pharm. Biopharm.* **2019**, *145*, 1–6. [CrossRef] [PubMed]

86. Gnopo, Y.M.D.; Mirsa, A.; Hsu, H.L.; DeLisa, M.P.; Daniel, S.; Putnam, D. Induced fusion and aggregation of bacterial outer membrane vesicles: Experimental and theoretical analysis. *J. Colloid Interface Sci.* **2020**, *578*, 522–532. [CrossRef] [PubMed]
87. Daleke-Schermerhorn, M.H.; Felix, T.; Soprova, Z.; Ten Hagen-Jongman, C.M.; Vikstrom, D.; Majlessi, L.; Beskers, J.; Follmann, F.; de Punder, K.; van der Wel, N.N.; et al. Decoration of outer membrane vesicles with multiple antigens by using an autotransporter approach. *Appl. Environ. Microbiol.* **2014**, *80*, 5854–5865. [CrossRef] [PubMed]
88. Wong, P.T.; Wang, S.H.; Ciotti, S.; Makidon, P.E.; Smith, D.M.; Fan, Y.; Schuler, C.F.; Baker, J.R.J. Formulation and characterization of nanoemulsion intranasal adjuvants: Effects of surfactant composition on mucoadhesion and immunogenicity. *Mol. Pharm.* **2014**, *11*, 531–544. [CrossRef] [PubMed]
89. Barnier Quer, C.; Elsharkawy, A.; Romeijn, S.; Kros, A.; Jiskoot, W. Cationic liposomes as adjuvants for influenza hemagglutinin: More than charge alone. *Eur. J. Pharm. Biopharm.* **2012**, *81*, 294–302. [CrossRef]
90. Pardi, N.; Hogan, M.J.; Porter, F.W.; Weissman, D. mRNA vaccines—A new era in vaccinology. *Nat. Rev. Drug Discov.* **2018**, *17*, 261–279. [CrossRef]
91. Maruggi, G.; Zhang, C.; Li, J.; Ulmer, J.B.; Yu, D. mRNA as a transformative technology for vaccine development to control infectious diseases. *Mol. Ther.* **2019**, *27*, 757–772. [CrossRef]
92. Kang, T.; Huang, Y.; Zhu, Q.; Cheng, H.; Pei, Y.; Feng, J.; Xu, M.; Jiang, G.; Song, Q.; Jiang, T.; et al. Necroptotic cancer cells-mimicry nanovaccine boosts anti-tumor immunity with tailored immune-stimulatory modality. *Biomaterials* **2018**, *164*, 80–97. [CrossRef]
93. Zhuang, X.; Qi, Y.; Wang, M.; Yu, N.; Nan, F.; Zhang, H.; Tian, M.; Li, C.; Lu, H.; Jin, N. mRNA vaccines encoding the HA protein of influenza A H1N1 virus delivered by cationic lipid nanoparticles induce protective immune responses in mice. *Vaccines* **2020**, *8*, 123. [CrossRef]
94. Guevara, M.L.; Persano, S.; Persano, F. Lipid-based vectors for therapeutic mRNA-based anti-cancer vaccines. *Curr. Pharm. Des.* **2019**, *25*, 1443–1454. [CrossRef]
95. Wang, C.; Liu, P.; Zhuang, Y.; Li, P.; Jiang, B.; Pan, H.; Liu, L.; Cai, L.; Ma, Y. Lymphatic-targeted cationic liposomes: A robust vaccine adjuvant for promoting long-term immunological memory. *Vaccine* **2014**, *32*, 5475–5483. [CrossRef]
96. Crooke, S.T.; Witztum, J.L.; Bennett, C.F.; Baker, B.F. RNA-targeted therapeutics. *Cell Metab.* **2018**, *27*, 714–739. [CrossRef] [PubMed]
97. Semple, S.C.; Akinc, A.; Chen, J.; Sandhu, A.P.; Mui, B.L.; Cho, C.K.; Sah, D.W.Y.; Stebbing, D.; Crosley, E.J.; Yaworski, E.; et al. Rational design of cationic lipids for siRNA delivery. *Nat. Biotechnol.* **2010**, *28*, 172–176. [CrossRef] [PubMed]
98. Heyes, J.; Palmer, L.; Bremner, K.; MacLachlan, I. Cationic lipid saturation influences intracellular delivery of encapsulated nucleic acids. *J. Control. Release* **2005**, *107*, 276–287. [CrossRef] [PubMed]
99. Geall, A.J.; Verma, A.; Otten, G.R.; Shaw, C.A.; Hekele, A.; Banerjee, K.; Cu, Y.; Beard, C.W.; Brito, L.A.; Krucker, T.; et al. Nonviral delivery of self-amplifying RNA vaccines. *Proc. Natl. Acad. Sci. USA* **2012**, *109*, 14604–14609. [CrossRef]
100. Shetab Boushehri, M.A.; Lamprecht, A. TLR4-based immunotherapeutics in cancer: A review of the achievements and shortcomings. *Mol. Pharm.* **2018**, *15*, 4777–4800. [CrossRef]
101. Meraz, I.M.; Savage, D.J.; Segura-Ibarra, V.; Li, J.; Rhudy, J.; Gu, J.; Serda, R.E. Adjuvant cationic liposomes presenting MPL and IL-12 induce cell death, suppress tumor growth, and alter the cellular phenotype of tumors in a murine model of breast cancer. *Mol. Pharm.* **2014**, *11*, 3484–3491. [CrossRef] [PubMed]
102. Kuai, R.; Ochyl, L.J.; Bahjat, K.S.; Schwendeman, A.; Moon, J.J. Designer vaccine nanodiscs for personalized cancer immunotherapy. *Nat. Mater.* **2017**, *16*, 489–496. [CrossRef]
103. Manolova, V.; Flace, A.; Bauer, M.; Schwarz, K.; Saudan, P.; Bachmann, M.F. Nanoparticles target distinct dendritic cell populations according to their size. *Eur. J. Immunol.* **2008**, *38*, 1404–1413. [CrossRef]
104. Tada, R.; Muto, S.; Iwata, T.; Hidaka, A.; Kiyono, H.; Kunisawa, J.; Aramaki, Y. Attachment of class B CpG ODN onto DOTAP/DC-chol liposome in nasal vaccine formulations augments antigen-specific immune responses in mice. *BMC Res. Notes* **2017**, *10*, 68. [CrossRef]
105. de Oliveira, C.M.; Fregnani, J.H.; Villa, L.L. HPV vaccine: Updates and highlights. *Acta Cytol.* **2019**, *63*, 159–168. [CrossRef] [PubMed]
106. Chen, W.; Yan, W.; Huang, L. A simple but effective cancer vaccine consisting of an antigen and a cationic lipid. *Cancer Immunol. Immunother.* **2008**, *57*, 517–530. [CrossRef] [PubMed]

107. Varypataki, E.M.; Benne, N.; Bouwstra, J.; Jiskoot, W.; Ossendorp, F. Efficient eradication of established tumors in mice with cationic liposome-based synthetic long-peptide vaccines. *Cancer Immunol. Res.* **2017**, *5*, 222–233. [CrossRef] [PubMed]
108. Brunel, F.; Darbouret, A.; Ronco, J. Cationic lipid DC-Chol induces an improved and balanced immunity able to overcome the unresponsiveness to the hepatitis B vaccine. *Vaccine* **1999**, *17*, 2192–2203. [CrossRef]
109. Friend, D.S.; Papahadjopoulos, D.; Debs, R.J. Endocytosis and intracellular processing accompanying transfection mediated by cationic liposomes. *Biochim. Biophys. Acta* **1996**, *1278*, 41–50. [CrossRef]
110. Hobernik, D.; Bros, M. DNA Vaccines-How Far From Clinical Use? *Int. J. Mol. Sci.* **2018**, *19*, 3605. [CrossRef]
111. Hermanson, G.; Whitlow, V.; Parker, S.; Tonsky, K.; Rusalov, D.; Ferrari, M.; Lalor, P.; Komai, M.; Mere, R.; Bell, M.; et al. A cationic lipid-formulated plasmid DNA vaccine confers sustained antibody-mediated protection against aerosolized anthrax spores. *Proc. Natl. Acad. Sci. USA* **2004**, *101*, 13601–13606. [CrossRef]
112. Perrie, Y.; McNeil, S.; Vangala, A. Liposome-mediated DNA immunisation via the subcutaneous route. *J. Drug Target.* **2003**, *11*, 555–563. [CrossRef]
113. Gregoriadis, G.; Bacon, A.; Caparros-Wanderley, W.; McCormack, B. A role for liposomes in genetic vaccination. *Vaccine* **2002**, *20*. [CrossRef]
114. Gregoriadis, G.; Saffie, R.; de Souza, J.B. Liposome-mediated DNA vaccination. *FEBS Lett.* **1997**, *402*, 107–110. [CrossRef]
115. Perrie, Y.; Barralet, J.E.; McNeil, S.; Vangala, A. Surfactant vesicle-mediated delivery of DNA vaccines via the subcutaneous route. *Int. J. Pharm.* **2004**, *284*, 31–41. [CrossRef] [PubMed]
116. Segal, A.W.; Gregoriadis, G.; Black, C.D. Liposomes as vehicles for the local release of drugs. *Clin. Sci. Mol. Med.* **1975**, *49*, 99–106. [CrossRef] [PubMed]
117. Szoka, F.C.; Xu, Y.; Zelphati, O. How are nucleic acids released in cells from cationic lipid-nucleic acid complexes? *J. Liposome Res.* **1996**, *6*, 567–587. [CrossRef]
118. Zelphati, O.; Szoka, F.C.J. Intracellular distribution and mechanism of delivery of oligonucleotides mediated by cationic lipids. *Pharm. Res.* **1996**, *13*, 1367–1372. [CrossRef]
119. Velinova, M.; Read, N.; Kirby, C.; Gregoriadis, G. Morphological observations on the fate of liposomes in the regional lymph nodes after footpad injection into rats. *Biochim. Biophys. Acta* **1996**, *1299*, 207–215. [CrossRef]
120. Smith, D.M.; Simon, J.K.; Baker, J.R.J. Applications of nanotechnology for immunology. *Nat. Rev. Immunol.* **2013**, *13*, 592–605. [CrossRef]
121. Wade, A.; Weller, P. *Pharmaceutical Excipients*, 2nd ed.; American Pharmaceutical Association: Washington, DC, USA; The Pharmaceutical Press: London, UK, 1994; ISBN 0 85369 305 6.
122. Cui, Z.; Qiu, F.; Sloat, B.R. Lecithin-based cationic nanoparticles as a potential DNA delivery system. *Int. J. Pharm.* **2006**, *313*, 206–213. [CrossRef]
123. Lonez, C.; Vandenbranden, M.; Ruysschaert, J.M. Cationic lipids activate intracellular signaling pathways. *Adv. Drug Deliv. Rev.* **2012**, *64*, 1749–1758. [CrossRef] [PubMed]
124. Bhardwaj, P.; Bhatia, E.; Sharma, S.; Ahamad, N.; Banerjee, R. Advancements in prophylactic and therapeutic nanovaccines. *Acta Biomater.* **2020**, *108*, 1–21. [CrossRef]
125. Mikelez-Alonso, I.; Aires, A.; Cortajarena, A.L. Cancer nano-immunotherapy from the injection to the target: The role of protein corona. *Int. J. Mol. Sci.* **2020**, *21*, 519. [CrossRef]
126. Fadeel, B. Hide and seek: Nanomaterial interactions with the immune system. *Front. Immunol.* **2019**, *10*, 133. [CrossRef]
127. Gilabert-Oriol, R.; Ryan, G.M.; Leung, A.W.Y.; Firmino, N.S.; Bennewith, K.L.; Bally, M.B. Liposomal formulations to modulate the tumour microenvironment and antitumour immune response. *Int. J. Mol. Sci.* **2018**, *19*, 2922. [CrossRef] [PubMed]
128. Gao, Y.; Wijewardhana, C.; Mann, J.F.S. Virus-like particle, liposome, and polymeric particle-based vaccines against HIV-1. *Front. Immunol.* **2018**, *9*, 345. [CrossRef] [PubMed]
129. Fischer, D.; Li, Y.; Ahlemeyer, B.; Krieglstein, J.; Kissel, T. In vitro cytotoxicity testing of polycations: Influence of polymer structure on cell viability and hemolysis. *Biomaterials* **2003**, *24*, 1121–1131. [CrossRef]
130. Monnery, B.D.; Wright, M.; Cavill, R.; Hoogenboom, R.; Shaunak, S.; Steinke, J.H.G.; Thanou, M. Cytotoxicity of polycations: Relationship of molecular weight and the hydrolytic theory of the mechanism of toxicity. *Int. J. Pharm.* **2017**, *521*, 249–258. [CrossRef]

131. Carrasco, L.D.; Sampaio, J.L.M.; Carmona-Ribeiro, A.M. Supramolecular cationic assemblies against multidrug-resistant microorganisms: Activity and mechanism of action. *Int. J. Mol. Sci.* **2015**, *16*, 6337–6352. [CrossRef] [PubMed]
132. Jeong, H.; Hwang, J.; Lee, H.; Hammond, P.T.; Choi, J.; Hong, J. In vitro blood cell viability profiling of polymers used in molecular assembly. *Sci. Rep.* **2017**, *7*, 9481. [CrossRef]
133. Carmona-Ribeiro, A.M.; Ortis, F.; Schumacher, R.I.; Armelin, M.C.S. Interactions between cationic vesicles and cultured mammalian cells. *Langmuir* **1997**, *13*, 2215–2218. [CrossRef]
134. Wang, X.; Zheng, K.; Si, Y.; Guo, X.; Xu, Y. Protein-polyelectrolyte interaction: Thermodynamic analysis based on the titration method (†). *Polymers* **2019**, *11*, 82. [CrossRef]
135. Singh, M.; Briones, M.; Ott, G.; O'Hagan, D. Cationic microparticles: A potent delivery system for DNA vaccines. *Proc. Natl. Acad. Sci. USA* **2000**, *97*, 811–816. [CrossRef]
136. Wusiman, A.; Gu, P.; Liu, Z.; Xu, S.; Zhang, Y.; Hu, Y.; Liu, J.; Wang, D.; Huang, X. Cationic polymer modified PLGA nanoparticles encapsulating Alhagi honey polysaccharides as a vaccine delivery system for ovalbumin to improve immune responses. *Int. J. Nanomed.* **2019**, *14*, 3221–3234. [CrossRef] [PubMed]
137. Wegmann, F.; Gartlan, K.H.; Harandi, A.M.; Brinckmann, S.A.; Coccia, M.; Hillson, W.R.; Kok, W.L.; Cole, S.; Ho, L.P.; Lambe, T.; et al. Polyethyleneimine is a potent mucosal adjuvant for viral glycoprotein antigens. *Nat. Biotechnol.* **2012**, *30*, 883–888. [CrossRef] [PubMed]
138. Sheppard, N.C.; Brinckmann, S.A.; Gartlan, K.H.; Puthia, M.; Svanborg, C.; Krashias, G.; Eisenbarth, S.C.; Flavell, R.A.; Sattentau, Q.J.; Wegmann, F. Polyethyleneimine is a potent systemic adjuvant for glycoprotein antigens. *Int. Immunol.* **2014**, *26*, 531–538. [CrossRef]
139. Carmona-Ribeiro, A.M.; de Melo Carrasco, L.D. Cationic antimicrobial polymers and their assemblies. *Int. J. Mol. Sci.* **2013**, *14*, 9906–9946. [CrossRef] [PubMed]
140. Vieira, D.B.; Carmona-Ribeiro, A.M. Cationic nanoparticles for delivery of amphotericin B: Preparation, characterization and activity in vitro. *J. Nanobiotechnol.* **2008**, *6*, 6. [CrossRef] [PubMed]
141. Melo, L.D.; Mamizuka, E.M.; Carmona-Ribeiro, A.M. Antimicrobial particles from cationic lipid and polyelectrolytes. *Langmuir* **2010**, *26*, 12300–12306. [CrossRef]
142. Bohidar, H.; Dubin, P.L.; Majhi, P.R.; Tribet, C.; Jaeger, W. Effects of protein-polyelectrolyte affinity and polyelectrolyte molecular weight on dynamic properties of bovine serum albumin-poly(diallyldimethylammonium chloride) coacervates. *Biomacromolecules* **2005**, *6*, 1573–1585. [CrossRef]
143. Kayitmazer, A.B.; Strand, S.P.; Tribet, C.; Jaeger, W.; Dubin, P.L. Effect of polyelectrolyte structure on protein-polyelectrolyte coacervates: Coacervates of bovine serum albumin with poly(diallyldimethylammonium chloride) versus chitosan. *Biomacromolecules* **2007**, *8*, 3568–3577. [CrossRef]
144. Xu, L.; Liu, Y.; Chen, Z.; Li, W.; Liu, Y.; Wang, L.; Liu, Y.; Wu, X.; Ji, Y.; Zhao, Y.; et al. Surface-engineered gold nanorods: Promising DNA vaccine adjuvant for HIV-1 treatment. *Nano Lett.* **2012**, *12*, 2003–2012. [CrossRef] [PubMed]
145. Kim, K.; Chen, W.C.W.; Heo, Y.; Wang, Y. Polycations and their biomedical applications. *Prog. Polym. Sci.* **2016**, *60*, 18–50. [CrossRef]
146. Shen, C.; Li, J.; Zhang, Y.; Li, Y.; Shen, G.; Zhu, J.; Tao, J. Polyethylenimine-based micro/nanoparticles as vaccine adjuvants. *Int. J. Nanomed.* **2017**, *12*, 5443–5460. [CrossRef] [PubMed]
147. Chen, X.; Wang, L.; Liu, Q.; Jia, J.; Liu, Y.; Zhang, W.; Ma, G.; Su, Z. Polycation-decorated PLA microspheres induce robust immune responses via commonly used parenteral administration routes. *Int. Immunopharmacol.* **2014**, *23*, 592–602. [CrossRef] [PubMed]
148. Benjaminsen, R.V.; Mattebjerg, M.A.; Henriksen, J.R.; Moghimi, S.M.; Andresen, T.L. The possible "proton sponge " effect of polyethylenimine (PEI) does not include change in lysosomal pH. *Mol. Ther.* **2013**, *21*, 149–157. [CrossRef]
149. Akinc, A.; Thomas, M.; Klibanov, A.M.; Langer, R. Exploring polyethylenimine-mediated DNA transfection and the proton sponge hypothesis. *J. Gene Med.* **2005**, *7*, 657–663. [CrossRef]
150. Le Bihan, O.; Chevre, R.; Mornet, S.; Garnier, B.; Pitard, B.; Lambert, O. Probing the in vitro mechanism of action of cationic lipid/DNA lipoplexes at a nanometric scale. *Nucleic Acids Res.* **2011**, *39*, 1595–1609. [CrossRef]

151. Démoulins, T.; Milona, P.; Englezou, P.C.; Ebensen, T.; Schulze, K.; Suter, R.; Pichon, C.; Midoux, P.; Guzmán, C.A.; Ruggli, N.; et al. Polyethylenimine-based polyplex delivery of self-replicating RNA vaccines. *Nanomed. Nanotechnol. Biol. Med.* **2016**, *12*, 711–722. [CrossRef] [PubMed]
152. Regnstrom, K.; Ragnarsson, E.G.E.; Koping-Hoggard, M.; Torstensson, E.; Nyblom, H.; Artursson, P. PEI—A potent, but not harmless, mucosal immuno-stimulator of mixed T-helper cell response and FasL-mediated cell death in mice. *Gene Ther.* **2003**, *10*, 1575–1583. [CrossRef]
153. Chen, J.; Li, Z.; Huang, H.; Yang, Y.; Ding, Q.; Mai, J.; Guo, W.; Xu, Y. Improved antigen cross-presentation by polyethyleneimine-based nanoparticles. *Int. J. Nanomed.* **2011**, *6*, 77–84. [CrossRef] [PubMed]
154. Qin, T.; Yin, Y.; Huang, L.; Yu, Q.; Yang, Q. H9N2 influenza whole inactivated virus combined with polyethyleneimine strongly enhances mucosal and systemic immunity after intranasal immunization in mice. *Clin. Vaccine Immunol.* **2015**, *22*, 421–429. [CrossRef]
155. Dhanwani, R.; Takahashi, M.; Sharma, S. Cytosolic sensing of immuno-stimulatory DNA, the enemy within. *Curr. Opin. Immunol.* **2018**, *50*, 82–87. [CrossRef]
156. Ma, Y.F.; Yang, Y.W. Delivery of DNA-based cancer vaccine with polyethylenimine. *Eur. J. Pharm. Sci.* **2010**, *40*, 75–83. [CrossRef] [PubMed]
157. Fischer, D.; Dautzenberg, H.; Kunath, K.; Kissel, T. Poly(diallyldimethylammonium chlorides) and their N-methyl-N-vinylacetamide copolymer-based DNA-polyplexes: Role of molecular weight and charge density in complex formation, stability, and in vitro activity. *Int. J. Pharm.* **2004**, *280*, 253–269. [CrossRef]
158. Alatorre-Meda, M.; Taboada, P.; Krajewska, B.; Willemeit, M.; Deml, A.; Klösel, R.; Rodríguez, J.R. DNA−Poly(diallyldimethylammonium chloride) Complexation and Transfection Efficiency. *J. Phys. Chem. B* **2010**, *114*, 9356–9366. [CrossRef] [PubMed]
159. Wang, Y.; Wang, X.; Wu, B.; Zhao, Z.; Yin, F.; Li, S.; Qin, X.; Chen, Q. Dispersion of single-walled carbon nanotubes in poly(diallyldimethylammonium chloride) for preparation of a glucose biosensor. *Sens. Actuators B Chem.* **2008**, *130*, 809–815. [CrossRef]
160. Sanches, L.M.; Petri, D.F.S.; de Melo Carrasco, L.D.; Carmona-Ribeiro, A.M. The antimicrobial activity of free and immobilized poly (diallyldimethylammonium) chloride in nanoparticles of poly (methylmethacrylate). *J. Nanobiotechnol.* **2015**, *13*, 58. [CrossRef] [PubMed]
161. Galvão, C.N.; Sanches, L.M.; Mathiazzi, B.I.; Ribeiro, R.T.; Petri, D.F.S.; Carmona-Ribeiro, A.M. Antimicrobial coatings from hybrid nanoparticles of biocompatible and antimicrobial polymers. *Int. J. Mol. Sci.* **2018**, *19*, 2965. [CrossRef]
162. Ribeiro, R.T.; Galvão, C.N.; Betancourt, Y.P.; Mathiazzi, B.I.; Carmona-Ribeiro, A.M. Microbicidal dispersions and coatings from hybrid nanoparticles of poly (methyl methacrylate), poly (diallyl dimethyl ammonium) chloride, lipids, and surfactants. *Int. J. Mol. Sci.* **2019**, *20*, 6150. [CrossRef]
163. Carmona-Ribeiro, A.M. Biomimetic nanomaterials from the assembly of polymers, lipids, and surfactants. In *Surfactants and Detergents*; Dutta, A.K., Ed.; IntechOpen: Rijeka, Croatia, 2019; pp. 1–16. ISBN 978-1-78984-661-4.
164. Leong, H.S.; Butler, K.S.; Brinker, C.J.; Azzawi, M.; Conlan, S.; Dufés, C.; Owen, A.; Rannard, S.; Scott, C.; Chen, C.; et al. On the issue of transparency and reproducibility in nanomedicine. *Nat. Nanotechnol.* **2019**, *14*, 629–635. [CrossRef]
165. Rehman, Z.U.; Hoekstra, D.; Zuhorn, I.S. Mechanism of polyplex- and lipoplex-mediated delivery of nucleic acids: Real-time visualization of transient membrane destabilization without endosomal lysis. *ACS Nano* **2013**, *7*, 3767–3777. [CrossRef]
166. Rejman, J.; Bragonzi, A.; Conese, M. Role of clathrin- and caveolae-mediated endocytosis in gene transfer mediated by lipo- and polyplexes. *Mol. Ther.* **2005**, *12*, 468–474. [CrossRef]
167. Siewert, C.; Haas, H.; Nawroth, T.; Ziller, A.; Nogueira, S.S.; Schroer, M.A.; Blanchet, C.E.; Svergun, D.I.; Radulescu, A.; Bates, F.; et al. Investigation of charge ratio variation in mRNA—DEAE-dextran polyplex delivery systems. *Biomaterials* **2019**, *192*, 612–620. [CrossRef]
168. Rice, J.M.; Madison, R.M. Subcutaneous injections of vaccine adjuvant DEAE-dextran induce local sarcomas in mice. *Nat. New Biol.* **1972**, *236*, 28. [CrossRef] [PubMed]
169. Houston, W.E.; Crabbs, C.L.; Kremer, R.J.; Springer, J.W. Adjuvant effects of diethylaminoethyl-dextran. *Infect. Immun.* **1976**, *13*, 1559–1562. [CrossRef] [PubMed]
170. Joo, I.; Emod, J. Adjuvant effect of DEAE-dextran on cholera vaccines. *Vaccine* **1988**, *6*, 233–237. [CrossRef]

171. Wittmann, G.; Bauer, K.; Mussgay, M. [Trials of vaccination of pigs with vaccines of inactivated foot-and-mouth disease (FMD) virus. II. Trials with ethyl ethyleneimine (EEI) inactivated virus and diethylaminoethyl dextran as an adjuvant]. *Arch. Gesamte Virusforsch.* **1970**, *29*, 139–158. [CrossRef]
172. Bakrania, A.K.; Variya, B.C.; Patel, S.S. Role of β-interferon inducer (DEAE-dextran) in tumorigenesis by VEGF and NOTCH1 inhibition along with apoptosis induction. *Front. Pharmacol.* **2017**, *8*, 930. [CrossRef]
173. Ji, W.; Panus, D.; Palumbo, R.N.; Tang, R.; Wang, C. Poly(2-aminoethyl methacrylate) with well-defined chain length for DNA vaccine delivery to dendritic cells. *Biomacromolecules* **2011**, *12*, 4373–4385. [CrossRef]
174. Chen, W.; Hong, Y.; Zhang, T.; Kong, D.; Zhang, M.; Zhang, Q.; Wang, C. Star-shaped poly(2-aminoethyl methacrylate)s as non-viral gene carriers: Exploring structure-function relationship. *Colloids Surf. B Biointerfaces* **2019**, *181*, 721–727. [CrossRef] [PubMed]
175. Farris, E.; Brown, D.M.; Ramer-Tait, A.E.; Pannier, A.K. Micro- and nanoparticulates for DNA vaccine delivery. *Exp. Biol. Med.* **2016**, *241*, 919–929. [CrossRef] [PubMed]
176. Mazid, R.; Tan, M.X.; Danquah, M.K. Molecular delivery of plasmids for genetic vaccination. *Curr. Pharm. Biotechnol.* **2013**, *14*, 615–622. [CrossRef] [PubMed]
177. Luhrs, P.; Schmidt, W.; Kutil, R.; Buschle, M.; Wagner, S.N.; Stingl, G.; Schneeberger, A. Induction of specific immune responses by polycation-based vaccines. *J. Immunol.* **2002**, *169*, 5217–5226. [CrossRef]
178. De Koker, S.; De Geest, B.G.; Singh, S.K.; De Rycke, R.; Naessens, T.; Van Kooyk, Y.; Demeester, J.; De Smedt, S.C.; Grooten, J. Polyelectrolyte microcapsules as antigen delivery vehicles to dendritic cells: Uptake, processing, and cross-presentation of encapsulated antigens. *Angew. Chem. Int. Ed.* **2009**, *48*, 8485–8489. [CrossRef] [PubMed]
179. Devriendt, B.; Baert, K.; Dierendonck, M.; Favoreel, H.; De Koker, S.; Remon, J.P.; De Geest, B.G.; Cox, E. One-step spray-dried polyelectrolyte microparticles enhance the antigen cross-presentation capacity of porcine dendritic cells. *Eur. J. Pharm. Biopharm.* **2013**, *84*, 421–429. [CrossRef] [PubMed]
180. Mattner, F.; Fleitmann, J.K.; Lingnau, K.; Schmidt, W.; Egyed, A.; Fritz, J.; Zauner, W.; Wittmann, B.; Gorny, I.; Berger, M.; et al. Vaccination with poly-L-arginine as immunostimulant for peptide vaccines: Induction of potent and long-lasting T-cell responses against cancer antigens. *Cancer Res.* **2002**, *62*, 1477–1480. [PubMed]
181. Maubant, S.; Banissi, C.; Beck, S.; Chauvat, A.; Carpentier, A.F. Adjuvant properties of cytosine-phosphate-guanosine oligodeoxynucleotide in combination with various polycations in an ovalbumin-vaccine model. *Nucleic Acid Ther.* **2011**, *21*, 231–240. [CrossRef] [PubMed]
182. Lingnau, K.; Egyed, A.; Schellack, C.; Mattner, F.; Buschle, M.; Schmidt, W. Poly-L-arginine synergizes with oligodeoxynucleotides containing CpG-motifs (CpG-ODN) for enhanced and prolonged immune responses and prevents the CpG-ODN-induced systemic release of pro-inflammatory cytokines. *Vaccine* **2002**, *20*, 3498–3508. [CrossRef]
183. Mulens-Arias, V.; Rojas, J.M.; Sanz-Ortega, L.; Portilla, Y.; Perez-Yague, S.; Barber, D.F. Polyethylenimine-coated superparamagnetic iron oxide nanoparticles impair in vitro and in vivo angiogenesis. *Nanomedicine* **2019**, *21*, 102063. [CrossRef] [PubMed]
184. Mulens-Arias, V.; Rojas, J.M.; Pérez-Yagüe, S.; Morales, M.P.; Barber, D.F. Polyethylenimine-coated SPIONs trigger macrophage activation through TLR-4 signaling and ROS production and modulate podosome dynamics. *Biomaterials* **2015**, *52*, 494–506. [CrossRef]
185. Zarei, H.; Kazemi Oskuee, R.; Hanafi-Bojd, M.Y.; Gholami, L.; Ansari, L.; Malaekeh-Nikouei, B. Enhanced gene delivery by polyethyleneimine coated mesoporous silica nanoparticles. *Pharm. Dev. Technol.* **2019**, *24*, 127–132. [CrossRef]
186. Lazarus, G.G.; Singh, M. In vitro cytotoxic activity and transfection efficiency of polyethyleneimine functionalized gold nanoparticles. *Colloids Surf. B. Biointerfaces* **2016**, *145*, 906–911. [CrossRef]
187. Wang, G.; Zhou, H.; Nian, Q.G.; Yang, Y.; Qin, C.F.; Tang, R. Robust vaccine formulation produced by assembling a hybrid coating of polyethyleneimine-silica. *Chem. Sci.* **2016**, *7*, 1753–1759. [CrossRef] [PubMed]
188. Li, A.W.; Sobral, M.C.; Badrinath, S.; Choi, Y.; Graveline, A.; Stafford, A.G.; Weaver, J.C.; Dellacherie, M.O.; Shih, T.Y.; Ali, O.A.; et al. A facile approach to enhance antigen response for personalized cancer vaccination. *Nat. Mater.* **2018**, *17*, 528–534. [CrossRef]
189. Minigo, G.; Scholzen, A.; Tang, C.K.; Hanley, J.C.; Kalkanidis, M.; Pietersz, G.A.; Apostolopoulos, V.; Plebanski, M. Poly L-lysine-coated nanoparticles: A potent delivery system to enhance DNA vaccine efficacy. *Vaccine* **2007**, *25*, 1316–1327. [CrossRef] [PubMed]

190. Gu, P.; Wusiman, A.; Wang, S.; Zhang, Y.; Liu, Z.; Hu, Y.; Liu, J.; Wang, D. Polyethylenimine-coated PLGA nanoparticles-encapsulated Angelica sinensis polysaccharide as an adjuvant to enhance immune responses. *Carbohydr. Polym.* **2019**, *223*, 115128. [CrossRef] [PubMed]
191. Salvador, A.; Sandgren, K.J.; Liang, F.; Thompson, E.A.; Koup, R.A.; Pedraz, J.L.; Hernandez, R.M.; Lore, K.; Igartua, M. Design and evaluation of surface and adjuvant modified PLGA microspheres for uptake by dendritic cells to improve vaccine responses. *Int. J. Pharm.* **2015**, *496*, 371–381. [CrossRef] [PubMed]
192. Arif, U.; Haider, S.; Haider, A.; Khan, N.; Alghyamah, A.A.; Jamila, N.; Khan, M.I.; Almasry, W.A.; Kang, I.K. Biocompatible polymers and their potential biomedical applications: A review. *Curr. Pharm. Des.* **2019**, *25*, 3608–3619. [CrossRef] [PubMed]
193. Shastri, V.P. Non-degradable biocompatible polymers in medicine: Past, present and future. *Curr. Pharm. Biotechnol.* **2003**, *4*, 331–337. [CrossRef] [PubMed]
194. Calzoni, E.; Cesaretti, A.; Polchi, A.; Di Michele, A.; Tancini, B.; Emiliani, C. Biocompatible polymer nanoparticles for drug delivery applications in cancer and neurodegenerative disorder therapies. *J. Funct. Biomater.* **2019**, *10*, 4. [CrossRef]
195. Makadia, H.K.; Siegel, S.J. Poly lactic-co-glycolic acid (PLGA) as biodegradable controlled drug delivery carrier. *Polymers* **2011**, *3*, 1377–1397. [CrossRef] [PubMed]
196. Malikmammadov, E.; Tanir, T.E.; Kiziltay, A.; Hasirci, V.; Hasirci, N. PCL and PCL-based materials in biomedical applications. *J. Biomater. Sci. Polym. Ed.* **2018**, *29*, 863–893. [CrossRef]
197. Lasprilla, A.J.R.; Martinez, G.A.R.; Lunelli, B.H.; Jardini, A.L.; Filho, R.M. Poly-lactic acid synthesis for application in biomedical devices—A review. *Biotechnol. Adv.* **2012**, *30*, 321–328. [CrossRef] [PubMed]
198. Rivera-Briso, A.L.; Serrano-Aroca, A. Poly(3-hydroxybutyrate-co-3-hydroxyvalerate): Enhancement strategies for advanced applications. *Polymers* **2018**, *10*, 732. [CrossRef] [PubMed]
199. Guan, G.; Azad, M.A.K.; Lin, Y.; Kim, S.W.; Tian, Y.; Liu, G.; Wang, H. Biological effects and applications of chitosan and chito-oligosaccharides. *Front. Physiol.* **2019**, *10*, 516. [CrossRef] [PubMed]
200. Younes, I.; Rinaudo, M. Chitin and chitosan preparation from marine sources. Structure, properties and applications. *Mar. Drugs* **2015**, *13*, 1133–1174. [CrossRef] [PubMed]
201. HPS, A.K.; Saurabh, C.K.; Adnan, A.S.; Nurul Fazita, M.R.; Syakir, M.I.; Davoudpour, Y.; Rafatullah, M.; Abdullah, C.K.; Haafiz, M.K.M.; Dungani, R. A review on chitosan-cellulose blends and nanocellulose reinforced chitosan biocomposites: Properties and their applications. *Carbohydr. Polym.* **2016**, *150*, 216–226.
202. Ali, U.; Karim, K.J.B.A.; Buang, N.A. A review of the properties and applications of poly (methyl methacrylate) (PMMA). *Polym. Rev.* **2015**, *55*, 678–705. [CrossRef]
203. Zaman, M.; Skwarczynski, M.; Malcolm, J.M.; Urbani, C.N.; Jia, Z.; Batzloff, M.R.; Good, M.F.; Monteiro, M.J.; Toth, I. Self-adjuvanting polyacrylic nanoparticulate delivery system for group A streptococcus (GAS) vaccine. *Nanomedicine* **2011**, *7*, 168–173. [CrossRef]
204. O'Hagan, D.T.; Singh, M. Microparticles as vaccine adjuvants and delivery systems. *Expert Rev. Vaccines* **2003**, *2*, 269–283. [CrossRef]
205. Carmona-Ribeiro, A.M.; Midmore, B.R. Synthetic bilayer adsorption onto polystyrene microspheres. *Langmuir* **1992**, *8*, 801–806. [CrossRef]
206. Carmona-Ribeiro, A.M.; de Moraes Lessa, M. Interactions between bilayer membranes and latex. *Colloids Surf. A Physicochem. Eng. Asp.* **1999**, *153*, 355–361. [CrossRef]
207. Xavier, G.R.S.; Carmona-Ribeiro, A.M. Cationic biomimetic particles of polystyrene/cationic bilayer/gramicidin for optimal bactericidal activity. *Nanomaterials* **2017**, *7*, 422. [CrossRef] [PubMed]
208. Moura, S.P.; Carmona-Ribeiro, A.M. Cationic bilayer fragments on silica at low Ionic strength: Competitive adsorption and colloid stability. *Langmuir* **2003**, *19*, 6664–6667. [CrossRef]
209. Ribeiro, R.T.; Braga, V.H.A.; Carmona-Ribeiro, A.M. Biomimetic cationic nanoparticles based on silica: Optimizing bilayer deposition from lipid films. *Biomimetics* **2017**, *2*, 20. [CrossRef] [PubMed]
210. Pereira, E.M.A.; Kosaka, P.M.; Rosa, H.; Vieira, D.B.; Kawano, Y.; Petri, D.F.S.; Carmona-Ribeiro, A.M. Hybrid materials from intermolecular associations between cationic lipid and polymers. *J. Phys. Chem. B* **2008**, *112*, 9301–9310. [CrossRef]
211. Melo, L.D.; Palombo, R.R.; Petri, D.F.S.; Bruns, M.; Pereira, E.M.A.; Carmona-Ribeiro, A.M. Structure-activity relationship for quaternary ammonium compounds hybridized with poly(methyl methacrylate). *ACS Appl. Mater. Interfaces* **2011**, *3*, 1933–1939. [CrossRef]

212. Naves, A.F.; Palombo, R.R.; Carrasco, L.D.M.; Carmona-Ribeiro, A.M. Antimicrobial particles from emulsion polymerization of methyl methacrylate in the presence of quaternary ammonium surfactants. *Langmuir* **2013**, *29*, 9677–9684. [CrossRef]
213. Mathiazzi, B.I.; Carmona-Ribeiro, A.M. Hybrid nanoparticles of poly (methyl methacrylate) and antimicrobial quaternary ammonium surfactants. *Pharmaceutics* **2020**, *12*, 340. [CrossRef]
214. Carmona-Ribeiro, A.M. Self-assembled antimicrobial nanomaterials. *Int. J. Environ. Res. Public Health* **2018**, *15*, 1408. [CrossRef]
215. Carmona-Ribeiro, A.M. Biomimetic lipid polymer nanoparticles for drug delivery. In *Nanoparticles in Biology and Medicine. Methods in Molecular Biology*; Ferrari, E., Soloviev, M., Eds.; Springer Nature: New York, NY, USA, 2020; Volume 2118, pp. 45–60. ISBN 978-1-0716-0318-5.
216. Han, J.; Zhao, D.; Li, D.; Wang, X.; Jin, Z.; Zhao, K. Polymer-Based Nanomaterials and Applications for Vaccines and Drugs. *Polymers* **2018**, *10*, 31. [CrossRef]
217. Bose, R.J.; Kim, M.; Chang, J.H.; Paulmurugan, R.; Moon, J.J.; Koh, W.G.; Lee, S.H.; Park, H. Biodegradable polymers for modern vaccine development. *J. Ind. Eng. Chem.* **2019**, *77*, 12–24. [CrossRef]
218. Nevagi, R.J.; Skwarczynski, M.; Toth, I. Polymers for subunit vaccine delivery. *Eur. Polym. J.* **2019**, *114*, 397–410. [CrossRef]
219. Pavot, V.; Berthet, M.; Rességuier, J.; Legaz, S.; Handké, N.; Gilbert, S.C.; Paul, S.; Verrier, B. Poly(lactic acid) and poly(lactic-co-glycolic acid) particles as versatile carrier platforms for vaccine delivery. *Nanomedicine* **2014**, *9*, 2703–2718. [CrossRef]
220. Moran, H.B.T.; Turley, J.L.; Andersson, M.; Lavelle, E.C. Immunomodulatory properties of chitosan polymers. *Biomaterials* **2018**, *184*, 1–9. [CrossRef]
221. Ebrahimian, M.; Hashemi, M.; Maleki, M.; Abnous, K.; Hashemitabar, G.; Ramezani, M.; Haghparast, A. Induction of a balanced Th1/Th2 immune responses by co-delivery of PLGA/ovalbumin nanospheres and CpG ODNs/PEI-SWCNT nanoparticles as TLR9 agonist in BALB/c mice. *Int. J. Pharm.* **2016**, *515*, 708–720. [CrossRef] [PubMed]
222. Ebrahimian, M.; Hashemi, M.; Maleki, M.; Hashemitabar, G.; Abnous, K.; Ramezani, M.; Haghparast, A. Co-delivery of dual toll-like receptor agonists and antigen in poly(lactic-co-glycolic) acid/polyethylenimine cationic hybrid nanoparticles promote efficient in vivo immune responses. *Front. Immunol.* **2017**, *8*, 1077. [CrossRef]
223. Kasturi, S.P.; Sachaphibulkij, K.; Roy, K. Covalent conjugation of polyethyleneimine on biodegradable microparticles for delivery of plasmid DNA vaccines. *Biomaterials* **2005**, *26*, 6375–6385. [CrossRef] [PubMed]
224. Zhou, X.; Liu, B.; Yu, X.; Zha, X.; Zhang, X.; Wang, X.; Jin, Y.; Wu, Y.; Chen, Y.; Shan, Y.; et al. Controlled release of PEI/DNA complexes from PLGA microspheres as a potent delivery system to enhance immune response to HIV vaccine DNA prime/MVA boost regime. *Eur. J. Pharm. Biopharm.* **2008**, *68*, 589–595. [CrossRef]
225. Duran, V.; Yasar, H.; Becker, J.; Thiyagarajan, D.; Loretz, B.; Kalinke, U.; Lehr, C.M. Preferential uptake of chitosan-coated PLGA nanoparticles by primary human antigen presenting cells. *Nanomedicine* **2019**, *21*, 102073. [CrossRef]
226. Pawar, D.; Mangal, S.; Goswami, R.; Jaganathan, K.S. Development and characterization of surface modified PLGA nanoparticles for nasal vaccine delivery: Effect of mucoadhesive coating on antigen uptake and immune adjuvant activity. *Eur. J. Pharm. Biopharm.* **2013**, *85*, 550–559. [CrossRef]
227. Chen, X.; Liu, Y.Y.; Wang, L.Y.; Liu, Y.; Weifeng, Z.; Fan, B.; Ma, X.; Yuan, Q.; Ma, G.; Su, Z. Enhanced humoral and cell-mediated immune responses generated by cationic polymer-coated PLA microspheres with adsorbed HBsAg. *Mol. Pharm.* **2014**, *11*, 1772–1784. [CrossRef]
228. Chaturvedi, M.; Kumar, M.; Pathak, K. A review on mucoadhesive polymer used in nasal drug delivery system. *J. Adv. Pharm. Technol. Res.* **2011**, *2*, 215–222. [CrossRef]
229. Slütter, B.; Bal, S.; Keijzer, C.; Mallants, R.; Hagenaars, N.; Que, I.; Kaijzel, E.; van Eden, W.; Augustijns, P.; Löwik, C.; et al. Nasal vaccination with N-trimethyl chitosan and PLGA based nanoparticles: Nanoparticle characteristics determine quality and strength of the antibody response in mice against the encapsulated antigen. *Vaccine* **2010**, *28*, 6282–6291. [CrossRef] [PubMed]
230. Park, Y.M.; Shin, B.A.; Oh, I.J. Poly(ι-lactic acid)/polyethylenimine nanoparticles as plasmid DNA carriers. *Arch. Pharm. Res.* **2008**, *31*, 96–102. [CrossRef] [PubMed]

231. Kim, I.S.; Lee, S.K.; Park, Y.M.; Lee, Y.B.; Shin, S.C.; Lee, K.C.; Oh, I.J. Physicochemical characterization of poly(L-lactic acid) and poly(D,L-lactide-co-glycolide) nanoparticles with polyethylenimine as gene delivery carrier. *Int. J. Pharm.* **2005**, *298*, 255–262. [CrossRef] [PubMed]
232. Yu, X.; Wen, T.; Cao, P.; Shan, L.; Li, L. Alginate-chitosan coated layered double hydroxide nanocomposites for enhanced oral vaccine delivery. *J. Colloid Interface Sci.* **2019**, *556*, 258–265. [CrossRef]
233. Jaafar, M.H.M.; Hamid, K.A. Chitosan-Coated Alginate Nanoparticles Enhanced Absorption Profile of Insulin Via Oral Administration. *Curr. Drug Deliv.* **2019**, *16*, 672–686. [CrossRef]
234. Biswas, S.; Chattopadhyay, M.; Sen, K.K.; Saha, M.K. Development and characterization of alginate coated low molecular weight chitosan nanoparticles as new carriers for oral vaccine delivery in mice. *Carbohydr. Polym.* **2015**, *121*, 403–410. [CrossRef]
235. Borges, O.; Silva, M.; de Sousa, A.; Borchard, G.; Junginger, H.E.; Cordeiro-da-Silva, A. Alginate coated chitosan nanoparticles are an effective subcutaneous adjuvant for hepatitis B surface antigen. *Int. Immunopharmacol.* **2008**, *8*, 1773–1780. [CrossRef]
236. Yuan, J.; Guo, L.; Wang, S.; Liu, D.; Qin, X.; Zheng, L.; Tian, C.; Han, X.; Chen, R.; Yin, R. Preparation of self-assembled nanoparticles of epsilon-polylysine-sodium alginate: A sustained-release carrier for antigen delivery. *Colloids Surf. B Biointerfaces* **2018**, *171*, 406–412. [CrossRef]
237. Setty, C.M.; Sahoo, S.S.; Sa, B. Alginate-coated alginate-polyethyleneimine beads for prolonged release of furosemide in simulated intestinal fluid. *Drug Dev. Ind. Pharm.* **2005**, *31*, 435–446. [CrossRef]
238. Wang, G.D.; Tan, Y.Z.; Wang, H.J.; Zhou, P. Autophagy promotes degradation of polyethyleneimine-alginate nanoparticles in endothelial progenitor cells. *Int. J. Nanomed.* **2017**, *12*, 6661–6675. [CrossRef]
239. Li, P.; Luo, Z.; Liu, P.; Gao, N.; Zhang, Y.; Pan, H.; Liu, L.; Wang, C.; Cai, L.; Ma, Y. Bioreducible alginate-poly(ethylenimine) nanogels as an antigen-delivery system robustly enhance vaccine-elicited humoral and cellular immune responses. *J. Control. Release* **2013**, *168*, 271–279. [CrossRef]
240. Tencomnao, T.; Klangthong, K.; Pimpha, N.; Chaleawlert-Umpon, S.; Saesoo, S.; Woramongkolchai, N.; Saengkrit, N. Acceleration of gene transfection efficiency in neuroblastoma cells through polyethyleneimine/poly(methyl methacrylate) core-shell magnetic nanoparticles. *Int. J. Nanomed.* **2012**, *7*, 2783–2792.
241. Zhu, J.; Tang, A.; Law, L.P.; Feng, M.; Ho, K.M.; Lee, D.K.L.; Harris, F.W.; Li, P. Amphiphilic core-shell nanoparticles with poly(ethylenimine) shells as potential gene delivery carriers. *Bioconjug. Chem.* **2005**, *16*, 139–146. [CrossRef]
242. Castaldello, A.; Brocca-Cofano, E.; Voltan, R.; Triulzi, C.; Altavilla, G.; Laus, M.; Sparnacci, K.; Ballestri, M.; Tondelli, L.; Fortini, C.; et al. DNA prime and protein boost immunization with innovative polymeric cationic core-shell nanoparticles elicits broad immune responses and strongly enhance cellular responses of HIV-1 tat DNA vaccination. *Vaccine* **2006**, *24*, 5655–5669. [CrossRef] [PubMed]
243. Santo, D.; Mendonça, P.V.; Lima, M.S.; Cordeiro, R.A.; Cabanas, L.; Serra, A.; Coelho, J.F.J.; Faneca, H. Poly(ethylene glycol)- block-poly(2-aminoethyl methacrylate hydrochloride)-Based Polyplexes as Serum-Tolerant Nanosystems for Enhanced Gene Delivery. *Mol. Pharm.* **2019**, *16*, 2129–2141. [CrossRef] [PubMed]
244. Dombu, C.; Carpentier, R.; Betbeder, D. Influence of surface charge and inner composition of nanoparticles on intracellular delivery of proteins in airway epithelial cells. *Biomaterials* **2012**, *33*, 9117–9126. [CrossRef] [PubMed]
245. Qiu, F.; Becker, K.W.; Knight, F.C.; Baljon, J.J.; Sevimli, S.; Shae, D.; Gilchuk, P.; Joyce, S.; Wilson, J.T. Poly(propylacrylic acid)-peptide nanoplexes as a platform for enhancing the immunogenicity of neoantigen cancer vaccines. *Biomaterials* **2018**, *182*, 82–91. [CrossRef]
246. Lynn, G.M.; Sedlik, C.; Baharom, F.; Zhu, Y.; Ramirez-Valdez, R.A.; Coble, V.L.; Tobin, K.; Nichols, S.R.; Itzkowitz, Y.; Zaidi, N.; et al. Peptide–TLR-7/8a conjugate vaccines chemically programmed for nanoparticle self-assembly enhance CD8 T-cell immunity to tumor antigens. *Nat. Biotechnol.* **2020**, *38*, 320–332. [CrossRef]
247. Woodrow, K.A.; Bennett, K.M.; Lo, D.D. Mucosal vaccine design and delivery. *Annu. Rev. Biomed. Eng.* **2012**, *14*, 17–46. [CrossRef]
248. Borchard, G.; Lueβen, H.L.; de Boer, A.G.; Verhoef, J.C.; Lehr, C.M.; Junginger, H.E. The potential of mucoadhesive polymers in enhancing intestinal peptide drug absorption. III: Effects of chitosan-glutamate and carbomer on epithelial tight junctions in vitro. *J. Control. Release* **1996**, *39*, 131–138. [CrossRef]

249. Men, Y.; Tamber, H.; Audran, R.; Gander, B.; Corradin, G. Induction of a cytotoxic T lymphocyte response by immunization with a malaria specific CTL peptide entrapped in biodegradable polymer microspheres. *Vaccine* **1997**, *15*, 1405–1412. [CrossRef]
250. Storni, T.; Kundig, T.M.; Senti, G.; Johansen, P. Immunity in response to particulate antigen-delivery systems. *Adv. Drug Deliv. Rev.* **2005**, *57*, 333–355. [CrossRef] [PubMed]
251. Singh, B.; Maharjan, S.; Jiang, T.; Kang, S.K.; Choi, Y.J.; Cho, C.S. Combinatorial approach of antigen delivery using M cell-homing peptide and mucoadhesive vehicle to enhance the efficacy of oral vaccine. *Mol. Pharm.* **2015**, *12*, 3816–3828. [CrossRef]
252. Gupta, N.K.; Tomar, P.; Sharma, V.; Dixit, V.K. Development and characterization of chitosan coated poly-(varepsilon-caprolactone) nanoparticulate system for effective immunization against influenza. *Vaccine* **2011**, *29*, 9026–9037. [CrossRef]
253. Mukherjee, A.; Waters, A.K.; Kalyan, P.; Achrol, A.S.; Kesari, S.; Yenugonda, V.M. Lipid-polymer hybrid nanoparticles as a next-generation drug delivery platform: State of the art, emerging technologies, and perspectives. *Int. J. Nanomed.* **2019**, *14*, 1937–1952. [CrossRef]
254. Dave, V.; Tak, K.; Sohgaura, A.; Gupta, A.; Sadhu, V.; Reddy, K.R. Lipid-polymer hybrid nanoparticles: Synthesis strategies and biomedical applications. *J. Microbiol. Methods* **2019**, *160*, 130–142. [CrossRef]
255. Carmona-Ribeiro, A.M.; Herrington, T.M. Phospholipid adsorption onto polystyrene microspheres. *J. Colloid Interface Sci.* **1993**, *156*, 19–23. [CrossRef]
256. Rapuano, R.; Carmona-Ribeiro, A.M. Physical adsorption of bilayer membranes on Silica. *J. Colloid Interface Sci.* **1997**, *193*, 104–111. [CrossRef]
257. Rapuano, R.; Carmona-Ribeiro, A.M. Supported bilayers on silica. *J. Colloid Interface Sci.* **2000**, *226*, 299–307. [CrossRef]
258. Carmona-Ribeiro, A.M. Bilayer vesicles and liposomes as interface agents. *Chem. Soc. Rev.* **2001**, *30*, 241–247. [CrossRef]
259. Pacheco, L.F.; Carmona-Ribeiro, A.M. Effects of synthetic lipids on solubilization and colloid stability of hydrophobic drugs. *J. Colloid Interface Sci.* **2003**, *258*, 146–154. [CrossRef]
260. Moura, S.P.; Carmona-Ribeiro, A.M. Biomimetic particles for isolation and reconstitution of receptor function. *Cell Biochem. Biophys.* **2006**, *44*, 446–452. [CrossRef]
261. Pereira, E.M.A.; Vieira, D.B.; Carmona-Ribeiro, A.M. Cationic bilayers on polymeric particles: Effect of low NaCl concentration on surface coverage. *J. Phys. Chem. B* **2004**, *108*, 11490–11495. [CrossRef]
262. Moura, S.P.; Carmona-Ribeiro, A.M. Biomimetic particles: Optimization of phospholipid bilayer coverage on silica and colloid stabilization. *Langmuir* **2005**, *21*, 10160–10164. [CrossRef]
263. Lincopan, N.; Carmona-Ribeiro, A.M. Lipid-covered drug particles: Combined action of dioctadecyldimethylammonium bromide and amphotericin B or miconazole. *J. Antimicrob. Chemother.* **2006**, *58*, 66–75. [CrossRef]
264. Barbassa, L.; Mamizuka, E.M.; Carmona-Ribeiro, A.M. Supramolecular assemblies of rifampicin and cationic bilayers: Preparation, characterization and micobactericidal activity. *BMC Biotechnol.* **2011**, *11*, 40. [CrossRef]
265. Carvalho, C.A.; Olivares-Ortega, C.; Soto-Arriaza, M.A.; Carmona-Ribeiro, A.M. Interaction of gramicidin with DPPC/DODAB bilayer fragments. *Biochim. Biophys. Acta* **2012**, *1818*, 3064–3071. [CrossRef]
266. Carmona-Ribeiro, A.M.; Carrasco, L.D.M. Fungicidal assemblies and their mode of action. *OA Biotechnol.* **2013**, *2*, 25. [CrossRef]
267. Ragioto, D.A.M.T.; Carrasco, L.D.M.; Carmona-Ribeiro, A.M. Novel gramicidin formulations in cationic lipid as broad-spectrum microbicidal agents. *Int. J. Nanomed.* **2014**, *9*, 3183–3192.
268. Carmona-Ribeiro, A.M.; de Melo Carrasco, L.D. Novel formulations for antimicrobial peptides. *Int. J. Mol. Sci.* **2014**, *15*, 18040–18083. [CrossRef] [PubMed]
269. Carrasco, L.D.; Bertolucci, R.J.; Ribeiro, R.T.; Sampaio, J.L.M.; Carmona-Ribeiro, A.M. Cationic nanostructures against foodborne pathogens. *Front. Microbiol.* **2016**, *7*, 1804. [CrossRef] [PubMed]
270. Carrasco, L.D.; Santos, H.C.; Sampaio, J.L.; Carmona-Ribeiro, A.M. Self-assembled antibiotic nanoparticles against intracellular bacteria. *Drug Deliv. Lett.* **2017**, *7*, 39–47.
271. Mamizuka, E.M.; Carmona-Ribeiro, A.M. Cationic liposomes as antimicrobial agents. In *Communicating Current Research and Educational Topics and Trends in Applied Microbiology*; Méndez Vilas, A., Ed.; Formatex: Badajoz, Spain, 2007; Volume 2, pp. 636–647. ISBN 9788461194223.

272. Moura, S.P.; Carmona-Ribeiro, A.M. Adsorption behavior of DODAB/DPPC vesicles on silica. *J. Colloid Interface Sci.* **2007**, *313*, 519–526. [CrossRef]
273. Carmona-Ribeiro, A.M.; Barbassa, L.; Melo, L. Antimicrobial Biomimetics. In *Biomimetic Based Applications*; George, A., Ed.; IntechOpen: Rijeka, Croatia, 2011; pp. 227–284. ISBN 978-953-307-195-4.
274. Tapias, G.N.; Sicchierolli, S.M.; Mamizuka, E.M.; Carmona-Ribeiro, A.M. Interactions between cationic vesicles and Escherichia coli. *Langmuir* **1994**, *10*, 3461–3465. [CrossRef]
275. Martins, L.M.S.; Mamizuka, E.M.; Carmona-Ribeiro, A.M. Cationic Vesicles as Bactericides. *Langmuir* **1997**, *13*, 5583–5587. [CrossRef]
276. Lima, E.G.; Gomes, L.R.; Carmona-Ribeiro, A.M. Stable indomethacin dispersions in water from drug, ethanol, cationic lipid and carboxymethyl-cellulose. *Pharm. Nanotechnol.* **2016**, *4*, 126–135. [CrossRef]
277. Grabowski, E.; Morrison, I. Particle size distribution from analysis of quasi-elastic light scattering data. In *Measurement of Suspended Particles by Quasi-Elastic Light Scattering*; John Wiley & Sons: New York, NY, USA, 1983; pp. 199–236.
278. Andersson, M.; Hammarstroem, L.; Edwards, K. Effect of Bilayer Phase Transitions on Vesicle Structure, and its Influence on the Kinetics of Viologen Reduction. *J. Phys. Chem.* **1995**, *99*, 14531–14538. [CrossRef]
279. Carmona-Ribeiro, A.M.; Castuma, C.E.; Sesso, A.; Schreier, S. Bilayer structure and stability in dihexadecyl phosphate dispersions. *J. Phys. Chem.* **1991**, *95*, 5361–5366. [CrossRef]
280. Gall, D. The adjuvant activity of aliphatic nitrogenous bases. *Immunology* **1966**, *11*, 369–386.
281. Dailey, M.O.; Hunter, R.L. The role of lipid in the induction of hapten-specific delayed hypersensitivity and contact sensitivity. *J. Immunol.* **1974**, *112*, 1526–1534. [PubMed]
282. Klinguer-Hamour, C.; Libon, C.; Plotnicky-Gilquin, H.; Bussat, M.C.; Revy, L.; Nguyen, T.; Bonnefoy, J.Y.; Corvaïa, N.; Beck, A. DDA adjuvant induces a mixed Th1/Th2 immune response when associated with BBG2Na, a respiratory syncytial virus potential vaccine. *Vaccine* **2002**, *20*, 2743–2751. [CrossRef]
283. Jain, V.; Gupta, A.; Pawar, V.K.; Asthana, S.; Jaiswal, A.K.; Dube, A.; Chourasia, M.K. Chitosan-assisted immunotherapy for intervention of experimental leishmaniasis via amphotericin B-loaded solid lipid nanoparticles. *Appl. Biochem. Biotechnol.* **2014**, *174*, 1309–1330. [CrossRef] [PubMed]
284. Bernocchi, B.; Carpentier, R.; Lantier, I.; Ducournau, C.; Dimier-Poisson, I.; Betbeder, D. Mechanisms allowing protein delivery in nasal mucosa using NPL nanoparticles. *J. Control. Release* **2016**, *232*, 42–50. [CrossRef]
285. Khademi, F.; Derakhshan, M.; Yousefi-Avarvand, A.; Najafi, A.; Tafaghodi, M. A novel antigen of Mycobacterium tuberculosis and MPLA adjuvant co-entrapped into PLGA:DDA hybrid nanoparticles stimulates mucosal and systemic immunity. *Microb. Pathog.* **2018**, *125*, 507–513. [CrossRef]
286. Rose, F.; Wern, J.E.; Ingvarsson, P.T.; van de Weert, M.; Andersen, P.; Follmann, F.; Foged, C. Engineering of a novel adjuvant based on lipid-polymer hybrid nanoparticles: A quality-by-design approach. *J. Control. Release* **2015**, *210*, 48–57. [CrossRef] [PubMed]
287. Fan, Y.; Sahdev, P.; Ochyl, L.J.; Akerberg, J.; Moon, J.J. Cationic liposome-hyaluronic acid hybrid nanoparticles for intranasal vaccination with subunit antigens. *J. Control. Release* **2015**, *208*, 121–129. [CrossRef]
288. Liu, L.; Ma, P.; Wang, H.; Zhang, C.; Sun, H.; Wang, C.; Song, C.; Leng, X.; Kong, D.; Ma, G. Immune responses to vaccines delivered by encapsulation into and/or adsorption onto cationic lipid-PLGA hybrid nanoparticles. *J. Control. Release* **2016**, *225*, 230–239. [CrossRef] [PubMed]



© 2020 by the authors. Licensee MDPI, Basel, Switzerland. This article is an open access article distributed under the terms and conditions of the Creative Commons Attribution (CC BY) license (http://creativecommons.org/licenses/by/4.0/).

2 | Objectives

2.1 General objective

The overall objective of this work was to determine the physical properties, in vitro cytotoxicity, and in vivo immunoadjuvant activity of cationic nanoparticles obtained by spontaneous interaction of ovalbumin (OVA) with poly(diallyl dimethylammonium) chloride (PDDA) or nanoparticles synthesized by emulsion polymerization of methyl methacrylate (MMA) in the presence of dimethyldioctadecylammonium bromide (DODAB) and PDDA, or DODAB alone as emulsifiers.

2.2 Specific objectives

- To establish a methodology for obtaining PDDA/OVA nanoparticles minimizing the concentration of free cationic polymer.
- To characterize the PDDA/OVA nanoparticles according to their physical properties and colloidal stability.
- To synthesize and characterize PMMA/DODAB/PDDA nanoparticles according to their physical properties, PMMA, DODAB, PDDA content, and core/shell dimensions.
- To synthesize and characterize PMMA/DODAB nanoparticles according to their physical properties, PMMA, DODAB content obtained employing DODAB in the form of films or fragments of bilayer.
- To determine the in vitro cytotoxicity of PDDA, OVA; PDDA/OVA PMMA/DODAB/PDDA,

and PMMA/DODAB nanoparticles as well as the cytotoxicity of large vesicles and bilayer fragments of DODAB.

- To evaluate the in vivo immune response elicited by PDDA/OVA, PMMA/DODAB/PDDA and PMMA/DODAB nanoparticles carrying OVA.

- To compare the immune response elicited by the four cationic adjuvants (PDDA/OVA, PMMA/DODAB/PDDA/OVA, PMMA/DODAB/OVA, and DODAB-BF/OVA).

3 | Microbicidal Dispersions and Coatings from Hybrid Nanoparticles of Poly (Methyl Methacrylate), Poly (Diallyl Dimethyl Ammonium) Chloride, Lipids, and Surfactants

International Journal of
Molecular Sciences

MDPI

Article

Microbicidal Dispersions and Coatings from Hybrid Nanoparticles of Poly (Methyl Methacrylate), Poly (Diallyl Dimethyl Ammonium) Chloride, Lipids, and Surfactants

Rodrigo Tadeu Ribeiro, Carolina Nascimento Galvão, Yunys Pérez Betancourt, Beatriz Ideriha Mathiazzi and Ana Maria Carmona-Ribeiro *

Biocolloids Laboratory, Departamento de Bioquímica, Instituto de Química, Universidade de São Paulo, Av. Prof. Lineu Prestes 748, 05508-000 São Paulo, Brazil; rodrigo@iq.usp.br (R.T.R.); carolinagalvao@usp.br (C.N.G.); y.betancourt@usp.br (Y.P.B.); bemathi@usp.br (B.I.M.)
* Correspondence: amcr@usp.br; Tel.: +55-011-3091-1887

Received: 12 November 2019; Accepted: 4 December 2019; Published: 6 December 2019



Abstract: Hybrid and antimicrobial nanoparticles (NPs) of poly (methyl methacrylate) (PMMA) in the presence of poly (diallyl dimethyl ammonium) chloride (PDDA) were previously obtained by emulsion polymerization in absence of surfactant with low conversion. In the presence of amphiphiles such as cetyl trimethyl ammonium bromide (CTAB), dioctadecyl dimethyl ammonium bromide (DODAB) or soybean lecithin, we found that conversion increased substantially. In this work, the effect of the amphiphiles on the NPs core-shell structure and on the antimicrobial activity of the NPs was evaluated. NPs dispersions casted on silicon wafers, glass coverslips or polystyrene substrates were also used to obtain antimicrobial coatings. Methods for characterizing the dispersions and coatings were based on scanning electron microscopy, dynamic light scattering, determination of thickness, rugosity, and wettability for the coatings and determination of colony-forming unities (log CFU/mL) of microbia after 1 h interaction with the coatings or dispersions. The amphiphiles used during PMMA/PDDA/amphiphile NPs synthesis reduced the thickness of the NPs PDDA shell surrounding each particle. The antimicrobial activity of the dispersions and coatings were due to PDDA—the amphiphiles were either washed out by dialysis or remained in the PMMA polymeric core of the NPs. The most active NPs and coatings were those of PMMA/PDDA/CTAB—the corresponding coatings showed the highest rugosity and total surface area to interact with the microbes. The dispersions and coatings obtained by casting of the NPs dispersions onto silicon wafers were hydrophilic and exhibited microbicidal activity against *Escherichia coli*, *Staphylococcus aureus*, and *Candida albicans*. In addition, a major effect of reduction in particle size revealed the suitability of nanometric and cationic NPs (sizes below 100 nm) represented by PMMA/PDDA/CTAB NPs to yield maximal microbicidal activity from films and dispersions against all microbia tested. The reduction of cell viability by coatings and dispersions amounted to 6–8 logs from [PDDA] ≥ minimal microbicidal concentration.

Keywords: hybrid polymeric nanoparticles; biocompatible polymer; antimicrobial cationic polymer; films from casting of nanoparticles; dynamic light scattering; coatings wettability; bacteria and fungus viability; bactericidal activity of hybrid coatings; *Escherichia coli*; *Staphylococcus aureus*; *Candida albicans*

1. Introduction

Several hybrid materials can exhibit antimicrobial activity [1–3]. For example, in restorative dentistry, inorganic antibacterial nanoparticles (NPs) incorporated to resin composites effectively reduce microorganism biofilm formation [4]. Examples of inorganic NPs with intrinsic antimicrobial activity are those made of ZnO, MgO, CuO, metallic silver, or gold, metal hydroxides such as $Mg(OH)_2$ [5]. In addition, colloidal NPs of biodegradable chitosan, lignin or dextran [5,6] or biocompatible poly (methacrylate)- and poly (acrylate)-based copolymers can be loaded with antibacterial agents [7]. The other class of hybrid nanomaterials encompasses the biomimetic antimicrobial NPs and coatings obtained from the assembly of polymers, surfactants, or lipids [8,9] or from the use of virus-like, bacteria-like, or biological structure-like nanomaterials carrying antimicrobials [10].

The variety of biomedical applications for antimicrobial NPs range from coating implants or catheters to drug delivery [11–13]. The very useful NPs can yield a variety of nanostructures. For example, NPs may form hybrid antimicrobial coatings and films [8,14–18].

Antimicrobial polymeric NPs of poly (methyl methacrylate) (PMMA) synthesized in the presence of the cationic antimicrobial polymer poly (diallyl dimethyl ammonium) chloride (PDDA) were first obtained in 2015 joining the biocompatible character of PMMA with the microbicidal property of the cationic PDDA [19]. PMMA is non-biodegradable, non-absorbable, non-hemolytic and non-toxic with several biomedical applications in dentistry, ophtalmics, orthopaedics, pharmaceutics, etc. [20,21].

Early reports on methyl acrylate (MA) or methyl methacrylate (MMA) polymerization using more than 1.9 wt % of monomer mass in oil-in-water microemulsions resulted in phase separation during polymerization [22–24]. In emulsion polymerization, nucleation in the micelles or monomer droplets is followed by particles growth [25,26]. The initiator reacts with MMA in the micelles and with MMA inside the droplets in the aqueous phase, yielding oligo radicals that co-localize with the monomers and continue the polymerization. PDDA present during NPs synthesis in absence of surfactant possibly stabilized the smaller droplets of MMA yielding PMMA/PDDA hybrid NPs with sizes around 200 nm of mean hydrodynamic diameter [19]. Coatings prepared by spin-coating PMMA and dioctadecyl dimethyl ammonium bromide (DODAB) or PMMA and cetyl trimethyl ammonium bromide (CTAB) displayed good antimicrobial activity against bacteria upon contact. Whereas CTAB diffused from the coating to the outer medium to kill bacteria, DODAB killed bacteria upon contact because its affinity for PMMA was higher than the one of CTAB and DODAB remained in the PMMA matrix [27,28]. In dispersion, some antimicrobial activity was also reported for PMMA/DODAB or PMMA/CTAB NPs prepared by emulsion polymerization over a range of high concentration of the quaternary ammonium amphiphiles [29].

In our laboratory, the synthesis of hybrid PMMA/PDDA NPs in absence of amphiphiles, their core-shell structure and their antimicrobial activity were described and compared with the one of the free PDDA polymer [19]. However, the yield of polymerization was low and PDDA immobilization in the NPs reduced its activity [19]. Later on, the coatings obtained by casting PMMA/PDDA NPs onto different substrates and their activity against *Escherichia coli* and *Staphylococcus aureus* were reported [17]. In addition, the use of amphiphiles as stabilizers during the NPs synthesis was shown to improve substantially the yield for the polymerization for obtaining the PMMA/PDDA/amphiphile NPs [17]. In this work, the PMMA/PDDA, PMMA/PDDA/DODAB, PMMA/PDDA/CTAB and PMMA/PDDA/lecithin NPs are further studied to ascertain the amphiphile effect on the core-shell NP structure and its effects on antimicrobial activity of the dispersions and coatings.

The results show that PDDA as an outer shell of core-shell nanoparticles or simply as an additive to dispersions and films was the dominant element imparting the antimicrobial effect. The dispersions and coatings obtained by the casting of the NPs dispersions onto silicon wafers were hydrophilic and exhibited microbicidal activity against *Escherichia coli*, *Staphylococcus aureus* and *Candida albicans.* In addition, a major effect of reduction in particle size and increased rugosity for the coatings was associated with CTAB and its molecular geometry. CTAB promoted the synthesis of the smallest NPs. Their casting onto hydrophilic surfaces generated coatings with the highest rugosity and microbicidal

activity. Nanometric and cationic NPs (sizes below 100 nm) of PMMA/PDDA/CTAB yielded maximal microbicidal activity for films and dispersions against all microbia tested amounting to 6–8 logs counting reduction from [PDDA] ≥ the minimal microbicidal concentration.

2. Results and Discussion

2.1. Physical and Antimicrobial Properties of PMMA/PDDA/Amphiphile Dispersions

SEM micrographs for the dried PMMA/PDDA/amphiphile dispersions after dialysis revealed uniform spherical NPs as synthesized in the presence of CTAB (Figure 1a), DODAB (Figure 1b) or lecithin (Figure 1c).

The micrographs on Figure 1 submitted to the ImageJ software yielded the mean diameter (D) of the dry NPs in the three dispersions (Table 1). As compared to the hydrodynamic diameter (Dz) obtained previously by dynamic light scattering (DLS) [17], the D values were smaller than the Dz ones for the NPs in water (Table 1).

The zeta-potentials (ζ) after dialysis remained positive, high and very similar to the ζ values for the PMMA/PDDA NPs obtained in absence of amphiphiles. The PDDA outer shell was responsible for the surface potential at the shear plane of the NPs in water dispersions (Table 1). In absence of PDDA, PMMA/DODAB, PMMA/CTAB, or PMMA/lecithin NPs exhibited zeta-potentials equal to 50, 26, and −21 mV, respectively [17]. In these cases, the amphiphile determined the surface potential at the shear plane of the NPs.

Figure 2 shows the effect of NaCl on Dz of PMMA/PDDA/DODAB, PMMA/PDDA/CTAB, and PMMA/PDDA/lecithin NPs. The effect of increasing [NaCl] was decreasing Dz possibly due to decreasing the thickness of the outer PDDA shell in water and screening of the positive charges on the outer polymer chains (Figure 2). This was consistent with the drying effect on particle size shown in Table 1 with D being generally smaller than Dz. The collapse of the outer and stretched PDDA polymer shell can take place either by drying the NP (Table 1) or by increasing the ionic strength thereby causing the collapse of the outer shell (Figure 2). Consistently, minimum Dz values were equal to the mean diameter D of the dry particles obtained by SEM (Table 1; Figure 2). Above the minimum Dz, further increasing [NaCl] lead to loss of colloidal stability and NPs aggregation with a substantial increase in Dz due to NPs aggregation (not shown). This occurred above 50, 20 and 50 mM NaCl for PMMA/PDDA/DODAB, PMMA/PDDA/CTAB, and PMMA/PDDA/lecithin NPs (Figure 2). Therefore, these simple experiments and considerations allowed determining the thickness of the outer PDDA shell in the different NPs as (Dz–D)/2 or as ($Dz–Dz_{minimum}$)/2. Furthermore, both determinations agreed (Table 1). Therefore, one can be confident that the shell thickness was properly obtained.

Previous data for PMMA/PDDA NPs obtained in absence of emulsifiers as compared to the antimicrobial effect of PDDA alone revealed that both similarly killed *E. coli* and *S. aureus* but PDDA was much more effective against *C. albicans* than the PMMA/PDDA NPs [19]. For the coatings cast from PMMA/PDDA NPs onto glass coverslips at 0.25 mg PDDA, the tests against bacteria (*E. coli* or *S. aureus*) yielded complete loss of cell viability but tests against *C. albicans* were not performed [17]. In this work, the antimicrobial properties of PMMA/PDDA/amphiphile dispersions were obtained for bacteria and fungus over a range of PDDA concentrations (Figure 3). The minimal microbicidal concentration (MMC) determined for each dispersion was shown in Table 2. The real potency of the dispersions was established over orders of magnitude using a logarithmic scale for the cell viability as a function of PDDA concentration. Microbial viability decreased by 10^7–10^8 viable colony forming unities (CFU) upon interaction with the NPs for 1 h (Figure 3; Table 2).

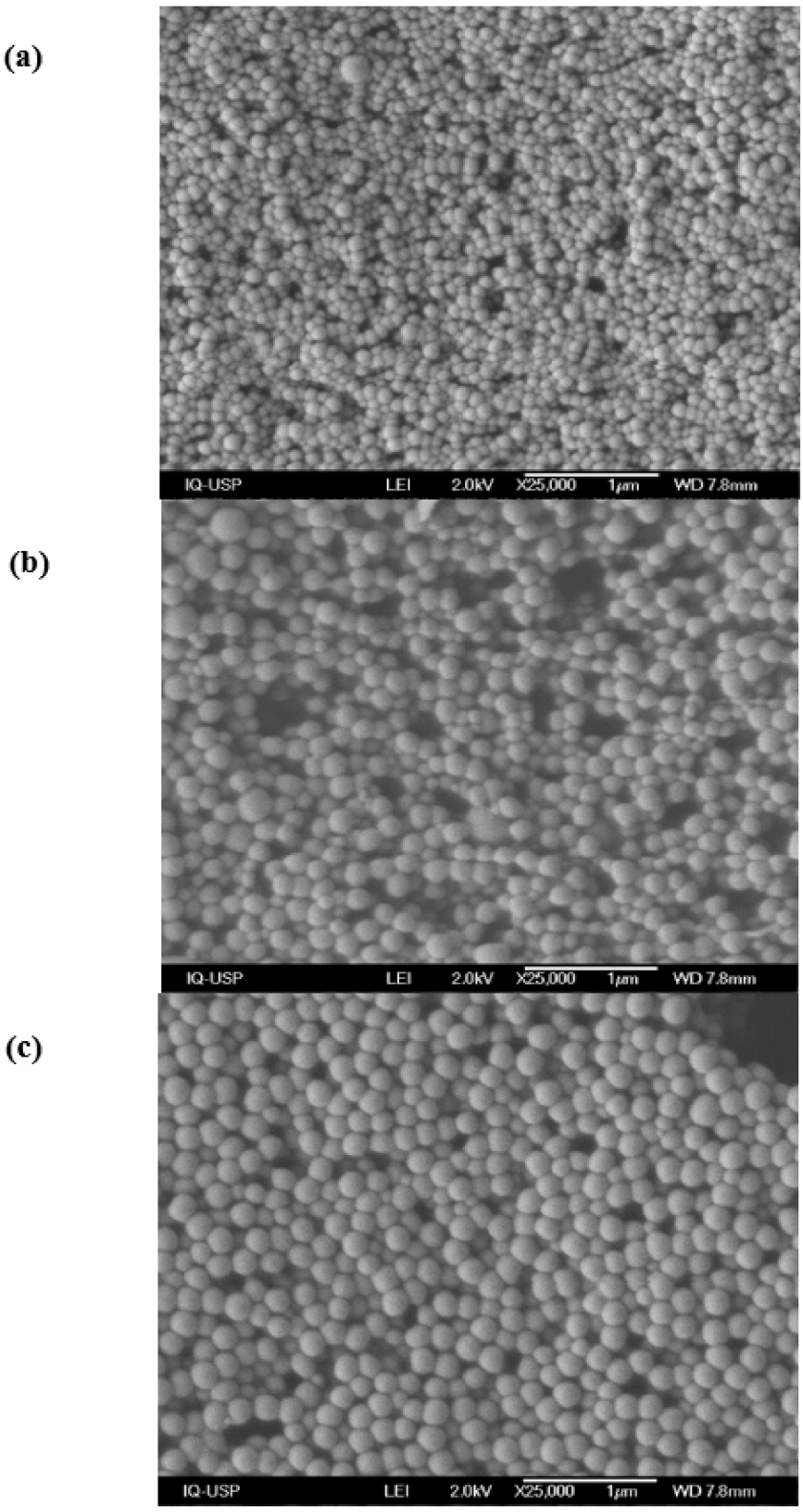


Figure 1. PMMA/PDDA/CTAB (**a**), PMMA/PDDA/DODAB (**b**) and PMMA/PDDA/lecithin coatings cast on silicon wafers from 50 μL droplets of nanoparticles (NPs) dispersions in water (**c**). The NPs were synthesized at 0.56 M MMA, 5 mg·mL^{-1} PDDA and 2 mM amphiphile (CTAB, DODAB, or lecithin). After synthesis, NPs were exhaustively dialyzed against water yielding final PDDA mass in the lyophilized coatings of 0.130 (**a**), 0.145 (**b**) and 0.140 mg (**c**). The bars represent 1000 nm.

Table 1. NPs physical properties as determined for dispersions aged 180 days. The mean hydrodynamic diameter (Dz), the polydispersity (P) and the zeta-potential (ζ) were obtained by dynamic light scattering (DLS). The mean diameter (D) was obtained for dry dispersions from scanning electron microscopy (SEM) and sizing analysis by the ImageJ software. The $Dz_{minimum}$ was obtained from the effect of [NaCl] on Dz in Figure 2. The NP shell thickness is Δ/2.

Dispersion	D/nm	Dz/nm	$Dz_{minimum}$/nm	Δ/2/nm	P	ζ/mV	Solids/mg·mL^{-1}	Conversion/%
PMMA/PDDA	164 ± 32	226 ± 3	166 ± 2	30	0.010 ± 0.010	51 ± 1	6 ± 1	11 ± 1
PMMA/PDDA/CTAB	97 ± 14	116 ± 1	98 ± 1	9	0.040 ± 0.010	50 ± 2	26 ± 1	79 ± 1
PMMA/PDDA/DODAB	183 ± 28	226 ± 1	194 ± 1	16	0.030 ± 0.020	54 ± 1	17 ± 1	47 ± 1
PMMA/PDDA/lecithin	190 ± 25	217 ± 2	194 ± 1	11.5	0.040 ± 0.020	55 ± 1	8 ± 1	24 ± 1

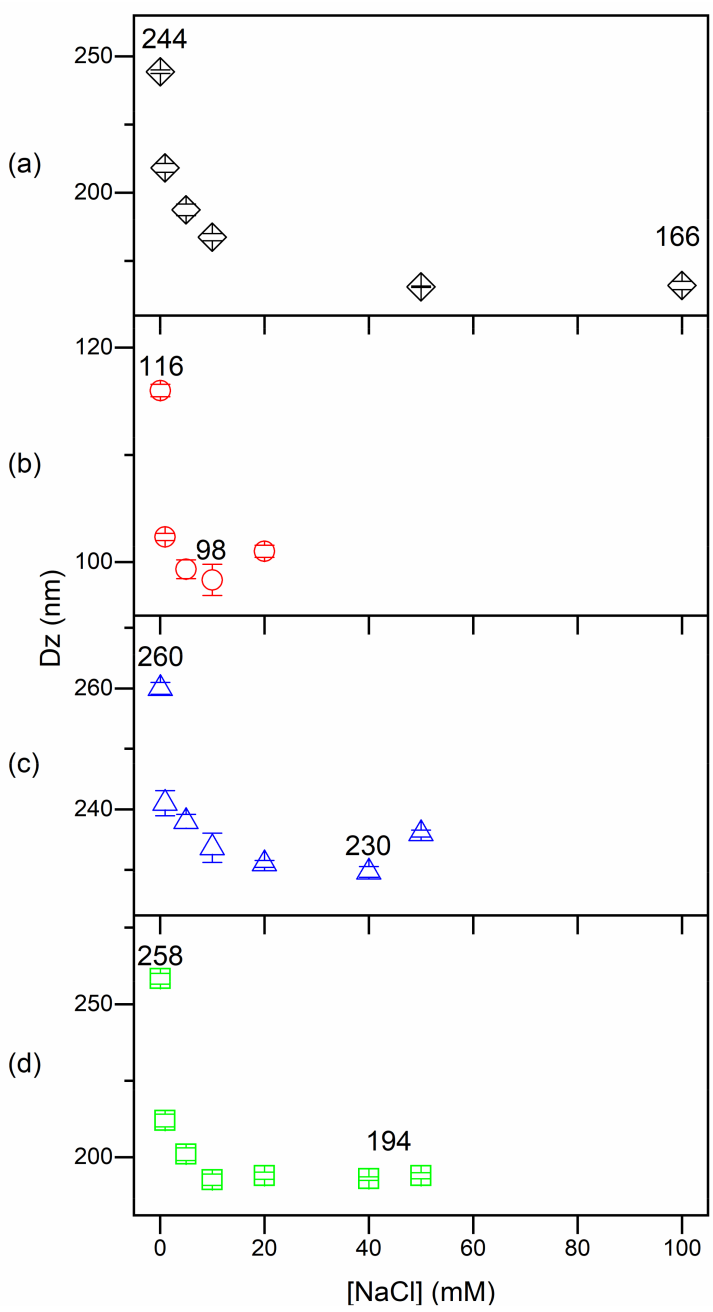


Figure 2. The collapse of the outer PDDA layer on PMMA/PDDA (**a**), PMMA/PDDA/DODAB (**b**), PMMA/PDDA/CTAB (**c**) and PMMA/PDDA/lecithin NPs (**d**) seen from Dz as a function of NaCl concentration.

From Figure 3 and Table 2, the most sensitive microorganism to the dispersions was *E. coli,* followed by *S. aureus* and *C. albicans.* The PMMA/PDDA/CTAB dispersions were the most effective dispersions killing the three strains by 7–8 logs in 1 h (Figure 3, Table 2). At this point, one should recall that all NPs exhibited hydrodynamic diameters of about 200 nm with the exception of the PMMA/PDDA/CTAB NPs with 90 ± 1 nm as Dz. Possibly, for this nanometric size especially; penetration of the NPs through the fungus cell wall and the cell membrane damaged these structures.

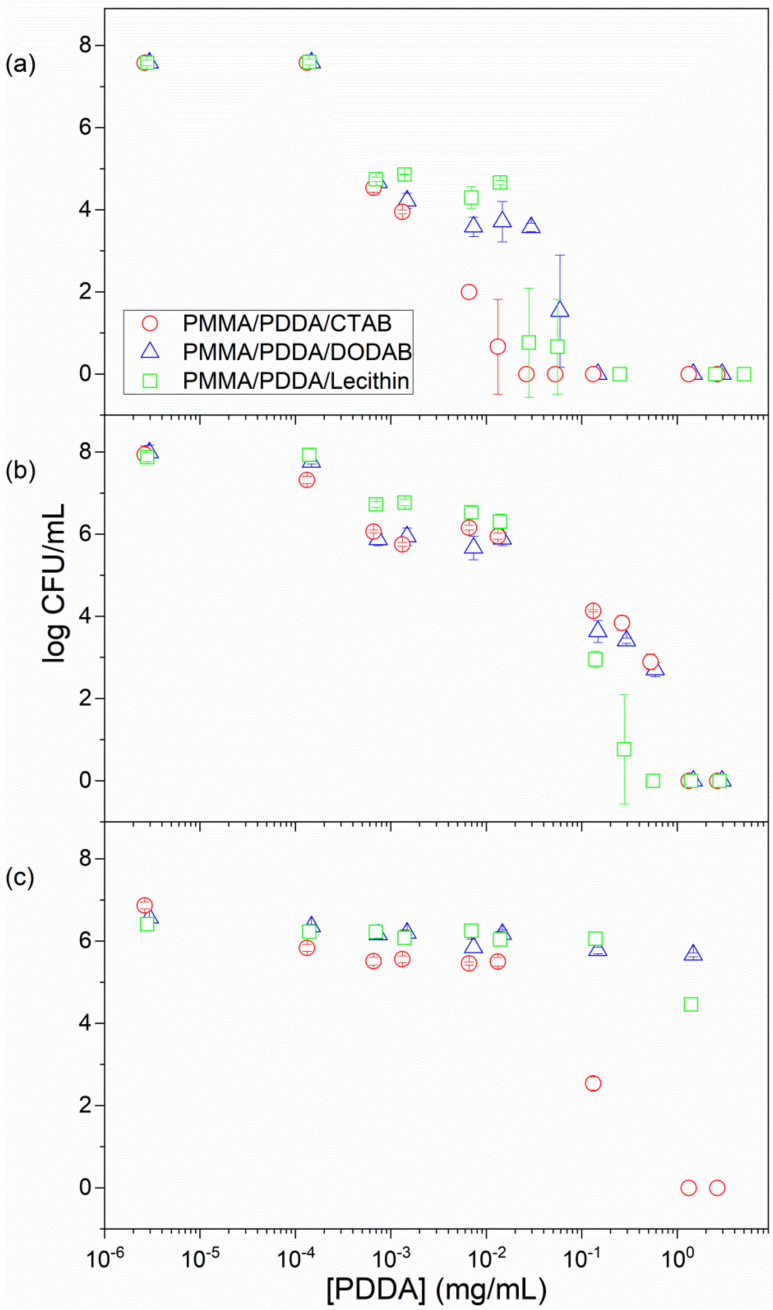


Figure 3. Antimicrobial activity of PMMA/PDDA/amphiphile dispersions after exhaustive dialysis against *E. coli* (**a**); *S. aureus* (**b**); *C. albicans* as a function of PDDA concentration (**c**). Cells and dispersions interacted for 1 h before plating for CFU counting.

Table 2. Microbicidal activities of PDDA, PMMA/PDDA and PMMA/PDDA/amphiphile dispersions plotted as minimal microbicidal concentrations (MMC).

Dispersion [1]	Minimal Microbicidal Concentration (MMC), mg·mL^{-1}		
	E. coli	*S. aureus*	*C. albicans*
PDDA [2]	0.005	>0.500	>0.005
PMMA/PDDA [2]	0.007	>0.500	>1.000
PMMA/PDDA/DODAB	0.100	1.000	>3.000
PMMA/PDDA/CTAB	0.030	1.000	1.310
PMMA/PDDA/Lecithin	0.250	0.550	>3.000

[1] Concentrations used for NPs synthesis were: [MMA] = 0.56 M; [PDDA] = 5 mg·mL^{-1}; [CTAB] = [DODAB] = [Lecithin] = 2 mM; [2] Data from reference [19].

For other assemblies with PDDA, PDDA doses required for killing *S. aureus* were always higher than those required for killing *P. aeruginosa*, a gram-negative bacterium [14]. Tetraalkyl ammonium compounds have been recognized as efficient blockers of the potassium channels KcsA of the Gram-negative *E. coli* [30].

Whereas the Gram-negative bacteria are very sensitive to all cationic compounds and assemblies, the Gram-positive *S. aureus* is less sensitive via a mechanism of resistance. A sensor system for cationic antimicrobial molecules in *Staphylococcus* sp. causes resistance to cationic antimicrobial agents [31]. A short extracellular loop with a high density of negatively charged amino acid residues would attract and interact with cationic antimicrobial compounds. Transduction of this interaction signal would trigger the D-alanylation of teichoic acids and the lysylation of phosphatidylglycerol, resulting in a decreased negative charge of the cell surface and membrane, respectively. Thereby there would be a decreased attraction for cationic molecules.

In order to evaluate the concentration of free and nanoparticle bound PDDA in the dispersions, the dispersions were dialyzed after synthesis and then centrifuged at 9,000 g in order to precipitate the NPs and separate them from their supernatant. The supernatant was then used to determine chloride concentration by micro-titration as previously described (see Methods). Since chloride is the PDDA counter-ion, its concentration is directly related to the PDDA concentration in mg·mL^{-1}. Another possible way for evaluating [PDDA] in the supernatant was its biological activity determined from inhibition of growth on *S. aureus* seeded agar plates (Figure 4). The inhibition zones against *S. aureus* depended on PDDA concentration in the wells numbered from 1 to 8; increasing [PDDA], increased the inhibition zone though the curve was not linear. Nevertheless, it was possible to estimate [PDDA] over a range of low concentrations (0–1.0 mg·mL^{-1}). After considering the dilution factor for the PMMA/PDDA/DODAB NPs after dialysis which was 2.8 the [PDDA] from the inhibition zone was 2.8 mg·mL^{-1} in reasonable agreement with the [PDDA] determined from chloride microtitration which was 2.5 mg·mL^{-1}. One should notice that PDDA cannot permeate the dialysis membrane so that the PDDA in the dialyzed dispersions will still be available to contribute to the inhibition zones. DODAB also would not permeate the dialysis membrane if it were not bound to the PMMA matrix as described before [27]. Table 3 shows the [PDDA] in the supernatants of the 4 different NPs dispersions determined by the two methods: chloride microtitration and inhibition zones against *S. aureus.*

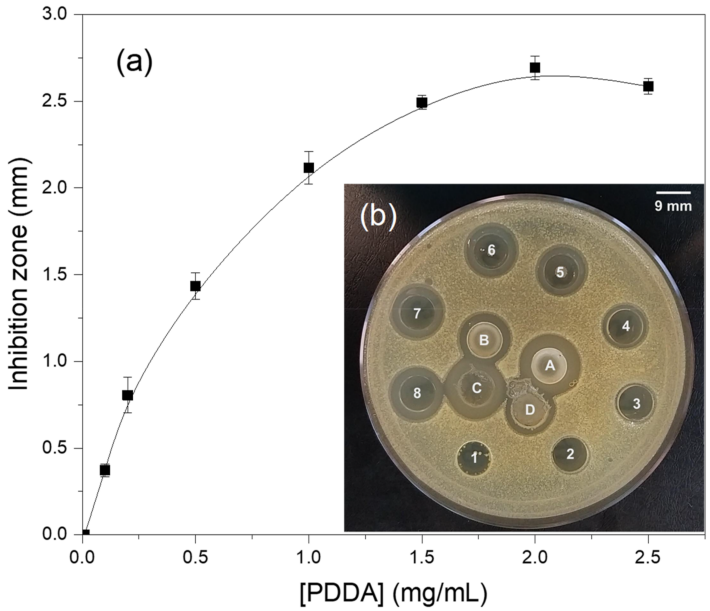


Figure 4. Inhibition zones against *S. aureus* as a function of PDDA concentration. From 1 to 8, 0.01, 0.2, 0.3, 0.5, 1,0, 1.5, 2.0 and 2.5 mg·mL^{-1} standard PDDA solutions were added to the 9 mm wells. In A, the PMMA/PDDA/DODAB dispersion before dialysis. In B, the same dispersion after dialysis (dilution factor of 2.8). In C, the supernatant of A. In D, the supernatant of B.

Table 3. PDDA concentration in the supernatant of NPs dispersion after dialysis. The experimental error for determining [PDDA] was around 10% of the mean values shown on the table.

Dispersion	$[PDDA]_{total}$/ mg·mL^{-1}	$[PDDA]_{supernatant}$/ mg·mL^{-1} Micro-Titration	$[PDDA]_{supernatant}$/ mg·mL^{-1} Inhibition Zone	$[PDDA]_{nanoparticles}$/ mg·mL^{-1}
PMMA/PDDA	4.2	3.2	3.5	0.7–1.0
PMMA/PDDA/DODAB	2.9	2.5	2.8	0.1–0.4
PMMA/PDDA/CTAB	2.6	1.9	2.8	0.0–0.7
PMMA/PDDA/lecithin	2.8	2.9	3.5	0.0–0.0

PDDA, DODAB and CTAB are all compounds with halides as counterions. Dispersions with DODAB or CTAB and PDDA may yield overestimated PDDA concentrations by the halide method. However, DODAB, despite not being permeable through the dialysis membrane, displayed high affinity for PMMA polymeric matrix and did not leach to the outer medium from PMMA coatings [27]. In addition, DODAB does not move through the agar and could not contribute to the inhibition zone observed for PMMA/PDDA/DODAB dialyzed NPs. Thus, for PMMA/PDDA/DODAB NPs after dialysis, both the microtitration and the determination of inhibition zones would give a reliable analysis of PDDA concentrations. On the other hand, CTAB was found to leach from PMMA coatings [27] and readily permeate the dialysis membrane (Figure 5). Thus CTAB would not be found in the supernatant of the dialyzed PMMA/PDDA/CTAB NPs—determination of PDDA concentration in the supernatant of dialyzed PMMA/PDDA/CTAB NPs would be reliable and not overestimated by the micro-titration method. Regarding the determination of inhibition zones, eventually, the lack of linear dependence of inhibition zones on [PDDA} would eventually yield poor determinations of concentration as indeed observed for PMMA/PDDA/lecithin dispersions. The composition of soybean lecithin includes negatively charged phospholipids and fatty acids [32], which would occupy the monomer droplet/water interface during PMMA synthesis eventually facilitating the incorporation of the positively charged PDDA in the PMMA NPs. However, the results on Table 3 show that the lecithin amphiphiles did not increase $[PDDA]_{nanoparticles}$. In summary, the use of amphiphiles during

PMMA/PDDA NPs synthesis did not improve PDDA attachment, entanglement, adsorption and/or mechanical immobilization to the NPs. It was in absence of surfactants, that the highest amount of PDDA became attached to the NPs yielding the most well-structured PDDA shell around the PMMA core (Tables 1 and 3; Figure 2). In the presence of amphiphiles, by determining [PDDA] in the supernatant of centrifuged NPs it was found that most PDDA molecules became poorly attached to the NPs. The amphiphiles indeed reduced the interaction of PDDA with the NPs and diminished the thickness of the NP shell.

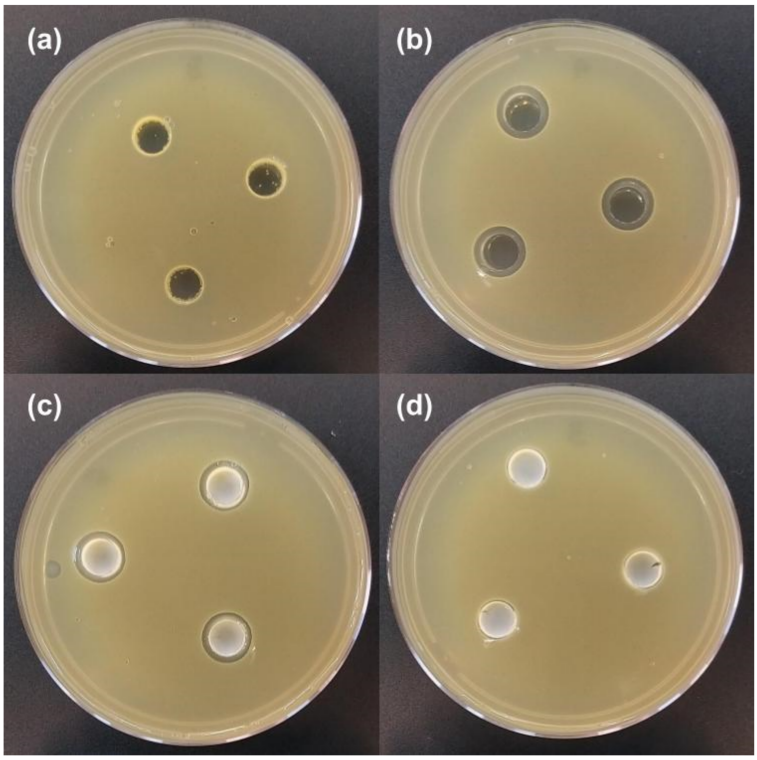


Figure 5. Inhibition zones against *S. aureus* for 0.1 mL of 2 mM DODAB (**a**), 2 mM CTAB (**b**); PMMA/CTAB NPs at 2 mM CTAB before dialysis (**c**) and PMMA/CTAB NPs after dialysis (**d**).

Figure 5 shows the different mobilities of DODAB or CTAB on *S. aureus* seeded agar plates. There was a lack of inhibition zones against *S. aureus* induced by 2mM DODAB in form of bilayer fragments [33] on Figure 5a. Inhibition zones occurred for 2 mM CTAB on Figure 5b and for PMMA/CTAB NPs at 2 mM CTAB before dialysis on Figure 5c. For PMMA/CTAB NPs after dialysis no inhibition zone was observed (Figure 5d). Whereas CTAB moved through the agar, DODAB bilayer fragments remained inside the limits of the sample wells. CTAB was no longer found in the PMMA/CTAB dialyzed NPs so that inhibition zones were not observed (Figure 5d).

In order to confirm that the location of PDDA in the PMMA/PDDA dispersions was mainly in the water phase (Table 3), the antimicrobial activity against *E. coli* was determined in the supernatant of centrifuged dispersions and compared to the total activity of the original dispersions. Figure 6 shows this comparison for dispersions and their supernatants against *E. coli.* The activity of the supernatants was slightly smaller than or equal to the one obtained using the original dispersions. This result was consistent with the predominant location of PDDA in the water phase and its poor association with the PMMA/PDDA/amphiphile NPs. The best association between PDDA and PMMA was achieved in absence of surfactants.

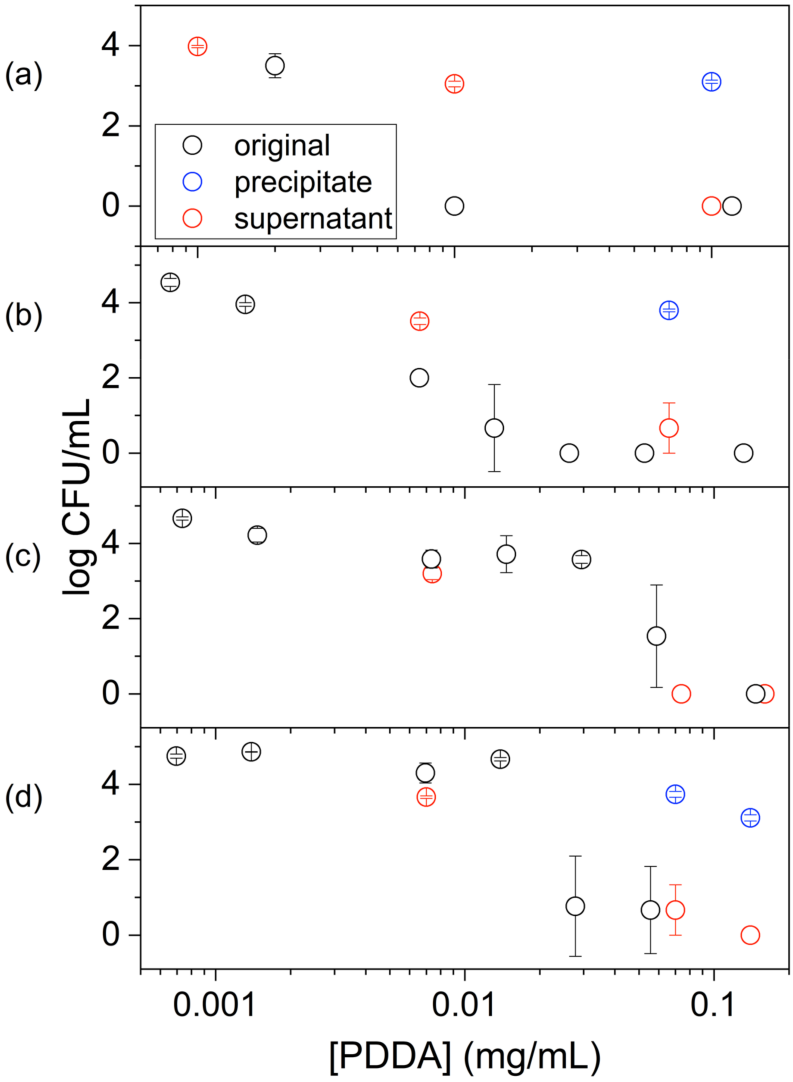


Figure 6. Activity of PDDA against *E. coli* in original dispersions (○), their precipitates (○) and supernatants (○). Dispersions are PMMA/ PDDA (**a**) or PMMA/PDDA/amphiphile where the amphiphile is CTAB (**b**), DODAB (**c**) or lecithin (**d**). Original dispersions are those obtained after exhaustive dialysis. Cells and dispersions or supernatants interacted for 1 h before plating for CFU counting. Dialysates were centrifuged (9000 g/40 min.) in order to separate NPs and supernatant for further separate the antimicrobial activity from the supernatant and the precipitate.

2.2. *Physical and Antimicrobial Properties of Coatings Prepared from PMMA/PDDA/Amphiphile Dispersions*

Figure 7 shows the macroscopic aspects of the PMMA/PDDA/amphiphile coatings obtained after casting and drying the NPs dispersions. The microscopic aspects of these coatings determined by SEM were also shown as the SEM micrographs previously shown as Figure 1. In general, their features were very similar to those previously described in detail for the PMMA/PDDA films in absence of amphiphiles on the three different substrates [17]. A uniform distribution of spherical nanoparticles of very similar size disposed in general side-by-side with some holes and discontinuities occurring at a low frequency showed the uniformity of the coatings.

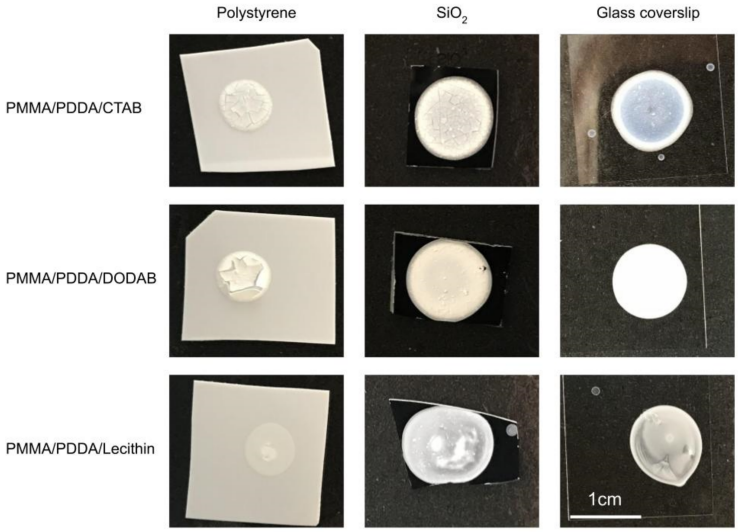


Figure 7. PMMA/PDDA/amphiphile films casted on three different surfaces (polystyrene, SiO_2, or glass) from 50 µL droplets of NPs dispersions in water. The NPs were synthesized at 0.56 M MMA, 5 mg·mL^{-1} PDDA and 2 mM amphiphile, where the amphiphile was CTAB, DODAB, or lecithin. After synthesis, dispersions were exhaustively dialyzed. From top to bottom, PDDA amount was 0.130, 0.145, and 0.140 mg and PMMA amount was 1.3, 0.85, and 0.4 mg. The mass ratio PMMA:PDDA was 10, 6, and 3 from top to bottom. The bar corresponding to 1 cm on the bottom right holds for all films.

The PMMA/PDDA/amphiphile coatings spread and adhered better to the hydrophilic surfaces such as the silicon wafers and the glass coverslips than to the hydrophobic polystyrene surfaces (Figure 7). The outer cationic PDDA shell on each NP interacted better with the anionic surfaces of silicon wafers or glass whereas the repulsion between the hydrophobic polystyrene surfaces; the hydrophilic PDDA shell of the NPs originated poor adherence and cracks on the PMMA/PDDA/amphiphile coatings (Figure 7). The coffee ring effect antagonized by the Marangoni effect was similar to effects previously described for coatings obtained from polymeric particles [34,35] as were the cracks visible for the coatings on the polystyrene surfaces [36]. Using lecithin as emulsifier resulted in some phase separation in the coatings that did not occur for CTAB and DODAB as emulsifiers (Figure 7).

In order to estimate the thickness of the coatings, simple calculations were performed as follows. The approximate area A for each coating on the hydrophilic substrates could be estimated considering spherical shape for the film with a radius of 0.5 cm: A = 0.785 cm^2. The solid content for each dispersion given in Table 1 was previously determined gravimetrically [17] so that the total mass of solids for each coating obtained from 0.05 mL could easily be calculated for each film. Considering each coating as a cylinder its volume will be its base area multiplied by its height. From the radius for the dry particles and the PMMA density (1.18 g·cm^{-3}), the volume and mass of each particle can be obtained. The total number of particles could be obtained from the total mass of the coating divided by the mass of one particle. The volume of the cylindrical films would then be given by the volume of each particle multiplied by the number of particles in each coating. Once known the volume of the cylinder, its thickness i.e., its height, could be estimated from the assumption of uniform coating and the division of the cylinder volume by its base area. From these simple calculations, the thicknesses for each film were estimated and added to Table 4.

Table 4. Physical properties of PMMA/PDDA/amphiphile coatings on silicon wafers. Casting of PMMA/PDDA/CTAB, PMMA/PDDA/DODAB, or PMMA/PDDA/lecithin NPs dispersions followed by drying under vacuum was compared to spin-coated [28] and PMMA/PDDA films [17].

Materials	Procedure	Thickness/μm	Rugosity R	Refractive Index	Contact Angle Θ_A/°
PMMA [1]	Spin-coating	0.091 ± 0.001	N.A.	1.4999 ± 0.004	76 ± 5
PMMA/PDDA [1]	Spin-coating	0.094 ± 0.003	N.A.	1.4951 ± 0.004	15 ± 1
PMMA/PDDA [2]	Casting	3.82	1.6	N.A.	9 ± 2
PMMA/PDDA/CTAB	Casting	12.70	4.0	N.A.	14 ± 1
PMMA/PDDA/DODAB	Casting	4.32	2.2	N.A.	47 ± 3
PMMA/PDDA/lecithin	Casting	9.17	3.0	N.A.	25 ± 1

[1] Data from reference [28]; [2] data from reference [17]; N.A. means non-available.

The coatings of PMMA/PDDA/amphiphile obtained by casting of the NPs dispersions onto silicon wafers were also evaluated regarding their wettability from contact angle determinations (Table 4). These characteristics of the hybrid films compared to those of pure PMMA coatings revealed higher wettability for the hybrid coatings than the one determined for PMMA films (Table 4).

Coatings obtained by casting the PMMA/PDDA dispersions yielded lower contact angles than those obtained by spin-coating. Possibly, some molecules of the hydrophilic PDDA immobilized as an outer layer of the PMMA/PDDA nanoparticle imparted a more hydrophilic character to the film surface than the one of the spin-coated PMMA/PDDA (Table 4).

For coatings obtained by casting and drying the PMMA/PDDA/amphiphile dispersions onto the silicon wafers, there was a consistent decrease of hydrophobicity meaning a decrease of contact angles Θ_A in the following order: Θ_A DODAB > Θ_A lecithin > Θ_A CTAB (Table 4). The presence of residual amphiphile possibly at the surface of the PMMA core reduced the hydrophilicity of the coatings in the expected order from CTAB to lecithin to DODAB. The more hydrophobic amphiphile was DODAB which has a small hydrophilic polar head and double-chained saturated hydrocarbon tails. Lecithin has a mixed composition of phospholipids and fatty acids, some of them unsaturated [32] thereby displaying an intermediate hydrophobicity between the double-chained DODAB and the single-chained surfactant CTAB.

Rugosity (R) is a measure of small-scale variations of amplitude in the height of a surface given by the ratio between the real surface area (A) and the geometric surface area (A_g) [37]. In the case of the NPs coatings from dispersions, R can be easily estimated due to the uniform size of the spherical NPs and the uniform general features of the coatings both microscopically (Figure 1) and macroscopically (Figure 7). The surface area for spherical NPs is given by $4\Pi(D/2)^2$, where D is the diameter of the dry NP. One needs to calculate the total number of NPs in a cross-section of the coating. The geometric area of the coating (A_g) is 0.785 cm^2. The film thickness divided by D yields the number of NPs layers per film. From the total number of NPs per coating divided by the number of NPs layers, the number of NPs per layer could be calculated. Since the area of the NPs is known multiplying this area per the number of NPs per layer divided by 2 will give the real surface area of the outer layer of the coating (A). Thus, R can be obtained from A/A_g (Table 4). The thicker the film, the rougher is its surface as depicted from the results on Table 4. Thus, in order to reduce the film rugosity, one should reduce the total amount of solid deposited. High rugosity might also mean a larger surface area to interact with the microbes and higher activity against the microbes.

As previously described, high conversion rates for the NPs synthesis depended on the presence of stabilizers, such as the amphiphiles used in this work, with the function of stabilizing the droplet/water interface during the polymerization [17]; only about 10% of the monomer mass added was converted into polymer in absence of the emulsifiers [19]. Here 2 mM amphiphile effectively lead to ≥80% monomer-to-polymer conversion but this was at the expenses of the core-shell nanoparticle structure; the PDDA shell around each PMMA core was practically lost due to the presence of amphiphile at the core-water interface of the NPs.

Coatings from the NPs were also tested for their antimicrobial activity. The coatings contained about 0.20 mg of PDDA and reduced cell viability to zero in many instances (Figure 8). The PMMA/PDDA/CTAB coatings yielded a larger reduction in final CFU countings for the three microorganisms tested at 0.18 mg of PDDA (Figure 8). The low NPs size and high rugosity of the coatings (R) also affected the activity. The roughest coating cast from the smallest NPs was the one with the highest activity, namely the coating cast from the PMMA/PDDA/CTAB NPs (Table 4; Figure 8).

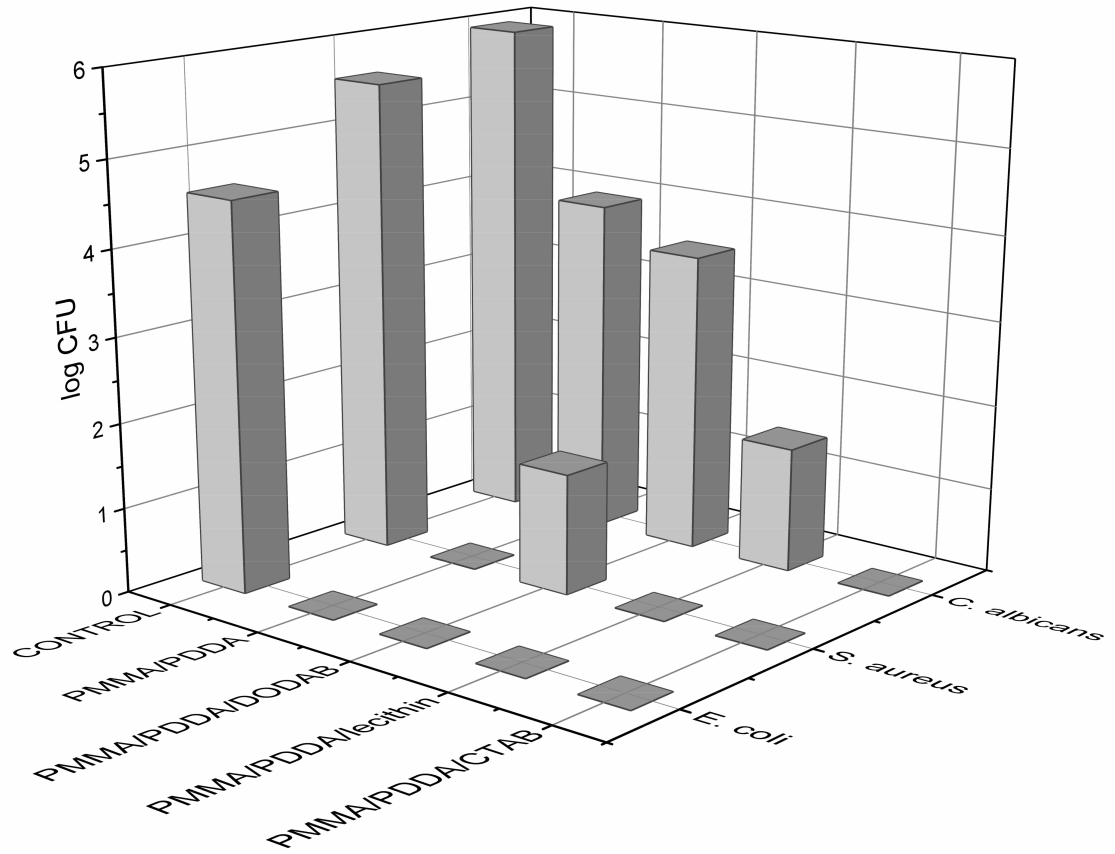


Figure 8. Microbicidal activity of PMMA/PDDA coatings on glass coverslips obtained from casting and drying under vacuum 50 µL of NPs dispersions in water obtained from 0.56 M MMA, 5 mg·mL^{-1} PDDA, 2 mM amphiphile CTAB or DODAB or lecithin during the polymerization and exhaustively dialysed thereafter. Since 5 mg·mL^{-1} of PDDA was used for NPs synthesis, in 0.05 mL of each dispersion used for the coatings, the PDDA amount active against microbes would be 0.25 mg. However, after dialysis, the final volume of the dialyzed dispersion increased inside the dialysis bags and diluted the dispersions by 10 to 12 (PMMA/PDDA), 10 to 19 (PMMA/PDDA/CTAB), 10 to 17 (PMMA/PDDA/DODAB), and 10 to 18 (PMMA/PDDA/lecithin); final PDDA amount in each coating was 0.210, 0.130, 0.145, and 0.140 mg, respectively.

At 2 mM lecithin, since lecithin contains phospholipids and fatty acids [32,38], a net negative charge (zeta-potential equal to −21 mV) was obtained for PMMA/lecithin NPs synthesized in absence of PDDA even after exhaustive dialysis [17]. At 2 mM DODAB or CTAB, the PMMA/DODAB or PMMA/CTAB NPs exhibited positive zeta-potentials [17]. However, the lower zeta-potential for PMMA/CTAB in comparison to the one for PMMA/DODAB NPs was deemed consistent with the reported affinity of DODAB for the PMMA polymeric matrix that did not occur for CTAB—CTAB diffused to the outer water medium from PMMA coatings [27,28]. In summary, although the three stabilizers indeed improved monomer-to-polymer conversion, PDDA imparted the electro-steric repulsion between the MMA droplets during NP synthesis and represented an additional stabilizing

factor for the PMMA/PDDA NPs. The use of cationic stabilizers such as DODAB and CTAB reduced PDDA shell surrounding the NPs (Figure 2).

In this work, one of the most interesting findings referred to the role of NPs size on the microbicidal activity. Figure 9 illustrated this finding showing that the frequency of multipoint attachment of the cells to the coatings cast from NPs can increase with the decrease in NPs size. Thereby the coatings made from small PMMA/PDDA/CTAB NPs would be more effective in killing the cells than those made from large PMMA/PDDA/DODAB or PMMA/PDDA/lecithin NPs.

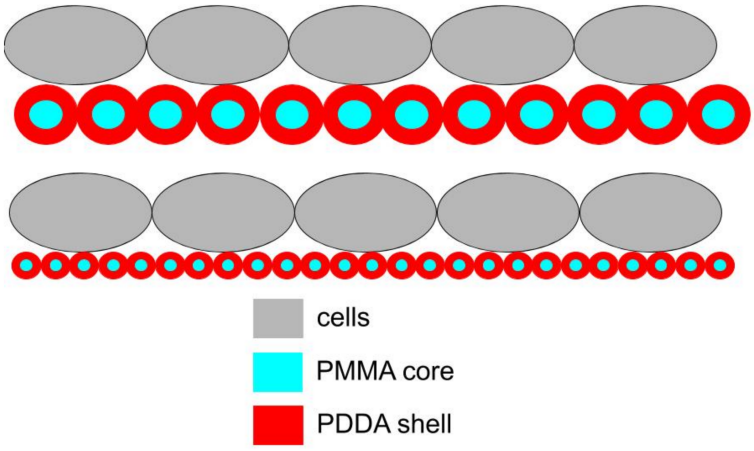


Figure 9. Scheme for the interaction between cells and coatings from PMMA/PDDA NPs illustrating a possible role of nanometric particle size on optimization of antimicrobial activity due to increase in the multipoint interaction between PDDA shell (in red) and cells (in grey). High rugosity for the films might also contribute to the increased surface area on the coating favouring the interaction with the microbial cells.

The reason for the small size of PMMA/PDDA/CTAB NPs in the dispersion can be related to the conical shape of the CTAB molecule, which favors high curvature for the MMA droplets during polymerization. The lipids DODAB or lecithin with molecular shapes closer to cylinders would not favor the curvature of the MMA droplets so that final particle size would be larger than the one for stabilizers with a conical shape.

By adding amphiphiles such as CTAB, DODAB and lecithin as surfactants, active as stabilizers during the NPs synthesis, a major question was raised regarding the effect of the stabilizers on the core-shell NPs structure. Would the quaternary ammonium, cationic amphiphiles hamper the location of cationic PDDA as a shell surrounding each PMMA NP core? Apparently, this indeed happened since the shell thickness was substantially reduced in the dispersions with the cationic amphiphiles as shown in Figure 2 and Table 1. Using the cationic amphiphiles as stabilizers, changed PDDA location from the NP shell to bulk water phase. This reduced the PDDA shell surrounding NPs PMMA core. The negatively charged lecithin possibly found also as closed bilayers in dispersion also might have withdrawn PDDA from the NPs shell to a certain extent thereby reducing the shell thickness (Figure 2; Table 1).

Other questions referred to the eventual contribution of CTAB or DODAB to the antimicrobial activity of the dispersions and coatings. The reason for this question was the reported activity of DODAB and CTAB as antimicrobial agents [8,14,16,29,39–42]. In this work, the antimicrobial properties of these ternary systems both as latexes dispersions in water and as coatings were determined. PDDA resulted in the most important microbicidal agent due to its location as an outer shell of the core-shell PMMA/PDDA NPs and/or its release to the water medium of amphiphile stabilized NPs. Residual CTAB or DODAB would either remain in the NPs polymer matrix or leach from the NPs and through the dialysis membrane leaving the dispersion during dialysis and barely contributing to the microbicidal

activity (Figure 5). PDDA did not leave the dispersions by dialysis so that free PDDA antimicrobial activity remained significant for dialyzed dispersions and their coatings.

3. Materials and Methods

3.1. Materials

MMA, PDDA, azobisisobutyronitrile (AIBN), NaCl, CTAB, DODAB, soybean lecithin, chloroform, agarose, and Mueller Hinton agar (MHA) were from Sigma-Aldrich (Darmstadt, Germany) and used without further purification. PDDA molecular weight was 100,000–200,000 g and came as a water solution at 20% PDDA. The composition of soybean lecithin includes several fatty acids and phospholipids [33,34]. Silicon <100> wafers were from Silicon Quest (USA) with a native oxide layer approximately 2 nm thick and used as substrates for casting the dispersions. The Si wafers with a native SiO_2 layer were cut into small pieces of ca 1 cm^2, cleaned with ethanol, and dried under an N_2 stream; they are smooth substrates for the coatings. The syntheses in 1 mM NaCl solution prepared with Milli-Q water yielded NPs dispersions by emulsion polymerization that underwent dialysis for purification using a cellulose acetate dialysis bag with molecular weight cut-off around 12,400 g/mol. All other reagents were analytical grade and used without further purification.

3.2. Preparation of Hybrid Nanoparticles (NPs) by Emulsion Polymerization

A variety of hybrid and polymeric NPs were obtained by polymerization of MMA at 70–80 °C for 1 h using 10 mL of aqueous solutions of NaCl 1 mM and PDDA and/or CTAB, DODAB or lecithin in accordance with compositions shown in Table 5 [17,19]. Briefly, a weak flux of nitrogen was applied to the solution during a few minutes before adding 0.0036 g of AIBN initiator and MMA. For dispersions containing surfactants or lipids, DODAB or lecithin was previously dissolved in chloroform in order to prepare lipid films under a nitrogen flux to evaporate the chloroform solvent [43,44]. 10 mL of the NaCl 1 mM solution was then added to the dried lipid films before proceeding with the NPs synthesis. In the case of CTAB, the required amount of CTAB in the NPs dispersion was directly added to the 1 mM NaCl solution before starting the NPs synthesis. NPs dispersions thus obtained were further purified by dialysis against Milli-Q water until water conductivity reached 5 μS/cm.

Table 5. Concentrations of MMA, PDDA, CTAB, DODAB and/or lecithin used to synthesize hybrid NPs by emulsion polymerization. The final PDDA concentrations departed from the expected value of 5 mg·mL^{-1} due to water entering the dialysis bag during dialysis. This was corrected to dilution after measuring the final volume of the dialyzed dispersion since the dispersions were used always after dialysis.

Dispersion	[MMA]/M	[PDDA]/ mg·mL^{-1}	[PDDA]$_{corrected}$/ mg·mL^{-1}	[CTAB]/mM	[DODAB]/mM	Lecithin/mM
PMMA/PDDA	0.56	5	4.2	-	-	-
PMMA/PDDA/CTAB	0.56	5	2.6	2	-	-
PMMA/PDDA/DODAB	0.56	5	2.9	-	2	-
PMMA/PDDA/lecithin	0.56	5	2.8	-	-	2

3.3. Determination of Zeta-Average Diameter (Dz), Polydispersity (P), and Zeta-Potential (ζ) for PMMA/PDDA NPs Dispersions

Size distributions, Dz, ζ, and P were checked for NPs dispersions by dynamic light-scattering (DLS) using a Zeta Plus–Zeta Potential Analyzer (Brookhaven Instruments Corporation, Holtsville, NY, USA) equipped with a laser of 677 nm with measurements at 90° (Table 1). P of the dispersions was determined by DLS following well defined mathematic equations [45]. Dz values were obtained from the log normal distribution of the light -scattered intensity curve against the diameter. ζ values were determined from the electrophoretic mobility (μ) and Smolukowski equation $\zeta = \mu\eta/\varepsilon$, where η

and ε are the viscosity and the dielectric constant of the medium, respectively. Samples were diluted 1:30 with a 1 mM NaCl water solution for performing the measurements at (25 ± 1) °C.

3.4. Preparation and Physical Characterization of Coatings from the NPs Dispersions by Casting from Photographs and Contact Angle Determinations

Films prepared by casting employed 0.05 mL of PMMA/PDDA, PMMA/CTAB/PDDA, PMMA/DODAB/PDDA, PMMA/lecithin/PDDA dispersions (Tables 1 and 3) casted onto three different surfaces: polystyrene, silicon wafers, or glass coverslips. After drying overnight under vacuum the films were photographed and characterized regarding their wettability. For determining antimicrobial activity films were cast onto glass coverslips. Wettability was evaluated by using a home build apparatus as previously described [46,47]. Sessile water droplets of 10 μL allowed determining the advancing contact angle (Θ_A) over the first five minutes after depositing the droplet on the films.

3.5. Microorganisms Growth and Determination of Cell Viability in the Presence of the PMMA/PDDA Dispersions and Coatings

E. coli ATCC (American Type Culture Collection) 25322, *S. aureus* ATCC 29213 and *Candida albicans* ATCC 90028 growth was from previously frozen stocks kept at −20 °C in the appropriate storage medium. The bacterial strains plated onto MHA were incubated at 37 °C/18–24 h before transferring some isolated colonies to an isotonic 0.264 M D-glucose solution and adjusting turbidity to 0.5 of the McFarland scale [48]. The 0.264 M D-glucose solution was used instead of any culture medium because cationic molecules are inactivated by the relatively high ionic strength or negatively charged molecules such as amino acids and polysaccharides. For determination of cell viability after interaction with the NPs, 0.1 mL of the cell suspensions (around 10^8 CFU/mL) were mixed with 0.9 mL of NPs dispersions diluted in the same D-glucose solution. Cell viabilities (log CFU/mL) were plotted as a function of PDDA concentration (mg·mL^{-1}).

60 μL of the bacterial suspensions were deposited on the coatings (obtained by casting of dispersions described on Tables 3 and 4 onto glass coverslips) and left in a water vapour saturated chamber for 1 h to prevent water evaporation from the droplet. Thereafter, the glass coverslips were transferred to 10 mL of 0.264 M D-glucose isotonic solution in Falcon tubes and vigorously stirred by vortexing before withdrawing 0.1 mL aliquots and preparing their 1:10 and 1:100 dilutions for plating on MHA plates, incubating the plates (37 °C/24 h) and counting the CFU. These readings were converted into CFU/mL and log (CFU/mL). When no counting was obtained, since the log function does not exist for zero, the CFU/mL counting was taken as 1 so that log CFU/mL could be taken as zero. Controls were bare glass coverslips.

3.6. Determination of Inhibition zones from NPs Dispersions and/or their Supernatants

S. aureus ATCC 29213 from previously frozen stocks kept at −20 °C in an appropriate storage medium was grown as described above and the bacterial suspension prepared in 0.264 M D-glucose had its turbidity adjusted according to 0.5 of the McFarland scale as previously described.

A growth medium containing 2.3% Muller-Hinton broth and 0.64% agar was prepared and sterilized. Into 50 mL of this growth medium, 0.5 mL of the *S. aureus* suspension was added and then carefully homogenized. Plates containing MHA were previously prepared and used to place micropipette tips with their bases positioned on the MHA in order to form wells with 9mm diameter where each antimicrobial sample can be applied, after pouring ca. 20 mL of the *S. aureus* culture. After agar hardening, the tips were removed and, in each well, 70 μL of the PDDA solutions at 0.01, 0.1, 0.2, 0.5, 1, 1.5, 2, and 2.5 mg·mL^{-1} PDDA or of the NPs dispersions were added.

3.7. Determination of PDDA by Chloride Microtitration

Chloride, as the PDDA counterion, was microtitrated to determine [PDDA] in $mg{\cdot}mL^{-1}$ after obtaining a standard curve for the linear dependence between PDDA and chloride concentrations. The method was previously described by Schales and Schales [49]. The detailed protocol for the halide microtitration can be found in reference [50].

4. Conclusions

The ternary systems composed of PMMA/PDDA/amphiphile NPs evaluated in dispersion or as coatings obtained by casting onto three different substrates displayed variable but important antimicrobial activity against three different pathogenic microbes, *E. coli*, *S. aureus* and *C. albicans.*

The macroscopic aspects for the coatings revealed homogeneous films on the hydrophilic silicon wafers or glass coverslips and cracked non-adherent coatings on the hydrophobic polystyrene surfaces. The amphiphiles employed during NPs synthesis changed the wettability of the coatings yielding contact angles that increased with the increase in the hydrophobicity of the amphiphile employed; thereby the lowest contact angle occurred in absence of amphiphile whereas the highest one occurred with DODAB as the most hydrophobic amphiphile as compared to CTAB or lecithin. At about 0.140 mg of PDDA in PMMA/PDDA/amphiphile dispersions casted and dried on the substrates, the coating with higher microbicidal activity was the one obtained from PMMA/PDDA/CTAB dispersions because the small NP size favoured both high frequency of contacts between PDDA in the outer NP medium for contacting the microbial cells; all pathogens present (10^4–10^6 CFU) completely lost their viability upon interaction with these coatings for 1 h.

The microbicidal activity of the ternary dispersions determined from cell viability curves over a broad range of PDDA concentrations revealed that the most sensitive microorganism to the dispersions was *E. coli*, followed by *S. aureus* and *C. albicans.* The PMMA/PDDA/CTAB dispersions were the most effective in killing the three microbial strains tested by 7–8 logs in 1 h. The nanometric and cationic NPs (sizes below 100 nm) of PMMA/PDDA/CTAB yielded maximal microbicidal activity either as dispersions or coatings. There were 6–8 logs reduction of cells viability from [PDDA] ≥ the minimal microbicidal concentration.

All NPs exhibited hydrodynamic diameters of about 200 nm with exception of the PMMA/PDDA/CTAB NPs with 90 ± 1 nm as Dz; this size allowed NPs penetration through the cell walls and cell membrane with significant damage to both structures and complete loss of cell viability at 0.030, 1.000, and 1.310 $mg{\cdot}mL^{-1}$ PDDA carried by the PMMA/PDDA/CTAB NPs against *E. coli, S. aureus* and *C. albicans*, respectively. In summary, in this work the presence of residual amphiphile stabilizers in PMMA/PDDA/amphiphile NPs revealed their important role during the emulsion polymerization that allowed high monomer-to-polymer conversion; however, the significant microbicidal agent in these NPs was only one, the cationic antimicrobial polymer PDDA, which exhibited the potency required to kill microbes over 6–8 logs of CFU countings.

The reduction in particle size and increased rugosity and surface area for the coatings were associated with CTAB and its molecular geometry. CTAB promoted the synthesis of the smallest NPs. Their casting onto hydrophilic surfaces generated coatings with the highest rugosity and microbicidal activity.

Finally, all three amphiphiles negatively affected the core-shell NPs structure, reducing the thickness of the shell in the core-shell NPs and releasing PDDA to the medium.

Author Contributions: Conceptualization, A.M.C.-R.; Data curation, A.M.C.-R.; Formal analysis, R.T.R., C.N.G., Y.P.B., B.I.M. and A.M.C.-R.; Funding acquisition, A.M.C.-R.; Investigation, R.T.R., C.N.G., Y.P.B., B.I.M. and A.M.C.-R.; Methodology, R.T.R., C.N.G., Y.P.B., B.I.M. and A.M.C.-R.; Project administration, A.M.C.-R.; Resources, A.M.C.-R.; Supervision, A.M.C.-R.; Validation, A.M.C.-R.; Writing – original draft, A.M.C.-R.; Writing – review & editing, A.M.C.-R.

Funding: Research support was from the Conselho Nacional de Desenvolvimento Científico e Tecnológico (CNPq) grant number 302352/2014-7 to the Project "Bioactive Supramolecular Assemblies" by A.M.C.-R. The APC was

also from CNPq grant number 302352/2014-7 C.N.G. and B.I.M. were recipients of undergraduate fellowships of the Programa Unificado de Bolsas da Universidade de São Paulo granted to the Project "Cationic Supramolecular Assemblies and their Films" by A.M.C.-R. Y.P.B. is the recipient of a PhD fellowship from CNPq. The authors gratefully acknowledge Professor Denise Freitas Siqueira Petri for allowing the use of the home-made apparatus for determining the wettability of some coatings.

Conflicts of Interest: The authors declare no conflict of interest. The funders had no role in the design of the study; in the collection, analyses, or interpretation of data; in the writing of the manuscript, and in the decision to publish the results.

Abbreviations

NPs	Nanoparticles
PMMA	poly (methylmethacrylate)
PDDA	poly (diallyldimethylammonium) chloride
CTAB	cetyltrimethylammonium bromide
DODAB	dioctadecyldimethylammonium bromide
CFU	colony forming unities
MMA	Methylmethacrylate
Θ_A	advancing contact angle
AIBN	Azobisisobutyronitrile
Dz	zeta-average diameter
P	Polydispersity
ζ	zeta-potential
MHA	Mueller-Hinton agar
DLS	dynamic light scattering
μ	electrophoretic mobility
η	viscosity of the medium
ε	dielectric constant of the medium
ATCC	american type culture collection

References

1. Carmona-Ribeiro, A.M.; Barbassa, L.; Melo, L.D. Antimicrobial Biomimetics. In *Biomimetic Based Applications*; Anne George; IntechOpen: Rijeka, Croatia, 2011; Volume 1, pp. 227–284. ISBN 978-953-307-195-4.
2. Carmona-Ribeiro, A.M. The Versatile Dioctadecyldimethylammonium Bromide. In *Application and Characterization of Surfactants*; Reza Najjar; IntechOpen: Rijeka, Croatia, 2017; Volume 1, pp. 157–181. ISBN 978-953-51-3325-4.
3. Vitiello, G.; Silvestri, B.; Luciani, G. Learning from Nature: Bioinspired Strategies Towards Antimicrobial Nanostructured Systems. *Curr. Top. Med. Chem.* **2018**, *18*, 22–41. [CrossRef] [PubMed]
4. Song, W.; Ge, S. Application of Antimicrobial Nanoparticles in Dentistry. *Molecules* **2019**, *24*, 1033. [CrossRef] [PubMed]
5. Halbus, A.F.; Horozov, T.S.; Paunov, V.N. Colloid particle formulations for antimicrobial applications. *Adv. Colloid Interface Sci.* **2017**, *249*, 134–148. [CrossRef] [PubMed]
6. Álvarez-Paino, M.; Muñoz-Bonilla, A.; Fernández-García, M. Antimicrobial Polymers in the Nano-World. *Nanomaterials* **2017**, *7*, 48. [CrossRef]
7. Thakral, S.; Thakral, N.K.; Majumdar, D.K. Eudragit®: A technology evaluation. *Expert Opin. Drug. Deliv.* **2013**, *10*, 131–149. [CrossRef]
8. Carmona-Ribeiro, A.M. Self-Assembled Antimicrobial Nanomaterials. *Int. J. Environ. Res. Public Health* **2018**, *15*, 1408. [CrossRef]
9. Carmona-Ribeiro, A.M. Biomimetic Nanomaterials from the Assembly of Polymers, Lipids, and Surfactants. In *Surfactants and Detergents*; Ashim Dutta; IntechOpen: London, UK, 2019; Volume 1, ISBN 978-1-78984-661-4.
10. Yang, G.; Chen, S.; Zhang, J. Bioinspired and Biomimetic Nanotherapies for the Treatment of Infectious Diseases. *Front. Pharmacol.* **2019**, *10*. [CrossRef]
11. Ferrer, M.C.C.; Hickok, N.J.; Eckmann, D.M.; Composto, R.J. Antibacterial Biomimetic Hybrid Films. *Soft Matter* **2013**, *8*, 2423–2431. [CrossRef]

12. Coll Ferrer, M.C.; Eckmann, U.N.; Composto, R.J.; Eckmann, D.M. Hemocompatibility and biocompatibility of antibacterial biomimetic hybrid films. *Toxicol. Appl. Pharmacol.* **2013**, *272*, 703–712. [CrossRef]
13. Coll Ferrer, M.C.; Dastgheyb, S.; Hickok, N.J.; Eckmann, D.M.; Composto, R.J. Designing nanogel carriers for antibacterial applications. *Acta Biomater.* **2014**, *10*, 2105–2111. [CrossRef]
14. Melo, L.D.; Mamizuka, E.M.; Carmona-Ribeiro, A.M. Antimicrobial Particles from Cationic Lipid and Polyelectrolytes. *Langmuir* **2010**, *26*, 12300–12306. [CrossRef] [PubMed]
15. Xavier, G.R.S.; Carmona-Ribeiro, A.M. Cationic Biomimetic Particles of Polystyrene/Cationic Bilayer/Gramicidin for Optimal Bactericidal Activity. *Nanomaterials* **2017**, *7*, 422. [CrossRef] [PubMed]
16. De Melo Carrasco, L.D.; Sampaio, J.L.M.; Carmona-Ribeiro, A.M. Supramolecular Cationic Assemblies against Multidrug-Resistant Microorganisms: Activity and Mechanism of Action. *Int. J. Mol. Sci.* **2015**, *16*, 6337–6352. [CrossRef] [PubMed]
17. Galvão, C.N.; Sanches, L.M.; Mathiazzi, B.I.; Ribeiro, R.T.; Petri, D.F.S.; Carmona-Ribeiro, A.M. Antimicrobial Coatings from Hybrid Nanoparticles of Biocompatible and Antimicrobial Polymers. *Int. J. Mol. Sci.* **2018**, *19*, 2965. [CrossRef] [PubMed]
18. Alvarez-Paino, M.; Juan-Rodríguez, R.; Cuervo-Rodríguez, R.; Tejero, R.; López, D.; López-Fabal, F.; Gómez-Garcés, J.L.; Muñoz-Bonilla, A.; Fernández-García, M. Antimicrobial films obtained from latex particles functionalized with quaternized block copolymers. *Colloids Surf B Biointerfaces* **2016**, *140*, 94–103. [CrossRef] [PubMed]
19. Sanches, L.M.; Petri, D.F.S.; de Melo Carrasco, L.D.; Carmona-Ribeiro, A.M. The antimicrobial activity of free and immobilized poly (diallyldimethylammonium) chloride in nanoparticles of poly (methylmethacrylate). *J. Nanobiotechnol.* **2015**, *13*, 58. [CrossRef] [PubMed]
20. Patra, C.N.; Priya, R.; Swain, S.; Kumar Jena, G.; Panigrahi, K.C.; Ghose, D. Pharmaceutical significance of Eudragit: A review. *Future J. Pharm. Sci.* **2017**, *3*, 33–45. [CrossRef]
21. Wijesinghe, W.P.S.L.; Mantilaka, M.M.M.G.P.G.; Karunarathne, T.S.E.F.; Rajapakse, R.M.G. Synthesis of a hydroxyapatite/poly(methyl methacrylate) nanocomposite using dolomite. *Nanoscale Adv.* **2019**, *1*, 86–88. [CrossRef]
22. Atik, S.S.; Thomas, J.K. Polymerized microemulsions. *J. Am. Chem. Soc.* **1981**, *103*, 4279–4280. [CrossRef]
23. Stoffer, J.O.; Bone, T. Polymerization in Water-in-Oil Microemulsion Systems Ii: Sem Investigation of Structure. *J. Dispers. Sci. Technol.* **1980**, *1*, 393–412. [CrossRef]
24. Jayakrishnan, A.; Shah, D.O. Polymerization of oil-in-water microemulsions: Polymerization of styrene and methyl methacrylate. *J. Polym. Sci. Polym. Lett. Ed.* **1984**, *22*, 31–38. [CrossRef]
25. Daniels, E.S.; Sudol, D.; El-Asser, M.S. Overview of Polymer Colloids: Preparation, Characterization, and Applications. In *Scientific Methods for the Study of Polymer Colloids and Their Applications*; Candau, F., Ottewill, R.H., Eds.; Kluwer Academic Press: Dordrecht, The Netherlands, 1990; ISBN 0-7923-0599-X.
26. Lichti, G.; Gilbert, R.G.; Napper, D.H. The mechanisms of latex particle formation and growth in the emulsion polymerization of styrene using the surfactant sodium dodecyl sulfate. *J. Polym. Sci. Polym. Chem. Ed.* **1983**, *21*, 269–291. [CrossRef]
27. Melo, L.D.; Palombo, R.R.; Petri, D.F.S.; Bruns, M.; Pereira, E.M.A.; Carmona-Ribeiro, A.M. Structure–Activity Relationship for Quaternary Ammonium Compounds Hybridized with Poly(methyl methacrylate). *ACS Appl. Mater. Interfaces* **2011**, *3*, 1933–1939. [CrossRef] [PubMed]
28. Pereira, E.M.A.; Kosaka, P.M.; Rosa, H.; Vieira, D.B.; Kawano, Y.; Petri, D.F.S.; Carmona-Ribeiro, A.M. Hybrid Materials from Intermolecular Associations between Cationic Lipid and Polymers. *J. Phys. Chem. B* **2008**, *112*, 9301–9310. [CrossRef] [PubMed]
29. Naves, A.F.; Palombo, R.R.; Carrasco, L.D.M.; Carmona-Ribeiro, A.M. Antimicrobial Particles from Emulsion Polymerization of Methyl Methacrylate in the Presence of Quaternary Ammonium Surfactants. *Langmuir* **2013**, *29*, 9677–9684. [CrossRef]
30. Raja, M.; Vales, E. Effects of sodium chloride on membrane fusion and on the formation of aggregates of potassium channel KcsA in Escherichia coli membrane. *Biophys. Chem.* **2009**, *142*, 46–54. [CrossRef]
31. Otto, M. Staphylococcus epidermidis—The "accidental" pathogen. *Nat. Rev. Microbiol.* **2009**, *7*, 555–567. [CrossRef]
32. Kagawa, Y.; Racker, E. Partial Resolution of the Enzymes Catalyzing Oxidative Phosphorylation VIII. Properties of a factor conferring oligomycin sensitivity on mitochondrial adenosine triphosphatase. *J. Biol. Chem.* **1966**, *241*, 2461–2466.

33. Carmona-Ribeiro, A.M. Lipid Bilayer Fragments and Disks in Drug Delivery. *Curr. Med. Chem.* **2006**, *13*, 1359–1370. [CrossRef]
34. Deegan, R.D.; Bakajin, O.; Dupont, T.F.; Huber, G.; Nagel, S.R.; Witten, T.A. Capillary flow as the cause of ring stains from dried liquid drops. *Nature* **1997**, *389*, 827–829. [CrossRef]
35. Hu, H.; Larson, R.G. Marangoni Effect Reverses Coffee-Ring Depositions. *J. Phys. Chem. B* **2006**, *110*, 7090–7094. [CrossRef] [PubMed]
36. Pauchard, L.; Parisse, F.; Allain, C. Influence of salt content on crack patterns formed through colloidal suspension desiccation. *Phys. Rev. E* **1999**, *59*, 3737–3740. [CrossRef]
37. McNaught, A.D.; Wilkinson, A. *Compendium of Chemical Terminology. (the "Gold Book")*, 2nd ed.; Blackwell Scientific Publications: Oxford, UK, 2019; ISBN 0-9678550-9-8.
38. Augusto, O.; Carmona-Ribeiro, A.M. Introducing model membranes and lipoperoxidation. *Biochem. Educ.* **1989**, *17*, 209–210. [CrossRef]
39. Campanhã, M.T.N.; Mamizuka, E.M.; Carmona-Ribeiro, A.M. Interactions between cationic liposomes and bacteria: the physical-chemistry of the bactericidal action. *J. Lipid Res.* **1999**, *40*, 1495–1500. [PubMed]
40. Martins, L.M.S.; Mamizuka, E.M.; Carmona-Ribeiro, A.M. Cationic Vesicles as Bactericides. *Langmuir* **1997**, *13*, 5583–5587. [CrossRef]
41. Vieira, D.B.; Carmona-Ribeiro, A.M. Cationic lipids and surfactants as antifungal agents: mode of action. *J. Antimicrob. Chemother.* **2006**, *58*, 760–767. [CrossRef]
42. Carmona Ribeiro, A.M.; Carrasco, L.D.M. Fungicidal assemblies and their mode of action. *OA Biotechnol.* **2013**, *2*, 25. [CrossRef]
43. Ribeiro, R.T.; Braga, V.H.A.; Carmona-Ribeiro, A.M. Biomimetic Cationic Nanoparticles Based on Silica: Optimizing Bilayer Deposition from Lipid Films. *Biomimetics* **2017**, *2*, 20. [CrossRef]
44. Sobral, C.N.C.; Soto, M.A.; Carmona-Ribeiro, A.M. Characterization of DODAB/DPPC vesicles. *Chem. Phys. Lipids* **2008**, *152*, 38–45. [CrossRef]
45. Grabowski, E.; Morrison, I. Particle size distribution from analysis of quasi-elastic light scattering data. In *Measurement of Suspended Particles by Quasi-Elastic Light Scattering*; Dahneke, B.E., Ed.; Wiley: New York, NY, USA, 1983; Volume 21, pp. 199–236.
46. Pereira, E.M.A.; Petri, D.F.S.; Carmona-Ribeiro, A.M. Synthetic Vesicles at Hydrophobic Surfaces. *J. Phys. Chem. B* **2002**, *106*, 8762–8767. [CrossRef]
47. Pereira, E.M.A.; Petri, D.F.S.; Carmona-Ribeiro, A.M. Adsorption of Cationic Lipid Bilayer onto Flat Silicon Wafers: Effect of Ion Nature and Concentration. *J. Phys. Chem. B* **2006**, *110*, 10070–10074. [CrossRef] [PubMed]
48. Chapin, K.; Lauderdale, T.L. Comparison of Bactec 9240 and Difco ESP blood culture systems for detection of organisms from vials whose entry was delayed. *J. Clin. Microbiol.* **1996**, *34*, 543–549. [PubMed]
49. Schales, O.; Schales, S. A simple and accurate method for the determination of chloride in biological fluids. *J. Biol. Chem.* **1941**, *140*, 879–884.
50. Carmona-Ribeiro, A.M. Preparation and Characterization of Biomimetic Nanoparticles for Drug Delivery. In *Nanoparticles in Biology and Medicine*; Methods in Molecular Biology; Humana Press: Totowa, NJ, USA, 2012; pp. 283–294. ISBN 978-1-61779-952-5.



© 2019 by the authors. Licensee MDPI, Basel, Switzerland. This article is an open access article distributed under the terms and conditions of the Creative Commons Attribution (CC BY) license (http://creativecommons.org/licenses/by/4.0/).

4 | Simple nanoparticles from the assembly of cationic polymer and antigen as immunoadjuvants

vaccines

MDPI

Article

Simple Nanoparticles from the Assembly of Cationic Polymer and Antigen as Immunoadjuvants

Yunys Pérez-Betancourt [1], Bianca de Carvalho Lins Fernandes Távora [2], Mônica Colombini [2], Eliana L. Faquim-Mauro [2] and Ana Maria Carmona-Ribeiro [1,*]

[1] Biocolloids Laboratory, Departamento de Bioquímica, Instituto de Química, Universidade de São Paulo, São Paulo 05508-000, Brazil; y.betancourt@usp.br

[2] Immunopathology Laboratory, Butantan Institute, São Paulo 05503-900, Brazil; bianca.tavora@butantan.gov.br (B.d.C.L.F.T.); eliana.faquim@butantan.gov.br (E.L.F.-M.); monica.colombini@butantan.gov.br (M.C.)

* Correspondence: amcr@usp.br; Tel.: +55-011-3091-1887

Received: 3 February 2020; Accepted: 24 February 2020; Published: 28 February 2020



Abstract: Since antigens are negatively charged, they combine well with positively charged adjuvants. Here, ovalbumin (OVA) (0.1 mg·mL^{-1}) and poly (diallyldimethylammonium chloride) (PDDA) (0.01 mg·mL^{-1}) yielded PDDA/OVA assemblies characterized by dynamic light scattering (DLS) and scanning electron microscopy (SEM) as spherical nanoparticles (NPs) of 170 ± 4 nm hydrodynamic diameter, 30 ± 2 mV of zeta-potential and 0.11 ± 0.01 of polydispersity. Mice immunization with the NPs elicited high OVA-specific IgG1 and low OVA-specific IgG2a production, indicating a Th-2 response. Delayed-type hypersensitivity reaction (DTH) was low and comparable to the one elicited by $Al(OH)_3$/OVA, suggesting again a Th-2 response. PDDA advantages as an adjuvant were simplicity (a single-component adjuvant), low concentration needed (0.01 mg·mL^{-1} PDDA) combined with antigen yielding neglectable cytotoxicity, and high stability of PDDA/OVA dispersions. The NPs elicited much higher OVA-specific antibodies production than $Al(OH)_3$/OVA. In vivo, the nano-metric size possibly assured antigen presentation by antigen-presenting cells (APC) at the lymph nodes, in contrast to the location of $Al(OH)_3$/OVA microparticles at the site of injection for longer periods with stimulation of local dendritic cells. In the future, it will be interesting to evaluate combinations of the antigen with NPs carrying both PDDA and elicitors of the Th-1 response.

Keywords: cationic polymer; poly (diallyldimethylammonium chloride); model antigen; ovalbumin; antigen/cationic polymer nanoparticles; poly-cation cytotoxicity; dynamic light scattering; scanning electron microscopy; ELISA assays; delayed-type hypersensitivity assay

1. Introduction

Adjuvants are essential components of modern vaccines; they enhance the magnitude and guide the type of adaptive immune response to produce the most effective form of immunity for each specific pathogen [1,2]. Adjuvants act, mostly, as antigen carriers or/and as pattern recognition receptors (PRR) agonists. The demand for adjuvants in vaccine formulations emerged from the application of purified antigens, which are poor immunogens due to lack of the danger signals of pathogens' entire cells, crucial for activating the innate immune system [1,3,4]. Currently, there are few adjuvants licensed for human use; aluminum-based adjuvants like $Al(OH)_3$ are the only ones approved worldwide performing the task of presenting negatively charged antigens due to their positive charge at the pH of water [5–7]. Other cationic adjuvants based on nanoparticles [8–11], liposomes [12–14], cationic bilayer fragments [8,15,16] or supported cationic bilayers on polymeric nanoparticles (NPs) [9], silica [17],

or cationic polymers on superparamagnetic iron oxide NPs [18] have also been proposed as effective micro or nanomaterials able to effectively interact with antigens and antigen-presenting cells (APC).

Major mechanisms for taking up the cationic assemblies depend on size [19,20]. Nanoparticles with 20–200 nm mean diameter are like viruses and usually taken up by endocytosis via clathrin-coated vesicles, caveolae, or their independent receptors, and preferentially ingested by dendritic cells (DC) [21]. Microparticles with 500–5000 nm diameter are like bacteria, captured by phagocytosis and primarily ingested by macrophages. All particles used in vaccine formulations are consequently internalized efficiently by APC by one or a combination of the quoted mechanisms [22,23]. Particles with diameters smaller than 500 nm, in particular the nano-sized ones with 40–100 nm diameter, are more efficient to promote CD8 and CD4 type 1 T-helper cells responses than those with diameters above 500 nm; large particles, more similar to Al $(OH)_3$, usually induce good T-helper cells type 2 improvement in antibody responses [22]. In summary, cationic micro and nanoparticles are effectively taken up both by macrophages and dendritic cells since electrostatic attraction promotes particle binding and subsequent internalization [11,14,20,24,25]. Cationic particles and liposomes containing dioctadecyldimethylammonium bromide (DODAB) cationic lipid [13,26] carrying *Mycobacterium tuberculosis* [13,27], *Chlamydia trachomatis* [11], or *Neisseria meningitides* antigens enhanced the cellular and humoral immune response against them [16,28].

Another important class of cationic adjuvants is represented by the cationic polymers despite their overt cytotoxicity [29–33]. They easily combine with oppositely charged proteins [34]. Particles of poly (lactic-co-glycolic acid) (PLGA) have been combined with cationic polymers like polyethyleneimine (PEI) or ε-poly-L-lysine (PLL) for improving antigen adsorption, colloidal stability, and the immune response [35]. Nanocomplexes of PEI and antigens (influenza hemagglutinin or herpes simplex virus type-2 glycoprotein D) delivered by the mucosal route activated APC in vivo, promoting dendritic cell trafficking to draining lymph nodes besides and eliciting a potent immune response against the viral subunit glycoproteins; a single intranasal administration elicited robust antibody-mediated protection [36]. Systemic administration of the same antigens with PEI induced both Th1/Th2 immune responses and higher titers of both antigen-binding and -neutralizing antibodies than alum [37].

The cationic antimicrobial polymer poly (diallyldimethylammonium chloride) (PDDA) is a poly-cation [38–40] able to combine with bovine serum albumin (BSA), yielding NPs with diameters around 50 nm [41,42]. In combination with HIV-1 DNA, nanorods of gold yielded particles of gold/PDDA/DNA, which elicited a Th-2 response that was higher than the one obtained using PEI or cetyltrimethylammonium bromide (CTAB). Stimulated cellular and humoral immunity, as well as T cell proliferation, were obtained in comparison with naked HIV-1 Env plasmid DNA treatment in vivo [43].

In this work, NPs of PDDA/ovalbumin are prepared, characterized by their physical properties, and evaluated as stimulators of the OVA-specific immune response. The results obtained by means of dynamic light scattering (DLS) show that cationic PDDA/OVA NPs at 0.01 and 0.1 mg·mL^{-1} PDDA and OVA, respectively, have 170 ± 4 nm of hydrodynamic diameter, 30 ± 2 mV of zeta-potential, and 0.11 ± 0.01 of polydispersity. These NPs used for mice immunization elicited potent Th-2 OVA-specific immune response. There were high OVA-specific IgG1 and low OVA-specific IgG2a production. Delayed-type hypersensitivity reaction (DTH) was low and comparable to the one elicited by $Al(OH)_3$/OVA, suggesting again a Th-2 response. PDDA advantages as an adjuvant are simplicity (a single-component adjuvant), low concentration needed (0.01 mg·mL^{-1} PDDA) combined with antigen yielding neglectable cytotoxicity, and high stability of PDDA/OVA dispersions. The NPs elicited much higher OVA-specific antibody production than $Al(OH)_3$/OVA.

2. Materials and Methods

2.1. Reagents and Stock Solutions

Poly (diallyldimethylammonium chloride) (PDDA), grade V ovalbumin (OVA), peroxidase-labeled streptavidin, and o-phenylenediamine (OPD) were purchased from Sigma Chemical Co. (St. Louis, MO, USA). OVA stock solutions (20 mg·mL^{-1}) were prepared in Milli-Q water (pH = 6.3) and purified to reduce endotoxin levels by means of a chromatographic procedure using polymyxin B columns (Pierce Biotechnology, Rockford, IL, USA). The concentration of purified OVA in the stock solution was determined by the bicinchoninic acid assay (BCA) [44] and adjusted to 10 mg·mL^{-1}. Aluminum hydroxide ($Al(OH)_3$) was purchased from Sanofi-Synthelabo, RJ, Brazil. PDDA molecular weight was <100,000 g and it was available as a water solution at 35% PDDA.

2.2. Preparation of the PDDA/OVA Nanoparticles (NPs)

PDDA/OVA NPs were obtained from aliquots of stock PDDA (10 mg·mL^{-1}) and OVA (10 mg·mL^{-1}) solutions vortexed for 30 s in Milli-Q water at room temperature. The turbid dispersions of NPs with good colloidal stability were used 1 h after preparation.

2.3. Determination of Physical Properties and Colloidal Stability for NPs Dispersions from Dynamic Light Scattering (DLS), Turbidimetry, and Scanning Electron Microscopy (SEM)

All dispersions were obtained in Milli-Q water. Size distribution, zeta-average diameter (Dz), zeta-potential (ζ), polydispersity (P), conductance (G), and colloidal stability for the dispersions were determined by DLS using a Zeta-Plus Zeta-Potential Analyzer (Brookhaven Instruments Corporation, Holtsville, NY) equipped with a 677 nm laser. The diameter from DLS is the mean hydrodynamic (zeta-average) diameter Dz unless otherwise stated. Zeta-potential (ζ) was determined from the electrophoretic mobility μ and Smoluchowski equation, $\zeta = \mu\eta/\varepsilon$, where η and ε are the viscosity and the dielectric constant of the medium, respectively. The physical properties of the dispersions (Dz, ζ, and polydispersity P) from the DLS technique were determined by applying well-defined mathematical equations [45]. The colloidal stability of the dispersions (at 0.01 and 0.1 mg·mL^{-1} of PDDA and OVA concentrations, respectively) was followed for 48 h by determining the effect of time on Dz, P, ζ, and G.

UV–Vis spectra of the PDDA/OVA dispersions were acquired at 25 °C using a Shimadzu UV-1800 spectrophotometer (SSI; Kyoto, Japan) from 200 to 800 nm in appropriate cuvettes against a Milli-Q blank of pure water.

For SEM experiments, the PDDA/OVA NPs dispersion in Milli-Q water (at 0.01 and 0.1 mg·mL^{-1} of PDDA and OVA concentrations, respectively) was placed on a round glass coverslip and dried overnight at room temperature before coating with a gold layer using a Leica EM SCD 050 sputtering apparatus for observation under a FEI Quanta 250 scanning electron microscope.

2.4. Cell Culture, Preparation of PDDA, OVA, or PDDA/OVA Solutions for Interaction with Cells, and Determination of Cell Viability in the Interaction Mixtures

L929 fibroblasts and J774A.1 macrophages cell lines were obtained from the American Type Culture Collection (ATCC; www.atcc.org) and cultured according to standard protocols for mammalian cells culture under sterile conditions, in an atmosphere of 90% humidity, 5% CO_2, at 37 °C in RPMI-1640 medium supplemented with 10% fetal bovine serum (FBS), 1 unit/mL of penicillin-streptomycin, and 2 mM L-glutamine. For interaction with cells, PDDA, OVA, and PDDA/OVA solutions were also prepared in RPMI-1640 medium supplemented with 10% fetal bovine serum (FBS), 1 unit/mL of penicillin-streptomycin, and 2 mM L-glutamine. The interaction between cells and solutions to be tested was performed as follows.

L929 fibroblasts and J774A.1 macrophages were plated into 96-well microtiter plates at a density of 10,000 cells/well and incubated for 12 h before replacing the culture medium by 100 µL of PDDA, OVA, or PDDA/OVA solutions. Thereafter, the mixtures were again incubated in a humidified CO_2 incubator for 3 and 24 h before determining the in vitro cytotoxicity of PDDA, OVA, and PDDA/OVA by the 3-(4,5-dimethylthiazol-2-yl)-2,5-diphenyl tetrazolium bromide (MTT) assay [46]. A MTT stock solution at 5 mg·mL^{-1} in PBS was filtered for sterilization and removal of insoluble MTT residues. Ten microliters of this stock MTT solution was added per well, each well containing 100 µL of the plated cells interacting with OVA, PDDA, PDDA/OVA. After incubation (37 °C/ 2 h), the supernatants were withdrawn and cells adhered to the wells were mixed meticulously with 100 µL of an isopropanol solution acidified to 0.04 N HCl in order to dissolve formazan crystals. The absorbance of each well was recorded at 570 nm on a Multiskan Ex Microelisa reader. As a control, cells mixed with the culture medium only yielded 100% of cell viability. Cell viability in the presence of OVA, PDDA, or OVA/PDDA solutions was expressed as % of the control.

2.5. Determination of Cells Morphology in the Presence of PDDA by Scanning Electron Microscopy (SEM)

L929 fibroblasts (ATCC CCL-1) were grown up to 80–100% confluency before taking aliquots of this culture to counting in a Neubauer chamber to add about 100,000 cells/well in wells that had received spherical coverslips (one coverslip per well) in plates with 24 wells/plate so that cells were allowed to adhere on the coverslips for 12 h. The culture medium was replaced by PDDA solutions at concentrations of 0.01, 0.1, and 1 mg·mL^{-1}, and the samples were incubated in a humidified CO_2 incubator for 3 h. Cells were then fixed in the Karnovsky buffer (5% glutaraldehyde, paraformaldehyde 4%, sodium cacodylate 0.1 M, and pH 7.2) for 3h before progressive dehydration was performed with added ethanol solutions (concentrations ranging from 7.5% to 100%; 15 min interaction with cells per concentration). Thereafter, the cells on the coverslips were further dried in a Leica CPD 030 critical-point dryer device and covered with gold in a Leica EM SCD 050 sputtering device for observation in an FEI Quanta 250 scanning electron microscope.

2.6. Immunization Scheme

Groups of five BALB/c mice were immunized subcutaneously at two separate sites on the base of the tail with a total injection volume of 0.2 mL/animal using solutions or dispersions at the final concentrations of adjuvants and/or OVA antigen shown in Table 1. A booster using the same dose employed for priming was carried out at 21 days post-immunization.

Ethical procedures for experimentation with animals were followed and were in accordance with guidelines approved by the Instituto Butantan's Committee of Ethics on Animal Research (protocol number 7912280219).

Table 1. Composition of solutions or dispersions in water used for immunization of four groups of five mice.

Group	Solution or Dispersion	[OVA] mg·mL^{-1}	[Al(OH)$_3$] mg·mL^{-1}	[PDDA] mg·mL^{-1}
1	Milli-Q water	0	0	0
2	OVA	0.1	0	0
3	Al(OH)$_3$/OVA	0.1	0.1	0
4	PDDA/OVA	0.1	0	0.01

2.7. Determination of OVA-Specific IgG1 and IgG2a Antibodies

For evaluation of the humoral response, five mice per group were bled through the ophthalmic plexus 14, 21, and 28 days after immunization and the serum individually analyzed by indirect enzyme-linked immunosorbent assay (ELISA). Briefly, 96-well polystyrene high-binding microtitre plates (Costar Corning Inc., Mass., USA) were coated overnight at 4 °C with 100 µL of OVA solution

(10 μg/mL in 0.01 M phosphate buffer saline (PBS), pH 7.2). The wells were blocked with 3% gelatin in PBS for 2 h and then incubated (1 h/37 °C) with serum samples serially diluted. In each well, 100 μL of goat anti-mouse biotin-conjugated IgG1 (1:1000) or IgG2a (1:500) (Southern Biotechnology Associates, AL, USA) were added to the corresponding plates and incubated for 1 h at 37 °C. Then, peroxidase-labeled streptavidin (100 μL of a 1:3000 dilution) was added and incubated for 1 h at 37 °C. Plates were washed three times after each incubation step with PBS containing 0.05% Tween 20 (PBST). Finally, 100 μL OPD substrate solution (1 mg·mL^{-1}) and H_2O_2 (1 μL/mL) diluted in 0.1 M citrate-phosphate (pH 5.0) were added to each well and incubated for 15 min at room temperature. The reaction was stopped by adding 50 μL of 2 M H_2SO_4 to each well. Absorbance was determined at 492 nm for individual wells using an ELISA plate reader (Multiskan Ex, Thermo Electron Corporation). The results were expressed for diluted serum samples as the mean absorbance ± standard deviation. The primary response of IgG1 was presented at dilution of 1/256 and the secondary response at 1/16348. The primary response of IgG2a was presented at dilutions 1/8 and the secondary response at 1/128, the dilutions chosen correspond to the linear part of the titration curve.

2.8. Determination of Delayed-Type Hypersensitivity Reaction (DTH)

For evaluation of the delayed-type hypersensitivity reaction, five mice/group on the fifth day post-immunization were injected at the left-hind footpad with a previously heated (1 h/80 °C) and denaturated OVA solution (30 μL, 2 μg/μL in saline). As a control, the same volume of saline was injected at the right-hind footpad of each animal. Differential footpad swelling was determined 24 h after injection with a Mitutoyo digital micrometer and considered as the difference between swelling of left and right paws for the same animal. The results were represented as arithmetic mean footpad swelling ± standard deviation.

2.9. Statistical Analysis

To compare results for different groups, two-way analysis of variance (ANOVA) followed by Tukey's multiple comparisons test was used. P-values below 0.05 were considered significant. Statistical analysis was performed using the Origin 2018 program (Origin Lab Corporation, Northampton, USA). Statistical analyses for IgG1 or IgG2a were performed separately.

3. Results and Discussion

3.1. Characterization of PDDA/OVA Dispersions Regarding Formation of Nanoparticles, Their Size, Surface Potential, Polydispersity, Morphology, and Colloidal Stability.

In order to ascertain the formation of nanoparticles from PDDA/OVA dispersions, the first property of the mixtures inferred by visual observation was the occurrence of a turbid appearance. The interaction between OVA and PDDA was driven by their opposite charges. OVA isoelectric point is around 4.5 [47]; its charge at the pH of water (6.3) is negative. PDDA, as a cationic antimicrobial polymer [40], is expected to interact electrostatically with OVA. In fact, PDDA and BSA and other negatively charged proteins interacted in dispersion to yield nanoparticles [41,42,48]. Figure 1 shows micrographs of PDDA/OVA dispersions obtained by SEM. These revealed the occurrence of NPs with a mean diameter (D) of dried NPs of D = 234 ± 42 nm as derived from ImageJ software. Typically, some aggregation due to the drying process (required by the SEM technique) might have slightly increased the mean size of the NPs. Indeed, using a method as DLS, the mean hydrodynamic diameter of the same NPs dispersion was Dz = 170 ± 4 nm (Figure 2a). The NPs at 0.1 mg·mL^{-1} OVA and 0.01 mg·mL^{-1} PDDA displayed a positive net charge (ζ = 30 ± 2), and the dispersion of NPs exhibited a relatively low polydispersity of P = 0.11 ± 0.01.

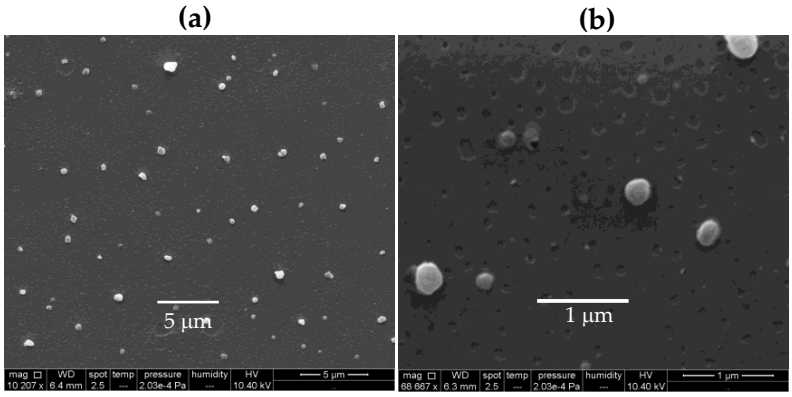


Figure 1. Scanning electron microscopy (SEM) of poly (diallyldimethylammonium chloride) (PDDA)/ ovalbumin (OVA) nanoparticles (NPs) at [PDDA] = 0.01 mg·mL^{-1} and [OVA] = 0.1 mg·mL^{-1} under low (**a**) and high magnification (**b**). The mean diameter (D) of dried NPs from ImageJ software was D = 234 ± 42 nm.

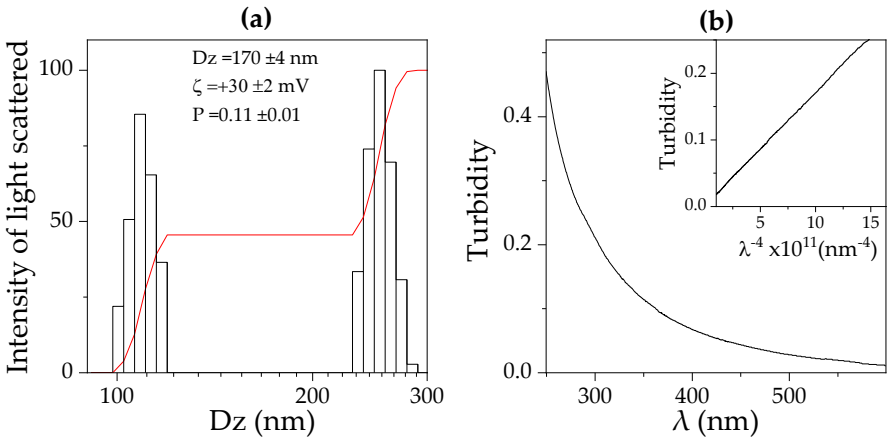


Figure 2. Intensity of light scattered by PDDA/OVA NPs in water obtained at 0.01 PDDA and 0.1 mg·mL^{-1} OVA: (**a**) as a function of the hydrodynamic diameter (Dz) determined by dynamic light scattering (DLS); (**b**) as a function of wavelength of the incident light (λ) determined from turbidimetry. Mean Dz, zeta potential (ζ), and polydispersity (P) for this dispersion are also given. The relationship between turbidity and λ^{-4} was linear with a regression coefficient of 0.90 (insert).

Curiously, the concentration of the OVA stock solution used to prepare the PDDA/OVA dispersions was important to define the PDDA/OVA NPs size (not shown). The lower the OVA stock solution concentration, the lower the size of PDDA/OVA NPs, possibly due to variable degrees of intermolecular OVA/OVA aggregation. At high concentrations, OVA/OVA aggregation in the stock solution would be higher than at low concentrations. In the literature, OVA/OVA aggregation with increasing OVA concentration has already been observed by other authors [49].

The nano-size of all PDDA/OVA NPs in water dispersion was reconfirmed by determining the dependence of turbidity on the wavelength of the incident light (λ). Rayleigh scattering by turbid dispersions of NPs means a linear dependence of turbidity with 1/λ^4 as the one shown in Figure 2b. Usually, Rayleigh scattering occurs for spherical particles in water dispersion with diameters very small compared with λ [50,51], showing that the PDDA/OVA NPs are indeed spherical and nano-sized.

We defined 0.1 and 0.01 mg·mL^{-1} as the OVA and PDDA concentrations, respectively, to be used throughout this study based on the experiments described next.

In order to evaluate the effect of [PDDA] on the physical properties of PDDA/OVA NPs at 0.1 mg·mL^{-1} OVA, the concomitant change in size (Dz), zeta-potential (ζ), polydispersity (P), and conductance (G) was obtained using the DLS apparatus. NPs size initially increased with PDDA concentration attaining a maximal value when ζ was zero meaning that absence of electrostatic repulsion between the NPs would cause loss of their colloidal stability (Figure 3a,b). Further increasing PDDA concentration to 0.01 mg·mL^{-1} re-stabilized the dispersion, yielding positive and relatively high zeta-potential (around 30 mV). This was the highest zeta-potential obtained over all ranges of PDDA concentrations tested. However, increasing [PDDA] above 0.01 mg·mL^{-1}, an increase in the conductance (G) of the dispersions revealed that further incorporation of PDDA onto NPs did not occur (Figure 3d). Additional PDDA remained in the bulk solution increasing G. The poly-cation nature of PDDA has indeed been shown to result in increasing conductance with increases in PDDA concentration in water solutions [52]. Over a range of high [PDDA], above 0.2 mg·mL^{-1} PDDA, the polydispersity (P) of the dispersions increased (Figure 3c), possibly due to PDDA-induced bridging flocculation and PDDA/OVA NPs aggregation [39].

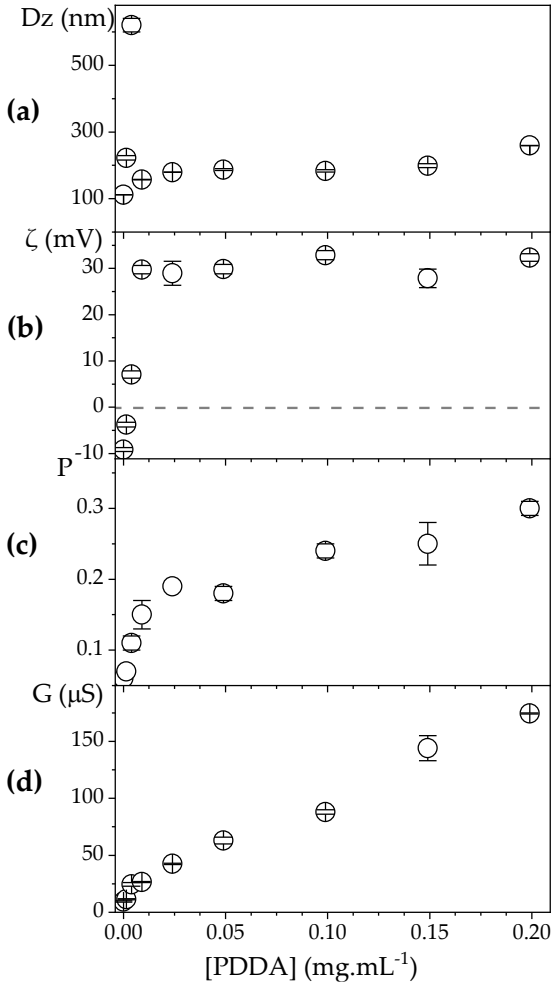


Figure 3. Effect of PDDA concentration on: (**a**) hydrodynamic diameter (Dz); (**b**) zeta potential (ζ); (**c**) polydispersity (P); (**d**) conductance (G) of PDDA/OVA NPs at [OVA] = 0.1 mg. mL^{-1}. The dashed line indicates zeta-potential (ζ) = 0 occurring around [PDDA] = 0.004 mg·mL^{-1}.

From the results in Figure 3, the best conditions for obtaining positively charged, stable, and nano-sized PDDA/OVA NPs became clear, namely, 0.1 and 0.01 mg·mL^{-1} for OVA and PDDA concentrations, respectively. At these concentrations, the usual cytotoxicity of cationic polymers is minimized [29]. The smallest concentration possible of the cationic polymer PDDA for obtaining the desired properties of the NPs was determined as 0.01 mg·mL^{-1} at 0.1 mg·mL^{-1} OVA (Figure 3). In Figure 4, using these same concentrations, the colloidal stability for the PDDA/OVA NPs in water was determined over the time remaining excellent during all the observation period (48 h) and possibly beyond (from visual and macroscopic observation). The NPs were stable colloids. Paul Dubin and co-workers also found good colloidal stability for PDDA/BSA NPs over 4 months [42].

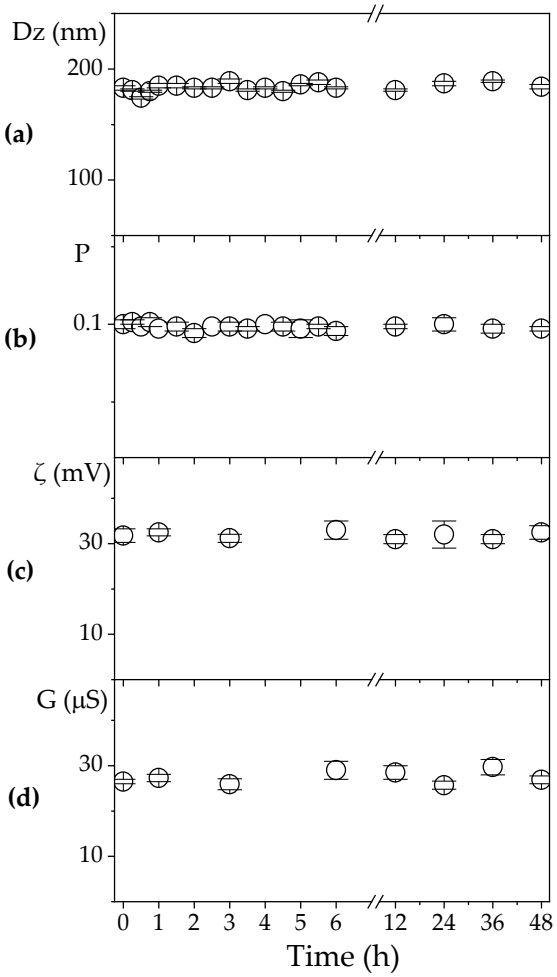


Figure 4. Effect of time on: (**a**) hydrodynamic diameter (Dz); (**b**) polydispersity (P); (**c**) zeta potential (ζ); (**d**) conductance (G) of PDDA/OVA NPs at [PDDA] = 0.01 mg·mL^{-1} and [OVA] = 0.1 mg. mL^{-1}.

3.2. Cytotoxicity of PDDA/OVA NPs Against Mammalian Cells in Culture

The cytotoxicity of the PDDA0.01/OVA0.1 formulation meaning 0.01 and 0.1 mg·mL-1 of PDDA and OVA concentrations was evaluated against two cell lines in culture, fibroblasts and macrophages, using two different techniques, the MTT assay and SEM.

In Figure 5, significant cytotoxicity for PDDA against the mammalian cells was obtained only above 0.01 mg·mL^{-1} for the two time points (3 and 24 h), and serum concentrations were tested (2% and 10% FBS). This agrees with data by Fischer and coworkers who determined low cytotoxicity

for 0.01 mg·mL^{-1} PDDA against fibroblasts. Along similar lines, hemolytic effects of PDDA did not occur at such low concentration [53].

The use of two serum concentrations aimed at finding an eventual effect of serum proteins neutralization of the positive charges on PDDA contributing to diminished cytotoxicity. The results in Figure 5 showed that both serum concentrations had a similar effect on cytotoxicity against the two cell lines. Possibly, at 0.01 mg·mL^{-1} PDDA, BFS at 2% was enough to combine with all PDDA molecules so that PDDA alone was not available to combine with the cells. On the other hand, at higher [PDDA], PDDA molecules that did not combine with BFS would attach to the cells exerting their cytotoxic activity. The hemolytic activity of PDDA was reported as important only above [PDDA] = 1 mg·mL^{-1} [29,33,53].

In agreement with the present findings, Fischer and co-workers also reported low cytotoxicity of PDDA against fibroblasts at 0.01 mg·mL^{-1} using the MTT assay besides showing that PDDA was less toxic against the cells than PEI or PLL [29].

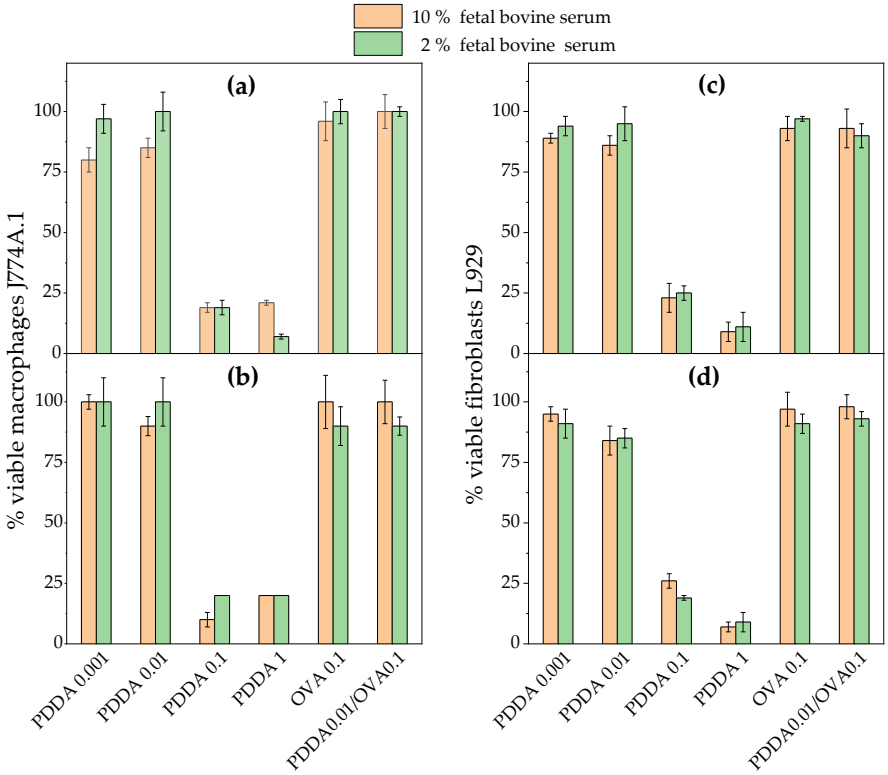


Figure 5. Cell viability (%) of macrophages (J774A.1) or fibroblasts (L929) in culture from the 3-(4,5-dimethylthiazol-2-yl)-2,5-diphenyl tetrazolium bromide (MTT) assay after incubation for 3 (**a**,**c**) or 24 h (**b**,**d**) with PDDA, OVA, and PDDA/OVA NPs. Concentrations are given in mg·mL^{-1}. One should notice that the formulation used for the immunology experiments were 0.01 and 0.1 mg. mL^{-1} of PDDA and OVA, respectively.

The effect of PDDA on morphology of the fibroblasts is presented in Figure 6. Holes could be seen on the cells indicating that the many debris observed in the SEM micrographs stemmed from the cell membrane, apparently withdraw from the cell by the cationic polymer PDDA. Similar cell debris were observed by Martinez et al. with 10 mM poly(allylamine hydrochloride) [31] and with linear or ramified PEI or PLL [30], suggesting a general feature of poly-cations acting by disruption of cell membranes. This also took place for multi-resistant bacteria submitted to PDDA assemblies with

anionic carboxymethylcellulose (CMC) for which both the cell wall and the cell membrane were lysed allowing the leakage of intracellular compounds [32].

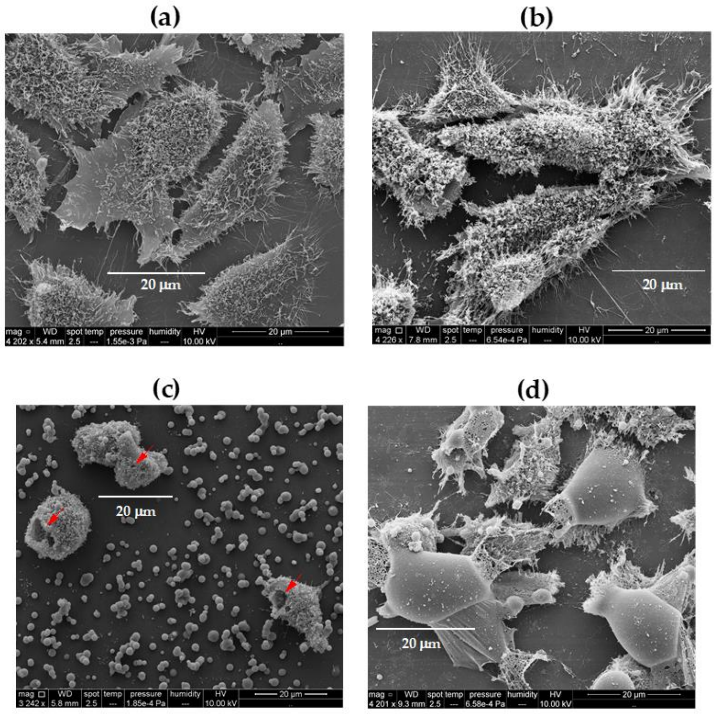


Figure 6. Scanning electron microscopy (SEM) of fibroblasts L929 incubated for 3 h with: (**a**) culture medium; (**b**) 0.01; (**c**) 0.1; (**d**) 1 mg·mL^{-1} PDDA. The red arrows indicate holes on the cells at 0.1 mg·mL^{-1} PDDA.

3.3. Immunoadjuvant Properties of PDDA/OVA NPs.

Adjuvants as $Al(OH)_3$ usually improve the antigen-specific production of IgG1, whereas adjuvants as the cationic lipid dioctadecyldimethylammonium bromide (DODAB) dispersed as bilayer assemblies usually implement the antigen-specific production of IgG2a [8,15,20,25,27]. Figure 7 shows the humoral responses of mice challenged with $Al(OH)_3$/OVA0.1 dispersion and PDDA0.01/OVA0.1 NPs as determined by ELISA for detection of IgG1 and IgG2a antibodies. The NPs displayed an immune response profile qualitatively very similar to the one of Al $(OH)_3$ [54] yielding an expressive increase in IgG1 and a discrete increase in IgG2a production as usual for a Th-2 implemented response by an adjuvant. However, in quantitative comparison with $Al(OH)_3$, PDDA as an adjuvant the NPs were more effective than $Al(OH)_3$/OVA for implementing OVA-specific IgG1 production. In the literature, the size histogram for $Al(OH)_3$ dispersion alone or carrying an antigen showed a broad size distribution with high polydispersity and low colloidal stability as depicted from the presence of precipitated material [17]. There was a much higher production of IgG1 than IgG2a, as depicted from the serum dilutions used to determine by ELISA both antibodies. Whereas the serum dilution used to determine the primary IgG1 production was 1/256, the one used to determine primary IgG2a production was 1/8 only. This means that the serum contained much larger IgG1 concentration than the one of IgG2a (Figure 7).

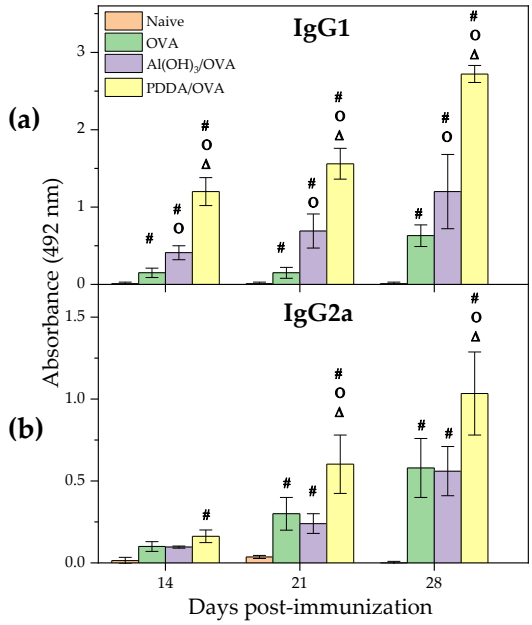


Figure 7. Humoral responses induced by OVA, Al $(OH)_3$/OVA, or PDDA/OVA NPs at concentrations given in Table 1. Mean absorbance at 492 nm± standard deviation related to anti-OVA IgG1 and IgG2a antibodies production was determined over time after immunization of BALB/c mice from sera collected on days 14 and 21 post-immunization (primary response) or on day 28 (secondary response). The primary IgG1 production was determined at 1/256 serum dilution whereas the secondary one was obtained at 1/16348 dilution. The primary IgG2a production was determined at 1/8 serum dilution whereas the secondary one was obtained at 1/128 dilution. $p < 0.05$ compared to naive group (#), $p < 0.05$ compared to OVA group (o), $p < 0.05$ compared to Al$(OH)_3$/OVA group (Δ).

The advantages of the PDDA/OVA NPs are their nano-size (Figures 1 and 2), high colloidal stability (Figure 4), and visual absence of precipitated material. Possible consequences in vivo would be the optimization of antigen presentation by APC at the lymph nodes. Indeed, Manolova and co-workers [55] found that nano-sized adjuvant/antigen assemblies directly delivered the antigen to the APC in the lymph nodes, whereas micro-sized ones stayed longer at the site of injection becoming mostly associated with dendritic cells (DC) from the site of injection. This could explain the higher production of IgG1 induced by PDDA/OVA NPs in comparison to Al$(OH)_3$ /OVA.

Other cationic polymers carrying antigen also improved the humoral response above the one obtained with the traditional Al$(OH)_3$. Diverse forms of PEI elicited potent mucosal adjuvant activity for viral subunit glycoprotein antigens; a single intranasal administration of influenza hemagglutinin or herpes simplex virus type-2 (HSV-2) glycoprotein D with PEI elicited robust antibody-mediated protection also superior to the one by existing experimental mucosal adjuvants [36].

Using other injection modes, PEI administered subcutaneously with viral glycoprotein (HIV-1 gp140) also enhanced antigen-specific serum IgG production. PEI elicited higher titers of both antigen-binding and -neutralizing antibodies than alum in mice and rabbits, and induced an increased proportion of antibodies reactive with native antigen. In an intraperitoneal model, PEI recruited neutrophils followed by monocytes to the site of administration and enhanced antigen uptake by antigen-presenting cells [37].

Gold nanorods modified with cationic CTAB, PDDA, and PEI were used as promising DNA vaccine adjuvants for HIV-1 treatment and, curiously, also yielded high ratios IgG1/IgG2a. Among these three cationic molecules, PDDA was the one yielding the higher ratios [43]. Plebanski and coworkers designed magnetic lipoplexes for enhanced DNA vaccine delivery combining PEI, superparamagnetic

iron oxide nanoparticles (SPIONs) with the mucoadhesive hyaluronic acid (HA) and a plasmid encoding a malaria antigen increasing IgG1, IgG2a, and IgG2b [10,18].

In order to ascertain the cell-mediated immunity induced by the PDDA/OVA NPs, the delayed-type hypersensitivity reaction in immunized mice was determined. The DTH response induced by PDDA/OVA was low and equal to the one observed in mice for $Al(OH)_3$/OVA (Figure 8). This reconfirms the Th-2 profile induced by PDDA/OVA NPs. Other Th-1 inducers such DODAB/OVA or DODAB/CpG/OVA gave footpad swellings above 1.25 mm in contrast to the value lower than 0.5 mm obtained for PDDA/OVA or $Al(OH)_3$/OVA [8,9,12,15,17]. Thus, the low DTH response agreed with the predominant Th-2 profile for PDDA/OVA NPs.

Recently, we described hybrid NPs made of poly (methyl methacrylate) (PMMA) in the presence of poly (diallyl dimethyl ammonium) chloride (PDDA) using dioctadecyl dimethyl ammonium bromide (DODAB) as an emulsifier and found that DODAB remains attached to the NPs core [56–59]. This system might bring interesting applications for antigen presentation since DODAB might eventually add the missing Th-1 response to the antigen-presenting NPs.

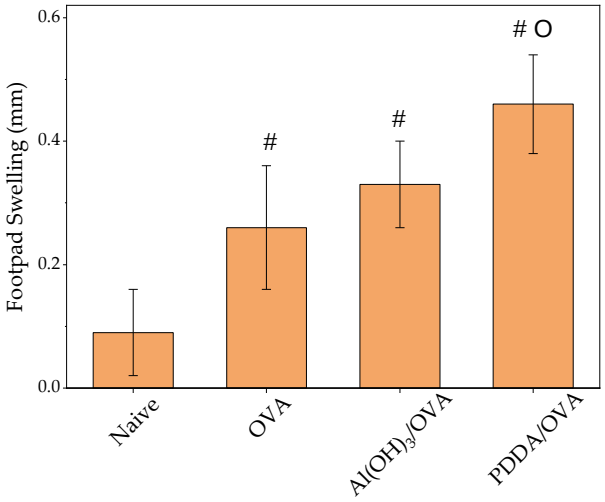


Figure 8. Mean footpad swelling ± standard deviation related to delayed-type hypersensitivity reaction of BALB/c mice immunized with OVA, $Al(OH)_3$/OVA, or PDDA/OVA NPs at concentrations given on Table 1. $p < 0.05$ compared to naive group (#), $p < 0.05$ compared to OVA group (o).

4. Conclusions

PDDA/OVA at 0.01 and 0.10 mg·mL^{-1} assembled as stable cationic nanoparticles in water with Dz = 170 nm ± 4, ζ = 30 mV ± 2, and P = 0.11 ± 0.01 effectively presented OVA to the immune system inducing a Th-2 type (humoral) response superior to the one induced by $Al(OH)_3$. One of the most important advantages of the PDDA system as an adjuvant is its simplicity; it is a single-component adjuvant. In addition, at the low PDDA concentration used, cytotoxicity of the cationic polymer became neglectable. At and above 0.1 mg·mL^{-1}, significant PDDA cytotoxicity against fibroblasts and macrophages in culture induced holes and cellular debris observable in SEM micrographs of the mammalian cells. PDDA/OVA NPs were nano-sized, stable, and well-dispersed in water without precipitated material. These properties would lead to in vivo optimization of antigen presentation by APC at the lymph nodes in contrast to the micro-sized $Al(OH)_3$/OVA dispersion that would remain at the site of injection staying longer at the site of injection and stimulating local dendritic cells. Determination of delayed-type hypersensitivity (DTH) reaction from footpad swelling revealed the low cellular response induced by PDDA/OVA similarly to $Al(OH)_3$ /OVA. In the future, it will be interesting to evaluate combinations of the antigen with NPs carrying both PDDA and elicitors of the Th-1 response such as cationic lipid and/or CpG. For continuing this work, the mechanism of PDDA-induced cell

death might be investigated from the morphology of the cell nucleus using a fluorescent label to discriminate between necrosis or apoptosis. The location of nanoparticles inside the cell will have to be assessed using an ovalbumin fluorescent label and the CD8+/CD4+ cell proliferation from flow cytometry and cytokines profile determination will reconfirm the Th-1/Th-2 response induced by PDDA/OVA NPs.

Author Contributions: Conceptualization, A.M.C.-R., E.L.F.-M., and Y.P.-B.; methodology, Y.P.-B., B.C.T., M.C., E.L.F.-M., and A.M.C.-R.; validation, A.M.C.-R., E.L.F.-M., and Y.P.-B.; formal analysis, A.M.C.-R., E.L.F.-M., and Y.P.-B.; investigation, Y.P.-B., B.d.C.L.F.T., M.C., E.L.F.-M., and A.M.C.-R.; resources, A.M.C.-R. and E.L.F.-M.; data curation, A.M.C.-R.; writing—original draft preparation, A.M.C.-R. and Y.P.-B.; writing—review and editing, A.M.C.-R. and Y.P.-B.; supervision, A.M.C.-R.; project administration, A.M.C.-R.; funding acquisition, A.M.C.-R. All authors have read and agreed to the published version of the manuscript.

Funding: This work was supported by Conselho Nacional de Desenvolvimento Científico e Tecnológico grants CNPq 302758/2019-4 and 302352/2014-7 to A.M.C.-R. and grant CNPq 312096/2018-6 to E.L.F.-M. Y.P.-B. is the recipient of a CNPq PhD fellowship (CNPq 140091/2019-0).

Acknowledgments: This work was supported by Conselho Nacional de Desenvolvimento Científico e Tecnológico grants CNPq 302758/2019-4 and 302352/2014-7 to A.M.C.R. Y.P.-B. is the recipient of a CNPq PhD fellowship (CNPq 140091/2019-0). We would like to thank Beatriz Mauricio from Cellular Biology Laboratory-Instituto Butantan for her kind technical assistance during SEM and Rodrigo Tadeu Ribeiro for his technical assistance during DLS and use of the Origin software.

Conflicts of Interest: The authors declare no conflict of interest. The funders had no role in the design of the study; in the collection, analyses, or interpretation of data; in the writing of the manuscript; or in the decision to publish the results.

References

1. Coffman, R.L.; Sher, A.; Seder, R.A. Vaccine adjuvants: Putting innate immunity to work. *Immunity* **2010**, *33*, 492–503. [CrossRef]
2. Bergmann-Leitner, E.S.; Leitner, W.W. Adjuvants in the driver's seat: How magnitude, type, fine specificity and longevity of immune responses are driven by distinct classes of immune potentiators. *Vaccines* **2014**, *2*, 252–296. [CrossRef]
3. Pasquale, A.; Preiss, S.; Silva, F.; Garçon, N. Vaccine adjuvants: From 1920 to 2015 and beyond. *Vaccines* **2015**, *3*, 320–343. [CrossRef] [PubMed]
4. Awate, S.; Babiuk, L.A.; Mutwiri, G. Mechanisms of action of adjuvants. *Front. Immunol.* **2013**, *4*, 114. [CrossRef] [PubMed]
5. HogenEsch, H.; O'Hagan, D.T.; Fox, C.B. Optimizing the utilization of aluminum adjuvants in vaccines: You might just get what you want. *Npj Vaccines* **2018**, *3*, 51. [CrossRef] [PubMed]
6. Martiñón, S.; Cisneros, A.; Villicaña, S.; Hernández-Miramontes, R.; Mixcoha, E.; Calderón-Vargas, P. Chemical and immunological characteristics of aluminum-based, oil-water emulsion, and bacterial-origin adjuvants. *J. Immunol. Res.* **2019**, *2019*, 3974127. [CrossRef]
7. Apostólico, J.d.S.; Lunardelli, V.A.S.; Coirada, F.C.; Boscardin, S.B.; Rosa, D.S. Adjuvants: Classification, modus operandi, and licensing. *J. Immunol. Res.* **2016**, *2016*, 1459394.
8. Lincopan, N.; Espindola, N.M.; Vaz, A.J.; da Costa, M.H.B.; Faquim-Mauro, E.; Carmona-Ribeiro, A.M. Novel immunoadjuvants based on cationic lipid: Preparation, characterization and activity in vivo. *Vaccine* **2009**, *27*, 5760–5771. [CrossRef]
9. Lincopan, N.; Espindola, N.M.; Vaz, A.J.; Carmona-Ribeiro, A.M. Cationic supported lipid bilayers for antigen presentation. *Int. J. Pharm.* **2007**, *340*, 216–222. [CrossRef]
10. Nawwab Al-Deen, F.M.; Selomulya, C.; Kong, Y.Y.; Xiang, S.D.; Ma, C.; Coppel, R.L.; Plebanski, M. Design of magnetic polyplexes taken up efficiently by dendritic cell for enhanced DNA vaccine delivery. *Gene Ther.* **2014**, *21*, 212–218. [CrossRef]
11. Rose, F.; Wern, J.E.; Gavins, F.; Andersen, P.; Follmann, F.; Foged, C. A strong adjuvant based on glycol-chitosan-coated lipid-polymer hybrid nanoparticles potentiates mucosal immune responses against the recombinant Chlamydia trachomatis fusion antigen CTH522. *J. Control. Release* **2018**, *271*, 88–97. [CrossRef] [PubMed]

12. Tsuruta, L.R.; Quintilio, W.; Costa, M.H.; Carmona-Ribeiro, A.M. Interactions between cationic liposomes and an antigenic protein: The physical chemistry of the immunoadjuvant action. *J. Lipid Res.* **1997**, *38*, 2003–2011. [PubMed]
13. Davidsen, J.; Rosenkrands, I.; Christensen, D.; Vangala, A.; Kirby, D.; Perrie, Y.; Agger, E.M.; Andersen, P. Characterization of cationic liposomes based on dimethyldioctadecylammonium and synthetic cord factor from M. tuberculosis (trehalose 6,6′-dibehenate)-a novel adjuvant inducing both strong CMI and antibody responses. *Biochim. Biophys. Acta* **2005**, *1718*, 22–31. [CrossRef] [PubMed]
14. Riehl, M.; Harms, M.; Hanefeld, A.; Baleeiro, R.B.; Walden, P.; Mader, K. Combining R-DOTAP and a particulate antigen delivery platform to trigger dendritic cell activation: Formulation development and in-vitro interaction studies. *Int. J. Pharm.* **2017**, *532*, 37–46. [CrossRef] [PubMed]
15. Rozenfeld, J.H.K.; Silva, S.R.; Raneia, P.A.; Faquim-Mauro, E.; Carmona-Ribeiro, A.M. Stable assemblies of cationic bilayer fragments and CpG oligonucleotide with enhanced immunoadjuvant activity in vivo. *J. Control. Release* **2012**, *160*, 367–373. [CrossRef] [PubMed]
16. De Almeida, A.F.; De Gaspari, E. Dioctadecyldimethylammonium bromide (DODAB-BF) as a new adjuvant for maternal-fetal immunization in mice against Neisseria meningitidis: Evaluation of humoral response. *Pathog. Dis.* **2018**, *76*, ftx128. [CrossRef] [PubMed]
17. Lincopan, N.; Santana, M.R.; Faquim-Mauro, E.; da Costa, M.H.B.; Carmona-Ribeiro, A.M. Silica-based cationic bilayers as immunoadjuvants. *BMC Biotechnol.* **2009**, *9*, 5. [CrossRef]
18. Nawwab Al-Deen, F.; Ma, C.; Xiang, S.D.; Selomulya, C.; Plebanski, M.; Coppel, R.L. On the efficacy of malaria DNA vaccination with magnetic gene vectors. *J. Control. Release* **2013**, *168*, 10–17. [CrossRef]
19. Xiang, S.D.; Scholzen, A.; Minigo, G.; David, C.; Apostolopoulos, V.; Mottram, P.L.; Plebanski, M. Pathogen recognition and development of particulate vaccines: Does size matter? *Methods* **2006**, *40*, 1–9. [CrossRef]
20. Carmona-Ribeiro, A.M. Cationic Nanostructures for Vaccines. In *Immune Response Activation*; Duc, G.H.T., Ed.; InTech: Rijeka, Croatia, 2014; pp. 1–45. ISBN 978-953-51-1374-4.
21. Pelkmans, L. Secrets of caveolae- and lipid raft-mediated endocytosis revealed by mammalian viruses. *Biochim. Biophys. Acta* **2005**, *1746*, 295–304. [CrossRef]
22. Fifis, T.; Gamvrellis, A.; Crimeen-Irwin, B.; Pietersz, G.A.; Li, J.; Mottram, P.L.; McKenzie, I.F.C.; Plebanski, M. Size-dependent immunogenicity: Therapeutic and protective properties of nano-vaccines against tumors. *J. Immunol.* **2004**, *173*, 3148–3154. [CrossRef] [PubMed]
23. O'Hagan, D.T.; MacKichan, M.L.; Singh, M. Recent developments in adjuvants for vaccines against infectious diseases. *Biomol. Eng.* **2001**, *18*, 69–85. [CrossRef]
24. Denis-Mize, K.S.; Dupuis, M.; MacKichan, M.L.; Singh, M.; Doe, B.; O'Hagan, D.; Ulmer, J.B.; Donnelly, J.J.; McDonald, D.M.; Ott, G. Plasmid DNA adsorbed onto cationic microparticles mediates target gene expression and antigen presentation by dendritic cells. *Gene Ther.* **2000**, *7*, 2105–2112. [CrossRef]
25. Carmona-Ribeiro, A.M. Nanomaterials based on lipids for vaccine development. In *Micro and Nano Technologies*; Skwarczynski, M., Toth, I.B.T.-M., Eds.; Elsevier: Oxford, UK; Cambridge, MA, USA, 2017; pp. 241–257. ISBN 978-0-323-39981-4.
26. Carmona-Ribeiro, A.M. The versatile dioctadecyldimethylammonium bromide. In *Application and Characterization of Surfactants*; Najjar, R., Ed.; InTech: Rijeka, Croatia, 2017; pp. 157–182. ISBN 978-953-51-3326-1.
27. Holten-Andersen, L.; Doherty, T.M.; Korsholm, K.S.; Andersen, P. Combination of the cationic surfactant dimethyl dioctadecyl ammonium bromide and synthetic mycobacterial cord factor as an efficient adjuvant for tuberculosis subunit vaccines. *Infect. Immun.* **2004**, *72*, 1608–1617. [CrossRef]
28. De Oliveira Santos, F.A.; Lincopan, N.; De Gaspari, E. Evaluation of intranasal and subcutaneous route of immunization in neonatal mice using DODAB-BF as adjuvant with outer membrane vesicles of Neisseria meningitis B. *Immunobiology* **2018**, *223*, 750–760. [CrossRef] [PubMed]
29. Fischer, D.; Li, Y.; Ahlemeyer, B.; Krieglstein, J.; Kissel, T. In vitro cytotoxicity testing of polycations: Influence of polymer structure on cell viability and hemolysis. *Biomaterials* **2003**, *24*, 1121–1131. [CrossRef]
30. Monnery, B.D.; Wright, M.; Cavill, R.; Hoogenboom, R.; Shaunak, S.; Steinke, J.H.G.; Thanou, M. Cytotoxicity of polycations: Relationship of molecular weight and the hydrolytic theory of the mechanism of toxicity. *Int. J. Pharm.* **2017**, *521*, 249–258. [CrossRef] [PubMed]
31. Martinez, J.S.; Keller, T.C.S.; Schlenoff, J.B. Cytotoxicity of free versus multilayered polyelectrolytes. *Biomacromolecules* **2011**, *12*, 4063–4070. [CrossRef]

32. Carrasco, L.D.d.M.; Sampaio, J.L.M.; Carmona-Ribeiro, A.M. Supramolecular cationic assemblies against multidrug-resistant microorganisms: Activity and mechanism of action. *Int. J. Mol. Sci.* **2015**, *16*, 6337–6352. [CrossRef]
33. Jeong, H.; Hwang, J.; Lee, H.; Hammond, P.T.; Choi, J.; Hong, J. In vitro blood cell viability profiling of polymers used in molecular assembly. *Sci. Rep.* **2017**, *7*, 9481. [CrossRef]
34. Wang, X.; Zheng, K.; Si, Y.; Guo, X.; Xu, Y. Protein-polyelectrolyte interaction: Thermodynamic analysis based on the titration method (†). *Polymers* **2019**, *11*, 82. [CrossRef] [PubMed]
35. Wusiman, A.; Gu, P.; Liu, Z.; Xu, S.; Zhang, Y.; Hu, Y.; Liu, J.; Wang, D.; Huang, X. Cationic polymer modified PLGA nanoparticles encapsulating Alhagi honey polysaccharides as a vaccine delivery system for ovalbumin to improve immune responses. *Int. J. Nanomed.* **2019**, *14*, 3221–3234. [CrossRef] [PubMed]
36. Wegmann, F.; Gartlan, K.H.; Harandi, A.M.; Brinckmann, S.A.; Coccia, M.; Hillson, W.R.; Kok, W.L.; Cole, S.; Ho, L.-P.; Lambe, T.; et al. Polyethyleneimine is a potent mucosal adjuvant for viral glycoprotein antigens. *Nat. Biotechnol.* **2012**, *30*, 883. [CrossRef] [PubMed]
37. Sheppard, N.C.; Brinckmann, S.A.; Gartlan, K.H.; Puthia, M.; Svanborg, C.; Krashias, G.; Eisenbarth, S.C.; Flavell, R.A.; Sattentau, Q.J.; Wegmann, F. Polyethyleneimine is a potent systemic adjuvant for glycoprotein antigens. *Int. Immunol.* **2014**, *26*, 531–538. [CrossRef] [PubMed]
38. Vieira, D.B.; Carmona-Ribeiro, A.M. Cationic nanoparticles for delivery of amphotericin B: Preparation, characterization and activity in vitro. *J. Nano Biotechnol.* **2008**, *6*, 6. [CrossRef] [PubMed]
39. Melo, L.D.; Mamizuka, E.M.; Carmona-Ribeiro, A.M. Antimicrobial particles from cationic lipid and polyelectrolytes. *Langmuir* **2010**, *26*, 12300–12306. [CrossRef] [PubMed]
40. Carmona-Ribeiro, A.M.; de Melo Carrasco, L.D. Cationic antimicrobial polymers and their assemblies. *Int. J. Mol. Sci.* **2013**, *14*, 9906–9946. [CrossRef]
41. Bohidar, H.; Dubin, P.L.; Majhi, P.R.; Tribet, C.; Jaeger, W. Effects of protein-polyelectrolyte affinity and polyelectrolyte molecular weight on dynamic properties of bovine serum albumin-poly(diallyldimethylammonium chloride) coacervates. *Biomacromolecules* **2005**, *6*, 1573–1585. [CrossRef]
42. Kayitmazer, A.B.; Strand, S.P.; Tribet, C.; Jaeger, W.; Dubin, P.L. Effect of polyelectrolyte structure on protein-polyelectrolyte coacervates: Coacervates of bovine serum albumin with poly(diallyldimethylammonium chloride) versus chitosan. *Biomacromolecules* **2007**, *8*, 3568–3577. [CrossRef]
43. Xu, L.; Liu, Y.; Chen, Z.; Li, W.; Liu, Y.; Wang, L.; Liu, Y.; Wu, X.; Ji, Y.; Zhao, Y.; et al. Surface-engineered gold nanorods: Promising DNA vaccine adjuvant for HIV-1 treatment. *Nano Lett.* **2012**, *12*, 2003–2012. [CrossRef]
44. Walker, J.M. The bicinchoninic acid (BCA) assay for protein quantitation. *Methods Mol. Biol.* **1994**, *32*, 5–8. [PubMed]
45. Grabowski, E.; Morrison, I. Particle size distribution from analysis of quasi-elastic light scattering data. In *Measurement of Suspended Particles by Quasi-Elastic Light Scattering*; John Wiley & Sons: New York, NY, USA, 1983; pp. 199–236.
46. Mosmann, T. Rapid colorimetric assay for cellular growth and survival: Application to proliferation and cytotoxicity assays. *J. Immunol. Methods* **1983**, *65*, 55–63. [CrossRef]
47. Niu, F.; Su, Y.; Liu, Y.; Wang, G.; Zhang, Y.; Yang, Y. Ovalbumin–gum arabic interactions: Effect of pH, temperature, salt, biopolymers ratio and total concentration. *Colloids Surf. B Biointerfaces* **2014**, *113*, 477–482. [CrossRef] [PubMed]
48. Wen, Y.; Dubin, P.L. Potentiometric studies of the interaction of bovine serum albumin and poly(dimethyldiallylammonium chloride). *Macromolecules* **1997**, *30*, 7856–7861. [CrossRef]
49. Ianeselli, L.; Zhang, F.; Skoda, M.W.A.; Jacobs, R.M.J.; Martin, R.A.; Callow, S.; Prevost, S.; Schreiber, F. Protein-protein interactions in ovalbumin solutions studied by small-angle scattering: Effect of ionic strength and the chemical nature of cations. *J. Phys. Chem. B* **2010**, *114*, 3776–3783. [CrossRef]
50. Carmona-Ribeiro, A.M.; Chaimovich, H. Salt-induced aggregation and fusion of dioctadecyldimethylammonium chloride and sodium dihexadecylphosphate vesicles. *Biophys. J.* **1986**, *50*, 621–628. [CrossRef]
51. Strutt, J.W. On the scattering of light by shells. *Proc. R. Soc. Lond. A Math. Phys. Sci.* **1918**, *94*, 296–300.
52. Karibyants, N.; Dautzenberg, H.; Cölfen, H. Characterization of PSS/PDADMAC-co-AA polyelectrolyte complexes and their stoichiometry using analytical ultracentrifugation. *Macromolecules* **1997**, *30*, 7803–7809. [CrossRef]

53. Sanches, L.M.; Petri, D.F.S.; de Melo Carrasco, L.D.; Carmona-Ribeiro, A.M. The antimicrobial activity of free and immobilized poly (diallyldimethylammonium) chloride in nanoparticles of poly (methylmethacrylate). *J. Nanobiotechnol.* **2015**, *13*, 58. [CrossRef]
54. Lindblad, E.B. Aluminium adjuvants—In retrospect and prospect. *Vaccine* **2004**, *22*, 3658–3668. [CrossRef]
55. Manolova, V.; Flace, A.; Bauer, M.; Schwarz, K.; Saudan, P.; Bachmann, M.F. Nanoparticles target distinct dendritic cell populations according to their size. *Eur. J. Immunol.* **2008**, *38*, 1404–1413. [CrossRef] [PubMed]
56. Ribeiro, R.T.; Galvão, C.N.; Betancourt, Y.P.; Mathiazzi, B.I.; Carmona-Ribeiro, A.M. Microbicidal dispersions and coatings from hybrid nanoparticles of poly (methyl methacrylate), poly (diallyl dimethyl ammonium) chloride, lipids, and surfactants. *Int. J. Mol. Sci.* **2019**, *20*, 6150. [CrossRef] [PubMed]
57. Galvão, C.N.; Sanches, L.M.; Mathiazzi, B.I.; Ribeiro, R.T.; Petri, D.F.S.; Carmona-Ribeiro, A.M. Antimicrobial coatings from hybrid nanoparticles of biocompatible and antimicrobial polymers. *Int. J. Mol. Sci.* **2018**, *19*, 2965. [CrossRef] [PubMed]
58. Pereira, E.M.A.; Kosaka, P.M.; Rosa, H.; Vieira, D.B.; Kawano, Y.; Petri, D.F.S.; Carmona-Ribeiro, A.M. Hybrid materials from intermolecular associations between cationic lipid and polymers. *J. Phys. Chem. B* **2008**, *112*, 9301–9310. [CrossRef]
59. Melo, L.D.; Palombo, R.R.; Petri, D.F.S.; Bruns, M.; Pereira, E.M.A.; Carmona-Ribeiro, A.M. Structure-activity relationship for quaternary ammonium compounds hybridized with poly(methyl methacrylate). *ACS Appl. Mater. Interfaces* **2011**, *3*, 1933–1939. [CrossRef]



© 2020 by the authors. Licensee MDPI, Basel, Switzerland. This article is an open access article distributed under the terms and conditions of the Creative Commons Attribution (CC BY) license (http://creativecommons.org/licenses/by/4.0/).

5 | Biocompatible lipid polymer cationic nanoparticles for antigen presentation

polymers

MDPI

Article

Biocompatible Lipid Polymer Cationic Nanoparticles for Antigen Presentation

Yunys Pérez-Betancourt [1], Bianca de Carvalho Lins Fernandes Távora [2], Eliana L. Faquim-Mauro [2] and Ana Maria Carmona-Ribeiro [1,*]

[1] Biocolloids Laboratory, Departamento de Bioquímica, Instituto de Química, Universidade de São Paulo, Avenida Professor Lineu Prestes, 748 Butantan, São Paulo 05508-000, Brazil; y.betancourt@usp.br
[2] Immunopathology Laboratory, Butantan Institute, Av. Vital Brasil, 1500 Butantan, São Paulo 05503-900, Brazil; bianca.tavora@butantan.gov.br (B.d.C.L.F.T.); eliana.faquim@butantan.gov.br (E.L.F.-M.)
* Correspondence: amcr@usp.br; Tel.: +55-11-3091-2164

Abstract: Biocompatible lipid polymer nanoparticles (NPs) previously used as antimicrobial agents are explored here as immuno-adjuvants. Poly (methyl methacrylate) (PMMA)/dioctadecyldimethylammonium bromide (DODAB)/poly (diallyldimethylammonium chloride) (PDDA) nanoparticles (NPs) were prepared by emulsion polymerization of methyl methacrylate (MMA) in the presence of DODAB and PDDA, with azobisisobutyronitrile (AIBN) as the initiator. NPs characterization after dialysis by dynamic light-scattering yielded 225 ± 2 nm hydrodynamic diameter (Dz), 73 ± 1 mV zeta-potential (ζ), and 0.10 ± 0.01 polydispersity (P). Ovalbumin (OVA) adsorption reduced ζ to 45 ± 2 mV. Balb/c mice immunized with NPs/OVA produced enhanced OVA-specific IgG1 and IgG2a, exhibited moderate delayed type hypersensitivity reaction, and enhanced cytokines production (IL-4, IL-10, IL-2, IFN-γ) by cultured spleen cells. There was no cytotoxicity against cultured macrophages and fibroblasts. Advantages of the PMMA/DODAB/PDDA NPs were high biocompatibility, zeta-potential, colloidal stability, and antigen adsorption. Both humoral and cellular antigen-specific immune responses were obtained.

Keywords: biocompatible polymer; cationic lipid; cationic polymer; ovalbumin; hybrid nanoparticles; humoral and cellular immune responses; protein delivery; vaccine adjuvants; cationic nanoparticles toxicity

check for updates

Citation: Pérez-Betancourt, Y.; Távora, B.d.C.L.F.; Faquim-Mauro, E.L.; Carmona-Ribeiro, A.M. Biocompatible Lipid Polymer Cationic Nanoparticles for Antigen Presentation. *Polymers* **2021**, *13*, 185. https://doi.org/10.3390/polym13020185

Received: 4 December 2020
Accepted: 4 January 2021
Published: 7 January 2021

Publisher's Note: MDPI stays neutral with regard to jurisdictional claims in published maps and institutional affiliations.

Copyright: © 2021 by the authors. Licensee MDPI, Basel, Switzerland. This article is an open access article distributed under the terms and conditions of the Creative Commons Attribution (CC BY) license (https://creativecommons.org/licenses/by/4.0/).

1. Introduction

Hybrid and cationic nanomaterials have been much explored in pharmaceutics for drug delivery [1,2], antimicrobial chemotherapy [3], dentistry [4], prosthetics [5], water treatment [6], and combination therapies against multidrug resistant pathogens [7,8]. These nanomaterials can have different shapes and compositions, yielding a variety of NPs and coatings.

The search for cationic NPs with potential as adjuvants for vaccines yielded many examples of polymer lipid [9–17], silica/cationic lipid [18,19], cationic polymer [20–22], gold/cationic polymer NPs [23], and iron-oxide/cationic polymer/antigen NPs [24]. Among the most important requirements of adjuvants for vaccines are biocompatibility and nanometric size [25].

Emulsion polymerization of methyl methacrylate (MMA), producing poly (methyl methacrylate) (PMMA), is well described in the literature [26]. In the presence of dioctadecyldimethylammonium bromide (DODAB) and poly (diallyl dimethylammonium) bromide (PDDA), emulsion polymerization of MMA yielded PMMA/DODAB/PDDA NPs [13,14]. These hybrid, PMMA-based NPs predominantly contained PMMA, a biocompatible polymer [27], displaying absence of cytotoxicity when tiny amounts of cationic components are used, as shown in this work.

Two different modes of interaction between lipids and polymers were previously disclosed: (1) Lipids phase-separating from polymers (low miscibility lipid/polymer); in

this case, bilayer adsorption sometimes took place on the surface of polymer NPs [10,28–30]. (2) Lipids mixing well with the polymer such as DODAB and PMMA [9,11,13,15,31].

DODAB and PDDA in the medium used for MMA emulsion polymerization yielded antimicrobial core–shell cationic PMMA/DODAB/PDDA NPs, where DODAB remained in the PMMA core whereas PDDA surrounded the NPs as a cationic shell at low ionic strength [13,14].

The electrostatic attraction between anionic antigens and cationic nanostructures has been the basis for antigen/adjuvant assemblies, where nanometric size is implied in direct antigen delivery to lymph nodes. This avoids reactions at the injection site caused by the permanence of adjuvant/antigen complexes, allowing rapid antigen delivery to lymph nodes dendritic cells [32,33]. This work emphasizes the importance of cationic, biocompatible, and nano-sized polymeric particles for antigen presentation to the immune system. Here, PMMA/DODAB/PDDA NPs synthesized by emulsion polymerization of MMA, in the presence of PDDA and DODAB, were evaluated as adjuvants in vivo while carrying ovalbumin (OVA) as the model antigen.

2. Materials and Methods

2.1. Materials

MMA, PDDA, azobisisobutyronitrile (AIBN), NaCl, DODAB, chloroform, grade V ovalbumin, peroxidase-labeled streptavidin, and concanavalin A were from Sigma-Aldrich. PDDA molecular weight <100,000 g came as a 35% water solution. OVA stock solution (20 mg/mL) in Milli-Q water was purified by chromatography (polymyxin B columns; Pierce Biotechnology, Rockford, IL, USA), analyzed by the bicinchoninic acid (BCA) assay, and adjusted to 10 mg/mL. $Al(OH)_3$ was from Sanofi-Synthelabo, RJ, Brazil. The NPs syntheses were performed in 1 mM NaCl solution. Milli-Q water was used for preparing all solutions and dispersions. For dialysis, a cellulose acetate bag with molecular weight cut-off around 12,400 g/mol was used. All other reagents were analytical grade and used without further purification.

2.2. Synthesis of NPs by Emulsion Polymerization Method

DODAB differs from surfactants by being a lipid. As such, the process for dispersing DODAB in the aqueous solution used as a reaction mixture requires a first step of preparing a DODAB chloroform solution so that a DODAB film can be obtained at the bottom of the glass assay tube by chloroform vaporization. This film in contact with the water solution will facilitate DODAB dispersion in the reaction mixture.

DODAB chloroform solution (10 mM) added to a glass tube (1.5 mL) was evaporated under nitrogen flux before adding 10 mL of 1 mM NaCl aqueous solution, 1 mL of 50 mg/mL PDDA, 0.20 mL of MMA 1.0 M followed by application of moderate nitrogen flux and AIBN addition (0.0036 g); polymerization occurred preferentially at 70–80 °C/1 h under periodic vortexing at 0.2 M MMA, 1.5 mM DODAB, 5 mg/mL PDDA [13,14]; the reaction mixture was extensively dialyzed until 5 μS/cm of water conductivity. These final concentrations in the reaction mixture were selected after systematic evaluation of the concentrations in the reaction mixture.

2.3. Determining Physical Properties of NPs by Dynamic Light-Scattering (DLS)

Dispersions were diluted 20 times for zeta-average diameter (Dz), zeta-potential (ζ), and polydispersity (P) DLS measurements using a Zeta-Plus Zeta-Potential Analyzer (Brookhaven Instruments Corporation, Holtsville, NY, USA), which was equipped with a 677 nm laser and dynamic light-scattering (DLS) at 90° for particle sizing. From fluctuations of scattered light intensity, the decay times of the fluctuations can be related to the diffusion constants and, therefore, to the sizes of the particles. Small particles moving rapidly cause faster decaying fluctuations than large particles moving slowly. The decay times of these fluctuations are determined in the time domain using a correlator. The fluctuating signal is processed by forming the autocorrelation function which decays exponentially with time

so that the relaxation of the fluctuations is directly related to the decay constant (Γ). The decay constant is given by Equation (1):

$$\Gamma = Dq^2 \quad (1)$$

where q depends on the scattering angle, the wavelength of the laser light, and refractive index of the suspending liquid and D is the translational diffusion coefficient.

Hydrodynamic particle diameter (Dz) is inversely related to D by the Stokes–Einstein Equation (2):

$$Dz = kT/(3\pi\eta D) \quad (2)$$

where k is the Boltzmann's constant, T is temperature in Kelvin, η is the viscosity of the suspending liquid, and D is the diffusion coefficient. Mean diameters were obtained by fitting data to log-normal size distributions that do not discriminate between one, two, or more different populations and always consider all scattering particles as belonging to one single Gaussian population. For the size distribution data, fitting was performed by the apparatus software using the non-negatively constrained least-squares (NNLS) algorithm, which is a model-independent technique allowing multimodal distributions to be achieved [34].

In order to define a relative width of size distributions, the polydispersity P is given by Equation (3):

$$P = \mu_2\Gamma^2 \quad (3)$$

where μ_2 is proportional to the variance of the "intensity" weighted diffusion coefficient distribution and carries information on the width of the size distribution. Polydispersity (P) has no units. It is close to zero (0.000 to 0.020) for monodisperse or nearly monodisperse samples, small (0.020 to 0.080) for narrow distributions, and larger for broader distributions. ζ was determined from electrophoretic mobility (μ) in 1 mM NaCl and the Smoluchowski equation (Equation (4)):

$$\zeta = \mu\eta/\varepsilon \quad (4)$$

where η is the medium viscosity and ε the medium dielectric constant.

2.4. Determining Solids Content, PDDA, and DODAB Concentration in NPs

Solids content (mg/mL) was obtained from lyophilizing and weighing 1 mL NPs dispersions. [PDDA] in NPs ($[PDDA]_p$) was obtained by subtracting free [PDDA] from added [PDDA]. Centrifuging dispersions (1 h/10,000 rpm) and pelleting NPs allowed the determination of [PDDA] in the supernatant from conductance, since [PDDA] and conductance displayed a linear relationship. During dialysis, PDDA attracted water by osmosis; increased volume after dialysis required measuring final volume after dialysis for precise calculations of final concentrations.

[DODAB] in NPs $[DODAB]_p$ was obtained from 1 mL dialyzed dispersion after centrifuging (1 h/10,000 rpm), supernatant withdrawing, and halide microtitration [35] in the supernatant containing Br^- and Cl^- from DODAB and PDDA, respectively. Subtracting supernatant [PDDA] (previously determined by conductimetry) from [halides] yielded the supernatant [DODAB] required for determining $[DODAB]_p$.

2.5. Determining NaCl Concentration Effect on NPs Dz

The core/shell NPs structure was determined as previously described [12,13]. Dialyzed NPs were centrifuged, the supernatant was removed, and the pellet was resuspended in pure water before 1:40 dilution in aqueous NaCl solutions (1–75 mM NaCl) and 30 min interaction for determining Dz by DLS. The core diameter was the minimal Dz (Dz_{min}) at collapse of the PDDA shell (salt screened PDDA charges); shell thickness was Dz_0–Dz_{min}, where Dz_0 is Dz in pure water.

2.6. Evaluation of NPs/OVA Interaction

The dialyzed and treated NPs contained 7.0, 0.32, and 0.7 mg/mL PMMA, DODAB, and PDDA, respectively; NPs (0.071 mL; 0.05 mg/mL PDDA) interacted 1 h with OVA stock solution over a [OVA] range before DLS measurements or [OVA] determination in the supernatants [36]. Adsorbed [OVA] was obtained from added minus free [OVA].

2.7. Determination of NPs Cytotoxicity by MTT Assay

L929 fibroblast and J774A.1 macrophage from American Type Culture Collection were cultured according to standard protocols (90% humidity, 5% CO_2, 37 °C), RPMI-1640/5% fetal bovine serum (FBS), 1 unit/mL penicillin-streptomycin, and 2 mM L-glutamine. NPs diluted in the same medium (0.1 mL) interacted with plated cells (10,000 cells/well; 12 h incubation) after withdrawing 0.1 mL of culture medium for incubation in a humidified CO_2 incubator for 3 and 24 h before determining the in vitro NPs' cytotoxicity using 3-(4,5-dimethylthiazol-2-yl)-2,5-diphenyl tetrazolium bromide (MTT). MTT (5 mg/mL in PBS) was filtered for sterilization and removal of insoluble residues before adding 10 µL of MTT solution per well containing 100 µL of the cells and NPs at different NPs concentrations. After incubation (37 °C/2 h), supernatant withdrawing, and mixing of adhered cells with 100 µL isopropanol solution in 0.04 N HCl, absorbance at 570 nm was determined on an ELISA reader; 100 % cell viability was given by cells in culture medium only.

2.8. Immunization Protocol

Four groups of five BALB/c male mice each were injected subcutaneously at two sites on the base of the tail with 0.2 mL/animal. Solutions or dispersions used for injection were: (1) pure water; (2) 0.1 mg/mL OVA; (3) 0.1 mg/mL OVA/0.1 mg/mL $Al(OH)_3$; (4) 0.1 mg/mL OVA in NPs with 0.52, 0.05, and 0.04 mg/mL of PMMA, PDDA, and DODAB, respectively. A booster (same dose/21 days post immunization) was injected. Guidelines for experiments with animals were from Instituto Butantan's Committee of Ethics on Animal Research (protocol 7912280219).

2.9. Determining OVA-Specific IgG1 and IgG2a

Blood from mice was collected from the ophthalmic plexus 14, 21, and 28 days after immunization yielded serum which was individually analyzed by the indirect enzyme-linked immunosorbent assay (ELISA); 96-well microtiter plates (Costar Corning Inc., Cambridge, MA, USA) were coated overnight at 4 °C with 100 µL 10 µg/mL OVA solution in 0.01 M phosphate buffer saline, pH 7.2. The wells were blocked (3% gelatin/PBS/2 h), incubated with serially diluted serum (1 h/37 °C), added of 100 µL goat anti-mouse biotin-conjugated IgG (1:1000) or IgG2a (1:500) (Southern Biotechnology Associates, AL, USA), and incubated (1 h/37 °C) again before adding peroxidase-labeled streptavidin (100 µL/1:3000 dilution) for 1 h incubation (at 37 °C), washing three times after each incubation step with PBS/0.05% Tween 20. Finally, 100 µL 1 mg/mL OPD solution and H_2O_2 (1 µL/mL) in 0.1 M citrate-phosphate (pH 5.0) were added per well for incubation (15 min/room temperature) before stopping the reaction with 0.05 mL 2 M H_2SO_4 per well. Absorbance was determined at 492 nm and results were expressed as mean values ± mean standard deviation. IgG1 and IgG2a primary responses were at 1/512 and 1/8; secondary responses, at 1/32696 and 1/256 dilutions, respectively. Results from different groups were compared using two-way variance analysis (ANOVA) and Tukey's test. p-values < 0.05 were significant. Separate statistics for IgG1 or IgG2a were performed.

2.10. Determining DTH from Footpad Swelling

Mice at day 5 post immunization were injected at the left-hind footpad with OVA, denatured by heating, in saline (2 mg/mL; 0.03 mL; 0.03 mL saline as control). Footpad swelling 24 h thereafter was measured with a micrometer as the difference between left and right footpads' swelling per animal and given as mean values ± mean standard deviation.

2.11. Culturing Spleen Cells for Cytokines Analysis

Two weeks after the second injection, spleen cells from five mice were gathered in RPMI 1640 with 10 mM HEPES, 50 μM 2-mercaptoethanol, 216 mg/L l-glutamine, and 5% FBS. Suspensions (12×10^6 cells/mL) distributed in tissue culture plates were incubated with medium containing 250 μg/mL OVA in a humidified CO_2 incubator for 72 h: medium only or 2.5 μg/mL concanavalin A (con A) were negative and positive controls, respectively. Thereafter, plates were centrifuged (5 min/1500 rpm) and the supernatants were collected for determining IL-2, IL-4, IL-10, and IFN-γ (sandwich ELISA kit; catalog #88-7711-44 Thermo Fisher Scientific). Detection limits were 0.03 (IL-10), 0.002 (IL-2), 0.004 (IL-4), and 0.015 ng/mL (IFN-γ); secretions are expressed as mean for two assays ± mean standard deviation.

3. Results and Discussion

3.1. Synthesis of PMMA/DODAB/PDDA NPs

The synthesis of PMMA NPs in the presence of DODAB or PDDA yielded poor conversion of MMA into PMMA using potassium persulfate as the initiator [11] or PDDA only, as the emulsifier [12]; conversion increased substantially with the AIBN initiator and DODAB/PDDA emulsifiers [13,14]. However, systematic evaluation of the effect of [MMA] or [PDDA] on the conversion or physical properties of the NPs dispersions had not been performed before.

The systematic effect of MMA and PDDA concentrations on yield of PMMA/DODAB/PDDA NPs synthesized using AIBN as the initiator is on Table 1. This table shows solid contents and yield for the synthesis of PMMA/DODAB/PDDA NPs (at 1.5 mM DODAB, 5 mg/mL PDDA, and 0.0036 g AIBN). The increment in MMA concentration increased the solid contents since MMA molecules available for polymerization increased. However, the yield decreased as [MMA] increased, meaning that not all monomers in the reaction mixture polymerized. This behavior differed from the one observed in the synthesis of PMMA/PDDA NPs in the absence of a surfactant. Under these conditions, over the same range of MMA and PDDA concentrations employed in this work, solids content fluctuated between 3.1 and 5.8 mg/mL, in contrast to the higher values achieved in Table 1, namely, 11–36 mg/mL [14]. The use of DODAB as an additional emulsifier in the synthesis of these NPs increased the mass of PMMA synthesized from MMA; this behavior was observed for all the tested MMA concentrations. However, using MMA concentrations above 0.2 M caused the appearance of precipitates during the synthesis. Increasing [MMA] decreased the yield, possibly because DODAB and PDDA concentrations were not enough to stabilize all the MMA droplets in the reaction mixture. During the synthesis of PMMA/PDDA NPs under the same conditions but in the absence of DODAB, the maximum yield was 25% at 0.05 M MMA, showing the essential role of DODAB as an emulsifier [14].

Table 1. Effect of methyl methacrylate concentration MMA on the solids content (mg/mL) and on the yield of the conversion of MMA into poly (methyl methacrylate) (PMMA). The dispersions of PMMA, dioctadecyl dimethylammonium bromide (DODAB) and polydiallyldimethylammonium bromide (PDDA) as PMMA/DODAB/PDDA nanoparticles (NPs) were synthesized using 1.5 mM of DODAB, 5 mg/mL of PDDA, and 0.0036 g azobisisobutyronitrile (AIBN). The data refer to samples just after synthesis and before dialysis.

[MMA]/M	Solids Content/mg mL^{-1}	Yield/%
0.10	11.0 ± 1.0	100
0.20	14.0 ± 1.0	70
0.30	21.0 ± 1.6	70
0.40	30.0 ± 2.1	75
0.50	31.0 ± 1.6	62
0.56	36.0 ± 2.4	64

The effect of MMA and PDDA concentrations on the physical properties of NPs obtained in the presence of DODAB 1.5 mM was explored to establish the best conditions for synthesizing PMMA/DODAB/PDDA NPs (Figure 1). Increasing MMA concentration increased D_Z (Figure 1a), probably due to increasing the growth in the mass of PMMA in the NPs, which did not affect the zeta-potential (Figure 1c) and slightly increased polydispersity over a range of [MMA] at 5 mg.mL^{-1} PDDA (Figure 1e).

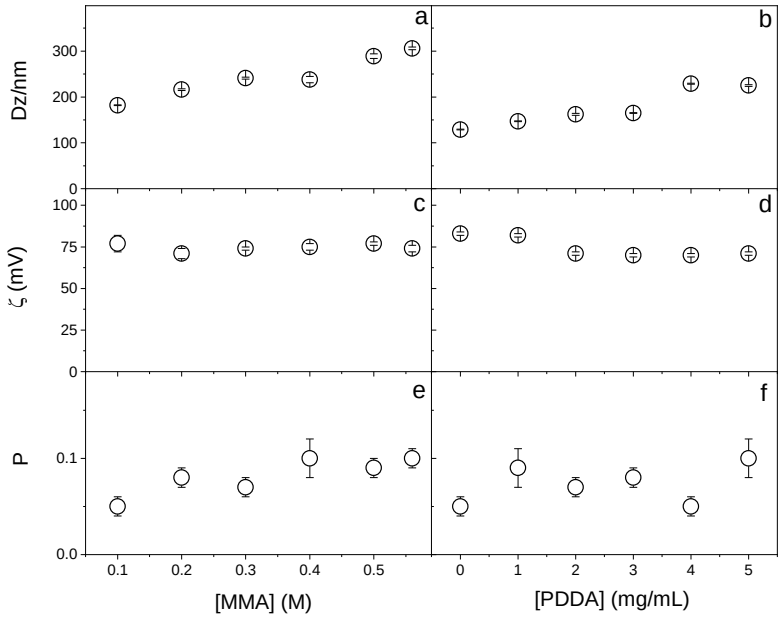


Figure 1. Effect of MMA or PDDA concentrations on (**a**,**b**) hydrodynamic diameter (Dz), (**c**,**d**) zeta-potential (ζ), and (**e**,**f**) polydispersity (P). All dispersions were synthesized by the emulsion polymerization method using 1.5 mM of DODAB and 0.0036 g of AIBN initiator. To evaluate the effect of MMA concentration, the synthesis was performed at 5 mg/mL of PDDA and to evaluate the effect of PDDA, 0.2 M MMA was used. Data points are mean values ± the mean standard deviation.

When increasing the PDDA concentration, Dz increased (Figure 1b) because more PDDA was incorporated into the NPs (as clarified in Figure 2); the zeta-potential remained constant (Figure 1d) and the polydispersity changed from 0.05 at 0 [PDDA] to 0.100 at 5 mg/mL [PDDA] (Figure 1f).

Figure 2 displays the effect of MMA or PDDA concentrations used in the synthesis of PMMA/DODAB/PDDA NPs on the concentration of DODAB and PDDA incorporated in the NPs.

Figure 2a,c show that maximal incorporation of the cationic components was reached from 0.1 M MMA. Figure 2b shows that the incorporation of PDDA increased with [PDDA]. Figure 2d shows that the incorporation of DODAB decreased with [PDDA]. The increment in PDDA concentration leads to an increase in mechanically immobilized PDDA in the NPs and to a simultaneous decrease in immobilized DODAB. The two cationic components, PDDA and DODAB, competed for the PMMA matrix. Increasing the PDDA concentration during NPs synthesis, the incorporated [DODAB] in the PMMA matrix decreased (Figure 2d).

From the data shown in Table 1 and Figures 1 and 2, 0.2 M MMA was selected for the synthesis of NPs to be used as adjuvants. At this concentration, no precipitates occurred and relatively high solids content (14 mg/mL) and yield (70%) were obtained. [PDDA] was selected as 5 mg/mL because this was the lowest concentration where maximal PDDA incorporation occurred.

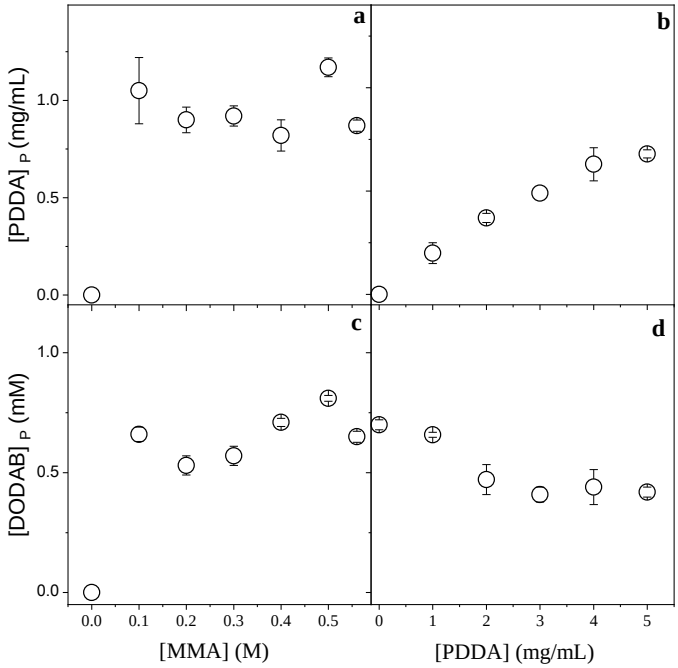


Figure 2. Effect of MMA and PDDA concentrations used in the NPs synthesis on $[PDDA]_P$ (**a**,**b**) and $[DODAB]_P$ in the PMMA/DODAB/PDDA NPs (**c**,**d**). All dispersions were synthesized by the emulsion polymerization method using 1.5 mM of DODAB and 0.0036 g AIBN. The effect of [MMA] on incorporation of the cationic components was performed at 5 mg/mL PDDA, whereas the effect of [PDDA] on incorporation of the cationic components was performed at 0.2 M MMA. These determinations were carried out after dialysis.

3.2. Properties and Cytotoxicity of PMMA/DODAB/PDDA NPs

First of all, PMMA/DODAB/PDDA NPs prepared with the AIBN initiator were treated to eliminate free DODAB and PMMA, assuring antigen adsorption to NPs only; treatment was pelleting dispersions, withdrawing and discarding supernatants, and resuspending the pellet in pure water. Table 2 shows the NPs' properties before and after treatment. Although main NPs' properties were not affected, the treatment reduced the conductance of the dispersion to practically zero due to the removal of free PDDA. PMMA density (1.18 g.cm^{-3}) [37], mean NP volume (5.3×10^{-15} cm^3), and mean mass per NP (6.2×10^{-12} mg) yielded 1.3×10^{12} particles/mL with 7.0 mg/mL PMMA in this stock dispersion and precise knowledge of particle number density, $[PDDA]_P$, and $[DODAB]_P$ (Table 2).

Table 2. Properties and composition of PMMA/DODAB/PDDA NPs: mean hydrodynamic diameter (Dz), zeta-potential (ζ), polydispersity (P), and conductance (G) after dialysis or after removal of free cationic components. Subscript P indicates concentration in NPs; asterisk indicates data for non-treated NPs after dialysis. Concentrations are given in mg mL^{-1}.

Dz/nm	ζ/mV	P	G/μS	$[PMMA]_P$	$[DODAB]_P$	$[PDDA]_P$
225 ± 2 *	70 ± 1 *	0.10 ± 0.02 *	92 ± 3 *			
217 ± 1	73 ± 1	0.12 ± 0.01	4 ± 2	7.0 ± 0.7	0.32 ± 0.03	0.70 ± 0.02

Core–shell dimensions in the NPs were evaluated using a method based on determining Dz as a function of [NaCl] [12]. When PDDA is fully charged (pure water), extended PDDA chains in the outer NP layer yielded the thickest shell. The NaCl screening effect on PDDA charges reduced shell thickness in comparison to the one in pure water. Figure 3 shows that the shell thickness at [NaCl] = 0 is 64 nm. Shell thickness for similar PMMA/PDDA NPs (in absence of DODAB) was 80 nm [12]; here, 64 nm seems consistent with DODAB in

the PMMA core, yielding a thinner PDDA shell due to PDDA electrostatic repulsion by DODAB in the core.

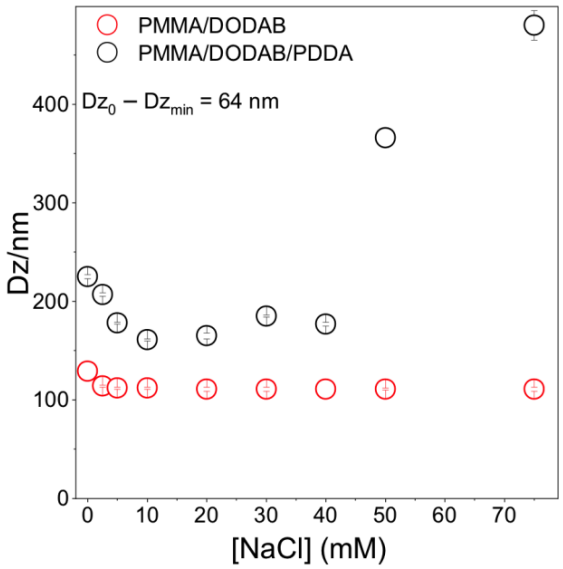


Figure 3. Effect of [NaCl] on PMMA/DODAB/PDDA or PMMA/DODAB NPs Dz. At [NaCl] = 0, Dz_0 =225 ± 2 nm. At 10 mM NaCl, Dz_{min} =161 ± 1 nm yielding 161 ± 1 nm core and 64 nm shell.

For [NaCl] > 40 mM, Dz increased with [NaCl] (Figure 3). Bridging flocculation has been observed for colloids with outer PDDA layers [16,38]. For PMMA/DODAB NPs, no bridging flocculation occurred; Dz was constant with increasing [NaCl] (Figure 3). PMMA/DODAB NPs high colloidal stability was due to embedded DODAB molecules in the PMMA core unaffected by outer NaCl.

At 0.05 mg/mL PDDA in PMMA/DODAB/PDDA NPs, 100% viability was observed against fibroblasts (Figure 2a); 80% viability after 24 h interaction was obtained against macrophages (Figure 4b). Cationic polyelectrolytes usually improve fibroblasts adhesion and proliferation on surfaces [39,40], in good agreement with our data (Figure 4a). Macrophages sensitivity to PDDA was observed for colloids with an outer PDDA layer [41]; at 0.1 mg/mL PDDA, fibroblasts exhibited major holes on cell membranes yielding 25% viability after 3 h interaction [20]. Free PDDA is very cytotoxic, whereas toxicity of immobilized PDDA is much more controllable. Macrophages interacting for 48 h with assemblies of DODAB/carboxymethylcellulose/PDDA containing 0.025 mg/mL PDDA were only 30% viable [41], whereas NPs containing 0.050 mg/mL immobilized PDDA yielded 80% macrophages viability for 24 h of interaction (Figure 4b). Mechanical PDDA immobilization in NPs prevented its complete interaction with the cells, avoiding the cell lysis related to free/penetrating cationic polymer chains. PDDA immobilization improved its biocompatibility by reducing cytotoxicity in comparison to free PDDA. In contrast to fibroblasts, macrophages were more sensitive to the cationic NPs, possibly due to their phagocytic ability. They avidly take up cationic NPs by direct translocation, endocytosis, or other mechanisms [21].

In fact, several pieces of evidence suggested that PDDA dose-dependent cytotoxicity can be reduced upon PDDA immobilization onto NPs. For example, against bacteria and fungus, immobilized PDDA was much less toxic than free PDDA [12]. The dose-dependent cytotoxicity of poly-cations, e.g., poly-lysine, poly-ethylene-imine, and PDDA, evaluated by MTT assay or lactate–dehydrogenase release, yielded 30% viability after 24 h interaction of fibroblasts with 0.1 mg/mL PDDA [42]. When reducing free PDDA dose to 0.01 mg/mL, about 100% fibroblasts remained viable [20,42].

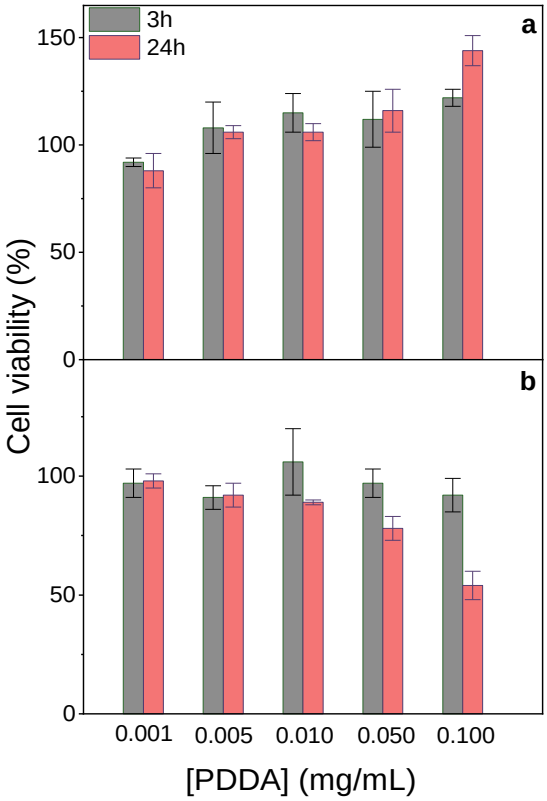


Figure 4. Effect of immobilized PDDA concentration on NPs on L929 fibroblasts (**a**) or J774A.1 macrophages viability (%) after 3 or 24 h interaction (**b**). The stock dispersion contained 0.7 mg/mL immobilized PDDA.

3.3. OVA/NPs Interaction

Figure 5 shows that OVA adsorption increased linearly with the added [OVA] until maximal OVA adsorption at 0.10–0.12 mg/mL OVA from 0.10 mg/mL of added OVA. Above 0.1 mg/mL of added [OVA], adsorption remained constant and equal to 0.1–0.12 mg/mL OVA. The lowest [OVA] added to obtain maximal adsorption was 0.1 mg/mL (Figure 5).

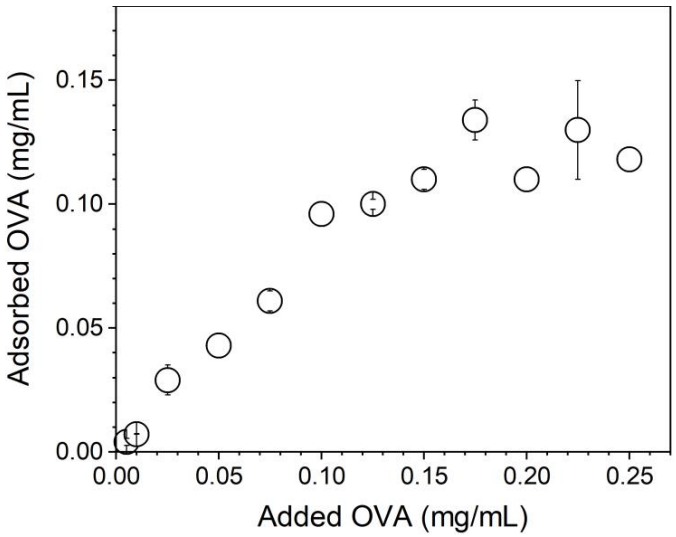


Figure 5. OVA adsorption isotherm onto PMMA/DODAB/PDDA NPs in Milli-Q water.

OVA concentration affected the physical properties of the PMMA/DODAB/PDDA NPs; at [OVA] = 0.17 mg/mL, zeta-potential was zero and NPs/OVA displayed poor colloidal stability with the occurrence of precipitates and poor DLS measurements (Figure 6). Outside this region, a good colloidal stability allowed for reliable DLS measurements. At 0.1 mg/mL OVA, cationic NPs displayed $\zeta = 45 \pm 2$ mV, P = 0.15 ± 0.02, and Dz = 242 ± 4 nm; this concentration of OVA was selected for the evaluation of NPs as adjuvants.

The colloidal stability after the NPs' synthesis and 72h dialysis was evaluated from measurements of the physical properties for the NPs at two time points: 1 and 6 h. For the NPs with OVA, a similar control was conducted revealing no changes in physical properties. All PMMA/DODAB/PDDA/OVA NPs injected in vivo were prepared and used 1 h after preparation.

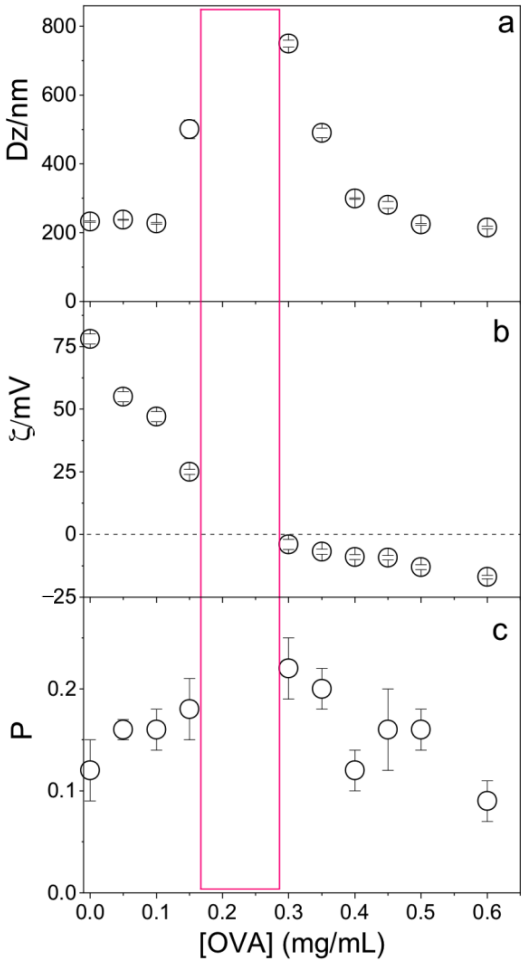


Figure 6. Effect of ovalbumin (OVA) concentration on (**a**) the mean hydrodynamic diameter (Dz), (**b**) zeta-potential (ζ), and (**c**) polydispersity (P) of PMMA/DODAB/PDDA NPs. The red rectangle indicates the zone where the dispersion was not colloidally stable and DLS measurements were not reliable.

The bare NPs (Dz = 217 ± 1 nm) adsorbed OVA, yielding 25 nm of an adsorbed layer (Figure 6). Silica/DODAB dispersions (Dz = 304 ± 2 nm) yielded Dz = 324 ± 8 nm at maximal adsorption with bovine serum albumin (BSA) or 20 nm BSA thickness [19]. It is interesting to compare the relative amount of protein that can be adsorbed onto a supported cationic bilayer and onto a cationic polymer shell surrounding solid NPs. Taking into account the 65.5 kDa (BSA) and 45 kDa molecular weight (OVA), if the same number of molecules had been adsorbed in both cases, at maximal adsorption, one would expect to

find a thicker BSA layer than the OVA layer on each NP. The experimental result yielded a thicker OVA layer than the BSA layer, showing that the number of OVA molecules adsorbed onto the PMMA/DODAB/PDDA NPs was higher than the number of BSA molecules adsorbed onto the silica/DODAB NPs at maximal adsorption for both systems. Possibly, different surfaces of the core–shell and silica/DODAB NPs interacted differently with the proteins. Whereas the former presented to the protein a cationic polymer layer with several protrusions and indentations due to the extended polymer chains, the latter were smooth cationic surfaces as provided by the adsorption of a DODAB cationic bilayer onto each silica NP. The total surface area for adsorption is higher in the former than in the latter cationic surface. The polymer shell was a more efficient rough surface for protein adsorption. Consistently, the maximal adsorption values obtained in both cases show that the adsorbed protein layer is indeed thicker at maximal adsorption for the core–shell NPs than for the silica/DODAB NPs. Adsorption is 2.5× higher on the core–shell than on the silica/DODAB NPs (Figure 5). For the polymer surface upon adding 0.100 mg/mL OVA, maximal adsorption was achieved at 0.100 mg/mL (Figure 5), whereas upon adding 0.050 mg/mL, maximal adsorption was achieved at 0.020 mg/mL [19].

3.4. PMMA/DODAB/PDDA NPs as Adjuvants

The adjuvant activity of NPs/OVA in vivo was evaluated from OVA-specific IgG1 and IgG2a production (Figure 7), the delayed type hypersensitivity (DTH) reaction from footpad swelling in mice (Figure 8), and determination of IL-2, IL-4, IL-10, and IFN-γ production by the spleen cells of the immunized mice in culture (Figure 9).

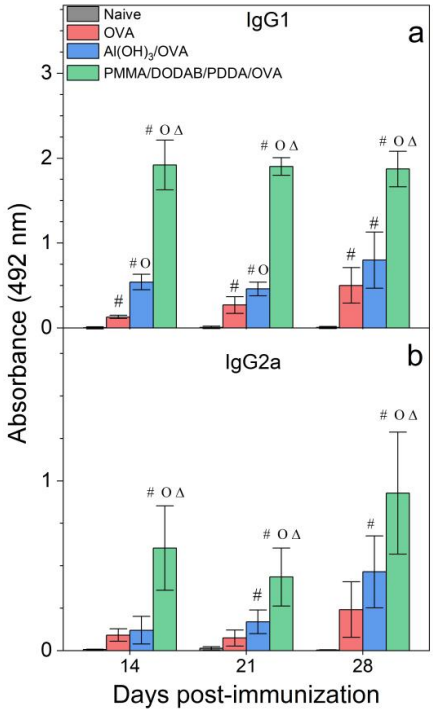


Figure 7. Humoral responses induced by OVA, $Al(OH)_3$/OVA, or PMMA/DODAB/PDDA/OVA NPs. Mean absorbance at 492 nm ± standard deviation related to anti-OVA IgG1 (**a**) and IgG2a (**b**) antibodies production was determined over time after immunization of BALB/c mice from sera collected on days 14 and 21 post immunization (primary response) or on day 28 (secondary response). Primary IgG1 production was determined at 1/512 serum dilution, whereas the secondary one was obtained at 1/32,696 dilution. Primary IgG2a production was determined at 1/8 serum dilution, whereas the secondary one was obtained at 1/256 dilution. $p < 0.05$ compared to the naive group (#), $p < 0.05$ compared to the OVA group (o), $p < 0.05$ compared to the $Al(OH)_3$/OVA group (Δ).

Adjuvants as $Al(OH)_3$ are of choice for implementing the antigen-specific production of IgG1 [43], whereas immune-adjuvants as vesicles or bilayer-fragments of the cationic lipid DODAB (DODAB BF) usually implement the antigen-specific production of IgG2a [17,44–46]. In Figure 7, NPs/OVA revealed their potent activity as inducers of humoral immune response in the production of IgG1, surpassing by about four times the primary response induced with the classical $Al(OH)_3$ adjuvant. The production of IgG2a (Figure 7) and the DTH reaction (Figure 8) followed similar patterns with the NPs, yielding much higher figures than the $Al(OH)_3$ adjuvant, a poor inducer of cellular immune responses [42].

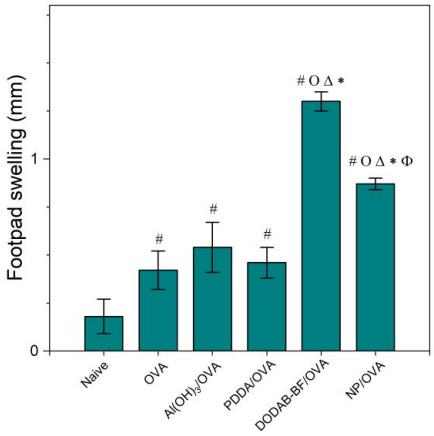


Figure 8. Mean footpad swelling ± standard deviation related to the delayed-type hypersensitivity reaction of BALB/c mice immunized with OVA, $Al(OH)_3$/OVA, PDDA/OVA [20], DODAB-BF/OVA [44], or PMMA/DODAB/PDDA NPs carrying OVA (NP/OVA). $p < 0.05$ compared to the naive group (#), $p < 0.05$ compared to the OVA group (o), $p < 0.05$ compared to the $Al(OH)_3$/OVA group (Δ), $p < 0.05$ compared to the PDDA/OVA group (*), or $p < 0.05$ compared to the DODAB-BF/OVA group (ϕ). The controls for PDDA/OVA and DODAB BF/OVA previously published (naïve, OVA) were very similar to those shown here for NP/OVA.

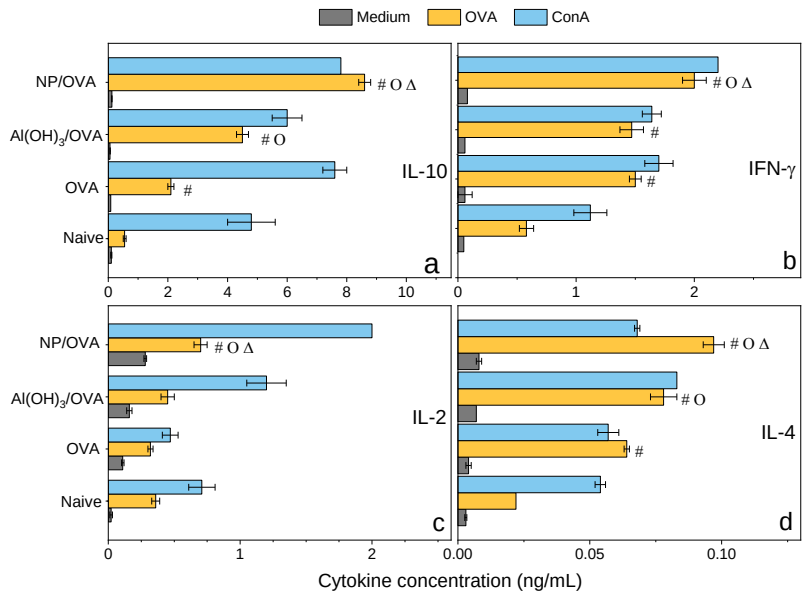


Figure 9. Cytokines profile (ng/mL) from the cultured spleen cells of BALB/c mice, naïve or immunized with OVA, $Al(OH)_3$/OVA, PMMA/DODAB/PDDA/OVA (NP/OVA). $p < 0.05$ compared to the naive group (#), $p < 0.05$ compared to the OVA group (o), $p < 0.05$ compared to the $Al(OH)_3$/OVA group (Δ). (**a**) IL-10, (**b**) IFN-γ, (**c**) IL-2, (**d**) IL-4.

DODAB BF/OVA and PMMA/DODAB/PDDA/OVA yielded a DTH response; $Al(OH)_3$/OVA or PDDA/OVA did not elicit a DTH response as previously reported in reference [20] (Figure 8). The NPs/OVA yielded both humoral and cellular immune responses (Figures 7 and 8).

Three different cationic nanoparticles have their performance as adjuvants compared in Table 3. They were: DODAB BF [44], PDDA/OVA NPs [20], and PMMA/DODAB/PDDA NPs (this work). OVA-specific IgG1 and IgG2 production and footpad swelling (FS) corresponding to the DTH reaction to OVA alone or carried by cationic NPs showed that DODAB BF were the most potent ones to induce DTH and IgG2a. PMMA/DODAB/PDDA NPs represented the most potent adjuvant to induce IgG1 response. The moderate increase in Th-1 response induced by the PMMA/DODAB/PDDA NPs could be explained by an eventual ability of cationic NPs to cross the cytoplasmic membrane by direct translocation, escaping endocytosis. Fluorescent giant vesicles made of phospholipid bilayers interacting with fluorescent cationic amidine polystyrene NPs of 20 nm diameter allowed the visualization of NPs adhesion and permeabilization of the model membrane to polymers of high molecular weight, indicating the formation of transient pores across bilayers and NP translocation [47]. In another study using molecular dynamics simulations, a model cell membrane allowed direct translocation of cationic gold nanoparticles (AuNPs) as well as HIV-1 Tat peptides; thereafter, the membrane resealed itself within a microsecond [48].

The three cationic adjuvants shown in Table 3 may have their adjuvant characteristics understood as the degree to which antigen delivery to the cytoplasm does or does not avoid endocytosis. Which factors would contribute to cytoplasm delivery of the carried antigen? Essentially, major factors would be direct translocation and the antigen/adjuvant strength of binding. The behavior of DODAB BF/OVA may have resulted from direct translocation and release of the antigen in the cytoplasm plus a relatively weak strength of binding between DODAB BF and antigen; this would explain the predominance of the Th-1 response. In contrast, PDDA/OVA behavior yielding predominance of Th-2 response could be explained by a high binding strength between PDDA and OVA in an entangled assembly and/or poor frequency of direct translocation with predominant internalization by endocytosis. The PMMA/DODAB/PDDA NPs would possibly become internalized by both routes (endocytosis and direct translocation) with the occurrence of an intermediate strength of binding between OVA and immobilized PDDA, so that some OVA molecules would be released from the NPs in the cytoplasm; overall, the Th-1 and Th-2 responses would occur for this system (Table 3).

Table 3. Comparison of IgG1 and IgG2a production and footpad swelling (FS) induced by the delayed type hypersensitivity reaction (DTH) to OVA alone or carried by three different cationic nanoparticles NPs: DODAB bilayer fragments (BF) [44], PDDA/OVA NPs [20], and PMMA/DODAB/PDDA NPs (this work). IgG1 and IgG2a production were depicted from absorbance at 492 nm (A492nm) determined at the serum dilutions (in brackets) and days 14 and 21 after immunization.

Assembly	Time/Days	A_{492nm} (IgG1)	A_{492nm} (IgG2a)	FS/mm
OVA	14	0.40 (1/128)	0.10(1/32)	0.3
	21	0.25 (1/128)	0.10(1/32)	
DODAB BF/OVA	14	1.45 (1/128)	0.70(1/32)	1.3
	21	0.80 (1/128)	0.40(1/32)	
PDDA/OVA	14	1.20 (1/256)	0.15(1/8)	0.5
	21	1.50 (1/256)	0.50(1/8)	
NPs/OVA	14	1.90 (1/512)	0.60(1/8)	0.9
	21	1.90 (1/512)	0.50(1/8)	

Confirmation of the mixed Th-1/Th-2 response was obtained by determining the cytokines profile induced in immunized mice 35 days after immunization and evaluated from cultured spleen cells production (Figure 9). At this point in time, one should expect

that too high responses (either Th-1 or Th-2) would have been dampened by the secretion of a regulatory cytokine such as IL-10 so that levels of this molecule would reflect down-regulation of too high Th-1 or Th-2 responses. Indeed, levels of IL-10 were very high and even higher than those elicited by $Al(OH)_3$ (Figure 9). IL-10 is produced by a diversity of cell types, including $CD8^+$, $CD4^+$, regulatory T cells, γδ-T cells, NK cells, NK-T cells, B cells, dendritic cells, eosinophils, mast cells, and monocytic cells; it is a cytokine with several pleiotropic effects in immunoregulation and inflammation [49–51]. IL-10 is an anti-inflammatory cytokine that downregulates the expression of Th-1 and Th-2 cytokines, MHC class II, and co-stimulatory B7-1/B7-2 molecules [49–51]. It maintains the balance of the immune response, allowing the clearance of infection while minimizing damage to the host [49,50]. The consequence of this activity, however, is that IL-10 can contribute to chronic infection [52].

The relatively low levels of IFN-γ and IL-2 determined in the spleen cells of mice immunized with the NPs/OVA at day 35 might reflect the regulatory activity of IL-10, although levels of these cytokines were still higher than those for the other groups (Figure 9).

IFN-γ enhances immune function by promoting the growth of Th-1 cells while inhibiting Th-2 cell growth and enhancing NK cytotoxic activity [49]. Furthermore, IFN-γ induces switching to IgG2a production by B cells and potentiates antigen presentation by activating dendritic cells and inducing MHC class I and class II gene expression on the surface of target cells [49]. IFN-γ is the major activator of macrophages, primarily through the induction of superoxide, nitric oxide production, and natural resistance-associated macrophage protein (NRAMP) gene expression [49,53]. At 6 days after immunization of mice with 18kDa-hsp antigen of *Mycobacterium leprae* presented by DODAB BF, 23 ng/mL IFN-γ and 0.6 ng/mL IL-10 secretions by cultured lymph node cells were determined [17]. In the present work, at day 35 after immunization with NPs/OVA, 2 ng/mL IFN-γ and 9.0 ng/mL IL-10 secretions by cultured lymph node cells were verified (Figure 9). Possibly the regulatory and dampening effect of this large secretion of IL-10 might be responsible for the low level of IFN-γ.

IL-2 is a proliferation factor of T cells [54]; the stimulation of naive $CD4^+$ T cells differentiation into Th-1 and Th-2 lymphocytes was reported [49,55]. IL-2 quantification for NPs/OVA yielded 0.8 ng/mL, about double the value determined for $Al(OH)_3$/OVA, suggesting that the double response induced by NPs/OVA (Th-1 and Th-2 types) required induction by doubled secretion of IL-2 (Figure 9).

Differentiation of naïve $CD4^+$ T cells into Th-2 cells requires signaling through the T cell receptor and an appropriate cytokine environment; IL-4 is critical for Th2 differentiation [49,56]. In our cytokines profile, IL-4 secretion induced by NPs-OVA was 0.1 ng/mL and even higher than the IL-4 secretion induced by $Al(OH)_3$/OVA, 0.07 ng/mL (Figure 9), agreeing with the compared IgG1 response shown for both systems (Figure 7a). The NPs/OVA are indeed better Th-2 inducers than $Al(OH)_3$/OVA. Our results also indicate that the formulation NPs/OVA was a better inductor of OVA-specific Th-1/Th-2 responses when compared with $Al(OH)_3$/OVA or OVA alone.

4. Conclusions

Cationic and biocompatible NPs of PMMA/DODAB/PDDA with Dz = 217 ± 1 nm, ζ = 73 ± 1 mV, and P = 0.12 ± 0.01 were investigated for their adjuvant properties while carrying the model antigen OVA. In addition, this system was compared with other cationic NPs and their immune responses in order to gain further insight into factors that determine Th-1 or Th-2 responses for cationic NPs. Two major factors were pointed out: (1) strength of adjuvant/antigen binding; (2) intracellular traffic with direct translocation across the cell membrane implying Th-1 response. DODAB BF/OVA, as Th-1 immune response inducers, translocated across the membrane to the cytoplasm releasing OVA; PDDA/OVA, as Th-2 inducers, did not release the protein in the cytoplasm requiring internalization by endocytosis; PMMA/DODAB/PDDA/OVA NPs were internalized by both routes, displaying both Th-1 and Th-2 responses. Among the three cationic systems useful as

adjuvants, the highest biocompatibility occurred for the PMMA/DODAB/PDDA NPs, since they were based mostly on PMMA, a biocompatible polymer.

Author Contributions: Conceptualization, A.M.C.-R., E.L.F.-M. and Y.P.-B.; methodology, Y.P.-B., B.d.C.L.F.T., E.L.F.-M. and A.M.C.-R.; validation, A.M.C.-R., E.L.F.-M. and Y.P.-B.; formal analysis, A.M.C.-R., E.L.F.-M. and Y.P.-B.; investigation, Y.P.-B., B.d.C.L.F.T., E.L.F.-M. and A.M.C.-R.; resources, A.M.C.-R. and E.L.F.-M.; data curation, A.M.C.-R.; writing—original draft preparation, A.M.C.-R. and Y.P.-B.; writing—review and editing, A.M.C.-R. and Y.P.-B.; supervision, A.M.C.-R.; project administration, A.M.C.-R.; funding acquisition, A.M.C.-R. and E.L.F.-M. All authors have read and agreed to the published version of the manuscript.

Funding: This work was supported by Conselho Nacional de Desenvolvimento Científico e Tecnológico (CNPq) by grants 302758/2019-4, 302352/2014-7 to A.M.C.-R.; 140091/2019-0 to Y.P.-B.; 312096/2018-6 to E.L.F.-M.) and Fundação de Amparo à Pesquisa do Estado de São Paulo (FAPESP) by grant 2019/17685-2 to A.M.C.-R. Y.P.-B. is the recipient of a CNPq Ph.D. fellowship (140091/2019-0) under A.M.C.-R. supervision for developing the project "Cationic Nanostructures for Vaccines".

Institutional Review Board Statement: The study was conducted according to the guidelines of the Declaration of Helsinki, and approved by the Ethics Committee of Butantan Institute (protocol code 7912280219, date of approval 04/2019).

Informed Consent Statement: Not applicable.

Data Availability Statement: All data available are reported in the article.

Acknowledgments: Y.P.-B. thanks CNPq for awarding a Ph.D. fellowship (140091/2019-0).

Conflicts of Interest: The authors declare no conflict of interest. The funders had no role in the design of the study; in the collection, analyses, or interpretation of data; in the writing of the manuscript, or in the decision to publish the results.

References

1. Date, T.; Nimbalkar, V.; Kamat, J.; Mittal, A.; Mahato, R.I.; Chitkara, D. Lipid-polymer hybrid nanocarriers for delivering cancer therapeutics. *J. Control. Release* **2018**, *271*, 60–73. [CrossRef] [PubMed]
2. Siewert, C.D.; Haas, H.; Cornet, V.; Nogueira, S.S.; Nawroth, T.; Uebbing, L.; Ziller, A.; Al-Gousous, J.; Radulescu, A.; Schroer, M.A.; et al. Hybrid biopolymer and lipid nanoparticles with improved transfection efficacy for mRNA. *Cells* **2020**, *9*, 2034. [CrossRef] [PubMed]
3. Zakharova, L.Y.; Pashirova, T.N.; Doktorovova, S.; Fernandes, A.R.; Sanchez-Lopez, E.; Silva, A.M.; Souto, S.B.; Souto, E.B. Cationic surfactants: Self-assembly, structure-activity correlation and their biological applications. *Int. J. Mol. Sci.* **2019**, *20*, 5534. [CrossRef] [PubMed]
4. Padovani, G.C.; Feitosa, V.P.; Sauro, S.; Tay, F.R.; Durán, G.; Paula, A.J.; Durán, N. Advances in dental materials through nanotechnology: Facts, perspectives and toxicological aspects. *Trends Biotechnol.* **2015**, *33*, 621–636. [CrossRef] [PubMed]
5. Ramasamy, M.; Lee, J. Recent nanotechnology approaches for prevention and treatment of biofilm-associated infections on medical devices. *BioMed Res. Int.* **2016**, *2016*, 1851242. [CrossRef] [PubMed]
6. Lu, F.; Astruc, D. Nanomaterials for removal of toxic elements from water. *Coord. Chem. Rev.* **2018**, *356*, 147–164. [CrossRef]
7. de Melo Carrasco, L.D.; Sampaio, J.L.M.; Carmona-Ribeiro, A.M. Supramolecular cationic assemblies against multidrug-resistant microorganisms: Activity and mechanism of action. *Int. J. Mol. Sci.* **2015**, *16*, 6337–6352. [CrossRef]
8. Mulani, M.S.; Kamble, E.E.; Kumkar, S.N.; Tawre, M.S.; Pardesi, K.R. Emerging strategies to combat ESKAPE pathogens in the era of antimicrobial resistance: A review. *Front. Microbiol.* **2019**, *10*, 539. [CrossRef] [PubMed]
9. Pereira, E.M.A.; Kosaka, P.M.; Rosa, H.; Vieira, D.B.; Kawano, Y.; Petri, D.F.S.; Carmona-Ribeiro, A.M. Hybrid materials from intermolecular associations between cationic lipid and polymers. *J. Phys. Chem. B* **2008**, *112*, 9301–9310. [CrossRef]
10. Lincopan, N.; Espindola, N.M.; Vaz, A.J.; Carmona-Ribeiro, A.M. Cationic supported lipid bilayers for antigen presentation. *Int. J. Pharm.* **2007**, *340*, 216–222. [CrossRef]
11. Naves, A.F.; Palombo, R.R.; Carrasco, L.D.M.; Carmona-Ribeiro, A.M. Antimicrobial particles from emulsion polymerization of methyl methacrylate in the presence of quaternary ammonium surfactants. *Langmuir* **2013**, *29*, 9677–9684. [CrossRef] [PubMed]
12. Sanches, L.M.; Petri, D.F.S.; de Melo Carrasco, L.D.; Carmona-Ribeiro, A.M. The antimicrobial activity of free and immobilized poly (diallyldimethylammonium) chloride in nanoparticles of poly (methylmethacrylate). *J. Nanobiotechnol.* **2015**, *13*, 58. [CrossRef] [PubMed]
13. Ribeiro, R.T.; Galvão, C.N.; Betancourt, Y.P.; Mathiazzi, B.I.; Carmona-Ribeiro, A.M. Microbicidal dispersions and coatings from hybrid nanoparticles of poly (methyl methacrylate), poly (diallyl dimethyl ammonium) chloride, lipids, and surfactants. *Int. J. Mol. Sci.* **2019**, *20*, 6150. [CrossRef] [PubMed]

14. Galvão, C.N.; Sanches, L.M.; Mathiazzi, B.I.; Ribeiro, R.T.; Petri, D.F.S.; Carmona-Ribeiro, A.M. Antimicrobial coatings from hybrid nanoparticles of biocompatible and antimicrobial polymers. *Int. J. Mol. Sci.* **2018**, *19*, 2965. [CrossRef] [PubMed]
15. Mathiazzi, B.I.; Carmona-Ribeiro, A.M. Hybrid nanoparticles of poly (methyl methacrylate) and antimicrobial quaternary ammonium surfactants. *Pharmaceutics* **2020**, *12*, 340. [CrossRef] [PubMed]
16. Melo, L.D.; Mamizuka, E.M.; Carmona-Ribeiro, A.M. Antimicrobial particles from cationic lipid and polyelectrolytes. *Langmuir* **2010**, *26*, 12300–12306. [CrossRef] [PubMed]
17. Lincopan, N.; Espindola, N.M.; Vaz, A.J.; da Costa, M.H.B.; Faquim-Mauro, E.; Carmona-Ribeiro, A.M. Novel immunoadjuvants based on cationic lipid: Preparation, characterization and activity in vivo. *Vaccine* **2009**, *27*, 5760–5771. [CrossRef] [PubMed]
18. Wei, X.-Q.; Zhang, W.-J.; Lai, L.; Mei, P.; Wu, L.-M.; Wang, Y.-Q. Different cationic surfactants-modified silica nanoparticles for Pickering emulsions. *J. Mol. Liq.* **2019**, *291*, 111341. [CrossRef]
19. Lincopan, N.; Santana, M.R.; Faquim-Mauro, E.; da Costa, M.H.B.; Carmona-Ribeiro, A.M. Silica-based cationic bilayers as immunoadjuvants. *BMC Biotechnol.* **2009**, *9*, 5. [CrossRef]
20. Pérez-Betancourt, Y.; Távora, B.C.L.F.; Colombini, M.; Faquim-Mauro, E.L.; Carmona-Ribeiro, A.M. Simple nanoparticles from the assembly of cationic polymer and antigen as immunoadjuvants. *Vaccines* **2020**, *8*, 105. [CrossRef]
21. Carmona-Ribeiro, A.M.; Pérez-Betancourt, Y. Cationic nanostructures for vaccines design. *Biomimetics* **2020**, *5*, 32. [CrossRef] [PubMed]
22. Lim, J.-W.; Na, W.; Kim, H.-O.; Yeom, M.; Park, G.; Kang, A.; Chun, H.; Park, C.; Oh, S.; Le, V.P.; et al. Cationic poly(amino acid) vaccine adjuvant for promoting both cell-mediated and humoral immunity against influenza virus. *Adv. Healthc. Mater.* **2019**, *8*, 1800953. [CrossRef] [PubMed]
23. Xu, L.; Liu, Y.; Chen, Z.; Li, W.; Liu, Y.; Wang, L.; Liu, Y.; Wu, X.; Ji, Y.; Zhao, Y.; et al. Surface-engineered gold nanorods: Promising DNA vaccine adjuvant for HIV-1 treatment. *Nano Lett.* **2012**, *12*, 2003–2012. [CrossRef] [PubMed]
24. Nawwab Al-Deen, F.M.; Selomulya, C.; Kong, Y.Y.; Xiang, S.D.; Ma, C.; Coppel, R.L.; Plebanski, M. Design of magnetic polyplexes taken up efficiently by dendritic cell for enhanced DNA vaccine delivery. *Gene Ther.* **2014**, *21*, 212–218. [CrossRef] [PubMed]
25. Wilson, K.L.; Howard, G.P.; Coatsworth, H.; Dinglasan, R.R.; Mao, H.-Q.; Plebanski, M. Biodegradable PLGA-b-PEG nanoparticles induce T helper 2 (Th2) immune responses and sustained antibody titers via TLR9 stimulation. *Vaccines* **2020**, *8*, 261. [CrossRef] [PubMed]
26. Gan, L.M.; Chew, C.H.; Ng, S.C.; Loh, S.E. Polymerization of methyl methacrylate in ternary systems: Emulsion and microemulsion. *Langmuir* **1993**, *9*, 2799–2803. [CrossRef]
27. Patra, C.N.; Priya, R.; Swain, S.; Jena, G.K.; Panigrahi, K.C.; Ghose, D. Pharmaceutical significance of Eudragit: A review. *Future J. Pharm. Sci.* **2017**, *3*, 33–45. [CrossRef]
28. Carmona-Ribeiro, A.M.; Midmore, B.R. Synthetic bilayer adsorption onto polystyrene microspheres. *Langmuir* **1992**, *8*, 801–806. [CrossRef]
29. Carmona-Ribeiro, A.M.; de Moraes Lessa, M. Interactions between bilayer membranes and latex. *Colloids Surf. A Physicochem. Eng. Asp.* **1999**, *153*, 355–361. [CrossRef]
30. Carmona-Ribeiro, A.M. Biomimetic nanomaterials from the assembly of polymers, lipids, and surfactants. In *Surfactants and Detergents*; Dutta, A.K., Ed.; IntechOpen: Rijeka, Croatia, 2019; pp. 1–16. ISBN 978-1-78984-661-4.
31. Melo, L.D.; Palombo, R.R.; Petri, D.F.S.; Bruns, M.; Pereira, E.M.A.; Carmona-Ribeiro, A.M. Structure-activity relationship for quaternary ammonium compounds hybridized with poly(methyl methacrylate). *ACS Appl. Mater. Interfaces* **2011**, *3*, 1933–1939. [CrossRef]
32. Manolova, V.; Flace, A.; Bauer, M.; Schwarz, K.; Saudan, P.; Bachmann, M.F. Nanoparticles target distinct dendritic cell populations according to their size. *Eur. J. Immunol.* **2008**, *38*, 1404–1413. [CrossRef] [PubMed]
33. Fifis, T.; Gamvrellis, A.; Crimeen-Irwin, B.; Pietersz, G.A.; Li, J.; Mottram, P.L.; McKenzie, I.F.C.; Plebanski, M. Size-dependent immunogenicity: Therapeutic and protective properties of nano-vaccines against tumors. *J. Immunol.* **2004**, *173*, 3148–3154. [CrossRef] [PubMed]
34. Grabowski, E.; Morrison, I. Particle Size Distribution from Analysis of Quasi-elastic Light Scattering Data. In *Measurement of Suspended Particles by Quasi-Elastic Light Scattering*; Dahneke, B., Ed.; Wiley-Interscience: New York, NY, USA, 1983; pp. 199–236.
35. Schales, O.; Schales, S.S. A simple and accurate method for the determination of chloride in biological fluids. *J. Biol. Chem* **1941**, *140*, 879–882. [CrossRef]
36. Walker, J.M. The bicinchoninic acid (BCA) assay for protein quantitation. *Methods Mol. Biol.* **1994**, *32*, 5–8. [CrossRef] [PubMed]
37. Van der Lee, A.; Hamon, L.; Holl, Y.; Grohens, Y. Density profiles in thin PMMA supported films investigated by X-ray reflectometry. *Langmuir* **2001**, *17*, 7664–7669. [CrossRef]
38. Stuart, M.A.C. Adsorbed polymers in colloidal systems: From statics to dynamics. *Polym. J.* **1991**, *23*, 669–682. [CrossRef]
39. Dubas, S.T.; Kittitheeranun, P.; Rangkupan, R.; Sanchavanakit, N.; Potiyaraj, P. Coating of polyelectrolyte multilayer thin films on nanofibrous scaffolds to improve cell adhesion. *J. Appl. Polym. Sci.* **2009**, *114*, 1574–1579. [CrossRef]
40. Behera, S.S.; Das, U.; Kumar, A.; Bissoyi, A.; Singh, A.K. Chitosan/TiO_2 composite membrane improves proliferation and survival of L929 fibroblast cells: Application in wound dressing and skin regeneration. *Int. J. Biol. Macromol.* **2017**, *98*, 329–340. [CrossRef]
41. Carrasco, L.D.; Santos, H.C.; Sampaio, J.L.; Carmona-Ribeiro, A.M. Self-assembled antibiotic nanoparticles against intracellular bacteria. *Drug Deliv. Lett.* **2017**, *7*, 39–47.

42. Fischer, D.; Li, Y.; Ahlemeyer, B.; Krieglstein, J.; Kissel, T. In vitro cytotoxicity testing of polycations: Influence of polymer structure on cell viability and hemolysis. *Biomaterials* **2003**, *24*, 1121–1131. [CrossRef]
43. Lindblad, E.B. Aluminium adjuvants—In retrospect and prospect. *Vaccine* **2004**, *22*, 3658–3668. [CrossRef] [PubMed]
44. Rozenfeld, J.H.K.; Silva, S.R.; Raneia, P.A.; Faquim-Mauro, E.; Carmona-Ribeiro, A.M. Stable assemblies of cationic bilayer fragments and CpG oligonucleotide with enhanced immunoadjuvant activity in vivo. *J. Control. Release* **2012**, *160*, 367–373. [CrossRef] [PubMed]
45. Carmona-Ribeiro, A.M. Cationic nanostructures for vaccines. In *Immune Response Activation*; Duc, G.H.T., Ed.; IntechOpen: Rijeka, Croatia, 2014; pp. 1–45; ISBN 978-953-51-1374-4.
46. Carmona-Ribeiro, A.M. Nanomaterials based on lipids for vaccine development. In *Micro and Nano Technologies*; Skwarczynski, M., Toth, I.B.T.-M., Eds.; Elsevier: Oxford, UK, 2017; pp. 241–257; ISBN 978-0-323-39981-4.
47. Li, S.; Malmstadt, N. Deformation and poration of lipid bilayer membranes by cationic nanoparticles. *Soft Matter* **2013**, *9*, 4969–4976. [CrossRef]
48. Lin, J.; Alexander-Katz, A. Cell membranes open "doors" for cationic nanoparticles/Biomolecules: Insights into uptake kinetics. *ACS Nano* **2013**, *7*, 10799–10808. [CrossRef] [PubMed]
49. Abbas, A.K.; Lichtman, A.H.; Pillai, S. *Cellular and Molecular Immunology*, 9th ed.; Elsevier Ltd.: Philadelphia, PA, USA, 2018; ISBN 9780323479783.
50. Kubo, T.; Morita, H.; Sugita, K.; Akdis, C.A. Introduction to mechanisms of allergic diseases. In *Middleton's Allergy Essentials*; O'Hehir, R.E., Holgate, S.T., Sheikh, A.B.T.-M.A.E., Eds.; Elsevier: Amsterdam, The Netherlands, 2017; pp. 1–27; ISBN 978-0-323-37579-5.
51. Couper, K.N.; Blount, D.G.; Riley, E.M. IL-10: The master regulator of immunity to infection. *J. Immunol.* **2008**, *180*, 5771–5777. [CrossRef] [PubMed]
52. Rojas, J.M.; Avia, M.; Martín, V.; Sevilla, N. IL-10: A multifunctional cytokine in viral infections. *J. Immunol. Res.* **2017**, *2017*, 6104054. [CrossRef]
53. Fritsche, G.; Dlaska, M.; Barton, H.; Theurl, I.; Garimorth, K.; Weiss, G. Nramp1 functionality increases inducible nitric oxide synthase transcription via stimulation of IFN regulatory factor 1 expression. *J. Immunol.* **2003**, *171*, 1994–1998. [CrossRef] [PubMed]
54. Taniguchi, T.; Minami, Y. The IL-2/IL-2 receptor system: A current overview. *Cell* **1993**, *73*, 5–8. [CrossRef]
55. Cote-Sierra, J.; Foucras, G.; Guo, L.; Chiodetti, L.; Young, H.A.; Hu-Li, J.; Zhu, J.; Paul, W.E. Interleukin 2 plays a central role in Th2 differentiation. *Proc. Natl. Acad. Sci. USA* **2004**, *101*, 3880–3885. [CrossRef]
56. Zhu, J. T helper 2 (Th2) cell differentiation, type 2 innate lymphoid cell (ILC2) development and regulation of interleukin-4 (IL-4) and IL-13 production. *Cytokine* **2015**, *75*, 14–24. [CrossRef]

6 | Cationic biocompatible polymer/lipid nanoparticles as immunoadjuvants

pharmaceutics

Article

Cationic and Biocompatible Polymer/Lipid Nanoparticles as Immunoadjuvants

Yunys Pérez-Betancourt [1], Péricles Marques Araujo [1], Bianca de Carvalho Lins Fernandes Távora [2,3], Daniele Rodrigues Pereira [2,3], Eliana Lima Faquim-Mauro [2,3] and Ana Maria Carmona-Ribeiro [1,*]

[1] Biocolloids Laboratory, Departamento de Bioquímica, Instituto de Química, Universidade de São Paulo, Avenida Professor Lineu Prestes, 748 Butantan, São Paulo 05508-000, Brazil; y.betancourt@usp.br (Y.P.-B.); periclesaraujo@usp.br (P.M.A.)
[2] Immunopathology Laboratory, Butantan Institute, Avenida Vital Brasil, 1500 Butantan, São Paulo 05503-900, Brazil; bianca.tavora@butantan.gov.br (B.d.C.L.F.T.); rodriguesdaniele663@gmail.com (D.R.P.); eliana.faquim@butantan.gov.br (E.L.F.-M.)
[3] Departamento de Imunologia, Instituto de Ciências Biomédicas, Universidade de São Paulo, Avenida Professor Lineu Prestes, 1730 Butantan, São Paulo 05508-000, Brazil
* Correspondence: amcr@usp.br

Abstract: Nanostructures have been of paramount importance for developing immunoadjuvants. They must be cationic and non-cytotoxic, easily assembling with usually oppositely charged antigens such as proteins, haptens or nucleic acids for use in vaccines. We obtained optimal hybrid nanoparticles (NPs) from the biocompatible polymer poly(methyl methacrylate) (PMMA) and the cationic lipid dioctadecyl dimethyl ammonium bromide (DODAB) by emulsion polymerization of methyl methacrylate (MMA) in the presence of DODAB. NPs adsorbed ovalbumin (OVA) as a model antigen and we determined their adjuvant properties. Interestingly, they elicited high double immune responses of the cellular and humoral types overcoming the poor biocompatibility of DODAB-based adjuvants of the bilayer type. The results suggested that the novel adjuvant would be possibly of use in a variety of vaccines.

Keywords: biocompatible polymer; cationic lipid; poly(methyl methacrylate); dioctadecyl dimethyl ammonium bromide; hybrid nanoparticles; ovalbumin; dynamic light scattering; nanoparticles cytotoxicity; delayed type hypersensitivity; cytokines profile

check for updates

Citation: Pérez-Betancourt, Y.; Araujo, P.M.; Távora, B.d.C.L.F.; Pereira, D.R.; Faquim-Mauro, E.L.; Carmona-Ribeiro, A.M. Cationic and Biocompatible Polymer/Lipid Nanoparticles as Immunoadjuvants. *Pharmaceutics* **2021**, *13*, 1859. https://doi.org/10.3390/pharmaceutics13111859

Academic Editors: Imran Saleem and Kan Kaneko

Received: 27 September 2021
Accepted: 3 November 2021
Published: 4 November 2021

Publisher's Note: MDPI stays neutral with regard to jurisdictional claims in published maps and institutional affiliations.

Copyright: © 2021 by the authors. Licensee MDPI, Basel, Switzerland. This article is an open access article distributed under the terms and conditions of the Creative Commons Attribution (CC BY) license (https://creativecommons.org/licenses/by/4.0/).

1. Introduction

In vaccine design, cationic nanostructures are very important as adjuvants for carrying antigens. Their nanometric size avoids retention by physiological barriers at the site of injection allowing them to reach lymph nodes and dendritic cells more easily [1–6]. They can be obtained from a variety of lipids, polymers or lipids and polymers, mostly as bilayer vesicles [7,8], open bilayer disks [9–13], lipid nanoparticles [14] or hybrid nanoparticles [15–21].

In particular, the cationic and synthetic lipid dioctadecyl dimethyl ammonium bromide (DODAB) self-assembles both as closed and large bilayer vesicles [8,22] or as open and cationic bilayer fragments or nanodisks (DODAB BF) with sizes below 100 nm that fuse upon relaxation of the surface potential due to the addition of monovalent salt [23]. DODAB bilayers can combine with a broad variety of antigens or enhancers of the immune response, such as proteins [7,10,24,25], peptides [18,26,27], oligonucleotides [11,28], mononucleotides [29,30] or nucleic acids [31,32], driving an enhanced cell-mediated immune response, but a poor humoral response in several instances [7,10,11,15].

The versatile character of the DODAB molecules and their assemblies directed our research to characterize the many DODAB interactions with oppositely charged particles such as polystyrene sulfate latexes [15,18,33–35] or silica [36–39]. This basic knowledge led to the optimized deposition of supported DODAB bilayers on polystyrene sulfate (PSS)

nanoparticles [15,18,35] or silica [38,39] as suitable immunoadjuvants and antigen carriers. The preparation and characterization of PSS/DODAB NPs, where a single DODAB bilayer surrounds each PSS NP was described [18].

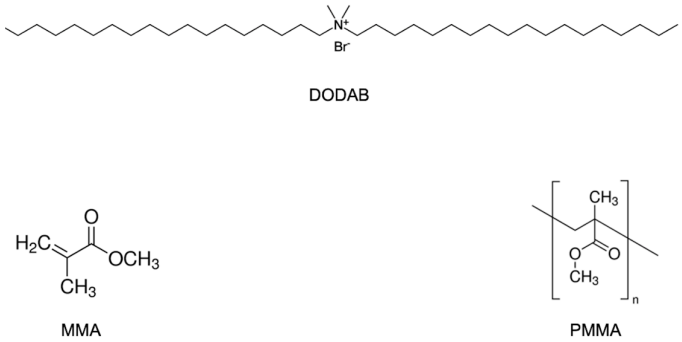
The good miscibility of DODAB with the biocompatible polymer poly(methylmethacrylate) (PMMA) [16,40] motivated the preparation of hybrid PMMA/DODAB NPs by emulsion polymerization of methylmethacrylate (MMA) in the presence of DODAB. These hybrid, cationic and nanometric PMMA/DODAB NPs were described previously [19]. Here we test the application of these PMMA/DODAB NPs as immuno-adjuvants carrying ovalbumin (OVA) as a model antigen. The advantages of the PMMA/DODAB NPs were biocompatibility, high affinity for oppositely charged antigens and induction of a mixed Th2/Th1 immune response.

2. Materials and Methods

2.1. Materials

MMA, azobisisobutyronitrile (AIBN), NaCl, DODAB, chloroform, grade V ovalbumin, ortho-phenilenediamine dihydrochloride (OPD), peroxidase—labeled streptavidin, and concanavalin A—were purchased from Sigma-Aldrich (Saint Louis, MO, USA). OVA stock solution was prepared in Milli-Q water at 15 mg/mL and was purified by chromatography (polymyxin B columns; Pierce Biotechnology, Rockford, IL, USA), analyzed by the bicinchoninic acid (BCA) assay, and adjusted to 10 mg/mL. $Al(OH)_3$ as adjuvant was purchased from Sanofi—Synthelabo, RJ, Brazil. Cellulose acetate membranes (12,400 g/mol molecular weight cut off) were used for dialyzing the nanoparticles dispersions. Analytical grade reagents were used throughout without purification.

The chemical structures for MMA, DODAB and PMMA are presented in Scheme 1.



Scheme 1. Chemical structures of dimethyl dioctadecyl ammonium bromide (DODAB), methyl methacrylate (MMA) and polymethyl methacrylate (PMMA).

2.2. Spreading of DODAB Films, Preparation of DODAB Bilayer Fragments (DODAB BF) and Synthesis of PMMA/DODAB NPs

Two different DODAB dispersions in water solution were prepared: (1) dispersions from DODAB films [27,41]; (2) DODAB bilayer fragments (BF) [8,9,42]. DODAB films on the bottom of glass tubes were obtained from a 10 mM DODAB solution in chloroform submitted to evaporation under nitrogen flow. For preparing DODAB BF, DODAB powder was sonicated for 15 min in 1 mM NaCl water solution using a macroprobe (85 W) and then centrifuged for pelleting titanium ejected from the tip (9300× *g*/1 h/4 °C).

The synthesis of PMMA/DODAB NPs was carried out by polymerizing MMA (emulsion polymerization) in the presence of DODAB and AIBN initiator [16,19,43]. In the tubes containing the dry DODAB films or DODAB bilayer fragments (BF), MMA (0.1 to 0.56 M), 0.036 g AIBN and 1 mM NaCl solution were added to a final volume of 10 mL and placed in a water bath at 70–80 °C for 1 h with periodic vortexing before exhaustive dialysis for eliminating unreacted monomer (4 L water, 6 times change, 72 h/Milli-Q water).

2.3. Determining Physical Properties of NPs by Dynamic Light-Scattering (DLS)

Dispersions were diluted 20 times for zeta-average diameter (Dz), zeta-potential (ζ) and polydispersity (P) DLS measurements using a Zeta-Plus Zeta-Potential Analyzer (Brookhaven Instruments Corporation, Holtsville, NY, USA), which was equipped with a 677 nm laser and dynamic light-scattering (DLS) at 90° for particle sizing. From fluctuations of scattered light intensity, the decay times of the fluctuations can be related to the diffusion constants and, therefore, to the sizes of the particles. Small particles moving rapidly cause faster decaying fluctuations than large particles moving slowly. The decay times of these fluctuations are determined in the time domain using a correlator. The fluctuating signal is processed by forming the autocorrelation function which decays exponentially with time so that the relaxation of the fluctuations is directly related to the decay constant (Γ). The decay constant is given by Equation (1):

$$\Gamma = Dq^2 \quad (1)$$

where q depends on the scattering angle, the wavelength of the laser light and refractive index of the suspending liquid and D is the translational diffusion coefficient.

Hydrodynamic particle diameter (Dz) is inversely related to D by the Stokes-Einstein Equation (2):

$$Dz = kT/(3\pi\eta D) \quad (2)$$

where k is the Boltzmann's constant, T is temperature in Kelvin, η is the viscosity of the suspending liquid, and D is the diffusion coefficient. Mean diameters were obtained by fitting data to log-normal size distributions that do not discriminate between one, two, or more different populations and always consider all scattering particles as belonging to one single Gaussian population. For the size distribution data, fitting was performed by the apparatus software using the non-negatively constrained least-squares (NNLS) algorithm, which is a model-independent technique allowing multimodal distributions to be achieved [44].

In order to define a relative width of size distributions, the polydispersity P is given by Equation (3):

$$P = \mu_2\Gamma^2 \quad (3)$$

where μ_2 is proportional to the variance of the "intensity" weighted diffusion coefficient distribution and carries information on the width of the size distribution. Polydispersity (P) has no units. It is close to zero (0.000 to 0.020) for monodisperse or nearly monodisperse samples, small (0.020 to 0.080) for narrow distributions and larger for broader distributions. ζ was determined from electrophoretic mobility (μ) in 1 mM NaCl and the Smoluchowski equation (Equation (4)):

$$\zeta = \mu\eta/\varepsilon \quad (4)$$

where η is the medium viscosity and ε the medium dielectric constant. DODAB differs from surfactants by being a lipid.

2.4. Determination of Solid Content and DODAB Concentration in NPs

Solid contents (mg/mL) in the dispersions were quantified by weighing 1 mL NPs dispersions before and after lyophilization as previously described [16,17,19,45]. Centrifuging dispersions (1 h/10,000 rpm) and pelleting NPs allowed the determination of DODAB concentration in the supernatant from halide microtitration [46]. DODAB concentration in NPs was obtained by subtracting DODAB concentration in the supernatant from DODAB concentration used for NPs synthesis [21,45].

2.5. Determination of Interaction of PMMA/DODAB NPs (20 mg/mL PMMA and 1.6 mM DODAB) and OVA

After washing out DODAB in the supernatant of a PMMA/DODAB NPs dispersion by centrifuging and re-suspending the initial dispersion three times in pure water, an aliquot

containing 0.50 mg/mL PMMA and 0.08 mM DODAB interacted with OVA over a range of OVA concentrations during 1 h interaction time. Thereafter, photos, DLS measurements and determination of OVA adsorption onto NPs from OVA analysis in the supernatants of the NPs/OVA mixtures were obtained [47]. Adsorbed [OVA] was obtained after centrifuging (10,000 rpm/1 h/25 °C) by subtracting OVA concentration in the supernatant from the OVA concentration added.

2.6. Determination of Cell Viability in the Presence of PMMA/DODAB NPs as Compared to the One with DODAB Vesicles and Bilayer Fragments

Three DODAB adjuvants were tested against cells in culture: PMMA/DODAB NPs, DODAB bilayer vesicles (DODAB LV) and DODAB BF. Stock dispersions of the three adjuvants were: (1) PMMA/DODAB NPs at 20 mg/mL PMMA and 1.6 mM DODAB; (2) DODAB LV at 10 mM DODAB in DODAB dispersions obtained by vortexing the DODAB powder in 1 mM NaCl solution above 47 °C [41]; (3) DODAB BF at 10 mM DODAB obtained by sonication in 1 mM NaCl with a macro-probe. Aliquots of each stock dispersion of adjuvants were mixed with cells' culture media over a range of DODAB concentrations (0.04, 0.08, 0.12, 0.16 mM DODAB for each adjuvant type). Thereafter 0.1 mL of each adjuvant type and concentration in culture medium were added to subconfluent layers of L929 fibroblasts or J774A.1 macrophages (American Type Culture Collection).

Cell lines were cultured according to standard protocols (90% humidity, 5% CO_2, 37 °C), RPMI—1640, 5% fetal bovine serum (FBS), 1% penicillin—streptomycin, 2 mM L—glutamine, and 0.25% 2—mercaptoethanol. In a humidified CO_2 incubator, 0.1 mL of DODAB-containing adjuvant previously diluted in the cells medium (0.1 mL) interacted with plated cells (10,000 cells/well) for 3 and 24 h. The 3-(4,5-dimethylthiazol-2-yl)-2,5-diphenyl tetrazolium bromide (MTT) assay evaluated cytotoxicity. Ten microliters of MTT solution in PBS (5 mg/mL MTT) was added per well. This stock MTT solution was previously filtered for sterilization and removal of insoluble residues. After incubation (37 °C/2 h), supernatant withdrawing, and mixing of adhered cells with 100 µL isopropanol solution in 0.04 N HCl, the absorbance at 570 nm was determined on an ELISA reader. One hundred percent of cell viability was given by cells in the culture medium only.

2.7. Immunization Protocol

Animals were immunized subcutaneously according to four groups with five BALB/c male mice each. They were injected with 0.1 mL of solution or dispersion on the base of the tail at two separate sites with 0.1 mL each (0.2 mL per animal in total). The composition of solutions or dispersions used for immunization is in Table 1. Animals received a booster with the same priming dose on day 21 after immunization.

Table 1. Solutions or dispersions in pure water used in mice immunization.

Group	Solution/ Dispersion	OVA mg/mL	$Al(OH)_3$ mg/mL	PMMA mg/mL	DODAB mM
1	Ultrapure water	0	0	0	0
2	Ovalbumin (OVA)	0.05	0	0	0
3	$Al(OH)_3$/OVA	0.05	0.10	0	0
4	PMMA/DODAB/OVA	0.05	0	0.50	0.08 [1]

[1] 0.08 mM DODAB is equivalent to 0.05 mg/mL.

2.8. OVA-Specific IgG1 and IgG2a Production by ELISA in Immunized Mice

Animals' blood was collected from the ophthalmic plexus at days 14, 21 and 28 postimmunization for serum individual analysis by indirect enzyme-linked immunosorbent assay (ELISA). Microtiter plates (Costar Corning Inc., Kennebunk, ME, USA) were incubated overnight at 4 °C with 0.1 mL OVA solution at 0.010 mg/mL in 0.01 M PBS, pH 7.2. Gelatin 3% in PBS blocked the wells for 2 h before adding serially diluted serum and further incubating the microplates for 1 h at 37 °C. 0.100 mL of goat anti-mouse biotin-conjugated

IgG1 (1:1000) or IgG2a (1:500) (Southern Biotechnology Associates, Birmingham, AL, USA) were added per well for incubation (1 h/37 °C). Thereafter, peroxidase-labeled streptavidin (0.100 mL/diluted 1:3000) was added and incubated for 1 h at 37 °C. Three-times washing was performed after each incubation step with PBS containing 0.05% Tween 20 (PBST). An amount of 0.1 mL of ortho-phenilenediamine dihydrochloride (OPD) substrate solution at 1 mg/mL and H_2O_2 (1 µL/mL) in 0.1 M citrate-phosphate at pH 5.0) were added per well for 15 min incubation at 25 °C. An amount of 0.050 mL of a H_2SO_4 solution (2 M) terminated the reaction. Optical density at 492 nm was read in an ELISA apparatus (Multiskan Ex, Thermo Electron Corporation, Waltham, MA, USA). Samples were diluted to fit inside the 0–1 absorbance range and data were shown. The results were expressed for diluted serum samples as the mean values ± standard deviation. For IgG1 dilution of 1:1024 corresponded to the primary response and 1/512,000, to the secondary one. For IgG2a, primary and secondary responses were present at 1:32 and 1:512 dilutions.

2.9. Determination of Delayed-Type Hypersensitivity Reaction (DTH)

DTH associated with cell-mediated immune response was evaluated from footpad swelling in mice [7,11,38,48]. At day 5 postimmunization, mice received injections of denaturated OVA in saline solution (0.030 mL of a 2 mg/mL OVA) at the left-hind footpad. Negative control was 0.030 mL of saline injected at the right-hind footpad of each animal. Footpad swelling at 24 h after injection was measured with a Mitutoyo digital micrometer. The difference between swelling of left and right hind footpads of a given 24 h after injection was taken as the individual footpad swelling. The mean footpad swelling ± standard deviation could be calculated considering all five animals in each group.

2.10. Determination of Cytokines Profile from Cultured Spleen Cells

Two weeks after the booster, spleen cells from spleens of five immunized mice of the same group were cultured in RPMI 1640 medium with 2 mM L—glutamine, 5% FBS and 0.25% 2-mercaptoethanol [21,49]. Suspensions (8×10^6 cells/mL) distributed in tissue culture plates were incubated with medium containing 250 µg/mL OVA in a humidified CO_2 incubator for 72 h. Negative and positive controls were medium only or 2.5 µg/mL concanavalin A (Con-A), respectively. Thereafter, plates were centrifuged (5 min/1500 rpm) and the supernatants collected for determining IL-2, IL-4, IL-10 and IFN-γ (sandwich ELISA kit, catalog number #88-7711-44, Thermo Fisher Scientific, Waltham, MA, USA). Detection limits were 30 (IL-10), 2 (IL-2), 4 (IL-4) and 15 pg/mL (IFN-γ); cytokine concentrations were expressed as mean of duplicate assays ± mean standard deviation.

2.11. Statistics Tests

The significance of results for different groups was evaluated using a two-way ANOVA variance analysis and the multiple comparisons Tukey's test. $p < 0.05$ meant significant differences between results. The software for statistical analysis was provided by the Origin 2018 program available from the Origin Lab Corporation, Northampton, MA, USA.

3. Results and Discussion

3.1. Synthesis of Nanoparticles (NP), NPs Physical Properties and Cytotoxicity against Cultured Cells

The background for synthesizing PMMA/DODAB NPs has been the high miscibility of DODAB and PMMA due to weak but numerous intermolecular interactions [40]. The hybrid coatings using PMMA/DODAB materials joined the high biocompatibility of PMMA [21,50,51] with the antimicrobial activity of the quaternary ammonium moiety of DODAB [52–55]. Here we take advantage of PMMA biocompatibility and DODAB activity as immunoadjuvant to obtain hybrid NPs of PMMA/DODAB. One should also recall the high surface potential of DODAB nanostructures, bilayer fragments and bilayer vesicles [56] favoring the adsorption of oppositely charged antigens, an essential property for combining antigen and adjuvant. The main physical properties of PMMA/DODAB NPs

obtained by emulsion polymerization of MMA in the presence of DODAB were on Figure 1.

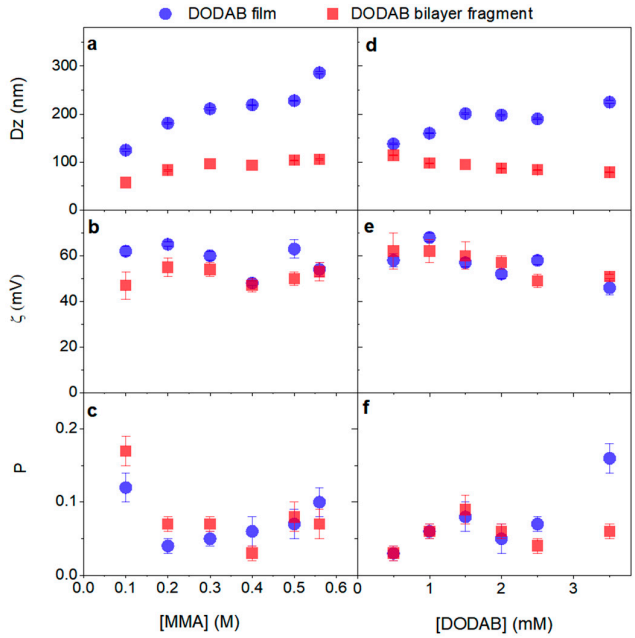


Figure 1. Effect of methyl methacrylate (MMA) concentration (**a**–**c**) or dioctadecyl dimethyl ammonium bromide (DODAB) concentration on main characteristics of PMMA/DODAB NPs synthesized by emulsion polymerization of MMA in the presence of DODAB (**d**–**f**). From dynamic light scattering (DLS), mean hydrodynamic diameter (Dz) (**a**,**d**), zeta—potential (ζ) (**b**,**e**) and polydispersity (P) (**c**,**f**) were determined for the dispersions in pure water. NPs in dispersion at 1.5 mM DODAB were synthesized over a range of [MMA]. NPs were also synthesized at 0.3 M MMA over a range of [DODAB].

Figure 1 showed the effect of MMA or DODAB concentration used during NPs synthesis on physical properties of PMMA/DODAB NPs. DODAB BF or DODAB dispersed as films on the bottom of the glass tube when used in the MMA polymerization medium yielded polymeric NPs further characterized by DLS for sizing, polydispersity (P) and zeta-potentials (ζ). Sizes (Dz) (Figure 1a), zeta-potentials (ζ) (Figure 1b) and polydispersities (P) (Figure 1c) were shown over a range of PMMA or DODAB concentrations. Nanometric size (50–80 nm) was mainly achieved using the DODAB BF during NPs synthesis over a range of MMA concentrations (Figure 1a). DODAB BF emulsified MMA better than DODAB films casted on the bottom of glass tubes. Therefore, in Figure 1a,d, NPs synthesized in the presence of DODAB BF (red points) were always smaller than those synthesized in the presence of DODAB films (blue points).

Over a range of low [MMA] (below 0.2 M MMA) in the reaction mixture, dispersions contained polydisperse NPs in contrast to the narrow size distribution obtained above 0.2 M MMA (Figure 1c). Thus [MMA] concentrations for nanometric sizes, high zeta-potential and narrow size distribution should be chosen above 0.2 M (concentration chosen was 0.3 M). Regarding the use of DODAB films for NPs synthesis, no signicant difference in zeta-potential and polydispersity was observed, but sizes tended to be always larger than the ones for NPs obtained from DODAB BF (Figure 1a–c).

At 0.3 M MMA, BFs confirmed their suitability to yield NPs sizes below 100 nm; DODAB films yielded always larger NPs (Figure 1d). This had already been observed on Figure 1a, where films yielded always larger NPs than those prepared in the presence of DODAB BF. Again, nanometric size (50–80 nm) was mainly achieved using the DODAB BF during NPs synthesis over a range of MMA concentrations (Figure 1d). DODAB BF emulsified MMA better than DODAB films casted on the bottom of glass tubes. Possibly,

DODAB BF present in the aqueous reaction medium organized the growing chains of PMMA in the core of the bilayer fragments at early stages of the polymerization. The high miscibility between PMMA and DODAB led to hybrid NPs where DODAB could be localized both in the polymer matrix and on the NP surface. Curiously, DODAB affinity for PMMA has been shown to be higher than the one for cetyltrimethylammonium bromide (CTAB): whereas DODAB remains in the polymer matrix, CTAB diffuses through the polymer network reaching the outer water medium [19,40,57].

Figure 1e,f confirmed similar zeta-potentials and polydispersities for NPs synthesized in the presence of DODAB BF or DODAB films.

Figure 2a showed the DODAB incorporation at 1.5 mM DODAB onto PMMA/DODAB NPs over a range of [MMA]. DODAB incorporation in the PMMA/DODAB NPs increased with [MMA] over a low range of [MMA] (0–0.3 M MMA). Above this range, further increasing [MMA] did not increase DODAB incorporation in the NPs.

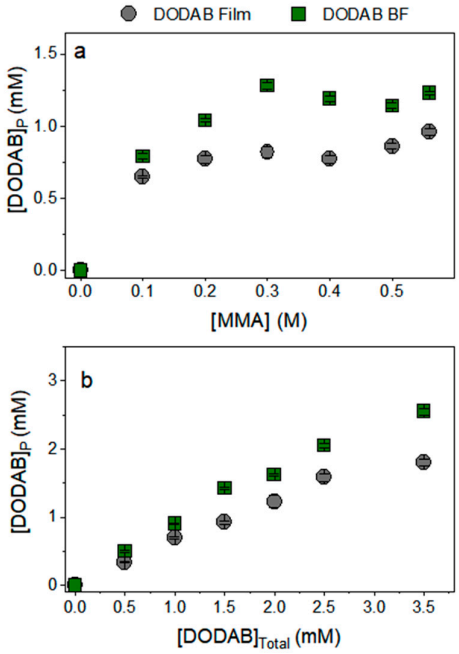


Figure 2. Incorporation of dioctadecyl dimethyl ammonium bromide (DODAB) in in poly(methyl methacrylate) (PMMA)/DODAB nanoparticles (NPs) as a function of methyl methacrylate concentration ([MMA]) using 1.5 mM DODAB (**a**) and as a function of DODAB concentration employing 0.3 M MMA (**b**).

From a certain MMA concentration it was not possible to disperse all PMMA as NPs due to lack of DODAB emulsifier; polymerization proceeded anyway yielding precipitated polymeric masses in the reaction mixtures; this occurred mainly over a range of [MMA] above 0.3 M (Figure 2a). Thus there is a need of establishing the saturation of PMMA with DODAB at a given concentration of MMA. For example, until 0.3 M MMA there was a linear dependence of DODAB incorporation from BF into PMMA/DODAB NPs (Figure 2a). However, it was observed that above 0.3 M MMA there were nonemulsified, precipitated polymer masses at the bottom of the assay tubes after NPs synthesis. For DODAB from films, the emulsification was even more hampered due to a lower availability of DODAB molecules to diffuse into the reaction mixture; at least for BF, the previous step of dispersing DODAB by sonication placed DODAB in a more suitable position as emulsifier for obtaining well dispersed polymeric NPs (Figure 2a,b). DODAB incorporation in NPs was always higher for polymerizations in the presence of BF than those in the presence of films (Figure 2). Furthermore, from DODAB added as BF, at 0.3 M MMA, there was a linear dependence of DODAB incorporation with the total DODAB concentration added to the

reaction mixture, at least up to 1.5 mM DODAB (Figure 2b). In addition, all DODAB added could become incorporated in the NPs (Figure 2b). Above 1.5 mM DODAB added not all DODAB became part of the NPs meaning that the maximal DODAB incorporation had been achieved at a certain proportion of MMA/DODAB, namely 0.3 M MMA and 1.5 mM DODAB (Figure 2b).

The initial study determining the optimal molar ratio for MMA/DODAB during polymerization, namely 0.3:0.0015 MMA:DODAB, suggested this ratio for synthesizing the NPs to be evaluated as antigen presenters. The concentrations used for NPs synthesis in the next experiments were 0.3 M MMA and 0.0020 M DODAB, considering that the cationic DODAB usually adsorbs onto all glass [58] or plastic containers [33]. In other words, we synthesized the NPs under a slight excess of DODAB, even though complete removal of DODAB by centrifuging, discarding the supernatant and resuspending in pure water was routinely done. For the final NPs, $[DODAB]_p$ was 1.62 mM.

In the presence of PMMA/DODAB NPs, DODAB BF and DODAB LV, determination of the viability of macrophages or fibroblasts in culture pointed out that DODAB concentration at 0.08 mM barely affected the macrophages and the fibroblasts after a period of 24 h interaction (Figure 3). In contrast with DODAB BF or DODAB LV, the PMMA/DODAB NPs resulted much less cytotoxic against the macrophages (Figure 3b). The [DODAB] selected to the next experiments on adjuvant activity of the NPs was selected as 0.08 mM DODAB.

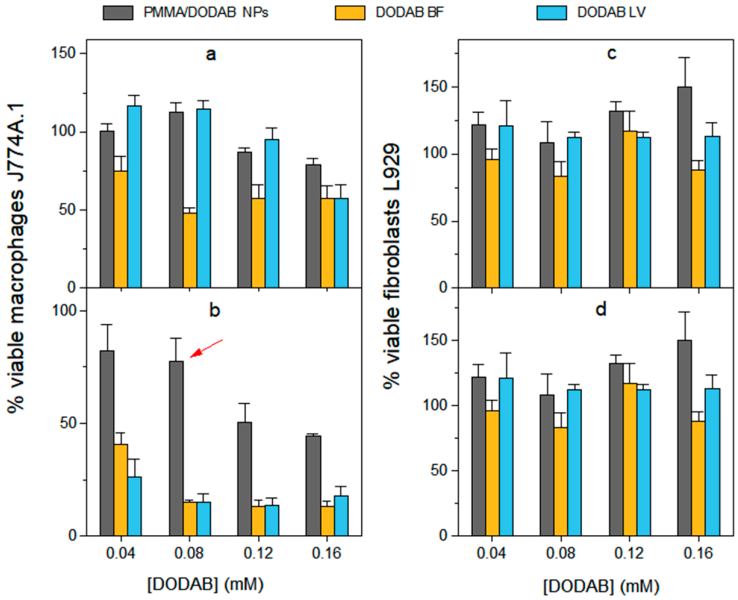


Figure 3. Cell viability of macrophages (J774A.1) or fibroblasts (L929) as affected by three different adjuvants containing dioctadecyl dimethyl ammonium bromide (DODAB) at 3 (**a**,**c**) and 24 h interaction time (**b**,**d**). The adjuvants were DODAB bilayer fragments (DODAB BF) (in yellow), DODAB bilayer vesicles (DODAB LV) (in blue) and poly (methyl methacrylate) (PMMA)/DODAB hybrid NPs (in gray). The DODAB concentration used for the three different adjuvants (PMMA/DODAB NPs, DODAB BF and DODAB LV) was indicated by the red arrow and corresponded to 0.08 mM DODAB.

One should notice that from a NPs dispersion of 20 mg/mL PMMA (determined from solid contents of the PMMA/DODAB dispersion) synthesized in the presence of 2.0 mM DODAB, after centrifuging to precipitate the NPs and determining the DODAB concentration in the supernatant as 0.38 mM the $[DODAB]_p$ would be 1.62 mM. From this dispersion with 20 mg/mL PMMA and 1.62 mM DODAB, aliquots were taken to yield the four final [DODAB] on Figure 3, namely, 0.04, 0.08, 0.12 and 0.16 mM DODAB; for PMMA, final concentrations were 0.25, 0.50, 0.75 and 1.00 mg/mL, respectively. Curiously, there was no cytotoxicity against the fibroblasts in the presence of all three adjuvants

over the 0–0.16 mM range of [DODAB] (Figure 3c,d). This result agrees with previous data on fibroblasts cell death in the presence of DODAB BF showing significant DODAB cytotoxicity only above 0.5 mM DODAB [59]. In summary, the use of DODAB mixed as a hybrid material with a biocompatible polymer such as PMMA advantageously reduced DODAB toxicity against the macrophages.

3.2. Ovalbumin Adsorption onto NPs, NPs/OVA Physical Properties and Colloidal Stability, and NPs/FITC-OVA Internalization in Macrophages

OVA adsorption onto PMMA/DODAB NPs was determined at 0.5 mg/mL PMMA over a range of added OVA concentrations. The reason for choosing this PMMA concentration was the possibility of comparing later on, the adjuvant effects of PMMA/DODAB with the previously described effects for PMMA/DODAB/PDDA NPs as adjuvants at this same concentration [21].

The oppositely charged OVA adsorbed onto PMMA/DODAB NPs at 0.5 mg/mL PMMA over a range of [OVA] yielding the macroscopic features shown on Figure 4a. Upon charge neutralization and zeta-potentials around zero, there was precipitation and loss of colloidal stability around 0.100–0.125 mg/mL of OVA (Figure 4a,d).

This behavior is usually obtained for interaction between NPs and oppositely charged molecules such as silica/DODAB [37], and polystyrene sulfate NPs/DODAB [15,33]. Around neutralization, large aggregates precipitate and polydispersity increases substantially; basically, it is not possible to use the DLS technique due to the absence of colloids in dispersion. The determination of colloidal stability was important to define OVA concentration to be combined with 0.5 mg/mL PMMA. To obtain positively charged NPs, their concentrations should be smaller than 0.1 mg/mL; furthermore, at 0.1 mg/mL OVA, aggregation and precipitation hampered the use of this OVA concentration. The OVA concentration chosen was 0.05 mg/mL in combination with 0.5 mg/mL PMMA/DODAB NPs. The reason for choosing 0.5 mg/mL PMMA/DODAB NPs was to compare later on the adjuvant effect with the one induced by PMMA/DODAB/PDDA NPs described previously at this same concentration [21].

The red point on Figure 4c–e showing the physical properties of NPs/OVA were obtained from a 1 mg/mL OVA stock solution. As compared to NPs/OVA obtained from a 10 mg/mL OVA stock solution (black points), sizes and polydispersities were smaller for the NPs obtained from the 1 mg/mL OVA. This was observed previously for concentrated OVA stock solutions and attributed to OVA-OVA interactions leading to OVA aggregation in the stock solution that remains to a certain extent after further dilution [60]. Thus, the stock OVA solution used was the one at 1 mg/mL OVA (red points in Figure 4c–e).

The OVA adsorption onto PMMA/DODAB NPs at 0.5 mg/mL PMMA increased linearly with added OVA concentration up to 0.1 mg/mL of added OVA (Figure 4b). Above this concentration NPs became saturated with OVA and further adsorption was substantially reduced. Therefore, 0.05 mg/mL of added OVA was suitable to ensure that all OVA added was adsorbed onto the NPs, no free OVA remained in solution.

In comparison with PMMA/DODAB/PDDA NPs (zeta-potentials around 70 mV), the present system with PMMA/DODAB NPs exhibited smaller zeta-potentials (around 30 mV) but maximal OVA adsorption was similarly around 0.10–0.12 mg/mL for both systems [21]. This can be better understood from the compared sizes for both NPs. PMMA/DODAB/PDDA NPs (Dz = 217 nm) were larger than PMMA/DODAB NPs (Dz = 81 nm). At 0.5 mg/mL PMMA for both NPs, the total surface area available for OVA adsorption is larger for the smaller NPs explaining why the lower zeta-potential resulted in similar adsorption to the one obtained with the PMMA/DODAB/PDDA NPs with higher zeta-potential. Small sizes compensated for the lower zeta-potentials.

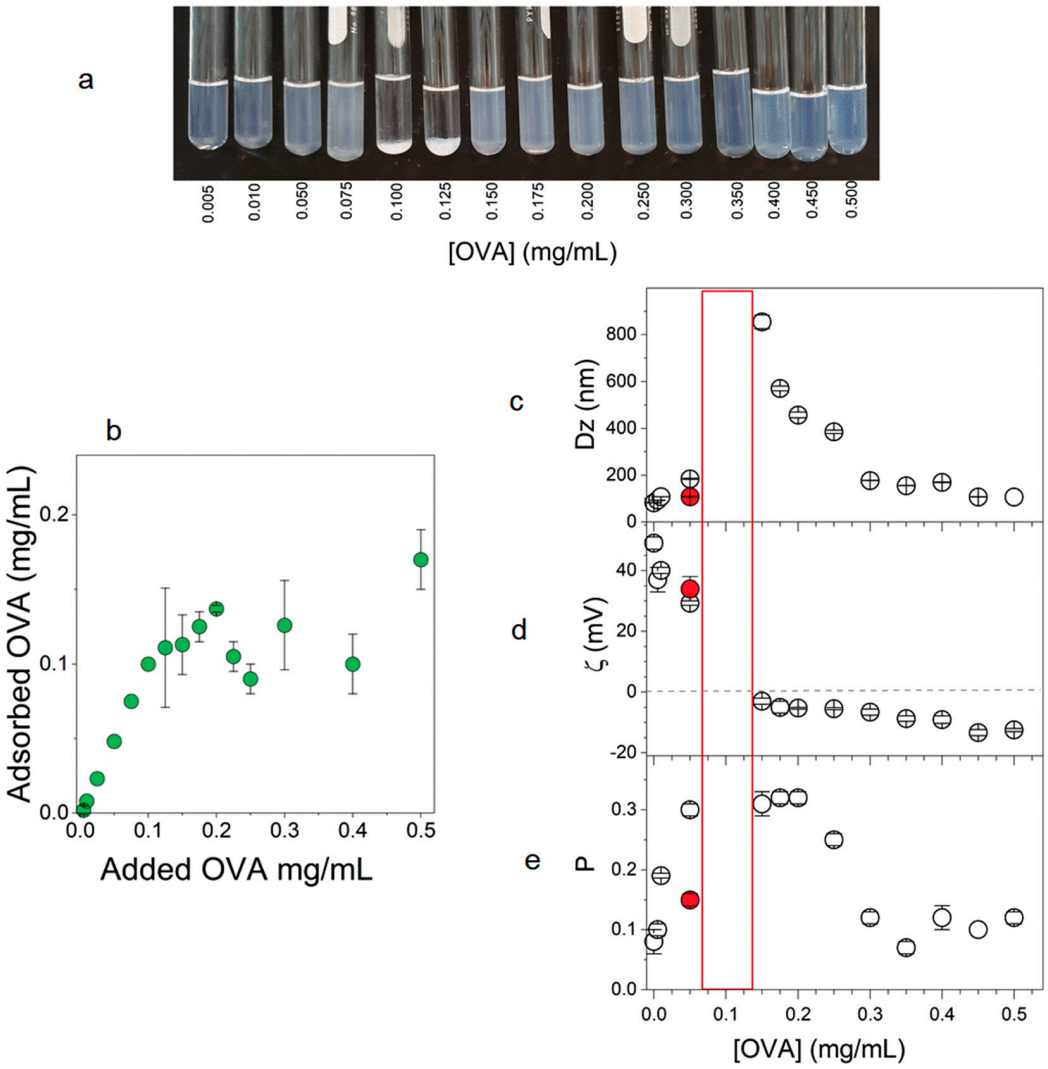


Figure 4. Poly(methyl methacrylate)/dioctadecyl dimethyl ammonium bromide (PMMA/DODAB) NPs at 0.5 mg/mL PMMA over a range of ovalbumin (OVA) concentrations: (**a**) photos of the dispersions; (**b**) OVA adsorption on NPs as a function of added OVA; (**c**) mean hydrodynamic diameter (Dz); (**d**) zeta-potential (ζ); (**e**) polydispersity of the dispersions (P). The stock solution of OVA used was 10 mg/mL whereas the red dot indicates properties of dispersions obtained from a 1 mg/mL OVA stock solution. The immunology tests were performed using the last stock solution of OVA. The red rectangle corresponds to the OVA concentration region of poor colloidal stability, meaning that DLS measurments could not be performed due to precipitation in the tubes.

3.3. Immune Response of NPs/OVA In Vivo: Improved Production of IgG1 and IgG2a

IgG1 and IgG2a OVA-specific antibodies production was enhanced substantially using NPs/OVA for immunization (Figure 5). Furthermore, NPs were as efficient as $Al(OH)_3$ as adjuvants inducing the IgG1 primary response on days 14 and 21 but surpassed alum regarding the secondary response on day 28 (Figure 5a). IgG2a production induced by NPs/OVA was substantially superior to the one induced by alum both for the primary and the secondary response, suggesting and important role of the novel NPs in promoting cellular immune response (Figure 5b). Similar NPs made of the biocompatible PMMA and a cationic polymer were previously used as adjuvants also yielding improved humoral response [21,43]. Emulsion polymerization of methyl methacrylate (MMA), producing poly(methyl methacrylate) (PMMA), is well described in the literature [61–63]. We have been studying the effect of adding cationic lipid, surfactant or polymer to obtain

cationic PMMA NPs useful as immunoadjuvants. Adding a cationic polymer to obtain PMMA/cationic polymer NPs, the IgG1 production was about four times higher than the one induced by alum [21] whereas in the present work, adding the cationic lipid DODAB to obtain PMMA/cationic lipid NPs, the IgG1 production was similar to the one induced by alum (Figure 5a). Production of IgG2a induced by PMMA/cationic lipid (Figure 5b) was four times higher than the one induced by PMMA/cationic polymer [21]. The cationic polymer PDDA was shown to enhance humoral response at levels superior to those attributed to polyethyleneimine (PEI) or cetyltrimethylammonium bromide (CTAB) adsorbed to gold nanorods [64].

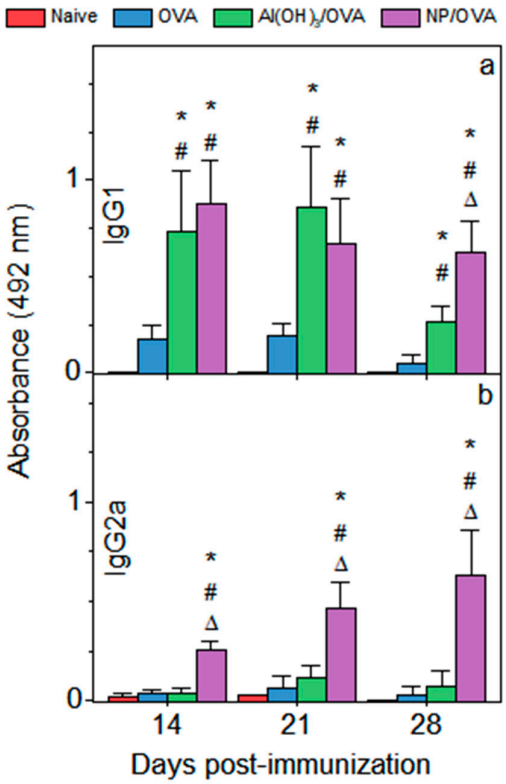


Figure 5. Antibody production in sera on days 14, 21 and 28 after immunization as induced by ovalbumin (OVA), $Al(OH)_3$/OVA and NPs/OVA. The mean absorbance measured at 492 nm ± standard deviation was relative to the production of OVA-specific IgG1 (**a**) or IgG2a (**b**). Serum dilution to present IgG1 primary response was 1/1024 and IgG2a primary response was showed at 1/32. Secondary response of IgG1 was displayed at 1/512,000 whereas IgG2a secondary response was presented at 1/512. $p < 0.05$ compared to the naive group (#), $p < 0.05$ compared to the OVA group (*), $p < 0.05$ compared to the $Al(OH)_3$/OVA group (Δ).

In order to obtain more quantitative data on IgG1 and IgG2a antibodies production, the endpoint titers were obtained in both cases and shown on Table 2. The qualitative data described on Figure 5 were reconfirmed by the titers' determination. PMMA/DODAB NPs induced indeed a mixed Th1-Th2 response in contrast to OVA alone or alum as adjuvant. Although OVA alone induced a certain production of IgG1, the production of IgG2a was basically neglectable (Table 2).

Table 2. Endpoint titer of OVA-specific IgG1, IgG2a and IgG1/IgG2a ratio determined 21 days after immunization.

Group	IgG1	IgG2a	IgG1/IgG2a
OVA	1434 ± 360	14 ± 10	102
$Al(OH)_3$/OVA	35,200 ± 13,000	58 ± 14	607
NPs/OVA	41,600 ± 15,648	358 ± 132	116

In summary, the NP structure determines the magnitude of both humoral and cellular responses when used as adjuvants. The cationic component as the outermost layer imparts high surface potential to the NPs and is seen by the immune system as a foreign body. The hybrid cationic lipid/PMMA NPs exhibit a lower surface potential due to uniform distribution of the cationic lipid in the polymer matrix and are not seen as so foreigner by the immune system.

Figure 6 shows the footpad swelling (FS) in mm for PMMA/DODAB NPs as compared to alum. The FS was 0.7 mm (Figure 6) and lower than the one previously determined for DODAB BF/OVA by Rozenfeld and coworkers, which was 1.3 mm [11]. Whereas the zeta-potential for PMMA/DODAB/OVA in this work is about 34 mV (Figure 4d), the zeta-potential for DODAB BF/OVA was determined as 21 mV [11]. The less charged nanostructure apparently induced the larger cellular response.

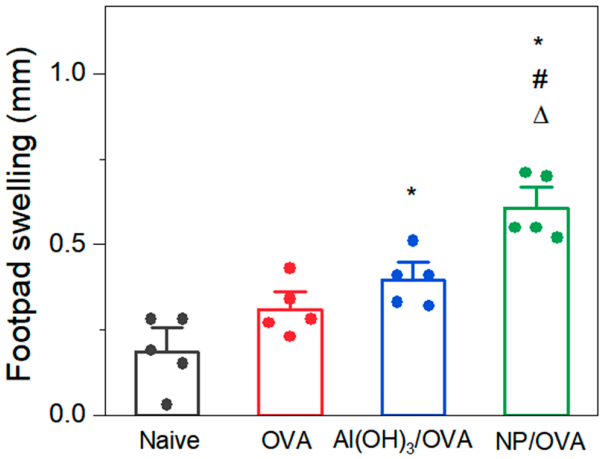


Figure 6. Delayed-type hypersensitivity reaction assessed as the mean footpad swelling ± standard deviation of animals immunized with ovalbumin (OVA), $Al(OH)_3$/OVA or PMMA/DODAB/OVA (NP/OVA). $p < 0.05$ compared to the naive group (*), $p < 0.05$ compared to the OVA group (#), $p < 0.05$ compared to the $Al(OH)_3$/OVA group (Δ).

Some cytokines elicited by medium (negative control), OVA or concanavalin-A in cultured spleen cells of animals previously immunized with water (naive), OVA, $Al(OH)_3$/OVA or PMMA/DODAB/OVA NPs allowed to reconfirm the intensity of humoral and cellular immune responses (Figure 7). Whereas IL-4 enhancement means improved humoral response (Figure 7a) and IL-10 enhancement relates to both humoral and cellular responses (Figure 7b), IL-2 (Figure 7c) and IFN-γ are typically produced in enhanced cellular immune response (Figure 7d). This profile perfectly agrees with previous results reported in this work where significant enhancements in both cellular (Figures 5b and 6) and humoral immune responses were indeed described (Figure 5a). IL-10 enhancement means a regulatory response against the pro-inflammatory effect of NPs/OVA in mice.

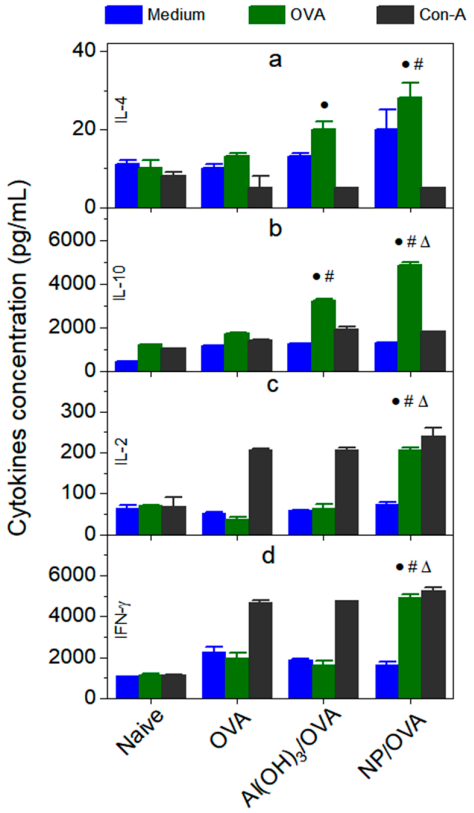


Figure 7. Production IL-4 (**a**), IL-10 (**b**), IL-2 (**c**) and IFN-γ (**d**) (pg/mL) elicited by cultured spleen cells obtained from naïve or animals immunized with ovalbumin (OVA), $Al(OH)_3$/OVA, PMMA/DODAB/OVA (NPs/OVA). $p < 0.05$ compared to the naive group (•), $p < 0.05$ compared to the OVA group (#), $p < 0.05$ compared to the $Al(OH)_3$/OVA group (Δ). Splenocytes were challenged with OVA, medium (negative control) and concanavalin-A (Con-A) (positive control).

In the presence of DODAB and poly(diallyl dimethylammonium chloride) (PDDA), emulsion polymerization of MMA yielded PMMA/DODAB/PDDA NPs [21,43,45]. These hybrid, PMMA-based NPs predominantly contained PMMA, a biocompatible polymer, displaying absence of cytotoxicity when tiny amounts of cationic components were used, as shown in this work. The comparison between PMMA/DODAB NPs (this work) and PMMA/DODAB/PDDA [21] showed some differences in the type of immune response. The former NPs induced preferentially a Th-1 response (higher IgG2a, IFN-γ and lower IL-10 for down regulation of inflammatory response induced by the PMMA/DODAB NP) as compared to the PMMA/DODAB/PDDA NPs that generated higher Th-2 response (lower IgG2a, IFN-γ and higher IL-10 attempting to reduce the NPs induced inflammatory effect).

The comparison between PMMA/DODAB NPs and DODAB bilayer fragments (BF) regarding the DTH response measured as footpad swelling (FS) also showed the mild inflammatory effect of the PMMA/DODAB NPs (FS = 0.70 mm) in comparison to DODAB BF (FS = 1.3).

Figure 8 shows schematically four different cationic nanostructures and their immune responses as studied in our group over the last 25 years.

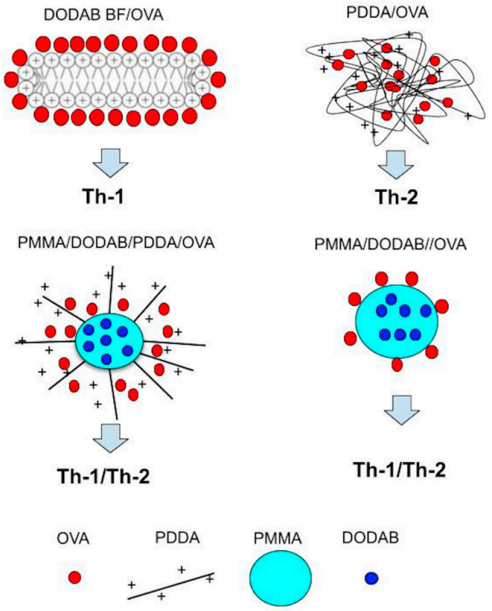


Figure 8. Cationic nanostructures from biocompatible polymer and cationic lipid and/or cationic polymer.

4. Conclusions

PMMA/DODAB NPs with nanometric sizes, high zeta-potential and narrow size distribution were obtained by emulsion polymerization of MMA in the presence of DODAB (at 0.3 M MMA and 2.0 mM DODAB). From DODAB films for NPs synthesis sizes were always larger than the ones for NPs obtained from DODAB BF. PMMA/DODAB NPs exhibited functional behavior as immunoadjuvants. They were non cytotoxic against macrophages and fibroblasts in culture, combined well with OVA, as model antigen, were nanometric, showing high zeta-potential, low polydispersity and high colloidal stability in water dispersions. NPs/OVA induced high production of OVA-specific IgG1 and IgG2a in immunized mice, high delayed type hypersensitivity reaction, high production of IFN-γ, regulatory cytokine IL-10, IL-2 and IL-4. Quantitative determination of IgG1 and IgG2a titers reconfirmed the induction of a mixed Th1-Th2 response induced by the PMMA/DODAB/OVA NPs. In summary, there was enhanced humoral and cellular responses against OVA carried by the novel biocompatible adjuvant.

Author Contributions: Conceptualization, A.M.C.-R., E.L.F.-M. and Y.P.-B.; methodology, Y.P.-B., B.d.C.L.F.T., E.L.F.-M., P.M.A., D.R.P. and A.M.C.-R.; validation, A.M.C.-R., E.L.F.-M. and Y.P.-B.; formal analysis, A.M.C.-R., E.L.F.-M. and Y.P.-B.; investigation, Y.P.-B., B.d.C.L.F.T., E.L.F.-M., P.M.A., D.R.P. and A.M.C.-R.; resources, A.M.C.-R. and E.L.F.-M.; data curation, A.M.C.-R.; writing—original draft preparation, A.M.C.-R. and Y.P.-B.; writing—review and editing, A.M.C.-R. and Y.P.-B.; supervision, A.M.C.-R.; project administration, A.M.C.-R.; funding acquisition, A.M.C.-R. and E.L.F.-M. All authors have read and agreed to the published version of the manuscript.

Funding: This work was supported by Conselho Nacional de Desenvolvimento Científico e Tecnológico (CNPq) by grants 302758/2019-4, 302352/2014-7 to A.M.C.-R.; 140091/2019-0 to Y.P.-B.; 312096/2018-6 to E.L.F.-M.) and Fundação de Amparo à Pesquisa do Estado de São Paulo (FAPESP) by grant 2019/17685-2 to A.M.C.-R and grant FAPESP 2019/17625-0 to E.L.F.-M. Y.P.-B. is the recipient of a CNPq Ph.D. fellowship (140091/2019-0) under A.M.C.-R. supervision for developing the project "Cationic Nanostructures for Vaccines".

Institutional Review Board Statement: The study was approved by the Ethics Committee of Butantan Institute (protocol code 7912280219, April 2019).

Informed Consent Statement: Not applicable.

Data Availability Statement: All data available are reported in the article.

Acknowledgments: Y.P.-B. thanks CNPq for awarding a Ph.D. fellowship (140091/2019-0). P.M.A. was the recipient of an undergraduate fellowship from the Programa Institucional de Bolsas de Iniciação Científica (PIBIC)-CNPq grant 139161/2020-1. D.R.P. thanks to Coordenação de Aperfeiçoamento de Pessoal de Nível Superior (CAPES) for granting a MSc fellowship (88887.467008/2019-00).

Conflicts of Interest: The authors declare no conflict of interest. The funders had no role in the design of the study; in the collection, analyses, or interpretation of data; in the writing of the manuscript, or in the decision to publish the results.

References

1. Manolova, V.; Flace, A.; Bauer, M.; Schwarz, K.; Saudan, P.; Bachmann, M.F. Nanoparticles Target Distinct Dendritic Cell Populations According to Their Size. *Eur. J. Immunol.* **2008**, *38*, 1404–1413. [CrossRef]
2. Fifis, T.; Gamvrellis, A.; Crimeen-Irwin, B.; Pietersz, G.A.; Li, J.; Mottram, P.L.; McKenzie, I.F.C.; Plebanski, M. Size-Dependent Immunogenicity: Therapeutic and Protective Properties of Nano-Vaccines against Tumors. *J. Immunol.* **2004**, *173*, 3148–3154. [CrossRef]
3. Xiang, S.D.; Scholzen, A.; Minigo, G.; David, C.; Apostolopoulos, V.; Mottram, P.L.; Plebanski, M. Pathogen Recognition and Development of Particulate Vaccines: Does Size Matter? *Methods* **2006**, *40*, 1–9. [CrossRef]
4. Carmona-Ribeiro, A.M. Cationic nanostructures for vaccines. In *Immune Response Activation*; Duc, G.H.T., Ed.; IntechOpen: Rijeka, Croatia, 2014; pp. 1–45, ISBN 978-953-51-1374-4.
5. Carmona-Ribeiro, A.M. Chapter Thirteen—Nanomaterials Based on Lipids for Vaccine Development. In *Micro and Nanotechnology in Vaccine Development*; Skwarczynski, M., Toth, I., Eds.; Micro and Nano Technologies; William Andrew Publishing: Norwich, NY, USA, 2017; pp. 241–257, ISBN 978-0-323-39981-4.
6. Mao, L.; Chen, Z.; Wang, Y.; Chen, C. Design and Application of Nanoparticles as Vaccine Adjuvants against Human Corona Virus Infection. *J. Inorg. Biochem.* **2021**, *219*, 111454. [CrossRef] [PubMed]
7. Tsuruta, L.R.; Quintilio, W.; Costa, M.H.; Carmona-Ribeiro, A.M. Interactions between Cationic Liposomes and an Antigenic Protein: The Physical Chemistry of the Immunoadjuvant Action. *J. Lipid Res.* **1997**, *38*, 2003–2011. [CrossRef]
8. Carmona-Ribeiro, A.M. Synthetic Amphiphile Vesicles. *Chem. Soc. Rev.* **1992**, *21*, 209–214. [CrossRef]
9. Carmona-Ribeiro, A.M. Lipid Bilayer Fragments and Disks in Drug Delivery. *Curr. Med. Chem.* **2006**, *13*, 1359–1370. [CrossRef]
10. Lincopan, N.; Espíndola, N.M.; Vaz, A.J.; da Costa, M.H.B.; Faquim-Mauro, E.; Carmona-Ribeiro, A.M. Novel Immunoadjuvants Based on Cationic Lipid: Preparation, Characterization and Activity In Vivo. *Vaccine* **2009**, *27*, 5760–5771. [CrossRef]
11. Rozenfeld, J.H.K.; Silva, S.R.; Raneia, P.A.; Faquim-Mauro, E.; Carmona-Ribeiro, A.M. Stable Assemblies of Cationic Bilayer Fragments and CpG Oligonucleotide with Enhanced Immunoadjuvant Activity In Vivo. *J. Control. Release Off. J. Control. Release Soc.* **2012**, *160*, 367–373. [CrossRef]
12. De Almeida, A.F.; De Gaspari, E. Dioctadecyldimethylammonium Bromide (DODAB-BF) as a New Adjuvant for Maternal-Fetal Immunization in Mice against Neisseria Meningitidis: Evaluation of Humoral Response. *Pathog. Dis.* **2018**, *76*, ftx128. [CrossRef] [PubMed]
13. Andersson, M.; Hammarstroem, L.; Edwards, K. Effect of Bilayer Phase Transitions on Vesicle Structure, and Its Influence on the Kinetics of Viologen Reduction. *J. Phys. Chem.* **1995**, *99*, 14531–14538. [CrossRef]
14. Baden, L.R.; El Sahly, H.M.; Essink, B.; Kotloff, K.; Frey, S.; Novak, R.; Diemert, D.; Spector, S.A.; Rouphael, N.; Creech, C.B.; et al. Efficacy and Safety of the MRNA-1273 SARS-CoV-2 Vaccine. *N. Engl. J. Med.* **2021**, *384*, 403–416. [CrossRef] [PubMed]
15. Lincopan, N.; Espindola, N.M.; Vaz, A.J.; Carmona-Ribeiro, A.M. Cationic Supported Lipid Bilayers for Antigen Presentation. *Int. J. Pharm.* **2007**, *340*, 216–222. [CrossRef]
16. Naves, A.F.; Palombo, R.R.; Carrasco, L.D.M.; Carmona-Ribeiro, A.M. Antimicrobial Particles from Emulsion Polymerization of Methyl Methacrylate in the Presence of Quaternary Ammonium Surfactants. *Langmuir* **2013**, *29*, 9677–9684. [CrossRef] [PubMed]
17. Sanches, L.M.; Petri, D.F.S.; de Melo Carrasco, L.D.; Carmona-Ribeiro, A.M. The Antimicrobial Activity of Free and Immobilized Poly(Diallyldimethylammonium) Chloride in Nanoparticles of Poly(Methylmethacrylate). *J. Nanobiotechnol.* **2015**, *13*, 58. [CrossRef]
18. Xavier, G.R.S.; Carmona-Ribeiro, A.M. Cationic Biomimetic Particles of Polystyrene/Cationic Bilayer/Gramicidin for Optimal Bactericidal Activity. *Nanomaterials* **2017**, *7*, 422. [CrossRef] [PubMed]
19. Mathiazzi, B.I.; Carmona-Ribeiro, A.M. Hybrid Nanoparticles of Poly(Methyl Methacrylate) and Antimicrobial Quaternary Ammonium Surfactants. *Pharmaceutics* **2020**, *12*, 340. [CrossRef]
20. Carmona-Ribeiro, A.M.; Pérez-Betancourt, Y. Cationic Nanostructures for Vaccines Design. *Biomimetics* **2020**, *5*, 32. [CrossRef]
21. Pérez-Betancourt, Y.; Távora, B.d.C.L.F.; Faquim-Mauro, E.L.; Carmona-Ribeiro, A.M. Biocompatible Lipid Polymer Cationic Nanoparticles for Antigen Presentation. *Polymers* **2021**, *13*, 185. [CrossRef]
22. Ribeiro, A.M.; Chaimovich, H. Preparation and Characterization of Large Dioctadecyldimethylammonium Chloride Liposomes and Comparison with Small Sonicated Vesicles. *Biochim. Biophys. Acta* **1983**, *733*, 172–179. [CrossRef]
23. Carmona-Ribeiro, A.M.; Chaimovich, H. Salt-Induced Aggregation and Fusion of Dioctadecyldimethylammonium Chloride and Sodium Dihexadecylphosphate Vesicles. *Biophys. J.* **1986**, *50*, 621–628. [CrossRef]

24. Carvalho, L.A.; Carmona-Ribeiro, A.M. Interactions between Cationic Vesicles and Serum Proteins. *Langmuir* **1998**, *14*, 6077–6081. [CrossRef]
25. Lincopan, N.; Carmona-Ribeiro, A.M. Protein Assembly onto Cationic Supported Bilayers. *J. Nanosci. Nanotechnol.* **2009**, *9*, 3578–3586. [CrossRef] [PubMed]
26. Carvalho, C.A.; Olivares-Ortega, C.; Soto-Arriaza, M.A.; Carmona-Ribeiro, A.M. Interaction of Gramicidin with DPPC/DODAB Bilayer Fragments. *Biochim. Biophys. Acta* **2012**, *1818*, 3064–3071. [CrossRef] [PubMed]
27. Ragioto, D.A.M.T.; Carrasco, L.D.M.; Carmona-Ribeiro, A.M. Novel Gramicidin Formulations in Cationic Lipid as Broad-Spectrum Microbicidal Agents. *Int. J. Nanomed.* **2014**, *9*, 3183–3192. [CrossRef]
28. Rozenfeld, J.H.K.; Oliveira, T.R.; Lamy, M.T.; Carmona-Ribeiro, A.M. Interaction of Cationic Bilayer Fragments with a Model Oligonucleotide. *Biochim. Biophys. Acta* **2011**, *1808*, 649–655. [CrossRef] [PubMed]
29. Kikuchi, I.S.; Viviani, W.; Carmona-Ribeiro, A.M. Nucleotide Insertion in Cationic Bilayers. *J. Phys. Chem. A* **1999**, *103*, 8050–8055. [CrossRef]
30. Nantes, I.L.; Correia, F.M.; Faljoni-Alario, A.; Kawanami, A.E.; Ishiki, H.M.; Amaral, A.T.; Carmona-Ribeiro, A.M. Nucleotide Conformational Change Induced by Cationic Bilayers. *Arch. Biochem. Biophys.* **2003**, *416*, 25–30. [CrossRef]
31. Rosa, H.; Petri, D.F.S.; Carmona-Ribeiro, A.M. Interactions between Bacteriophage DNA and Cationic Biomimetic Particles. *J. Phys. Chem. B* **2008**, *112*, 16422–16430. [CrossRef]
32. Kikuchi, I.S.; Carmona-Ribeiro, A.M. Interactions between DNA and Synthetic Cationic Liposomes. *J. Phys. Chem. B* **2000**, *104*, 2829–2835. [CrossRef]
33. Carmona-Ribeiro, A.M.; Midmore, B.R. Synthetic Bilayer Adsorption onto Polystyrene Microspheres. *Langmuir* **1992**, *8*, 801–806. [CrossRef]
34. Carmona-Ribeiro, A.M.; de Moraes Lessa, M. Interactions between Bilayer Membranes and Latex. *Colloids Surf. A Physicochem. Eng. Asp.* **1999**, *153*, 355–361. [CrossRef]
35. Pereira, E.M.A.; Vieira, D.B.; Carmona-Ribeiro, A.M. Cationic Bilayers on Polymeric Particles: Effect of Low NaCl Concentration on Surface Coverage. *J. Phys. Chem. B* **2004**, *108*, 11490–11495. [CrossRef]
36. Rapuano, R.; Carmona-Ribeiro, A.M. Supported Bilayers on Silica. *J. Colloid Interface Sci.* **2000**, *226*, 299–307. [CrossRef]
37. Moura, S.P.; Carmona-Ribeiro, A.M. Cationic Bilayer Fragments on Silica at Low Ionic Strength: Competitive Adsorption and Colloid Stability. *Langmuir* **2003**, *19*, 6664–6667. [CrossRef]
38. Lincopan, N.; Santana, M.R.; Faquim-Mauro, E.; da Costa, M.H.B.; Carmona-Ribeiro, A.M. Silica-Based Cationic Bilayers as Immunoadjuvants. *BMC Biotechnol.* **2009**, *9*, 5. [CrossRef] [PubMed]
39. Ribeiro, R.T.; Braga, V.H.A.; Carmona-Ribeiro, A.M. Biomimetic Cationic Nanoparticles Based on Silica: Optimizing Bilayer Deposition from Lipid Films. *Biomimetics* **2017**, *2*, 20. [CrossRef]
40. Pereira, E.M.A.; Kosaka, P.M.; Rosa, H.; Vieira, D.B.; Kawano, Y.; Petri, D.F.S.; Carmona-Ribeiro, A.M. Hybrid Materials from Intermolecular Associations between Cationic Lipid and Polymers. *J. Phys. Chem. B* **2008**, *112*, 9301–9310. [CrossRef]
41. Sobral, C.N.C.; Soto, M.A.; Carmona-Ribeiro, A.M. Characterization of DODAB/DPPC Vesicles. *Chem. Phys. Lipids* **2008**, *152*, 38–45. [CrossRef] [PubMed]
42. Carmona-Ribeiro, A.M. Self-Assembled Antimicrobial Nanomaterials. *Int. J. Environ. Res. Public Health* **2018**, *15*, 1408. [CrossRef]
43. Galvão, C.N.; Sanches, L.M.; Mathiazzi, B.I.; Ribeiro, R.T.; Petri, D.F.S.; Carmona-Ribeiro, A.M. Antimicrobial Coatings from Hybrid Nanoparticles of Biocompatible and Antimicrobial Polymers. *Int. J. Mol. Sci.* **2018**, *19*, 2965. [CrossRef] [PubMed]
44. Grabowski, E.; Morrison, I. Particle size distribution from analysis of quasi-elastic light-scattering data. In *Measurement of Suspended Particles by Quasi-Elastic Light-Scattering*; Dahneke, B., Ed.; Wiley Interscience: New York, NY, USA, 1983; pp. 199–236, ISBN 0-471-87289-X.
45. Ribeiro, R.T.; Galvão, C.N.; Betancourt, Y.P.; Mathiazzi, B.I.; Carmona-Ribeiro, A.M. Microbicidal Dispersions and Coatings from Hybrid Nanoparticles of Poly(Methyl Methacrylate), Poly(Diallyl Dimethyl Ammonium) Chloride, Lipids, and Surfactants. *Int. J. Mol. Sci.* **2019**, *20*, 6150. [CrossRef]
46. Schales, O.; Schales, S.S. A Simple and Accurate Method for the Determination of Chloride in Biological Fluids. *J. Biol. Chem.* **1941**, *140*, 879–882. [CrossRef]
47. Walker, J.M. The Bicinchoninic Acid (BCA) Assay for Protein Quantitation. *Methods Mol. Biol.* **1994**, *32*, 5–8. [CrossRef]
48. Hilgers, L.A.; Snippe, H. DDA as an Immunological Adjuvant. *Res. Immunol.* **1992**, *143*, 494–503; discussion 574–576. [CrossRef]
49. Lage, R.S.; Oliveira, G.C.; Busek, S.U.; Guerra, L.L.; Giunchetti, R.C.; Corrêa-Oliveira, R.; Reis, A.B. Analysis of the Cytokine Profile in Spleen Cells from Dogs Naturally Infected by Leishmania Chagasi. *Vet. Immunol. Immunopathol.* **2007**, *115*, 135–145. [CrossRef] [PubMed]
50. Patra, C.N.; Priya, R.; Swain, S.; Kumar Jena, G.; Panigrahi, K.C.; Ghose, D. Pharmaceutical Significance of Eudragit: A Review. *Future J. Pharm. Sci.* **2017**, *3*, 33–45. [CrossRef]
51. Carmona-Ribeiro, A.M.; Araújo, P.M. Antimicrobial Polymer-Based Assemblies: A Review. *Int. J. Mol. Sci.* **2021**, *22*, 5424. [CrossRef] [PubMed]
52. Martins, L.M.S.; Mamizuka, E.M.; Carmona-Ribeiro, A.M. Cationic Vesicles as Bactericides. *Langmuir* **1997**, *13*, 5583–5587. [CrossRef]
53. Sicchierolli, S.M.; Mamizuka, E.M.; Carmona-Ribeiro, A.M. Bacteria Flocculation and Death by Cationic Vesicles. *Langmuir* **1995**, *11*, 2991–2995. [CrossRef]

54. Tapias, G.N.; Sicchierolli, S.M.; Mamizuka, E.M.; Carmona-Ribeiro, A.M. Interactions between Cationic Vesicles and *Escherichia coli*. *Langmuir* **1994**, *10*, 3461–3465. [CrossRef]
55. Campanhã, M.T.; Mamizuka, E.M.; Carmona-Ribeiro, A.M. Interactions between Cationic Liposomes and Bacteria: The Physical-Chemistry of the Bactericidal Action. *J. Lipid Res.* **1999**, *40*, 1495–1500. [CrossRef]
56. Carmona-Ribeiro, A.M.; Midmore, B.R. Surface Potential in Charged Synthetic Amphiphile Vesicles. *J. Phys. Chem.* **1992**, *96*, 3542–3547. [CrossRef]
57. Melo, L.D.; Palombo, R.R.; Petri, D.F.S.; Bruns, M.; Pereira, E.M.A.; Carmona-Ribeiro, A.M. Structure–Activity Relationship for Quaternary Ammonium Compounds Hybridized with Poly(Methyl Methacrylate). *ACS Appl. Mater. Interfaces* **2011**, *3*, 1933–1939. [CrossRef] [PubMed]
58. Rapuano, R.; Carmona-Ribeiro, A.M. Physical Adsorption of Bilayer Membranes on Silica. *J. Colloid Interface Sci.* **1997**, *193*, 104–111. [CrossRef] [PubMed]
59. Carmona-Ribeiro, A.M.; Ortis, F.; Schumacher, R.I.; Armelin, M.C.S. Interactions between Cationic Vesicles and Cultured Mammalian Cells. *Langmuir* **1997**, *13*, 2215–2218. [CrossRef]
60. Perez-Betancourt, Y.; de Carvalho Lins Fernandes Távora, B.; Colombini, M.; Faquim-Mauro, E.L.; Carmona-Ribeiro, A.M. Simple Nanoparticles from the Assembly of Cationic Polymer and Antigen as Immunoadjuvants. *Vaccines* **2020**, *8*, 105. [CrossRef]
61. Gan, L.M.; Chew, C.H.; Ng, S.C.; Loh, S.E. Polymerization of Methyl Methacrylate in Ternary Systems: Emulsion and Microemulsion. *Langmuir* **1993**, *9*, 2799–2803. [CrossRef]
62. Arif, U.; Haider, S.; Haider, A.; Khan, N.; Alghyamah, A.A.; Jamila, N.; Khan, M.I.; Almasry, W.A.; Kang, I.-K. Biocompatible Polymers and Their Potential Biomedical Applications: A Review. *Curr. Pharm. Des.* **2019**, *25*, 3608–3619. [CrossRef]
63. Webster, O.W. Group Transfer Polymerization: A Critical Review of Its Mechanism and Comparison with Other Methods for Controlled Polymerization of Acrylic Monomers. In *New Synthetic Methods*; Springer: Berlin/Heidelberg, Germany, 2004; pp. 1–34, ISBN 978-3-540-36458-0.
64. Xu, L.; Liu, Y.; Chen, Z.; Li, W.; Liu, Y.; Wang, L.; Liu, Y.; Wu, X.; Ji, Y.; Zhao, Y.; et al. Surface-Engineered Gold Nanorods: Promising DNA Vaccine Adjuvant for HIV-1 Treatment. *Nano Lett.* **2012**, *12*, 2003–2012. [CrossRef]

7 | Cationic nanostructures as adjuvants for vaccines

Metadata of the chapter that will be visualized online

Chapter Title	Cationic Nanostructures as Adjuvants for Vaccines	
Copyright Year	2022	
Copyright Holder	The Author(s), under exclusive license to Springer Science+Business Media, LLC, part of Springer Nature	
Corresponding Author	Family Name	**Carmona-Ribeiro**
	Particle	
	Given Name	**Ana Maria**
	Suffix	
	Division	Biocolloids Laboratory, Departamento de Bioquímica, Instituto de Química
	Organization	Universidade de São Paulo
	Address	São Paulo, Brazil
	Email	amcr@usp.br
Author	Family Name	**Mathiazzi**
	Particle	
	Given Name	**Beatriz Ideriha**
	Suffix	
	Division	Biocolloids Laboratory, Departamento de Bioquímica, Instituto de Química
	Organization	Universidade de São Paulo
	Address	São Paulo, Brazil
Author	Family Name	**Pérez-Betancourt**
	Particle	
	Given Name	**Yunys**
	Suffix	
	Division	Biocolloids Laboratory, Departamento de Bioquímica, Instituto de Química
	Organization	Universidade de São Paulo
	Address	São Paulo, Brazil
Abstract	Spherical or discoidal lipid polymer nanostructures bearing cationic charges successfully adsorb a variety of oppositely charged antigens (Ag) such as proteins, peptides, nucleic acids, or oligonucleotides. This report provides instructions for the preparation and physical characterization of four different cationic nanostructures able to combine and deliver antigens to the immune system: (1) dioctadecyl dimethylammonium bromide (DODAB) bilayer fragments (DODAB BF); (2) polystyrene sulfate (PSS) nanoparticles (NPs) covered with one cationic dioctadecyl dimethylammonium bromide bilayer (DODAB) named (PSS/DODAB); (3) cationic NPs of biocompatible polymer poly(methyl methacrylate) (PMMA) prepared by emulsion polymerization of the methyl	

	methacrylate (MMA) monomer in the presence of DODAB BF (PMMA/ DODAB NPs); (4) antigen NPs (NPs) where the cationic polymer poly (diallyl dimethyl ammonium chloride) (PDDA) directly combined at nontoxic and low dose with the antigen (Ag); when the oppositely charged model antigen is ovalbumin (OVA), NPs are named PDDA/OVA. These nanostructures provide adequate microenvironments for carrying and delivering antigens to the antigen-presenting cells of the immune system.
Keywords (separated by '-')	Polymeric NPs - Cationic lipid - Bilayer fragments or nanodisks - Cationic polymer - Model antigen ovalbumin - Poly(diallyl dimethyl ammonium) chloride - Poly(methylmethacrylate) - Dioctadecyl dimethylammonium bromide - Immunoadjuvants

Chapter 10

Cationic Nanostructures as Adjuvants for Vaccines

Ana Maria Carmona-Ribeiro, Beatriz Ideriha Mathiazzi, and Yunys Pérez-Betancourt

Abstract

Spherical or discoidal lipid polymer nanostructures bearing cationic charges successfully adsorb a variety of oppositely charged antigens (Ag) such as proteins, peptides, nucleic acids, or oligonucleotides. This report provides instructions for the preparation and physical characterization of four different cationic nanostructures able to combine and deliver antigens to the immune system: (1) dioctadecyl dimethylammonium bromide (DODAB) bilayer fragments (DODAB BF); (2) polystyrene sulfate (PSS) nanoparticles (NPs) covered with one cationic dioctadecyl dimethylammonium bromide bilayer (DODAB) named (PSS/DODAB); (3) cationic NPs of biocompatible polymer poly(methyl methacrylate) (PMMA) prepared by emulsion polymerization of the methyl methacrylate (MMA) monomer in the presence of DODAB BF (PMMA/DODAB NPs); (4) antigen NPs (NPs) where the cationic polymer poly(diallyl dimethyl ammonium chloride) (PDDA) directly combined at nontoxic and low dose with the antigen (Ag); when the oppositely charged model antigen is ovalbumin (OVA), NPs are named PDDA/OVA. These nanostructures provide adequate microenvironments for carrying and delivering antigens to the antigen-presenting cells of the immune system.

Keywords Polymeric NPs, Cationic lipid, Bilayer fragments or nanodisks, Cationic polymer, Model antigen ovalbumin, Poly(diallyl dimethyl ammonium) chloride, Poly(methylmethacrylate), Dioctadecyl dimethylammonium bromide, Immunoadjuvants

1 Introduction

Cationic structures of nanometric size are especially suitable to carry and deliver antigens directly to antigen-presenting cells (APC) in the lymph nodes easily overcoming anatomical barriers from the injection site [1, 2]. They can be obtained from a variety of lipids, polymers, or lipids and polymers mostly as bilayer vesicles [3], open bilayer disks [4–6], or hybrid nanoparticles (NPs) [5, 7–14]. Cationic nanostructures applied to vaccine design were recently reviewed [15].

In particular, the cationic and synthetic lipid dioctadecyldimethylammonium bromide (DODAB) self-assembles as both

Sunil Thomas (ed.), *Vaccine Design: Methods and Protocols, Vol. 3. Resources for Vaccine Development*, Methods in Molecular Biology, vol. 2412, https://doi.org/10.1007/978-1-0716-1892-9_10,
© The Editor(s) (if applicable) and The Author(s), under exclusive license to Springer Science+Business Media, LLC, part of Springer Nature 2022

Uncorrected Proof

closed and large bilayer vesicles [16, 17] or as open and cationic bilayer fragments or nanodisks (DODAB BF). The sizes of DODAB BF are below 100 nm, they are stabilized by the electrostatic repulsion, and they fuse to yield large vesicles upon addition of monovalent salt and screening of the surface potential [18]. DODAB bilayers can combine with a broad variety of antigens or enhancers of the immune response such as proteins [3, 19, 20], peptides [11, 21, 22], oligonucleotides [6, 23], mononucleotides [24, 25], or nucleic acids [26, 27] driving an enhanced cell-mediated immune response but a poor humoral response in several instances [3, 5–7]. The preparation and characterization of DODAB BF dispersions in water (Fig. 1) is stated in Subheading 3.1.

The versatile DODAB assemblies also interact with oppositely charged particles such as polystyrene sulfate (PSS) latexes [7, 11, 29–31] or silica [32–35]. Optimal deposition of DODAB bilayers on PSS NPs [7, 11, 31] or silica was achieved [34, 35] paving the way for their use as suitable immunoadjuvants and antigen carriers. Subheading 3.2 describes the preparation and characterization of PSS/DODAB NPs (Fig. 2), where a single DODAB bilayer surrounds each PSS NP [11].

The good miscibility of DODAB with the biocompatible polymer poly(methylmethacrylate) (PMMA) [8, 36] led to the synthesis of polymeric PMMA/DODAB NPs by emulsion polymerization of methylmethacrylate (MMA) in the presence of DODAB BF [14]. Subheading 3.3 describes this synthesis yielding the hybrid, cationic, and nanometric PMMA/DODAB NPs (Fig. 3). The cationic, hydrophilic, and antimicrobial polymer PDDA [10, 37, 38] combined by electrostatic attraction with oppositely charged biopolymers such as bovine serum albumin (BSA) [39] and ovalbumin (OVA) also yielded cationic NPs [13]. This led to the proposition of PDDA as a suitable immunoadjuvant combined with antigens; at low PDDA doses, its toxicity was nondetectable. Furthermore, PDDA/antigen NPs (Fig. 4) enhanced the humoral response to levels even higher than those elicited by the classical adjuvant alum [13]. Subheading 3.4 of the protocol details the PDDA/ovalbumin (OVA) NP preparation.

Uncorrected Proof

2 Materials

Prepare all solutions using analytical grade reagents and ultrapure water (prepared by purifying deionized water to attain a sensitivity of 18 M Ω cm at 25 °C). All reagents should be prepared at room temperature unless indicated otherwise. DODAB dispersions should be freshly prepared and used within 1–2 days after dispersion. Polymeric microspheres should be stored refrigerated at 4 °C to avoid microbial growth.

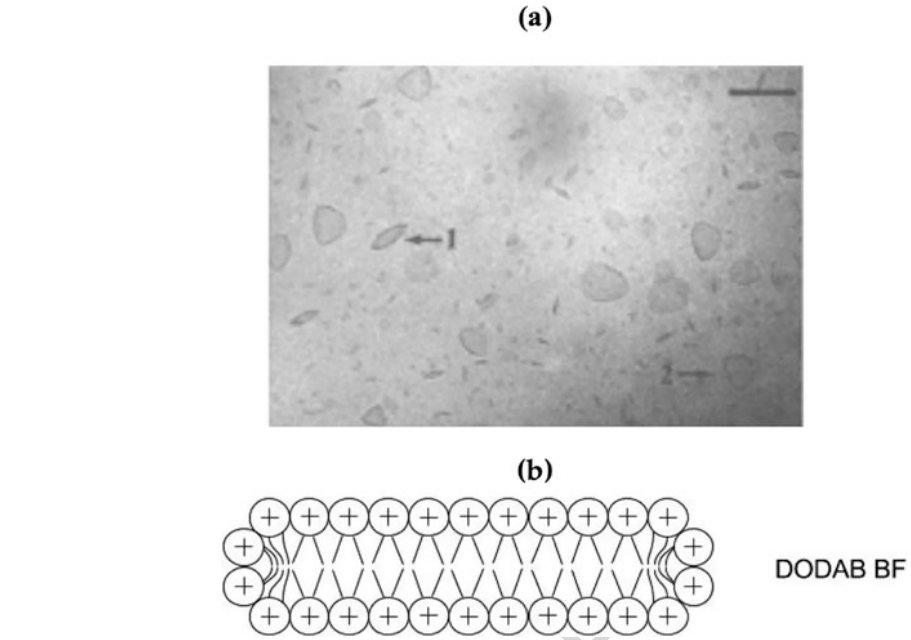


Fig. 1 (**a**) Bilayer fragments of dioctadecyldimethylammonium bromide (DODAB BF) visualized face-on and edge-on by cryo-transmission electron microscopy where the bar denotes 100 nm and the scheme shows a cross section of DODAB BF. The micrograph was adapted with permission from [28]. (**b**) Schematic representation of a DODAB BF cross section

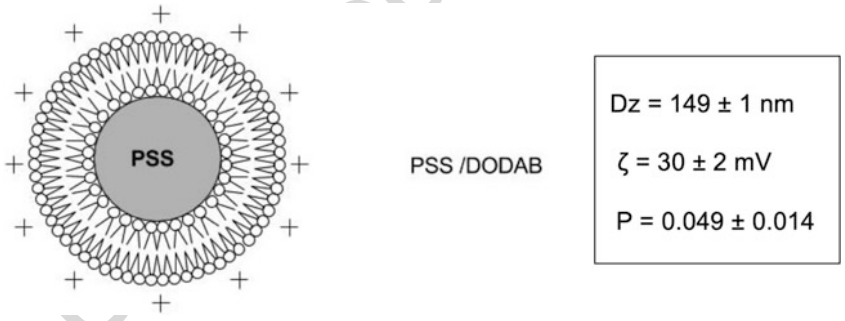


Fig. 2 Scheme of a cross section of a polystyrene sulfate nanoparticle (PSS) supporting a cationic bilayer of dioctadecyldimethylammonium bromide (DODAB). The mean hydrodynamic diameter (Dz), the zeta-potential (ζ) and the polydispersity of the dispersion in 1 mM NaCl were from ref. 11

2.1 Preparation and Characterization of DODAB BF

1. 1 mM NaCl solution in water.
2. DODAB BF: add 32.0 mg of the DODAB powder in 25 mL of a 1 mM NaCl solution in water. Make fresh on the day of the experiment (*see* **Notes 1** and **2**).
3. 10 mM $Hg(NO_3)_2$/0.04 M HNO_3 stock solution. Store in a dark vessel to protect this solution from light.

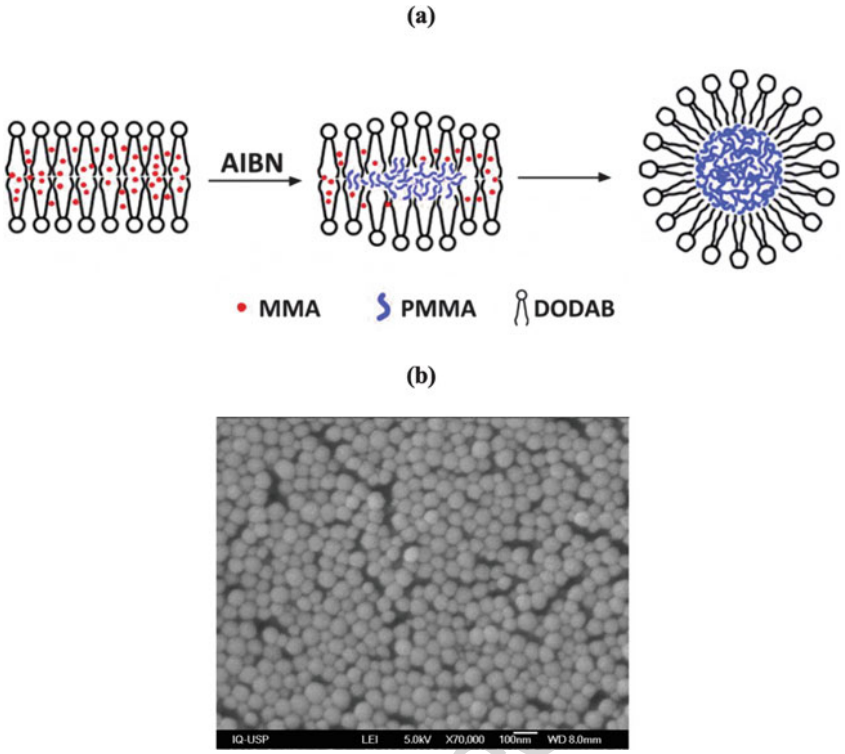


Fig. 3 Scheme illustrating the polymerization of methyl methacrylate (MMA) in the presence of DODAB BF using AIBN as initiator. The PMMA/DODAB hybrid NPs in 1 mM NaCl are shown in the scanning electron micrograph. From DLS, in 1 mM NaCl aqueous solution, these NPs exhibited Dz = 75 ± 1 nm, $\zeta = 49 \pm 4$ mV, and $P = 0.037 \pm 0.005$ [14] AU1

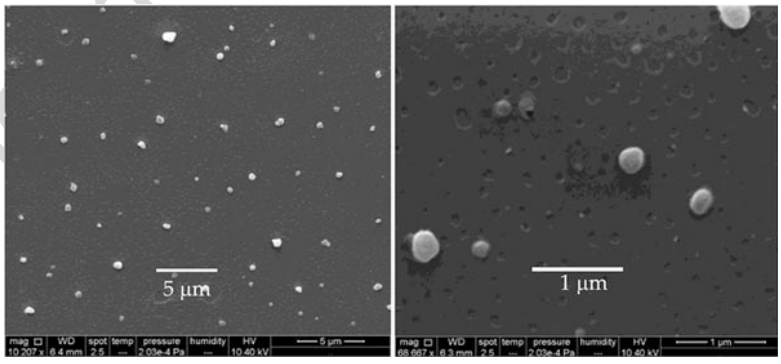


Fig. 4 Scanning electron micrographs of PDDA/OVA NPs under low and high magnification. NPs were obtained at 0.01 mg/mL PDDA and 0.1 mg/mL OVA in pure water. The mean diameter (*D*) of dry NPs evaluated from the micrographs using the ImageJ software was 234 ± 42 nm. The same NPs dispersion evaluated by DLS in pure water yielded Dz = 170 ± 4 nm, $\zeta = 30 \pm 2$ mV, and $P = 0.11 \pm 0.01$ [13]

Uncorrected

4. 0.01N HCl solution: prepare by diluting standard solution of 0.1N HCl tenfold (*see* **Note 3**).
5. 1 mM $Hg(NO_3)_2$ in 0.04 M HNO_3: make 1:10 dilution of 10 mM $Hg(NO_3)_2$ in 0.04 M HNO_3 (*see* **Note 4**).
6. 0.01 mg/mL diphenylcarbazone ethanolic solution: dissolve 50 μg of diphenylcarbazone in 5 mL ethanol (*see* **Note 5**).
7. Macrotip probe powered by an ultrasound source at a nominal output of 90 W (*see* **Note 6**).
8. High speed refrigerated centrifuge capable of 20,000 × *g*, e.g., Model SCR20B.
   (Hitachi) equipped with a RPR20-2-3079 rotor (*see* **Note 7**).
9. DLS and Zeta-potential Analyzer for particle sizing, zeta-potential analysis, and determination of polydispersity (*see* **Notes 8** and **9**). Cuvettes with four transparent faces for DLS instrument.

2.2 Preparation and Characterization of PSS/DODAB NPs

1. 5.97×10^{13} particles/mL PSS dispersion of polymeric particles (Interfacial Dynamics Corporation) with nominal diameters around 140 nm (*see* **Note 10**).
2. DODAB BF at 2 mM DODAB prepared as in the previous protocol (**protocol 1**).
3. Combine PSS NPs and DODAB BF in the following order:
   (i) 0.2 mL of the stock PSS dispersion.
   (ii) 2.5 mL of the 2 mM DODAB BF dispersion.
   (iii) 2.3 mL of 1 mM NaCl solution.
   Allow the components to interact for 1 h at 25 °C (*see* **Note 11**).
4. DLS and Zeta-potential Analyzer for particle sizing, zeta-potential analysis, and determination of polydispersity (*see* again **Notes 8** and **9**). Cuvettes with four transparent faces for DLS instrument.
5. High-speed refrigerated centrifuge capable of 20,000 × *g*, e.g., Model SCR20B.
   (Hitachi) equipped with a RPR20-2-3079 rotor.
6. Sonicator macroprobe (1 cm diameter).

2.3 Preparation and Characterization of PMMA/DODAB NPs

Uncorrected Proof

2.3.1 Preparation of DODAB BF Dispersion at 10 mM in 1 mM NaCl

1. 1 mM NaCl solution in water.
2. 10 mM DODAB BF dispersion: add 160.0 mg of the DODAB powder in 25 mL of a 1 mM NaCl solution in water. Make fresh on the day of the experiment (*see* again **Notes 1** and **2**).
3. 10 mM $Hg(NO_3)_2$/0.04 M HNO_3 stock solution. Store in a dark vessel to protect this solution from light.
4. 0.01N HCl solution: Prepare by diluting standard solution of 0.1N HCl tenfold (*see* again **Note 3**).
5. 1 mM $Hg(NO_3)_2$ in 0.04 M HNO_3: make 1:10 dilution of 10 mM $Hg(NO_3)_2$ in 0.04 M HNO_3 (*see* again **Note 4**).
6. 0.01 mg/mL diphenylcarbazone ethanolic solution: dissolve 50 μg of diphenylcarbazone in 5 mL ethanol (*see* again **Note 5**).
7. Macrotip probe powered by an ultrasound source at a nominal output of 90 W (*see* again **Note 6**).
8. High-speed refrigerated centrifuge capable of 20,000 × *g*, e.g., Model SCR20B.
   (Hitachi) equipped with a RPR20-2-3079 rotor (*see* again **Note 7**).
9. DLS and Zeta-potential Analyzer for particle sizing, zeta-potential analysis and determination of polydispersity (*see* again **Notes 8** and **9**). Cuvettes with four transparent faces for DLS instrument.

2.3.2 Synthesis of PMMA/DODAB NPs by Emulsion Polymerization

1. 1 mM NaCl solution in water.
2. MMA at least 99% pure.
3. Initiator AIBN powder.
4. Glass assay tube of 28 mL closed with a cap.
5. Vortex.
6. Magnetic stirrer with a hot plate.
7. Water bath at 80 °C suitable for using with the magnetic stirrer.
8. Cellulose acetate dialysis membranes with a molecular weight cut-off around 12,400 g/mol.
9. DLS and Zeta-potential Analyzer for particle sizing, zeta-potential analysis and determination of polydispersity (*see* **Notes 8** and **9**). Cuvettes with four transparent faces for DLS instrument.
10. High-speed refrigerated centrifuge capable of 20,000 × *g*, e.g., Model SCR20B.
    (Hitachi) equipped with a RPR20-2-3079 rotor (*see* again **Note 7**).

Uncorrected Proof

11. 10 mM $Hg(NO_3)_2$/0.04 M HNO_3 stock solution. Store in a dark vessel to protect this solution from light.
12. 0.01N HCl solution: Prepare by diluting standard solution of 0.1N HCl tenfold (*see* again **Note 3**).
13. 1 mM $Hg(NO_3)_2$ in 0.04 M HNO_3: make 1:10 dilution of 10 mM $Hg(NO_3)_2$ in 0.04 M HNO_3 (*see* again **Note 4**).
14. 0.01 mg/mL diphenylcarbazone ethanolic solution: dissolve 50 μg of diphenylcarbazone in 5 mL ethanol (*see* again **Note 5**).

2.4 Preparation and Characterization of PDDA/OVA NPs.

1. Stock solution of PDDA 10 mg/mL: Dilute 0.262 mL of PDDA and complete up to 10 mL of Milli Q water, mix thoroughly on vortex. Store solution at room temperature.
2. Stock solution of OVA 10 mg/mL: Dissolve 10 mg of OVA in 1 mL of Milli Q water, stir the mixture at low rpm and room temperature during 30 min. OVA stock solution must be prepared on the day of the experiment.
3. Vortex.
4. DLS and Zeta-potential Analyzer for particle sizing, zeta-potential analysis and determination of polydispersity (*see* **Notes 8** and **9**). Cuvettes for DLS instrument.
5. Stirrer.

3 Methods

3.1 Preparation and Characterization of DODAB BF

1. To make a dispersion of DODAB BF, sonicate the freshly prepared DODAB/1 mM NaCl solution with a macrotip probe at a nominal output of 90 W for 20 min. Maintain the temperature at 60 °C.
2. Centrifuge the dispersion for 60 min at 10,000 × *g* and 4 °C in order to eliminate residual titanium particles ejected from the macrotip probe. Discard the dark titanium pellet by withdrawing the supernatant of DODAB BF with a Pasteur pipette.
3. Determine DODAB analytical concentrations in the dispersion by halide microtitration using the analytical solution of Hg $(NO_3)_2$ and two or three droplets of the ethanol diphenyl carbazone solution as indicator of endpoint.
4. Adjust DODAB concentration in the DODAB BF dispersion to 2 mM. Aliquots of this dispersion will be used for combination with antigen.

3.2 Preparation and Characterization of PSS/DODAB NPs

1. To prepare the DODAB BF dispersions, sonicate DODAB powder in the 1 mM NaCl water solution with a macrotip for 15 min (80–90 mW).

Uncorrected Proof

t.1 **Table 1**
Physical properties of cationic nanostructured adjuvants dispersed in water as determined by DLS. Mean hydrodynamic diameter (Dz), zeta-potential (ζ), and polydispersity (P) of the adjuvant dispersions were determined by DLS following protocols 1–4 AU3

t.2 Protocol	Adjuvant	Dz (nm)	ζ (mV)	P	References
t.3 1	DODAB BF	73 ± 4	41 ± 3	0.29 ± 0.03	[5]
t.4 2	PSS/DODAB	149 ± 1	30 ± 2	0.05 ± 0.01	[11]
t.5 3	PMMA/DODAB	75 ± 1	49 ± 5	0.04 ± 0.01	[14]
t.6 4	PDDA/OVA	170 ± 4	30 ± 2	0.11 ± 0.01	[13]

2. To precipitate titanium residues ejected from the macrotip, centrifuge the sonicated DODAB dispersion at 10,000 × *g* in a refrigerated centrifuge for 40 min at 15 °C.
3. Determine DODAB and NaCl analytical concentrations in the dispersion by halide microtitration using the analytical solution of $Hg(NO_3)_2$ and two or three droplets of the ethanolic diphenylcarbazone solution as indicator of endpoint.
4. Combine PSS NPs and DODAB BF in the following order:
   (i) 0.2 mL of the stock PSS dispersion.
   (ii) 2.5 mL of the 2 mM DODAB BF dispersion.
   (iii) 2.3 mL of 1 mM NaCl solution.
5. Allow the components to interact for 1 h at 25 °C (*see* **Note 11**).
6. Determine zeta-average diameters, zeta-potentials and polydispersities for all dispersions using DLS instrument. Follow manufacturer procedures to conduct DLS measurements. Results should be very similar to those in Table 1 (*see* **Note 12**).

3.3 Preparation and Characterization of PMMA/DODAB NPs

3.3.1 Preparation of DODAB BF Dispersion at 10 mM in 1 mM NaCl

1. To make a dispersion of DODAB BF, sonicate the freshly prepared DODAB/1 mM NaCl solution with a macrotip probe at a nominal output of 90 W for 20 min. Maintain the temperature at 60 °C.
2. Centrifuge the dispersion for 60 min at 10,000 × *g* and 4 °C in order to eliminate residual titanium particles ejected from the macrotip probe. Discard the dark titanium pellet by withdrawing the supernatant of DODAB BF with a Pasteur pipette.
3. Determine DODAB analytical concentrations in the dispersion by halide microtitration using the analytical solution of $Hg(NO_3)_2$ and two or three droplets of the ethanol diphenyl carbazone solution as indicator of endpoint.

Uncorrected Proof

3.3.2 Synthesis of PMMA/DODAB NPs by Emulsion Polymerization

1. Prepare a heating system using the magnetic stirrer with a hot plate and a magnet into the water bath at 80 °C.
2. In the glass assay tube of 28 mL with a cap, transfer 2 mL of 10 mM DODAB BF dispersion and 7.57 mL of 1 mM NaCl solution in water.
3. Apply a flow of nitrogen gas for 1 min to the contents of the tube in order to eliminate oxygen.
4. Add 0.43 mL of MMA 99%, close the tube with a cap and mix using vortex for 30 s.
5. Add 3.6 mg of AIBN powder and vortex again.
6. Place the assay tube containing the reaction mixture in the water bath and keep it at 80 °C for 1 h, vortexing every 2 min.
7. Withdraw the assay tube containing the reaction mixture from the water bath and allow the reaction system to reach room temperature.
8. Transfer the contents of the tube in the dialysis bag and purify by dialysis against 2 L of ultrapure water (3×) for 24 h.
9. For particle characterization after dialysis, use dilutions of 20–30 times of the original dispersions.
10. Transfer 2 mL of the diluted PMMA/DODAB dispersion into a DLS cuvette for determining its zeta-average diameter and zeta-potential. Follow manufacturer procedures to conduct DLS measurements. These should yield small cationic particles with zeta-potential around +49 mV and the diameter around 75 nm.
11. Centrifuge the original dispersion for 60 min at 10,000 × *g* and 4 °C before the analytical determination of the DODAB concentration in the supernatant by halide microtitration. Withdraw the supernatant with a Pasteur pipette for determining DODAB concentration.
12. Determine DODAB concentration in the PMMA/DODAB NPs by halide microtitration of the supernatant, using the analytical solution of $Hg(NO_3)_2$ and two or three droplets of the ethanol diphenyl carbazone solution as indicator of endpoint.

3.4 Preparation and Characterization of PDDA/OVA NPs

1. To prepare 10 mL of PDDA/OVA NPs, combine the stock solutions as follows:
   (i) In a tube containing 9.89 mL of Milli Q water, add 0.01 mL of PDDA stock solution and vortex thoroughly.
   (ii) Into the solution obtained in (i), add 0.1 mL of stock solution of OVA and vortex for 30 s (*see* **Note 13**).
2. Transfer 2 mL of the PDDA/OVA dispersion into a DLS cuvette for determining zeta-average diameter and zeta-

Uncorrected Proof

potential of the dispersion. Follow manufacturer procedures to conduct DLS measurements. These should yield small cationic particles with zeta-potential around 30 mV and the diameter around 170 nm.

4 Notes

1. This should yield 2 mM DODAB final concentration.
2. DODAB dispersions should be always prepared above the mean gel-to-liquid crystalline phase transition temperature of the DODAB bilayer that is around 45 °C [40]. Thus, DODAB should be dispersed in 1 mM NaCl aqueous solution always at temperatures above 50 °C. Sonication will raise the temperature above 50 °C, so further heating the sample is not required. Other important property to note is the low stability of the BFs in moderate to high ionic strength solutions. Above 10 mM concentrations of monovalent salts, DODAB BFs will fuse to yield larger assemblies [18].
3. This solution will be used for titrating the previous solution and determining its analytical $Hg(NO_3)_2$ concentration.
4. This solution will be used to microtitrate bromide (in DODAB dispersions) or chloride (in 1 mM NaCl solution). Details on the microtitration procedure where the mercury caption forms a complex with halides can be found on refs. 41–43.
5. This solution allows determining the endpoint of the halide microtitration where the indicator changes color at the end point.
6. This will disperse the DODAB powder in the 1 mM NaCl solution for 20 min to yield the BFs dispersion.
7. This will centrifuge the sonicated DODAB dispersion aiming at precipitation of titanium microparticles ejected from the tip of the macro-probe.
8. We used a ZetaPlus Zeta-potential Analyzer (Brookhaven Instruments Corporation, Holtsville, NY) equipped with a 677-nm laser and dynamic light scattering at 90°.
9. Mean hydrodynamic diameters should be obtained by fitting intensity of light scattered to log-normal size distributions which do not discriminate between one, two, or more different populations and consider all scattering particles as belonging to one single Gaussian population. On the other hand, for the size distribution data, fitting should be done using the non-negatively constrained least squares (NNLS) algorithm available from the light scattering apparatus, which is a model-independent technique allowing to achieve multimodal

Uncorrected Proof

distributions [44]. ζ is usually determined from electrophoretic mobility μ in 1 mM NaCl and the Smoluchowski's equation: $\zeta = \mu\eta/\varepsilon$, where η is the medium viscosity and ε the medium dielectric constant: this is also provided by the apparatus software. The electrode of the apparatus should be used only over a low range of ionic strength (0–5 mM monovalent salt). High conductivities can damage the electrode.

10. The PSS original particles purchased from Interfacial Dynamics Corporation have their particle number density, size, surface charge density, and polydispersity specified in a specifications sheet provided by the supplier. In this protocol, the stock dispersion of anionic PSS NPs, nominal mean diameter from scanning electron micrographs of 0.137 ± 0.003 μm, 415,124 cm^2/g of specific surface area (SSA), surface charge density of 0.79 $\mu C/cm^2$, and −43 ± 3 mV of zeta-potential were obtained from the stock dispersion containing 5.97×10^{13} particles/mL. This stock dispersion can be further diluted in 1 mM NaCl solution in order to obtain the final desired NP concentration. PSS and DODAB BF should be prepared in 1 mM NaCl because this represents an adequate ionic strength to assemble DODAB BFs as a single bilayer onto PSS particles by fusion of adsorbed and adjacent BFs [31].
11. The knowledge of the accurate concentrations of DODAB in dispersion should allow calculation of the DODAB amount required to cover all particles with one bilayer:

    The final concentrations are 2.4×10^{12} particles/mL and 1 mM DODAB. This DODAB concentration is approximately the concentration required to allow coverage of each particle with a DODAB bilayer [11].
12. Note that upon coverage of each particle with a bilayer, the zeta-average diameter should increase by the equivalent of two bilayer thicknesses (one bilayer thickness is 4–5 nm).
13. Upon mixing PDDA and OVA in solution, formation of NPs is associated with the appearance of turbidity in the dispersion due to the light scattered by them.

Uncorrected Proof

Acknowledgments

This work was supported by grant 2019/17685-2, São Paulo Research Foundation (FAPESP) and 302758/2019-4, Conselho Nacional de Pesquisa e Desenvolvimento Tecnológico (CNPq). Y. P.-B is the recipient of a PhD fellowship from CNPq.

AU4

References

1. Xiang SD, Scholzen A, Minigo G, David C et al (2006) Pathogen recognition and development of particulate vaccines: does size matter? Methods 40:1–9. https://doi.org/10.1016/j.ymeth.2006.05.016
2. Manolova V, Flace A, Bauer M et al (2008) NPs target distinct dendritic cell populations according to their size. Eur J Immunol 38:1404–1413. https://doi.org/10.1002/eji.200737984
3. Tsuruta LR, Quintilio W, Costa MH et al (1997) Interactions between cationic liposomes and an antigenic protein: the physical chemistry of the immunoadjuvant action. J Lipid Res 38:2003–2011. https://www.jlr.org/content/38/10/2003.long
4. Carmona-Ribeiro AM (2006) Lipid bilayer fragments and disks in drug delivery. Curr Med Chem 13:1359–1370. https://doi.org/10.2174/092986706776872925
5. Lincopan N, Espindola NM, Vaz AJ et al (2009) Novel immunoadjuvants based on cationic lipid: preparation, characterization and activity in vivo. Vaccine 27:5760–5771. https://doi.org/10.1016/j.vaccine.2009.07.066
6. Rozenfeld JHK, Silva SR, Raneia PA et al (2012) Stable assemblies of cationic bilayer fragments and CpG oligonucleotide with enhanced immunoadjuvant activity in vivo. J Control Release 160:367–373. https://doi.org/10.1016/j.jconrel.2011.10.017
7. Lincopan N, Espindola NM, Vaz AJ et al (2007) Cationic supported lipid bilayers for antigen presentation. Int J Pharm 340:216–222. https://doi.org/10.1016/j.ijpharm.2007.03.014
8. Naves AF, Palombo RR, Carrasco LDM et al (2013) Antimicrobial particles from emulsion polymerization of methyl methacrylate in the presence of quaternary ammonium surfactants. Langmuir 29:9677–9684. https://doi.org/10.1021/la401527j
9. Carmona-Ribeiro AM (2014) Cationic nanostructures for vaccines. In: Guy Huynh Thien Duc GHT (ed) Immune response activation, 1st edn. IntechOpen, Rijeka, pp 1–45. https://www.intechopen.com/books/immune-response-activation/cationic-nanostructures-for-vaccines
10. Sanches LM, Petri DFS, de Melo Carrasco LD et al (2015) The antimicrobial activity of free and immobilized poly (diallyldimethylammonium) chloride in NPs of poly (methylmethacrylate). J Nanobiotechnol 13:58. https://jnanobiotechnology.biomedcentral.com/articles/10.1186/s12951-015-0123-3
11. Xavier GRS, Carmona-Ribeiro AM (2017) Cationic biomimetic particles of polystyrene/cationic bilayer/gramicidin for optimal bactericidal activity. Nanomaterials 7:12. https://doi.org/10.3390/nano7120422
12. Carmona-Ribeiro AM (2017) Nanomaterials based on lipids for vaccine development. In: Skwarczynski M, Toth I (eds) Micro- and nano-technology in vaccine development. Elsevier, Oxford, pp 241–257. https://doi.org/10.1016/B978-0-323-39981-4.00013-0
13. Perez-Betancourt Y, Tavora BCLF, Colombini M et al (2020) Simple nanoparticles from the assembly of cationic polymer and antigen as immunoadjuvants. Vaccine 8:105. https://doi.org/10.3390/vaccines8010105
14. Mathiazzi BI, Carmona-Ribeiro AM (2020) Hybrid NPs of poly (methyl methacrylate) and antimicrobial quaternary ammonium surfactants. Pharmaceutics 12:340. https://doi.org/10.3390/pharmaceutics12040340
15. Carmona-Ribeiro AM, Pérez-Betancourt Y (2020) Cationic nanostructures for vaccines design. Biomimetics 5:32. https://doi.org/10.3390/biomimetics5030032
16. Ribeiro AMC, Chaimovich H (1983) Preparation and characterization of large dioctadecyldimethylammonium chloride liposomes and comparison with small sonicated vesicles. Biochim Biophys Acta 733:172–179. https://doi.org/10.1016/0005-2736(83)90103-7
17. Carmona-Ribeiro AM (1992) Synthetic amphiphile vesicles. Chem Soc Rev 21:209–214. https://doi.org/10.1039/CS9922100209
18. Carmona-Ribeiro AM, Chaimovich H (1986) Salt-induced aggregation and fusion of dioctadecyldimethylammonium chloride and sodium dihexadecylphosphate vesicles. Biophys J 50:621–628. https://doi.org/10.1016/S0006-3495(86)83501-9
19. Carvalho LA, Carmona-Ribeiro AM (1998) Interactions between cationic vesicles and serum proteins. Langmuir 14:6077–6081. https://doi.org/10.1021/la980345j
20. Lincopan N, Carmona-Ribeiro AM (2009) Protein assembly onto cationic supported bilayers. J Nanosci Nanotechnol 9:3578–3586. https://doi.org/10.1166/jnn.2009.NS33
21. Carvalho CA, Olivares-Ortega C, Soto-Arriaza MA, Carmona-Ribeiro AM (2012) Interaction of gramicidin with DPPC/DODAB bilayer

Uncorrected Proof

fragments. Biochim Biophys Acta 1818:3064–3071. https://doi.org/10.1016/j.bbamem.2012.08.008

22. Ragioto DAMT, Carrasco LDM, Carmona-Ribeiro AM (2014) Novel gramicidin formulations in cationic lipid as broad-spectrum microbicidal agents. Int J Nanomedicine 9:3183–3192. https://doi.org/10.2147/IJN.S65289
23. Rozenfeld JHK, Oliveira TR, Lamy MT et al (2011) Interaction of cationic bilayer fragments with a model oligonucleotide. Biochim Biophys Acta 1808:649–655. https://doi.org/10.1016/j.bbamem.2010.11.036
24. Kikuchi IS, Viviani W, Carmona-Ribeiro AM (1999) Nucleotide insertion in cationic bilayers. J Phys Chem A 103:8050–8055. https://doi.org/10.1021/jp9911090
25. Nantes IL, Correia FM, Faljoni-Alario A et al (2003) Nucleotide conformational change induced by cationic bilayers. Arch Biochem Biophys 416:25–30. https://doi.org/10.1016/S0003-9861(03)00280-7
26. Rosa H, Petri DFS, Carmona-Ribeiro AM (2008) Interactions between bacteriophage DNA and cationic biomimetic particles. J Phys Chem B 112:16422–16430. https://doi.org/10.1021/jp806992f
27. Kikuchi IS, Carmona-Ribeiro AM (2000) Interactions between DNA and synthetic cationic liposomes. J Phys Chem B 104:2829–2835. https://doi.org/10.1021/jp9935891
28. Andersson M, Hammarstroem L, Edwards K (1995) Effect of bilayer phase transitions on vesicle structure, and its influence on the kinetics of viologen reduction. J Phys Chem 99:14531–14538. https://doi.org/10.1021/j100039a047
29. Carmona-Ribeiro AM, Midmore BR (1992) Synthetic bilayer adsorption onto polystyrene microspheres. Langmuir 8:801–806. https://doi.org/10.1021/la00039a013
30. Carmona-Ribeiro AM, de Moraes LM (1999) Interactions between bilayer membranes and latex. Colloids Surf A Physicochem Eng Asp 153:355–361. https://doi.org/10.1016/S0927-7757(98)00532-9
31. Pereira EMA, Vieira DB, Carmona-Ribeiro AM (2004) Cationic bilayers on polymeric particles: effect of low NaCl concentration on surface coverage. J Phys Chem B 108:11490–11495. https://doi.org/10.1021/jp060737w
32. Rapuano R, Carmona-Ribeiro AM (2000) Supported bilayers on silica. J Colloid Interface Sci 226:299–307. https://doi.org/10.1006/jcis.2000.6824
33. Moura SP, Carmona-Ribeiro AM (2003) Cationic bilayer fragments on silica at low ionic strength: competitive adsorption and colloid stability. Langmuir 19:6664–6667. https://doi.org/10.1021/la034334o
34. Lincopan N, Santana MR, Faquim-Mauro E et al (2009) Silica-based cationic bilayers as immunoadjuvants. BMC Biotechnol 9:5. https://doi.org/10.1186/1472-6750-9-5
35. Ribeiro RT, Braga VHA, Carmona-Ribeiro AM (2017) Biomimetic cationic NPs based on silica: optimizing bilayer deposition from lipid films. Biomimetics 2:20. https://doi.org/10.3390/biomimetics2040020
36. Pereira EMA, Kosaka PM, Rosa H et al (2008) Hybrid materials from intermolecular associations between cationic lipid and polymers. J Phys Chem B 112:9301–9310. https://doi.org/10.1021/jp801297t
37. Vieira DB, Carmona-Ribeiro AM (2008) Cationic NPs for delivery of amphotericin B: preparation, characterization and activity in vitro. J Nanobiotechnol 6:6. https://doi.org/10.1186/1477-3155-6-6
38. Melo LD, Mamizuka EM, Carmona-Ribeiro AM (2010) Antimicrobial particles from cationic lipid and polyelectrolytes. Langmuir 26:12300–12306. https://doi.org/10.1021/la101500s
39. Bohidar H, Dubin PL, Majhi PR et al (2005) Effects of protein-polyelectrolyte affinity and polyelectrolyte molecular weight on dynamic properties of bovine serum albumin-poly (diallyldimethylammonium chloride) coacervates. Biomacromolecules 6:1573–1585. https://doi.org/10.1021/bm049174p
40. Nascimento DB, Rapuano R, Lessa MM et al (1998) Counterion effects on properties of cationic vesicles. Langmuir 14:7387–7391. https://doi.org/10.1021/la980845c
41. Schales O, Schales SS (1941) A simple and accurate method for the determination of chloride in biological fluids. J Biol Chem 140:879–884
42. Carmona-Ribeiro AM (2012) Preparation and characterization of biomimetic nanoparticles for drug delivery. Methods Mol Biol 906:283–294. https://doi.org/10.1007/978-1-61779-953-2_22
43. Carmona-Ribeiro AM (2020) Biomimetic lipid polymer nanoparticles for drug delivery. Methods Mol Biol 2118:45–60. https://doi.org/10.1007/978-1-0716-0319-2_4
44. Grabowski E, Morrison I (1983) Particle size distribution from analysis of quasi-elastic light

Uncorrected Proof

scattering data. In: Danecke B (ed) Measurement of suspended particles by quasi-elastic light scattering. Wiley-Interscience, New York, pp 199–236

Uncorrected Proof

Author Queries

Chapter No.: 10 498165_2_En

Query Refs.	Details Required	Author's response
AU1	Part labels 'a and b' are mentioned in the artwork Fig. 3 but they are missing in the caption. Please check.	
AU2	Please provide appropriate section numbering for protocol 1.	
AU3	Please suggest whether Protcols 1 to 4 can be changed to Subheading 3.1 to 3.4 both in Table and in its caption.	
AU4	References have been sorted to maintain sequential order. Please confirm if correct.	

Uncorrected Proof

8 | Conclusions

Cationic and biocompatible PDDA/OVA, PMMA/DODAB/PDDA, and PMMA/DODAB nanoparticles were prepared and characterized regarding their physical properties, toxicity and immunoadjuvant activity. PDDA/OVA nanoparticles were prepared easily from the self-assembly of PDDA and OVA driven by electrostatic interactions; PMMA/DODAB and PMMA/DODAB/PDDA nanoparticles were synthesized by emulsion polymerization method in the presence of the cationic components. The three nanoparticles were stable colloids in water dispersions with nanometric size and narrow particle size distributions. Cationic PDDA/OVA nanoparticles were obtained practically in absence of free PDDA, while PMMA/DODAB/PDDA and PMMA/DODAB nanoparticles were obtained without free cationic components, assuring low toxicity in vitro. The toxicity of free PDDA was dose-dependent and displayed higher cytotoxicity as compared to immobilized PDDA. Likewise, the toxicity of hybrid PMMA/DODAB nanoparticles was smaller than those determined for DODAB large vesicles and DODAB bilayer fragments demonstrating, that the immobilization of PDDA and DODAB augments their biocompatibility. Nanoparticles were suitable to induce an improved immune response, determined by antibody and cytokine production and delayed-type hypersensitivity reaction, as compared with the antigen without adjuvant or antigen carried by aluminum hydroxide. The comparison of the four adjuvants (PDDA/OVA, PMMA/DODAB/PDDA/OVA, PMMA/DODAB/OVA, and DODAB-BF/OVA) showed that nanoparticles bearing PDDA elicited an immune response with a clear bias toward the Th2 type with high titers of IgG1, implying that PDDA preferentially induces this type of response. On the other hand, PMMA/DODAB nanoparticles and DODAB-

BF/OVA generated a more equitable Th1/Th2 response, in agreement with previous work describing high DODAB-induced Th1-biased response. We hypothesized that the strength of the interaction between antigens and cationic adjuvants affects the resultant immune response; the stronger interaction would lead to a Th2 immune response, while the weaker interaction would favor a Th1 immune response due to release of the antigen to cytosol and MHC class I presentation.

9 | Perspectives

1. To evaluate the genotoxic effect of PDDA, PMMA/DODAB/PDDA, and PMMA/DODAB nanoparticles using comet or micronucleus assays.

2. To study the mechanism through which PDDA enhances the immune response and mechanisms of activation of the Th2 immune response, emphasizing in the activation of NLRP3 inflammasome determined by quantification of IL-18 and IL-1β production in cultured lymphocytes.

3. To evaluate the ability of PDDA/OVA, PMMA/DODAB, and PMMA/DODAB/PDDA nanoparticles to deliver the antigens directly into lymph nodes by analyzing nanoparticles' biodistribution and in vivo fluorescence.

3. To identify the principal mechanisms by which PDDA/OVA, PMMA/DODAB/PDDA, and PMMA/DODAB nanoparticles are taken up by antigen-presenting cells by blocking the main mechanisms of cell internalization before quantifying the amount of fluorescent-antigen internalized using flow cytometry and fluorescent microscopy.

4. To identify if PDDA/OVA, PMMA/DODAB/PDDA, and PMMA/DODAB escape from endosomes using fluorescence microscopy to track the fate of antigens after internalization.

5. To assess the ability of PDDA/OVA, PMMA/DODAB/PDDA, and PMMA/DODAB nanoparticles to induce expression of MHC and co-stimulatory molecules in antigen-presenting cells using specific fluorescent-labeled antibodies and quantifying the fluorescence by flow cytometry.

6. To implement PDDA and PMMA/DODAB/PDDA, PMMA/DODAB as carriers of protein antigens different of OVA and assess the antibody, DTH, and cytokine production.

7. To test PDDA and PMMA/DODAB/PDDA, PMMA/DODAB nanoparticles as carriers for RNA and DNA vaccines and assess the resulting immune response by quantifying the antibody, DTH, and cytokine production.

8. To determine the capacity of PDDA, and PMMA/DODAB/PDDA, PMMA/DODAB nanoparticles as mucosal adjuvants using antigens from major pathogens such as influenza virus and SARS-CoV-2 virus and assessing the production of neutralizing IgA.

Bibliography

AALST, S. van; LUDWIG, I. S.; KOOTEN, P. J. S. van; ZEE, R. van der; EDEN, W. van; BROERE, F. Dynamics of APC recruitment at the site of injection following injection of vaccine adjuvants. Vaccine, v. 35, n. 12, p. 1622–1629, mar. 2017. ISSN 0264-410X. Disponível em: <https://www.sciencedirect.com/science/article/pii/S0264410X17301688>. Citado na página 22.

ABBAS, A. K.; LICHTMAN, A. H.; PILLAI, S. Cellular and molecular immunology. 9th. ed. Philadelphia, PA, USA: Elsevier Ltd, 2018. Pages: 608. ISBN 978-0-323-47978-3. Citado 3 vezes nas páginas 15, 16 e 17.

AKIRA, S. Innate immunity and adjuvants. Philosophical transactions of the Royal Society of London. Series B, Biological sciences, v. 366, n. 1579, p. 2748–2755, out. 2011. Citado na página 16.

ALMEIDA, A. F. de; GASPARI, E. D. Dioctadecyldimethylammonium bromide (DODAB-BF) as a new adjuvant for maternal-fetal immunization in mice against Neisseria meningitidis: evaluation of humoral response. Pathogens and disease, v. 76, n. 1, p. ftx128–ftx128, fev. 2018. Place: United States. Citado na página 32.

ANDERLUZZI, G.; LOU, G.; GALLORINI, S.; BRAZZOLI, M.; JOHNSON, R.; O'HAGAN, D. T.; BAUDNER, B. C.; PERRIE, Y. Investigating the Impact of Delivery System Design on the Efficacy of Self-Amplifying RNA Vaccines. Vaccines, v. 8, n. 2, 2020. ISSN 2076-393X. Disponível em: <https://www.mdpi.com/2076-393X/8/2/212>. Citado 2 vezes nas páginas 33 e 35.

ANDERLUZZI, G.; SCHMIDT, S. T.; CUNLIFFE, R.; WOODS, S.; ROBERTS, C. W.; VEGGI, D.; FERLENGHI, I.; O'HAGAN, D. T.; BAUDNER, B. C.; PERRIE, Y. Rational design of adjuvants for subunit vaccines: The format of cationic adjuvants affects the induction of antigen-specific antibody responses. Journal of Controlled Release, v. 330, p. 933–944, fev. 2021. ISSN 0168-3659. Disponível em: <https://www.sciencedirect.com/science/article/pii/S0168365920306477>. Citado na página 33.

APOSTóLICO, J. d. S.; LUNARDELLI, V. A. S.; COIRADA, F. C.; BOSCARDIN, S. B.; ROSA, D. S. Adjuvants: classification, modus operandi, and licensing. Journal of immunology research, v. 2016, p. 1459394–1459394, 2016. Edition: 2016/05/04 Publisher: Hindawi Publishing Corporation. Citado na página 22.

AWATE, S.; BABIUK, L. A.; MUTWIRI, G. Mechanisms of action of adjuvants. Frontiers in immunology, v. 4, p. 114–114, 2013. Publisher: Frontiers Media SA. Disponível em: <http://www.ncbi.nlm.nih.gov/pubmed/23720661>. Citado 5 vezes nas páginas 21, 22, 23, 24 e 27.

BALL, T.; CARRIèRE, A.; BARBEAU, B. Comparison of two online flocculation monitoring techniques for predicting turbidity removal by granular media filtration. Environmental technology, v. 32, n. 9-10, p. 1095–1105, jul. 2011. ISSN 0959-3330. Place: England. Citado na página 29.

BARON, L.; GOMBAULT, A.; FANNY, M.; VILLERET, B.; SAVIGNY, F.; GUILLOU, N.; PANEK, C.; BERT, M. L.; LAGENTE, V.; RASSENDREN, F.; RITEAU, N.; COUILLIN, I. The NLRP3 inflammasome is activated by nanoparticles through ATP, ADP and adenosine. Cell Death & Disease, v. 6, n. 2, p. e1629–e1629, fev. 2015. ISSN 2041-4889. Disponível em: <https://doi.org/10.1038/cddis.2014.576>. Citado na página 27.

BEHZADI, S.; SERPOOSHAN, V.; TAO, W.; HAMALY, M. A.; ALKAWAREEK, M. Y.; DREADEN, E. C.; BROWN, D.; ALKILANY, A. M.; FAROKHZAD, O. C.; MAHMOUDI, M. Cellular uptake of nanoparticles: journey inside the cell. Chemical Society reviews, v. 46, n. 14, p. 4218–4244, jul. 2017. ISSN 1460-4744. Disponível em: <https://pubmed.ncbi.nlm.nih.gov/28585944>. Citado 2 vezes nas páginas 25 e 26.

BENJAMINSEN, R. V.; MATTEBJERG, M. A.; HENRIKSEN, J. R.; MOGHIMI, S. M.; ANDRESEN, T. L. The possible “proton sponge ” effect of polyethylenimine (PEI) does not include change in lysosomal pH. Molecular Therapy, v. 21, n. 1, p. 149–157, 2013. Disponível em: <http://www.sciencedirect.com/science/article/pii/S1525001616305706>. Citado na página 30.

BLANCO, E.; SHEN, H.; FERRARI, M. Principles of nanoparticle design for overcoming biological barriers to drug delivery. Nature Biotechnology, v. 33, n. 9, p. 941–951, set. 2015. ISSN 1546-1696. Disponível em: <https://doi.org/10.1038/nbt.3330>. Citado na página 25.

BLANCO, J. C. G.; BOUKHVALOVA, M. S.; SHIREY, K. A.; PRINCE, G. A.; VOGEL, S. N. New insights for development of a safe and protective RSV vaccine. Human vaccines, v. 6, n. 6, p. 482–492, jun. 2010. Citado na página 19.

BOHIDAR, H.; DUBIN, P. L.; MAJHI, P. R.; TRIBET, C.; JAEGER, W. Effects of protein-polyelectrolyte affinity and polyelectrolyte molecular weight on dynamic properties of bovine serum albumin-poly(diallyldimethylammonium chloride) coacervates. Biomacromolecules, v. 6, n. 3, p. 1573–1585, 2005. Citado na página 31.

BRINKMAN, J. A.; FAUSCH, S. C.; WEBER, J. S.; KAST, W. M. Peptide-based vaccines for cancer immunotherapy. Expert opinion on biological therapy, v. 4, n. 2, p. 181–198, fev. 2004. Citado na página 18.

CARMONA-RIBEIRO, A. M. Biomimetic nanoparticles: preparation, characterization and biomedical applications. International journal of nanomedicine, v. 5, p. 249–259, abr. 2010. Citado na página 35.

CARMONA-RIBEIRO, A. M. Cationic nanostructures for vaccines. In: DUC, G. H. T. (Ed.). Immune Response Activation. 1. ed. Rijeka, Croatia: IntechOpen, 2014. p. 1–45. ISBN 978-953-51-1374-4. Citado na página 26.

CARMONA-RIBEIRO, A. M. Nanomaterials based on lipids for vaccine development. In: SKWARCZYNSKI, M.; TOTH, I. B. T. M. (Ed.). Micro and Nano Technologies. Oxford, UK: Elsevier, 2017. p. 241–257. ISBN 978-0-323-39981-4. Disponível em: <http://www.sciencedirect.com/science/article/pii/B9780323399814000130>. Citado na página 33.

CARMONA-RIBEIRO, A. M. The versatile dioctadecyldimethylammonium bromide. In: NAJJAR, R. (Ed.). Application and Characterization of Surfactants. 1. ed. IntechOpen, 2017. p. 157–182. ISBN 978-953-51-3326-1. Disponível em: <https://www.intechopen.com/books/application-and-characterization-of-surfactants/the-versatile-dioctadecyldimethylammonium-bromide>. Citado na página 33.

CARMONA-RIBEIRO, A. M. Biomimetic lipid polymer nanoparticles for drug delivery. In: FERRARI SOLOVIEV, M. E. (Ed.). Nanoparticles in Biology and Medicine. Methods in Molecular Biology. New York: [s.n.], 2020. v. 2118, p. 45–60. ISBN 978-1-07-160318-5. Citado na página 35.

CARMONA-RIBEIRO, A. M.; CARRASCO, L. D. de M. Cationic antimicrobial polymers and their assemblies. International journal of molecular sciences, v. 14, n. 5, p. 9906–9946, maio 2013. Citado na página 27.

CARMONA-RIBEIRO, A. M.; PéREZ-BETANCOURT, Y. Cationic nanostructures for vaccines design. Biomimetics (Basel, Switzerland), v. 5, n. 3, jul. 2020. Citado 7 vezes nas páginas 21, 23, 26, 32, 33, 34 e 35.

CHAPLIN, D. D. Overview of the immune response. The Journal of allergy and clinical immunology, v. 125, n. 2 Suppl 2, p. S3–S23, fev. 2010. ISSN 1097-6825. Disponível em: <https://pubmed.ncbi.nlm.nih.gov/20176265>. Citado na página 17.

CHEN, J.; LI, Z.; HUANG, H.; YANG, Y.; DING, Q.; MAI, J.; GUO, W.; XU, Y. Improved antigen cross-presentation by polyethyleneimine-based nanoparticles. International journal of nanomedicine, v. 6, p. 77–84, jan. 2011. Citado na página 30.

CHEN, W.; YAN, W.; HUANG, L. A simple but effective cancer vaccine consisting of an antigen and a cationic lipid. Cancer immunology, immunotherapy : CII, v. 57, n. 4, p. 517–530, abr. 2008. Citado na página 18.

CHUA, B. Y.; SEKIYA, T.; JACKSON, D. C. Making Inactivated and Subunit-Based Vaccines Work. Viral Immunology, v. 31, n. 2, p. 150–158, 2018. Disponível em: <https://doi.org/10.1089/vim.2017.0146>. Citado na página 19.

CHUMAKOV, K.; AVIDAN, M. S.; BENN, C. S.; BERTOZZI, S. M.; BLATT, L.; CHANG, A. Y.; JAMISON, D. T.; KHADER, S. A.; KOTTILIL, S.; NETEA, M. G.; SPARROW, A.; GALLO, R. C. Old vaccines for new infections: Exploiting innate immunity to control COVID-19 and prevent future pandemics. Proceedings of the National Academy of Sciences, v. 118, n. 21, 2021. ISSN 0027-8424. Publisher: National Academy of Sciences _eprint: https://www.pnas.org/content/118/21/e2101718118.full.pdf. Disponível em: <https://www.pnas.org/content/118/21/e2101718118>. Citado na página 18.

COFFMAN, R. L.; SHER, A.; SEDER, R. A. Vaccine adjuvants: putting innate immunity to work. Immunity, v. 33, n. 4, p. 492–503, out. 2010. Citado 3 vezes nas páginas 17, 20 e 22.

CUI, Z. DNA vaccine. Advances in genetics, v. 54, p. 257–289, 2005. Citado na página 20.

DAUTZENBERG, H.; HOLZAPFEL, G.; LUKANOFF, B. Methods for a comprehensive characterization of microcapsules based on polyelectrolyte complexes. Biomater Artif Cells Immobilization Biotechnol, v. 21, n. 3, p. 399–405, 1993. Citado na página 29.

DAVE, V.; TAK, K.; SOHGAURA, A.; GUPTA, A.; SADHU, V.; REDDY, K. R. Lipid-polymer hybrid nanoparticles: Synthesis strategies and biomedical applications. Journal of Microbiological Methods, v. 160, p. 130–142, 2019. Disponível em: <http://www.sciencedirect.com/science/article/pii/S0167701219300533>. Citado 2 vezes nas páginas 34 e 35.

DENIS-MIZE, K. S.; DUPUIS, M.; SINGH, M.; WOO, C.; UGOZZOLI, M.; O'HAGAN, D. T.; DONNELLY, J. J. r.; OTT, G.; MCDONALD, D. M. Mechanisms of increased immunogenicity for DNA-based vaccines adsorbed onto cationic microparticles. Cellular immunology, v. 225, n. 1, p. 12–20, set. 2003. ISSN 0008-8749. Place: Netherlands. Citado na página 20.

DEVRIENDT, B.; BAERT, K.; DIERENDONCK, M.; FAVOREEL, H.; KOKER, S. D.; REMON, J. P.; GEEST, B. G. D.; COX, E. One-step spray-dried polyelectrolyte microparticles enhance the antigen cross-presentation capacity of porcine dendritic cells. European Journal of Pharmaceutics and Biopharmaceutics, v. 84, n. 2, p. 421–429, 2013. Disponível em: <http://www.sciencedirect.com/science/article/pii/S0939641112003827>. Citado na página 32.

DHANWANI, R.; TAKAHASHI, M.; SHARMA, S. Cytosolic sensing of immuno-stimulatory DNA, the enemy within. Current opinion in immunology, v. 50, p. 82–87, fev. 2018. Citado na página 30.

DUPUIS, M.; DENIS-MIZE, K.; WOO, C.; GOLDBECK, C.; SELBY, M. J.; CHEN, M.; OTTEN, G. R.; ULMER, J. B.; DONNELLY, J. J.; OTT, G.; MCDONALD, D. M. Distribution of DNA Vaccines Determines Their Immunogenicity After Intramuscular Injection in Mice. The Journal of Immunology, v. 165, n. 5, p. 2850–2858, 2000. Publisher: American Association of Immunologists. Disponível em: <https://www.jimmunol.org/content/165/5/2850>. Citado na página 20.

DéMOULINS, T.; MILONA, P.; ENGLEZOU, P. C.; EBENSEN, T.; SCHULZE, K.; SUTER, R.; PICHON, C.; MIDOUX, P.; GUZMáN, C. A.; RUGGLI, N.; MCCULLOUGH, K. C. Polyethylenimine-based polyplex delivery of self-replicating RNA vaccines. Nanomedicine: Nanotechnology, Biology and Medicine, v. 12, n. 3, p. 711–722, 2016. Disponível em: <http://www.sciencedirect.com/science/article/pii/S1549963415002038>. Citado na página 30.

ESFAHANI, K.; ROUDAIA, L.; BUHLAIGA, N.; RINCON, S. D.; PAPNEJA, N.; MILLER, W. A Review of Cancer Immunotherapy: From the Past, to the Present, to the Future. Current Oncology, v. 27, n. 12, 2020. ISSN 1718-7729. Citado na página 18.

FAN, Y.-N.; LI, M.; LUO, Y.-L.; CHEN, Q.; WANG, L.; ZHANG, H.-B.; SHEN, S.; GU, Z.; WANG, J. Cationic lipid-assisted nanoparticles for delivery of mRNA cancer vaccine. Biomater. Sci., v. 6, n. 11, p. 3009–3018, 2018. Publisher: The Royal Society of Chemistry. Disponível em: <http://dx.doi.org/10.1039/C8BM00908B>. Citado na página 21.

FINDLOW, J.; KNUF, M. Immunogenicity and safety of meningococcal group A, C, W and Y tetanus toxoid conjugate vaccine: review of clinical and real-world evidence. Future Microbiology, v. 14, n. 7, p. 563–580, 2019. Disponível em: <https://doi.org/10.2217/fmb-2018-0343>. Citado na página 19.

FISCHER, D.; LI, Y.; AHLEMEYER, B.; KRIEGLSTEIN, J.; KISSEL, T. In vitro cytotoxicity testing of polycations: influence of polymer structure on cell viability and hemolysis. Biomaterials, v. 24, n. 7, p. 1121–1131, mar. 2003. Citado na página 29.

FOX, C. B.; KRAMER, R. M.; V, L. B.; DOWLING, Q. M.; VEDVICK, T. S. Working together: interactions between vaccine antigens and adjuvants. Therapeutic advances in vaccines, v. 1, n. 1, p. 7–20, maio 2013. ISSN 2051-0136. Publisher: SAGE Publications. Disponível em: <https://pubmed.ncbi.nlm.nih.gov/24757512>. Citado na página 26.

FRöHLICH, E. The role of surface charge in cellular uptake and cytotoxicity of medical nanoparticles. International journal of nanomedicine, v. 7, p. 5577–5591, 2012. ISSN 1178-2013. Edition: 2012/11/02 Publisher: Dove Medical Press. Disponível em: <https://pubmed.ncbi.nlm.nih.gov/23144561>. Citado na página 26.

GALL, D.; KNIGHT, P. A.; HAMPSON, F. Adjuvant activity of polyelectrolytes. Immunology, v. 23, n. 4, p. 569–575, out. 1972. Citado na página 29.

GALLUCCI, S.; MATZINGER, P. Danger signals: SOS to the immune system. Current Opinion in Immunology, v. 13, n. 1, p. 114–119, 2001. Disponível em: <https://www.sciencedirect.com/science/article/pii/S0952791500001916>. Citado na página 20.

GALVãO, C. N.; SANCHES, L. M.; MATHIAZZI, B. I.; RIBEIRO, R. T.; PETRI, D. F. S.; CARMONA-RIBEIRO, A. M. Antimicrobial coatings from hybrid nanoparticles of biocompatible and antimicrobial polymers. International Journal of Molecular Sciences, v. 19, n. 10, p. 2965–2965, 2018. ISSN 1422-0067. Citado 2 vezes nas páginas 37 e 38.

GAO, S.; HOLKAR, A.; SRIVASTAVA, S. Protein-Polyelectrolyte Complexes and Micellar Assemblies. Polymers, v. 11, n. 7, jun. 2019. Citado na página 28.

GARG, A.; DEWANGAN, H. K. Nanoparticles as Adjuvants in Vaccine Delivery. Critical reviews in therapeutic drug carrier systems, v. 37, n. 2, p. 183–204, 2020. ISSN 2162-660X 0743-4863. Place: United States. Citado na página 25.

GARG, A. D.; AGOSTINIS, P. Cell death and immunity in cancer: From danger signals to mimicry of pathogen defense responses. Immunological Reviews, v. 280, n. 1, p. 126–148, 2017. Disponível em: <https://onlinelibrary.wiley.com/doi/abs/10.1111/imr.12574>. Citado na página 20.

GHAFFARIFAR, F. Plasmid DNA vaccines: where are we now? Drugs of today (Barcelona, Spain : 1998), v. 54, n. 5, p. 315–333, maio 2018. Citado na página 20.

GU, P.; WUSIMAN, A.; WANG, S.; ZHANG, Y.; LIU, Z.; HU, Y.; LIU, J.; WANG, D. Polyethylenimine-coated PLGA nanoparticles-encapsulated Angelica sinensis polysaccharide as an adjuvant to enhance immune responses. Carbohydrate Polymers, v. 223, p. 115128–115128, 2019. Disponível em: <http://www.sciencedirect.com/science/article/pii/S0144861719307957>. Citado na página 31.

HALLMAN, M.; RäMET, M.; EZEKOWITZ, R. A. Toll-like Receptors as Sensors of Pathogens. Pediatric Research, v. 50, n. 3, p. 315–321, set. 2001. ISSN 1530-0447. Disponível em: <https://doi.org/10.1203/00006450-200109000-00004>. Citado na página 16.

HARUSH-FRENKEL, O.; ROZENTUR, E.; BENITA, S.; ALTSCHULER, Y. Surface charge of nanoparticles determines their endocytic and transcytotic pathway in polarized MDCK cells. Biomacromolecules, v. 9, n. 2, p. 435–443, fev. 2008. ISSN 1526-4602 1525-7797. Place: United States. Citado na página 26.

HASSON, S. S. A. A.; AL-BUSAIDI, J. K. Z.; SALLAM, T. A. The past, current and future trends in DNA vaccine immunisations. Asian Pacific Journal of Tropical Biomedicine, v. 5, n. 5, p. 344–353, 2015. Disponível em: <https://www.sciencedirect.com/science/article/pii/S222116911530366X>. Citado na página 20.

HELLER, C.; SCHWENTENWEIN, M.; RUSSMüLLER, G.; KOCH, T.; MOSER, D.; SCHOPPER, C.; VARGA, F.; STAMPFL, J.; LISKA, R. Vinylcarbonates and vinylcarbamates: Biocompatible monomers for radical photopolymerization. Journal of Polymer Science Part A: Polymer Chemistry, v. 49, n. 3, p. 650–661, fev. 2011. ISSN 0887-624X. Publisher: John Wiley & Sons, Ltd. Disponível em: <https://doi.org/10.1002/pola.24476>. Citado na página 37.

HENGGE, U. R.; BENNINGHOFF, B.; RUZICKA, T.; GOOS, M. Topical immunomodulators–progress towards treating inflammation, infection, and cancer. The Lancet. Infectious diseases, v. 1, n. 3, p. 189–198, out. 2001. Citado na página 20.

HENRIKSEN-LACEY, M.; BRAMWELL, V. W.; CHRISTENSEN, D.; AGGER, E.-M.; ANDERSEN, P.; PERRIE, Y. Liposomes based on dimethyldioctadecylammonium promote a depot effect and enhance immunogenicity of soluble antigen. Journal of controlled release : official journal of the Controlled Release Society, v. 142, n. 2, p. 180–186, mar. 2010. ISSN 1873-4995 0168-3659. Place: Netherlands. Citado na página 33.

IDREES, H.; ZAIDI, S. Z. J.; SABIR, A.; KHAN, R. U.; ZHANG, X.; HASSAN, S.-u. A Review of Biodegradable Natural Polymer-Based Nanoparticles for Drug Delivery Applications. Nanomaterials, v. 10, n. 10, 2020. ISSN 2079-4991. Disponível em: <https://www.mdpi.com/2079-4991/10/10/1970>. Citado na página 37.

IVANOV, K.; GARANINA, E.; RIZVANOV, A.; KHAIBOULLINA, S. Inflammasomes as Targets for Adjuvants. Pathogens (Basel, Switzerland), v. 9, n. 4, p. 252, mar. 2020. ISSN 2076-0817. Publisher: MDPI. Disponível em: <https://pubmed.ncbi.nlm.nih.gov/32235526>. Citado 2 vezes nas páginas 23 e 24.

JANSSENS, S.; BEYAERT, R. Role of Toll-like receptors in pathogen recognition. Clinical microbiology reviews, v. 16, n. 4, p. 637–646, out. 2003. ISSN 0893-8512. Publisher: American Society for Microbiology. Disponível em: <https://pubmed.ncbi.nlm.nih.gov/14557290>. Citado na página 16.

JIA, J.; WANG, Z.; YUE, T.; SU, G.; TENG, C.; YAN, B. Crossing Biological Barriers by Engineered Nanoparticles. Chemical Research in Toxicology, v. 33, n. 5, p. 1055–1060, maio 2020. ISSN 0893-228X. Publisher: American Chemical Society. Disponível em: <https://doi.org/10.1021/acs.chemrestox.9b00483>. Citado na página 25.

KARCH, C. P.; BURKHARD, P. Vaccine technologies: From whole organisms to rationally designed protein assemblies. Biochemical pharmacology, v. 120, p. 1–14, nov. 2016. Citado na página 20.

KAUR, R.; BRAMWELL, V. W.; KIRBY, D. J.; PERRIE, Y. Pegylation of DDA:TDB liposomal adjuvants reduces the vaccine depot effect and alters the Th1/Th2 immune responses. Journal of Controlled Release, v. 158, n. 1, p. 72–77, fev. 2012. ISSN 0168-3659. Disponível em: <https://www.sciencedirect.com/science/article/pii/S0168365911009643>. Citado na página 33.

KAYITMAZER, A. B.; SEEMAN, D.; MINSKY, B. B.; DUBIN, P. L.; XU, Y. Protein–polyelectrolyte interactions. Soft Matter, v. 9, n. 9, p. 2553–2583, 2013. Publisher: The Royal Society of Chemistry. Disponível em: <http://dx.doi.org/10.1039/C2SM27002A>. Citado 2 vezes nas páginas 28 e 29.

KHADEMI, F.; DERAKHSHAN, M.; YOUSEFI-AVARVAND, A.; NAJAFI, A.; TAFAGHODI, M. A novel antigen of Mycobacterium tuberculosis and MPLA adjuvant co-entrapped into PLGA:DDA hybrid nanoparticles stimulates mucosal and systemic immunity. Microbial pathogenesis, v. 125, p. 507–513, dez. 2018. Citado na página 35.

KHADEMI, F.; TAHERI, R.-A.; AVARVAND, A. Y.; VAEZ, H.; MOMTAZI-BOROJENI, A. A.; SOLEIMANPOUR, S. Are chitosan natural polymers suitable as adjuvant/delivery system for anti-tuberculosis vaccines? Microbial pathogenesis, v. 121, p. 218–223, ago. 2018. Citado na página 30.

KHAN, I.; SAEED, K.; KHAN, I. Nanoparticles: Properties, applications and toxicities. Arabian Journal of Chemistry, v. 12, n. 7, p. 908–931, nov. 2019. ISSN 1878-5352. Disponível em: <https://www.sciencedirect.com/science/article/pii/S1878535217300990>. Citado na página 25.

KHAN, K. H. DNA vaccines: roles against diseases. Germs, v. 3, n. 1, p. 26–35, mar. 2013. ISSN 2248-2997. Publisher: National Institute of Infectious Diseases “Prof. Dr. Matei Balş”, Romania, and the European Academy of HIV/AIDS and Infectious Diseases. Disponível em: <https://pubmed.ncbi.nlm.nih.gov/24432284>. Citado na página 20.

KIZILAY, E.; KAYITMAZER, A. B.; DUBIN, P. L. Complexation and coacervation of polyelectrolytes with oppositely charged colloids. Advances in Colloid and Interface Science, v. 167, n. 1, p. 24–37, 2011. Disponível em: <http://www.sciencedirect.com/science/article/pii/S0001868611001242>. Citado na página 27.

KORSHOLM, K. S.; AGGER, E. M.; FOGED, C.; CHRISTENSEN, D.; DIETRICH, J.; ANDERSEN, C. S.; GEISLER, C.; ANDERSEN, P. The adjuvant mechanism of cationic dimethyldioctadecylammonium liposomes. Immunology, v. 121, n. 2, p. 216–226, jun. 2007. Citado na página 33.

KURODA, E.; COBAN, C.; ISHII, K. J. Particulate adjuvant and innate immunity: past achievements, present findings, and future prospects. International reviews of immunology, v. 32, n. 2, p. 209–220, abr. 2013. Citado na página 24.

LI, S.; MALMSTADT, N. Deformation and poration of lipid bilayer membranes by cationic nanoparticles. Soft Matter, v. 9, n. 20, p. 4969–4976, 2013. Publisher: The Royal Society of Chemistry. Disponível em: <http://dx.doi.org/10.1039/C3SM27578G>. Citado na página 26.

LIM, J. J.; GRINSTEIN, S.; ROTH, Z. Diversity and Versatility of Phagocytosis: Roles in Innate Immunity, Tissue Remodeling, and Homeostasis. Frontiers in Cellular and Infection Microbiology, v. 7, p. 191, 2017. ISSN 2235-2988. Disponível em: <https://www.frontiersin.org/article/10.3389/fcimb.2017.00191>. Citado na página 15.

LIN, J.; ALEXANDER-KATZ, A. Cell membranes open "doors" for cationic nanoparticles/Biomolecules: insights into uptake kinetics. ACS Nano, v. 7, n. 12, p. 10799–10808, dez. 2013. Publisher: American Chemical Society. Disponível em: <https://doi.org/10.1021/nn4040553>. Citado na página 26.

LINCOPAN, N.; ESPINDOLA, N. M.; VAZ, A. J.; COSTA, M. H. B. da; FAQUIM-MAURO, E.; CARMONA-RIBEIRO, A. M. Novel immunoadjuvants based on cationic lipid: preparation, characterization and activity in vivo. Vaccine, v. 27, n. 42, p. 5760–5771, set. 2009. Citado na página 32.

LUHRS, P.; SCHMIDT, W.; KUTIL, R.; BUSCHLE, M.; WAGNER, S. N.; STINGL, G.; SCHNEEBERGER, A. Induction of specific immune responses by polycation-based vaccines. Journal of immunology (Baltimore, Md. : 1950), v. 169, n. 9, p. 5217–5226, nov. 2002. Citado 2 vezes nas páginas 31 e 32.

MANOLOVA, V.; FLACE, A.; BAUER, M.; SCHWARZ, K.; SAUDAN, P.; BACHMANN, M. F. Nanoparticles target distinct dendritic cell populations according to their size. European journal of immunology, v. 38, n. 5, p. 1404–1413, maio 2008. Citado na página 26.

MARRACK, P.; MCKEE, A. S.; MUNKS, M. W. Towards an understanding of the adjuvant action of aluminium. Nature reviews. Immunology, v. 9, n. 4, p. 287–293, abr. 2009. Citado na página 21.

MARTINEZ, J. S.; KELLER, T. C. S.; SCHLENOFF, J. B. Cytotoxicity of free versus multilayered polyelectrolytes. Biomacromolecules, v. 12, n. 11, p. 4063–4070, nov. 2011. Publisher: American Chemical Society. Disponível em: <https://doi.org/10.1021/bm201142x>. Citado na página 29.

MATHIAZZI, B. I.; CARMONA-RIBEIRO, A. M. Hybrid nanoparticles of poly (methyl methacrylate) and antimicrobial quaternary ammonium surfactants. Pharmaceutics, v. 12, n. 4, abr. 2020. Citado 3 vezes nas páginas 12, 35 e 36.

MATTNER, F.; FLEITMANN, J.-K.; LINGNAU, K.; SCHMIDT, W.; EGYED, A.; FRITZ, J.; ZAUNER, W.; WITTMANN, B.; GORNY, I.; BERGER, M.; KIRLAPPOS, H.; OTAVA, A.; BIRNSTIEL, M. L.; BUSCHLE, M. Vaccination with poly-L-arginine as immunostimulant for peptide vaccines: induction of potent and long-lasting T-cell responses against cancer antigens. Cancer research, v. 62, n. 5, p. 1477–1480, mar. 2002. Citado na página 32.

MEDZHITOV, R.; JANEWAY, C. J. Innate immunity. The New England journal of medicine, v. 343, n. 5, p. 338–344, ago. 2000. ISSN 0028-4793. Place: United States. Citado na página 16.

MEKA, V. S.; SING, M. K.; PICHIKA, M. R.; NALI, S. R.; KOLAPALLI, V. R.; KESHARWANI, P. A comprehensive review on polyelectrolyte complexes. Drug Discovery Today, v. 22, n. 11, p. 1697–1706, nov. 2017. ISSN 1359-6446. Disponível em: <https://www.sciencedirect.com/science/article/pii/S1359644617301265>. Citado na página 29.

MELO, L. D.; PALOMBO, R. R.; PETRI, D. F. S.; BRUNS, M.; PEREIRA, E. M. A.; CARMONA-RIBEIRO, A. M. Structure-activity relationship for quaternary ammonium compounds hybridized with poly(methyl methacrylate). ACS applied materials & interfaces, v. 3, n. 6, p. 1933–1939, jun. 2011. Citado na página 35.

MENG, F.; KWON, S.; WANG, J.; YEO, Y. Immunoactive drug carriers in cancer therapy. In: PARK, K. (Ed.). Biomaterials for Cancer Therapeutics (Second Edition). Woodhead Publishing, 2020. p. 53–94. ISBN 978-0-08-102983-1. Disponível em: <https://www.sciencedirect.com/science/article/pii/B978008102983100003X>. Citado na página 30.

MINOR, P. D. Live attenuated vaccines: Historical successes and current challenges. Virology, v. 479-480, p. 379–392, maio 2015. ISSN 1096-0341 0042-6822. Place: United States. Citado na página 19.

MONNERY, B. D.; WRIGHT, M.; CAVILL, R.; HOOGENBOOM, R.; SHAUNAK, S.; STEINKE, J. H. G.; THANOU, M. Cytotoxicity of polycations: relationship of molecular weight and the hydrolytic theory of the mechanism of toxicity. International journal of pharmaceutics, v. 521, n. 1-2, p. 249–258, abr. 2017. Citado na página 29.

MOURA, S. P.; CARMONA-RIBEIRO, A. M. Biomimetic particles for isolation and reconstitution of receptor function. Cell biochemistry and biophysics, v. 44, n. 3, p. 446–452, 2006. Citado na página 35.

MUKHERJEE, A.; WATERS, A. K.; KALYAN, P.; ACHROL, A. S.; KESARI, S.; YENUGONDA, V. M. Lipid-polymer hybrid nanoparticles as a next-generation drug delivery platform: state of the art, emerging technologies, and perspectives. International journal of nanomedicine, v. 14, p. 1937–1952, 2019. Citado 2 vezes nas páginas 34 e 35.

MUTWIRI, G.; GERDTS, V.; HURK, S. van Drunen Littel-van den; AURAY, G.; ENG, N.; GARLAPATI, S.; BABIUK, L. A.; POTTER, A. Combination adjuvants: the next generation of adjuvants? Expert Review of Vaccines, v. 10, n. 1, p. 95–107, jan. 2011. ISSN 1476-0584. Publisher: Taylor & Francis. Disponível em: <https://doi.org/10.1586/erv.10.154>. Citado na página 24.

NANOMEDICINE and the COVID-19 vaccines. Nature Nanotechnology, v. 15, n. 12, p. 963–963, dez. 2020. ISSN 1748-3395. Disponível em: <https://doi.org/10.1038/s41565-020-00820-0>. Citado na página 21.

NAVES, A. F.; PALOMBO, R. R.; CARRASCO, L. D. M.; CARMONA-RIBEIRO, A. M. Antimicrobial particles from emulsion polymerization of methyl methacrylate in the presence of quaternary ammonium surfactants. Langmuir : the ACS journal of surfaces and colloids, v. 29, n. 31, p. 9677–9684, ago. 2013. Citado na página 35.

ORTEGA-MUNOZ, M.; GIRON-GONZALEZ, M. D.; SALTO-GONZALEZ, R.; JODAR-REYES, A. B.; JESUS, S. E. D.; LOPEZ-JARAMILLO, F. J.; HERNANDEZ-MATEO, F.; SANTOYO-GONZALEZ, F. Polyethyleneimine-Coated Gold Nanoparticles: Straightforward Preparation of Efficient DNA Delivery Nanocarriers. Chemistry, an Asian journal, v. 11, n. 23, p. 3365–3375, dez. 2016. Citado na página 29.

PARDI, N.; HOGAN, M. J.; PORTER, F. W.; WEISSMAN, D. mRNA vaccines - a new era in vaccinology. Nature reviews. Drug discovery, v. 17, n. 4, p. 261–279, abr. 2018. ISSN 1474-1784. Edition: 2018/01/12. Disponível em: <https://pubmed.ncbi.nlm.nih.gov/29326426>. Citado na página 21.

PASHINE, A.; VALIANTE, N. M.; ULMER, J. B. Targeting the innate immune response with improved vaccine adjuvants. Nature medicine, v. 11, n. 4 Suppl, p. S63–8, abr. 2005. Citado na página 22.

PASQUALE, A.; PREISS, S.; SILVA, F.; GARçON, N. Vaccine adjuvants: from 1920 to 2015 and beyond. Vaccines, v. 3, n. 2, p. 320–343, abr. 2015. Publisher: Multidisciplinary Digital Publishing Institute. Disponível em: <http://www.mdpi.com/2076-393X/3/2/320>. Citado 6 vezes nas páginas 17, 19, 20, 21, 22 e 24.

PATI, R.; SHEVTSOV, M.; SONAWANE, A. Nanoparticle Vaccines Against Infectious Diseases. Frontiers in immunology, v. 9, p. 2224–2224, out. 2018. ISSN 1664-3224. Publisher: Frontiers Media S.A. Disponível em: <https://pubmed.ncbi.nlm.nih.gov/30337923>. Citado na página 25.

PATRA, J. K.; DAS, G.; FRACETO, L. F.; CAMPOS, E. V. R.; RODRIGUEZ-TORRES, M. D. P.; ACOSTA-TORRES, L. S.; DIAZ-TORRES, L. A.; GRILLO, R.; SWAMY, M. K.; SHARMA, S.; HABTEMARIAM, S.; SHIN, H.-S. Nano based drug delivery systems: recent developments and future prospects. Journal of nanobiotechnology, v. 16, n. 1, p. 71–71, set. 2018. ISSN 1477-3155. Publisher: BioMed Central. Disponível em: <https://pubmed.ncbi.nlm.nih.gov/30231877>. Citado na página 25.

PAULIS, L. E.; MANDAL, S.; KREUTZ, M.; FIGDOR, C. G. Dendritic cell-based nanovaccines for cancer immunotherapy. Current opinion in immunology, v. 25, n. 3, p. 389–395, jun. 2013. Citado na página 16.

PEREIRA, E. M. A.; KOSAKA, P. M.; ROSA, H.; VIEIRA, D. B.; KAWANO, Y.; PETRI, D. F. S.; CARMONA-RIBEIRO, A. M. Hybrid materials from intermolecular associations between cationic lipid and polymers. The journal of physical chemistry. B, v. 112, n. 31, p. 9301–9310, ago. 2008. Citado na página 35.

POLLARD, A. J.; BIJKER, E. M. A guide to vaccinology: from basic principles to new developments. Nature Reviews Immunology, v. 21, n. 2, p. 83–100, fev. 2021. ISSN 1474-1741. Disponível em: <https://doi.org/10.1038/s41577-020-00479-7>. Citado 2 vezes nas páginas 18 e 22.

PULENDRAN, B.; AHMED, R. Immunological mechanisms of vaccination. Nature immunology, v. 12, n. 6, p. 509–517, jun. 2011. ISSN 1529-2916 1529-2908. Citado 3 vezes nas páginas 15, 18 e 19.

PULENDRAN, B.; ARUNACHALAM, P. S.; O'HAGAN, D. T. Emerging concepts in the science of vaccine adjuvants. Nature Reviews Drug Discovery, v. 20, n. 6, p. 454–475, jun. 2021. ISSN 1474-1784. Disponível em: <https://doi.org/10.1038/s41573-021-00163-y>. Citado na página 27.

RAHMAN, F.; CARBAUGH, D. J.; WRIGHT, J. T.; RAJAN, P.; PANDYA, S. G.; KAYA, S. A review of polymethyl methacrylate (PMMA) as a versatile lithographic resist – With emphasis on UV exposure. Microelectronic Engineering, v. 224, p. 111238, mar. 2020. ISSN 0167-9317. Disponível em: <https://www.sciencedirect.com/science/article/pii/S0167931720300265>. Citado na página 37.

REED, S. G.; ORR, M. T.; FOX, C. B. Key roles of adjuvants in modern vaccines. Nature Medicine, v. 19, n. 12, p. 1597–1608, dez. 2013. ISSN 1546-170X. Disponível em: <https://doi.org/10.1038/nm.3409>. Citado na página 22.

REGNSTROM, K.; RAGNARSSON, E. G. E.; KOPING-HOGGARD, M.; TORSTENSSON, E.; NYBLOM, H.; ARTURSSON, P. PEI - a potent, but not harmless, mucosal immuno-stimulator of mixed T-helper cell response and FasL-mediated cell death in mice. Gene therapy, v. 10, n. 18, p. 1575–1583, set. 2003. Citado na página 30.

RIBEIRO, R. T.; BRAGA, V. H. A.; CARMONA-RIBEIRO, A. M. Biomimetic cationic nanoparticles based on silica: optimizing bilayer deposition from lipid films. Biomimetics (Basel, Switzerland), v. 2, n. 4, out. 2017. Citado na página 35.

RIBEIRO, R. T.; GALVãO, C. N.; BETANCOURT, Y. P.; MATHIAZZI, B. I.; CARMONA-RIBEIRO, A. M. Microbicidal dispersions and coatings from hybrid nanoparticles of poly (methyl methacrylate), poly (diallyl dimethyl ammonium) chloride, lipids, and surfactants. International Journal of Molecular Sciences, v. 20, n. 24, p. 6150–6150, dez. 2019. Publisher: MDPI. Citado 2 vezes nas páginas 37 e 38.

RIEDEL, S. Edward Jenner and the history of smallpox and vaccination. Proceedings (Baylor University. Medical Center), v. 18, n. 1, p. 21–25, jan. 2005. Publisher: Baylor Health Care System. Disponível em: <https://pubmed.ncbi.nlm.nih.gov/16200144>. Citado na página 18.

ROCHE, P. A.; FURUTA, K. The ins and outs of MHC class II-mediated antigen processing and presentation. Nature reviews. Immunology, v. 15, n. 4, p. 203–216, abr. 2015. ISSN 1474-1741. Edition: 2015/02/27. Disponível em: <https://pubmed.ncbi.nlm.nih.gov/25720354>. Citado na página 33.

RODRIGUES, C. M. C.; PLOTKIN, S. A. Impact of Vaccines; Health, Economic and Social Perspectives. Frontiers in Microbiology, v. 11, p. 1526, 2020. ISSN 1664-302X. Disponível em: <https://www.frontiersin.org/article/10.3389/fmicb.2020.01526>. Citado na página 18.

ROSE, F.; WERN, J. E.; INGVARSSON, P. T.; WEERT, M. van de; ANDERSEN, P.; FOLLMANN, F.; FOGED, C. Engineering of a novel adjuvant based on lipid-polymer hybrid nanoparticles: A quality-by-design approach. Journal of controlled release : official journal of the Controlled Release Society, v. 210, p. 48–57, jul. 2015. Citado na página 35.

ROZENFELD, J. H. K.; OLIVEIRA, T. R.; LAMY, M. T.; CARMONA-RIBEIRO, A. M. Interaction of cationic bilayer fragments with a model oligonucleotide. Biochimica et biophysica acta, v. 1808, n. 3, p. 649–655, mar. 2011. Citado na página 32.

ROZENFELD, J. H. K.; SILVA, S. R.; RANEIA, P. A.; FAQUIM-MAURO, E.; CARMONA-RIBEIRO, A. M. Stable assemblies of cationic bilayer fragments and CpG oligonucleotide with enhanced immunoadjuvant activity in vivo. Journal of controlled release : official journal of the Controlled Release Society, v. 160, n. 2, p. 367–373, jun. 2012. Citado 2 vezes nas páginas 32 e 33.

SAHIN, U.; KARIKó, K.; TüRECI, mRNA-based therapeutics — developing a new class of drugs. Nature Reviews Drug Discovery, v. 13, n. 10, p. 759–780, out. 2014. ISSN 1474-1784. Disponível em: <https://doi.org/10.1038/nrd4278>. Citado na página 21.

SALLUSTO, F.; LANZAVECCHIA, A.; ARAKI, K.; AHMED, R. From vaccines to memory and back. Immunity, v. 33, n. 4, p. 451–463, out. 2010. ISSN 1097-4180. Disponível em: <https://pubmed.ncbi.nlm.nih.gov/21029957>. Citado na página 18.

SANCHES, L. M.; PETRI, D. F. S.; CARRASCO, L. D. de M.; CARMONA-RIBEIRO, A. M. The antimicrobial activity of free and immobilized poly (diallyldimethylammonium) chloride in nanoparticles of poly (methylmethacrylate). Journal of nanobiotechnology, v. 13, p. 58–58, set. 2015. Citado 3 vezes nas páginas 12, 29 e 38.

SANDERS, B.; KOLDIJK, M.; SCHUITEMAKER, H. Inactivated Viral Vaccines. In: NUNNALLY, B. K.; TURULA, V. E.; SITRIN, R. D. (Ed.). Vaccine Analysis: Strategies, Principles, and Control. Berlin, Heidelberg: Springer Berlin Heidelberg, 2015. p. 45–80. ISBN 978-3-662-45024-6. Disponível em: <https://doi.org/10.1007/978-3-662-45024-6_2>. Citado na página 19.

SANTOS, F. A. de O.; LINCOPAN, N.; GASPARI, E. D. Evaluation of intranasal and subcutaneous route of immunization in neonatal mice using DODAB-BF as adjuvant with outer membrane vesicles of Neisseria meningitis B. Immunobiology, v. 223, n. 12, p. 750–760, dez. 2018. Citado na página 32.

SAROJA, C.; LAKSHMI, P.; BHASKARAN, S. Recent trends in vaccine delivery systems: A review. International journal of pharmaceutical investigation, v. 1, n. 2, p. 64–74, abr. 2011. ISSN 2230-9713. Publisher: Medknow Publications & Media Pvt Ltd. Disponível em: <https://pubmed.ncbi.nlm.nih.gov/23071924>. Citado na página 24.

SCHIJNS, V.; FERNáNDEZ-TEJADA, A.; BARJAKTAROVIć, ; BOUZALAS, I.; BRIMNES, J.; CHERNYSH, S.; GIZURARSON, S.; GURSEL, I.; JAKOPIN, ; LAWRENZ, M.; NATIVI, C.; PAUL, S.; PEDERSEN, G. K.; ROSANO, C.; ANGULO, A. Ruiz-de; SLüTTER, B.; THAKUR, A.; CHRISTENSEN, D.; LAVELLE, E. C. Modulation of immune responses using adjuvants to facilitate therapeutic vaccination. Immunological Reviews, v. 296, n. 1, p. 169–190, 2020. _eprint: https://onlinelibrary.wiley.com/doi/pdf/10.1111/imr.12889. Disponível em: <https://onlinelibrary.wiley.com/doi/abs/10.1111/imr.12889>. Citado na página 22.

SCHLAKE, T.; THESS, A.; FOTIN-MLECZEK, M.; KALLEN, K.-J. Developing mRNA-vaccine technologies. RNA biology, v. 9, n. 11, p. 1319–1330, nov. 2012.

ISSN 1555-8584. Edition: 2012/10/12 Publisher: Landes Bioscience. Disponível em: <https://pubmed.ncbi.nlm.nih.gov/23064118>. Citado na página 21.

SCHORK, F. J.; RAY, W. H. The dynamics of the continuous emulsion polymerization of methylmethacrylate. Journal of Applied Polymer Science, v. 34, n. 3, p. 1259–1276, ago. 1987. ISSN 0021-8995. Publisher: John Wiley & Sons, Ltd. Disponível em: <https://doi.org/10.1002/app.1987.070340331>. Citado na página 37.

SHAKYA, A. K.; NANDAKUMAR, K. S. Applications of polymeric adjuvants in studying autoimmune responses and vaccination against infectious diseases. Journal of the Royal Society, Interface, v. 10, n. 79, p. 20120536–20120536, fev. 2013. Citado 3 vezes nas páginas 12, 23 e 24.

SHEN, C.; LI, J.; ZHANG, Y.; LI, Y.; SHEN, G.; ZHU, J.; TAO, J. Polyethylenimine-based micro/nanoparticles as vaccine adjuvants. International journal of nanomedicine, v. 12, p. 5443–5460, 2017. Citado na página 30.

SHEPPARD, N. C.; BRINCKMANN, S. A.; GARTLAN, K. H.; PUTHIA, M.; SVANBORG, C.; KRASHIAS, G.; EISENBARTH, S. C.; FLAVELL, R. A.; SATTENTAU, Q. J.; WEGMANN, F. Polyethyleneimine is a potent systemic adjuvant for glycoprotein antigens. International Immunology, v. 26, n. 10, p. 531–538, maio 2014. Citado na página 30.

SINGH, M.; BRIONES, M.; OTT, G.; O'HAGAN, D. Cationic microparticles: A potent delivery system for DNA vaccines. Proceedings of the National Academy of Sciences of the United States of America, v. 97, n. 2, p. 811–816, jan. 2000. Citado na página 20.

SINGH, M.; KAZZAZ, J.; UGOZZOLI, M.; CHESKO, J.; O'HAGAN, D. T. Charged polylactide co-glycolide microparticles as antigen delivery systems. Expert opinion on biological therapy, v. 4, n. 4, p. 483–491, abr. 2004. Citado na página 31.

SPROUSE, D.; REINEKE, T. M.; DAVIS, M. E. Polymeric Delivery Vehicles for Exogenous Nucleic Acid Delivery. In: Reference Module in Materials Science and Materials Engineering. Elsevier, 2016. ISBN 978-0-12-803581-8. Disponível em: <https://www.sciencedirect.com/science/article/pii/B9780128035818015162>. Citado na página 27.

STEINMAN, R. M.; HEMMI, H. Dendritic cells: translating innate to adaptive immunity. Current topics in microbiology and immunology, v. 311, p. 17–58, 2006. ISSN 0070-217X. Place: Germany. Citado na página 17.

STROMBERG, Z. R.; FISCHER, W.; BRADFUTE, S. B.; KUBICEK-SUTHERLAND, J. Z.; HRABER, P. Vaccine Advances against Venezuelan, Eastern, and Western Equine Encephalitis Viruses. Vaccines, v. 8, n. 2, jun. 2020. ISSN 2076-393X. Citado na página 19.

TIZARD, I. R. Adjuvants and adjuvanticity. Vaccines for Veterinarians, p. 75–86.e1, 2021. Edition: 2020/07/10. Disponível em: <https://www.ncbi.nlm.nih.gov/pmc/articles/PMC7348637/>. Citado na página 24.

TSURUTA, L. R.; QUINTILIO, W.; COSTA, M. H.; CARMONA-RIBEIRO, A. M. Interactions between cationic liposomes and an antigenic protein: the physical chemistry of the

immunoadjuvant action. Journal of lipid research, v. 38, n. 10, p. 2003–2011, out. 1997. Citado 2 vezes nas páginas 32 e 33.

VALETTI, N. W.; BRASSESCO, M. E.; PICó, G. A. Polyelectrolytes–protein complexes: a viable platform in the downstream processes of industrial enzymes at scaling up level. Journal of Chemical Technology \& Biotechnology, v. 91, n. 12, p. 2921–2928, 2016. Disponível em: <https://onlinelibrary.wiley.com/doi/abs/10.1002/jctb.5050>. Citado na página 28.

WANDREY, C.; HERNáNDEZ-BARAJAS, J.; HUNKELER, D. Diallyldimethylammonium Chloride and its Polymers. In: 1, C.; HERNáNDEZ-BARAJAS, J.; HUNKELER, D.; REDDINGER, J. L.; REYNOLDS, J. R.; WANDREY, C. (Ed.). Radical Polymerisation Polyelectrolytes. Berlin, Heidelberg: Springer Berlin Heidelberg, 1999. p. 123–183. ISBN 978-3-540-70733-2. Disponível em: <https://doi.org/10.1007/3-540-70733-6_3>. Citado na página 28.

WANG, X.; ZHENG, K.; SI, Y.; GUO, X.; XU, Y. Protein-polyelectrolyte interaction: thermodynamic analysis based on the titration method (†). Polymers, v. 11, n. 1, p. 82–82, jan. 2019. Publisher: MDPI. Disponível em: <https://www.ncbi.nlm.nih.gov/pubmed/30960066>. Citado 3 vezes nas páginas 27, 28 e 29.

WANG, Z.-B.; XU, J. Better Adjuvants for Better Vaccines: Progress in Adjuvant Delivery Systems, Modifications, and Adjuvant–Antigen Codelivery. Vaccines, v. 8, n. 1, 2020. ISSN 2076-393X. Disponível em: <https://www.mdpi.com/2076-393X/8/1/128>. Citado 2 vezes nas páginas 21 e 24.

WEGMANN, F.; GARTLAN, K. H.; HARANDI, A. M.; BRINCKMANN, S. A.; COCCIA, M.; HILLSON, W. R.; KOK, W. L.; COLE, S.; HO, L.-P.; LAMBE, T.; PUTHIA, M.; SVANBORG, C.; SCHERER, E. M.; KRASHIAS, G.; WILLIAMS, A.; BLATTMAN, J. N.; GREENBERG, P. D.; FLAVELL, R. A.; MOGHADDAM, A. E.; SHEPPARD, N. C.; SATTENTAU, Q. J. Polyethyleneimine is a potent mucosal adjuvant for viral glycoprotein antigens. Nature Biotechnology, v. 30, p. 883–888, ago. 2012. Publisher: Nature Publishing Group, a division of Macmillan Publishers Limited. All Rights Reserved. Disponível em: <https://doi.org/10.1038/nbt.2344>. Citado 3 vezes nas páginas 29, 30 e 31.

WEINBERGER, B. Adult vaccination against tetanus and diphtheria: the European perspective. Clinical and experimental immunology, v. 187, n. 1, p. 93–99, jan. 2017. ISSN 1365-2249 0009-9104. Citado na página 19.

XAVIER, G. R. S.; CARMONA-RIBEIRO, A. M. Cationic biomimetic particles of polystyrene/cationic bilayer/gramicidin for optimal bactericidal activity. Nanomaterials (Basel, Switzerland), v. 7, n. 12, dez. 2017. Citado na página 35.

XU, L.; LIU, Y.; CHEN, Z.; LI, W.; LIU, Y.; WANG, L.; LIU, Y.; WU, X.; JI, Y.; ZHAO, Y.; MA, L.; SHAO, Y.; CHEN, C. Surface-engineered gold nanorods: promising DNA vaccine adjuvant for HIV-1 treatment. Nano letters, v. 12, n. 4, p. 2003–2012, abr. 2012. Citado 2 vezes nas páginas 29 e 31.

YAZDI, A. S.; GUARDA, G.; RITEAU, N.; DREXLER, S. K.; TARDIVEL, A.; COUILLIN, I.; TSCHOPP, J.; FELDMANN, M. Nanoparticles activate the NLR pyrin domain containing 3

(Nlrp3) inflammasome and cause pulmonary inflammation through release of IL-1 and IL-1. Proceedings of the National Academy of Sciences of the United States of America, v. 107, n. 45, p. 19449–19454, 2010. ISSN 00278424. Publisher: National Academy of Sciences. Disponível em: <http://www.jstor.org/stable/25748694>. Citado na página 27.

ZHANG, C.; MARUGGI, G.; SHAN, H.; LI, J. Advances in mRNA Vaccines for Infectious Diseases. Frontiers in Immunology, v. 10, p. 594, 2019. ISSN 1664-3224. Disponível em: <https://www.frontiersin.org/article/10.3389/fimmu.2019.00594>. Citado na página 21.

ZHANG, L.; WU, S.; QIN, Y.; FAN, F.; ZHANG, Z.; HUANG, C.; JI, W.; LU, L.; WANG, C.; SUN, H.; LENG, X.; KONG, D.; ZHU, D. Targeted Codelivery of an Antigen and Dual Agonists by Hybrid Nanoparticles for Enhanced Cancer Immunotherapy. Nano letters, v. 19, n. 7, p. 4237–4249, jul. 2019. ISSN 1530-6992 1530-6984. Place: United States. Citado na página 35.

ZHAO, L.; SETH, A.; WIBOWO, N.; ZHAO, C.-X. X.; MITTER, N.; YU, C.; MIDDELBERG, A. P. Nanoparticle vaccines. Vaccine, v. 32, n. 3, p. 327–337, 2014. ISSN 1873-2518 (Electronic)\r0264-410X (Linking). Citado 2 vezes nas páginas 25 e 26.

ZHU, M.; WANG, R.; NIE, G. Applications of nanomaterials as vaccine adjuvants. Human vaccines & immunotherapeutics, v. 10, n. 9, p. 2761–2774, 2014. Citado na página 25.